Investigation of the Signalling and Function of NOD2

A thesis submitted to the University of Oxford

for the degree of doctor of philosophy

Dr Andrew Oliver Seaward Brain

Jesus College Trinity Term 2011

Translational Gastroenterology Unit

Nuffield Department of Medicine

University of Oxford

© 2011 Andrew Oliver Seaward Brain

All rights reserved

This dissertation is the result of my own work and includes nothing that is the outcome of work done in collaboration except where specifically indicated in the text.

No part of this dissertation has already been, or is currently being submitted, by the author for any other degree or diploma or other qualification.

This dissertation does not exceed 50,000 words, exclusive of appendices, bibliography, diagrams and tables.

All trademarks used in this dissertation are acknowledged to be the property of their respective owners.

Abstract

NOD2 is an intracellular innate immune receptor expressed in dendritic cells and gastrointestinal epithelial cells. Polymorphisms in the NOD2 gene convey a strong predisposition to Crohn's disease (CD), a form of inflammatory bowel disease. Understanding the function of NOD2, and in what way it is aberrant in the presence of NOD2 polymorphisms, would confer a valuable paradigm for understanding Crohn's pathogenesis.

CD is thought to arise both from defects in the gut mucosal barrier and from a dysregulated Th17 immune response to commensal gut flora. Aberrant expression of IL-23 is present in both human CD and in murine models of colitis. Wild-type NOD2 contributes to NFκB activation and pro-inflammatory cytokine production on recognition of its cognate ligand, a function that is lost in CD-associated mutations. How the predominantly loss-of-function CD-NOD2 contributes to the pro-inflammatory response present in Crohn's is not yet understood.

In this thesis a set of experiments is described that aim to shed light on the function of NOD2, firstly through identification of negative regulators of immune activation that are dependent on NOD2 for their expression. This work identifies the microRNAs that are expressed following NOD2 triggering in human dendritic cells. Specifically, up-regulation of the miR-29 family was found to be dependent on wild-type NOD2 function. A number of novel miR-29 targets and their functional consequences are presented, including the cytokine subunits IL-12p40 and IL-23p19, directly linking NOD2 polymorphisms and aberrant IL-23 expression.

Secondly, a project aiming to identify components of the NOD2 signalling complex (or signalosome) is described. To this end I employed a model system that involved tagging NOD2, and stable expression in a human cell line. These clones were validated for expression and function before an immunoprecipitation protocol was optimised. Mass spectrometry analysis of these samples identified the known NOD2-interacting protein Erbin.

Contents

Abstract iii

List of Tables xiv

List of Figures xiv

Abbreviations xvii

Acknowledgements xxxii

1 Introduction 1

1.1 The Gastrointestinal tract in health and disease 1

1.2 Defective Immunity 2

1.2.1 Genetics 2

1.2.2 Autophagy 4

1.2.3 ATG16L1 5

1.2.4 IRGM 6

1.2.5 IL-23/ Th17 pathway 8

1.2.6 Unfolded Protein Response 9

1.3 GI Barrier Function 10

1.3.1 The GIT forms a large environmental interface 10

1.3.2 Mucus Layer 11

1.3.3 Epithelial Organisation 11

1.3.4 Anti-microbial Peptides 12

1.4 Gastrointestinal Flora 14

1.4.1 The microbial flora is intimately linked with GIT inflammation 14

1.4.2 Anti-inflammatory commensals 15

1.4.3 Disease-associated bacteria 16
1.4.4 Defining the normal gut microflora 16
1.4.5 Dysbiosis in Crohn's disease 18
1.5 NOD2 19
1.5.1 NOD2 Introduction 19
1.5.2 NOD2 discovery and structure 19
1.5.3 NOD2 expression in Dendritic cells 21
1.6 NOD2 and Immunity 23
1.6.1 NOD2 signalling 23
1.6.2 NOD2-signalling regulators: A20 23
1.6.3 NOD2-signalling regulators: directly interacting proteins 24
1.6.4 NOD2-signalling: MAPK activation 26
1.7 NOD2 in context 27
1.7.1 NOD2 and Toll-like receptors 28
1.7.2 NOD2: TLR2 29
1.7.3 NOD2: TLR4 30
1.7.4 Other NOD2: TLR interactions 31
1.7.5 NOD2: TLR interaction mechanisms 31
1.7.6 NOD2 pre-stimulation 33
1.7.7 NOD2: TLR summary 34
1.8 NOD2 and Nod-like receptors 34
1.8.1 Inflammasome activators 35
1.8.2 NOD2: NLRC4 37
1.8.3 NOD2: NLRP3 38
1.8.4 NOD2: NLRP1 40

1.9 NOD2 and Autophagy 41
1.10 NOD2 and ER stress 42
1.11 NOD2 and Adaptive Immunity 43
1.11.1 NOD2 in DCs 43
1.11.2 NOD2 T cell-intrinsic function 45
1.12 NOD2 and Epithelial Barrier Function 45
1.12.1 NOD2 and epithelial extracellular bacterial control 45
1.12.2 Defensins 45
1.12.3 DMTB1 47
1.13 NOD2 and epithelial intracellular bacterial control 47
1.13.1 GRIM-19 47
1.13.2 DUOX2 48
1.14 NOD2 and the Microbiome 48
1.14.1 NOD2 microbiota: mice 49
1.14.2 NOD2 microbiota: humans 50
1.15 NOD2 function: Of mice and men 51
1.16 NOD2 Summary 52

2 Material and Methods 55

2.1 Molecular Biology Methods 55
2.1.1 Polymerase chain reaction 55
2.1.2 Mini / Maxipreps 55
2.1.3 Restriction digest 57
2.1.4 Western Blot 57
2.1.5 DC Nucleofection 58

2.1.6 Preparation of Human Monocyte-derived Dendritic Cells 59
2.1.7 Quantitative PCR mRNA 59
2.1.8 Quantitative PCR microRNA 60
2.2 MDDC stimulation and FACS analysis 61
2.3 NOD2 homozygote Crohn's disease patient selection 61
2.4 NOD2 Genotyping 61
2.5 MicroRNA Array 62
2.6 Quantitative PCR of miRNAs identified by microRNA array 62
2.7 miRNA Target Prediction and DNA array 63
2.8 Quantitative PCR of potential miR-29 targets 63
2.9 siRNA confirmation by Western Blot 64
2.10 miRNA target confirmation by Western Blot 64
2.11 Bacterial Killing Assay 65
2.12 ELISA 66
2.13 Luciferase Reporter Assay 66
2.14 3'UTR Sequence Primers 67
2.15 DC + T cell co-culture 67
2.16 CFSE Labelling and FACS analysis 68
2.17 Maxi-prep and linearisation EGFP-C1 68
2.18 PCR of NOD2 from pUNO-NOD2 70
2.19 PCR of FS1007insC NOD2 from pUNO-NOD2 70
2.20 Ligation of NOD2/ FS1007insC NOD2 and linearised EGFP-C1 71
2.21 Diagnostic digest and sequencing of NOD2 constructs 71
2.22 HEK293 Stable Clones 71
2.22.1 G418 Kill Curve 71

2.22.2 Stable Transfection and single cell sorting 72
2.23 Clone Testing 72
2.23.1 FACS Analysis of GFP expression 73
2.23.2 Western Blot 73
2.23.3 Confocal microscopy 73
2.23.4 IL-8 ELISA 74
2.24 NOD2 IP 74
2.24.1 MAPK 44-42 Phosphoblot 74
2.24.2 IP Conditions 75
2.24.3 Preparation for Mass Spectrometry Analysis 75
2.24.4 Immunoprecipitation Immunoblot 76
2.25 Statistical Analyses 76

3 NOD2 control of microRNA expression in human DCs 77

3.1 Introduction 77
3.1.1 MicroRNA discovery and function 77
3.1.2 MicroRNA genesis 78
3.1.3 MicroRNA Clustering 79
3.2 MicroRNAs and Innate Immunity 80
3.2.1 miR-155 81
3.2.2 miR-146a 83
3.2.3 miR-145 84
3.2.4 miR-9 84
3.2.5 miR-27b 84
3.2.6 miR-147 84

3.2.7 miR-21 85
3.2.8 Let-7 86
3.2.9 miR-125b 87
3.2.10 miR-132 87
3.2.11 Summary 88
3.3 Aims 89
3.4 Results 89
3.5 Genotyping 89
3.6 Initial Stimulation of Dendritic Cells, and Validation of Conditions 91
3.7 microRNA Microarray: NOD2 affects miRNA expression in DCs 93
3.8 qPCR Analysis of miRNA Results 97
3.9 NOD2 induces miR-29a and 29b in human DCs 102
3.10 NOD2 induces miRNA family 29a, 29b, 29c in DCs 104
3.11 miR-29 expression is dependent on RIPK-2 and wild-type NOD2 106
3.12 Discussion 107

4 MicroRNA-29 targets and functional effects in DCs 114

4.1 Introduction 114
4.1.1 MicroRNA Targeting 114
4.1.2 Predicted targeting: Algorithms 114
4.1.3 Detecting miRNA: mRNA targeting 115
4.1.4 Individual miRNA target identification 115
4.1.5 Screening methods for miRNA targets 116
4.2 Methods undertaken to detect miR-29 targets 117
4.3 miR-29 published targets 117

4.3.1 miR-29 and malignancy 118
4.3.2 miR-29 and the extracellular matrix 120
4.3.3 Other miR-29 published targets 121
4.4 Aims 122
4.5 Potential miR-29 Targets 122
4.6 qPCR assessment of potential miR-29 targets in DCs 123
4.7 miR-29 published targets 127
4.7.1 MCL-1 is a miR-29 target in DCs 127
4.7.2 MCL-1 and miR-29 modulate AIEC handling in DCs 129
4.7.3 miR-29 and Wnt signalling 133
4.8 Other miR-29 published targets 136
4.8.1 CDC42 137
4.8.2 TTP, PI3K p85, B7-H3 138
4.9 Predicted miR-29 targets 139
4.9.1 A20/ TNFAIP3 139
4.10 Other miR-29 predicted targets 144
4.10.1 TNFRSF1A 144
4.10.2 TRAF4 146
4.10.3 CX3CL1 147
4.10.4 IL-1RAP 147
4.11 Discussion 148

5 MicroRNA-29 controls IL-23 in human DCs 151

5.1 Introduction 151
5.2 Aims 152

5.3 Results 152

5.3.1 miRNA 29 influences the expression of multiple inflammatory genes in DCs including IL-12p40 152

5.4 Other miR-29 targets 159

5.4.1 DNMT3A 161

5.4.2 TNFSF15 161

5.4.3 IL-19 162

5.5 miR-29 down-regulates IL-12p40 164

5.5.1 miR-29 directly targets IL-12p40 3'UTR 168

5.6 miR-29 down-regulates IL-23 175

5.6.1 miR-29 down-regulates IL-12p40 and IL-23p19 in a dose-responsive manner 179

5.6.2 IL-23p19 is indirectly targeted by miR-29 via ATF2 181

5.7 Crohn's patient DCs expressing NOD2 variants are defective in miR-29 expression and down-regulation of IL-12p40 expression at the end of an immune response 185

5.8 miR-29 decreases IL-17 expression by regulating IL-23 in DC + T cell co-culture 187

5.9 Discussion 189

6 NOD2 Immunoprecipitation 193

6.1 Introduction 193

6.2 Aims 197

6.3 Results 198

6.3.1 PCR of NOD2 from pUNO-NOD2 198

6.3.2 FS1007insC NOD2 PCR 200
6.3.3 EGFP-C1 vector 200
6.3.4 NOD2 and FS1007insC NOD2 cloning into EGFP-C1 203
6.4 HEK293 cell transfection and clonal selection 205
6.5 NOD2-GFP and FS1007insC NOD2-GFP distribution 208
6.6 NOD2-GFP and FS1007insC NOD2-GFP function 209
6.7 Timing of NOD2 stimulation 210
6.8 Immunoprecipitation 214
6.9 IP Optimisation 217
6.10 Mass Spectrometry Analysis 222
6.11 Discussion 223

7 General Discussion 227

7.1 Introduction 227
7.2 IP Project 227
7.3 miRNA Project 227
7.3.1 miRNA expression in human DCs 228
7.3.2 miR-29 targets 231
7.4 Further Work 233

Bibliography 235

Tables

Table 2.1 PCR primers for luciferase assays 66

Table 2.2 3'UTR Sequence Primers 67

Table 3.1 miRNA Array Results 96

Table 4.1 Potential miR-29 Targets 123

Table 5.1 RNA preparation for DNA Array 154

Table 6.1 Sequencing of NOD2 constructs 204

Table 6.2 Mass Spectrometry Results 223

Figures

Figure 1.3 Domain Organisation of ATG16L1 and NOD2 5

Figure 1.4 NOD2 Crosstalk with TLRs 31

Figure 1.5 NLR Signalling 34

Figure 2.1 EGFP-C1 Vector Map 69

Figure 3.1 microRNA Genesis 79

Figure 3.2 miRNA Experiment Protocol 90

Figure 3.3 NOD2 Genotyping 91

Figure 3.4 DC characterisation by FACS 92

Figure 3.5 miRNA Preparation for miRNA Array 93

Figure 3.6 miRNA Array Results 96

Figure 3.7 qPCR Reference Control Assessment 98

Figure 3.8 qPCR Assessment of miR-155 and miR-146a 100

Figure 3.9 qPCR Assessment of Let-7i, Let-7e, miR-572, miR-16 101

Figure 3.10 NOD2 induces miR-29a and 29b in human MDDCs 103

Figure 3.11 NOD2 induces both of the niR-29 clusters in DCs 105

Figure 3.12 miR-29 expression is dependent on RIPK-2 and WT NOD2 107

Figure 4.1 miR-29 antimiR and premiR assessment by qPCR 123

Figure 4.2 qPCR assessment of potential miR-29 targets in DCs 125

Figure 4.3 MCL-1 is a miR-29 target in DCs 129

Figure 4.4 MCL-1 and miR-29 modulate bacterial killing in DCs 131

Figure 4.5 miR-29 and WNT signalling in DCs 136

Figure 4.6 miR-29 targets in DCs by WB: Published Targets 137

Figure 4.7 Analysis of miR-29 potential target A20 in DCs 142

Figure 4.8 miR-29 targets in DCs by WB: Predicted Targets 145

Figure 5.1 DNA Array results 155

Figure 5.2 DNA Array results: Ingenuity analysis 156

Figure 5.3 qPCR assessment of DNA Array results 158

Figure 5.4 WB and ELISA assessment of DNA Array results 160

Figure 5.5 miR-29 down-regulates IL-12p40 166

Figure 5.6 IL-12p40 3'UTR PCR and cloning into luciferase vector 169

Figure 5.7 miR-29 directly targets IL-12p40 3'UTR 173

Figure 5.8 miR-29 preferentially regulates IL-23 176

Figure 5.9 miR-29 does not affect IL-6, TGFβ1, or IL-10 178

Figure 5.10 miR-29 dose-response 180

Figure 5.11 miR-29 controls IL-23p19 indirectly 182

Figure 5.12 miR-29 controls IL-23p19 by down-regulating ATF2 184

Figure 5.13 NOD2 mutant DCs fail to control IL-12/23p40 186

Figure 5.14 miR-29 in DCs mediates IL-17 production from T cells via IL-23 188
Figure 6.1 NOD2 IP Experimental Design 194
Figure 6.2 NOD2 PCR: Optimising PCR conditions 199
Figure 6.3 NOD2 PCR and Diagnostic Digest 200
Figure 6.4 EGFP-C1 Vector Maxi-Prep and Linearisation 202
Figure 6.5 NOD2 cloning into EGFP-C1 Vector 204
Figure 6.6 FACS Analysis of Transfection Efficiency 206
Figure 6.7 NOD2-GFP and FS1007insC NOD2-GFP Clones 208
Figure 6.8 Distribution of NOD2-GFP and FS1007insC NOD2-GFP 209
Figure 6.9 NOD2 Clone Function: IL-8 ELISA 210
Figure 6.10 MAPK 44-42 Western Blot 211
Figure 6.11 Mechanisms of HEK293 MAPK 44-42 activation 213
Figure 6.12 Optimum MDP stimulation times 214
Figure 6.13 Original IP result: Silver Stain 216
Figure 6.14 IP conditions: Protein loss assessment 218
Figure 6.15 Determination of elution method 219
Figure 6.16 Preclear steps and lysate concentration 220
Figure 6.17 Optimised IP as assessed by Silver Stain 222

Abbreviations

A20/ TNFAIP3	Tumour necrosis factor alpha-induced protein 3
AA	Amino acid
AAMP	Angio-associated migratory cell protein
AChE	Acetylcholinesterase
AGO	Argonaute
AICDA	Activation-induced cytidine deaminase
AIEC	Adherent-invasive *Escherichia coli*
AIRE	Autoimmune regulator
Akt1	V-akt murine thymoma viral oncogene homolog 1
ALP	Alkaline phosphatase
AM	AntimiR
AMC	AntimiR control
AOX1	Aldehyde oxidase 1
AP-1	Activator protein 1
APC	Antigen-presenting cell
ARE	AU-rich elements
ASC	Apoptosis-associated speck-like protein containing a CARD
ATF2/ 6	Activating transcription factor 2/ 6
ATG5/ 6/ 7/ 12	Autophagy related 5/ 6/ 7/ 12
ATG16L1	Autophagy related 16-like 1
ATP	Adenosine triphosphate
B7-H3	B7 homolog 3

BACH2	BTB and CNC homology 1, basic leucine zipper transcription factor 2
BAD	BCL2-associated agonist of cell death
BAK	BCL2-antagonist/ killer 1
BAX	BCL2-associated X protein
BC	Buffy coat
BCL-2	B-cell CLL/ lymphoma 2
BDKRB2	Bradykinin receptor B2
BID	BH3 interacting domain death agonist
BIK	BCL2-interacting killer (apoptosis-inducing)
BIM	BCL2-like 11 (apoptosis facilitator)
BH3	BCL-2 homology domain 3
BMDM	Bone marrow-derived macrophage
B-Myb	Myeloblastosis viral oncogene homolog (avian)-like 2
BSA	Bovine serum albumin
C11Orf30	Chromosome 11 open reading frame 30
Ca^{++}	Calcium
CAPN10	Calpain 10
CAPS	Cryopyrin-associated periodic syndromes
CARD	Caspase activation and recruitment domain
CCD	Coiled coil domain
CCL	Chemokine ligand
CCR	Chemokine receptor
CD	Crohn's disease
CD40L	CD40 ligand

CDC42	Cell division cycle 42
CDH1	Cadherin 1, type 1, E-cadherin
cDNA	Complementary deoxyribonucleic acid
CDK4/ 6	Cyclin-dependent kinase 4 and 6
CDKAL1	CDK5 regulatory subunit associated protein 1-like 1
CEACAM6	Carcinoembryonic antigen-related cell adhesion molecule 6
CENTB1	Centaurin beta1
CHOP	c/EBP-homologous protein
Chr	Chromosome
cIAP1/ 2	Cellular inhibitor of apoptosis proteins 1 and 2
CLDN1	Claudin 1
Clec7a	C-type lectin domain family 7 member a
CLL	Chronic lymphocytic leukaemia
CLR	C-type lectin receptors
CNOT8	CCR4-NOT transcription complex subunit 8
CNV	Copy number variation
CPEB4	Cytoplasmic polyadenylation element binding protein 4
cREL	Reticuloendotheliosis viral oncogene homolog
CREM	cAMP responsive element modulator
CXCL	Chemokine (C-X-C motif) ligand
CX3CL1	Chemokine (C-X3-C motif) ligand 1
CX3CR1	Chemokine (C-X3-C motif) receptor 1
2D-DIGE	Two-dimensional differentiation in-gel electrophoresis

D10	DMEM +10% foetal calf serum, glutamine, and penicillin/ streptomycin
DAMP	Damage associated molecular pattern
DAP	Death-associated protein
DAPI	4’,6-diamidino-2-phenylindole
DC	Dendritic cell
DC-SIGN	DC-specific intracellular adhesion molecule-3 grabbing nonintegrin
DENND1B	DENN/MADD domain containing 1B
DGCR8	DiGeorge syndrome critical region gene 8
DKK1	Dikkopf-1
DMEM	Dulbecco's Modified Eagle's Medium
DMTB1	Deleted in malignant brain tumours 1
DNA	Deoxyribonucleic acid
DNMT3A	DNA methyltransferase 3A
DNTP	Deoxyribonucleotide triphosphate
DR3	Death domain receptor 3
DRB*103	Major histocompatibility complex, class II, DR beta 1
DROSHA	Double-stranded RNA-specific endoribonuclease
DSS	Dextran sodium sulphate
DTT	Dithiothreitol
DUOX2	Dual oxidase 2
E2F1	E2F transcription factor 1
ECL	Enhanced chemiluminescence
ECM	Extracellular matrix

ELISA	Enzyme-linked immunosorbent assay
ER	Endoplasmic reticulum
ERAP2	Endoplasmic reticulum aminopeptidase 2
Erk	Extracellular signal-regulated protein kinase
EST	Expressed sequence tag
FACS	Fluorescence associated cell sorting
FADD	Fas-associating death domain-containing protein
FADS1	Fatty acid desaturase 1
FCGR2A	Fc fragment of IgG, low affinity IIa, receptor (CD32)
FCS	Foetal calf serum
FIIND	Function to find domain
FOXP3	Forkhead box P3
FSL1	Synthetic diacylated lipoprotein – TLR2/ TLR6 ligand
FS1007insC	Frame-shift NOD2 polymorphism
Fzd5	Frizzled 5
GALC	Galactosylceramidase
GAPDH	Glyceraldehyde 3-phosphate dehydrogenase
GCKR	Glucokinase (hexokinase 4) regulator
GFP	Green fluorescent protein
GI	Gastrointestinal
GIT	Gastrointestinal tract
Gli	Glioma-associated oncogene family zinc finger 1
GMCSF	Granulocyte-macrophage colony-stimulating factor
GNA12	Guanine nucleotide binding protein (G protein) alpha 12
GO	Gene ontology

GPR65	G-protein coupled receptor 65
GRIM-19	Genes associated with retinoid-IFN-induced mortality 19
GRP78	Glucose-regulated protein 78
GWAS	Genome-wide association study
HBP1	HMG-box transcription factor 1
HBS	Hepes Buffer Saline
HD	Human defensin
HDAC4	Histone deacetylase 4
HEK293	Human embryonic kidney 293 cells
HITS-CLIP	High-throughput sequencing of RNA isolated by crosslinking immunoprecipitation
HKLM	Heat killed *Listeria Monocytogenes* – TLR2 ligand
HLA	Human leucocyte antigen
HMGB1	High mobility group box 1
HNF4A	Hepatocyte nuclear factor 4, alpha
hnRNP A1	Heterogenous nuclear ribonucleoprotein A1
HSP	Heat shock protein
IBD	Inflammatory Bowel Disease
ICAM	Intercellular adhesion molecule
ICOSLG	Inducible T-cell co-stimulator ligand
IDO	Indoleamine 2,3-dioxygenase 1
IEC	Intestinal epithelial cells
IFN	Interferon
IKK	IκB kinase
IL	Interleukin

IL-1F9	Interleukin 1 family member 9
IL-1RAP	Interleukin-1 receptor accessory protein
IL-1RI / 2	Interleukin 1 receptor, type I / 2
IL-1RN	Interleukin 1 receptor antagonist
IL-12B	Interleukin 12B / IL-12p40
IL-18RAP	Interleukin-18 receptor accessory protein
IL-23R	Interleukin-23 receptor
IL2RA	Interleukin 2 receptor alpha
IL-20Rα/ β	Interleukin 20 receptor alpha/ beta
IL-7R	Interleukin 7 receptor
IL8RA / RB	Chemokine (C-X-C motif) receptor 2
IP	Immunoprecipitation
IP IB	Immunoprecipitation Immunoblot
IRAK-1/ 2	IL-1 receptor-associated kinase 1/ 2
IRE1	Inositol-requiring 1
IRF5	Interferon regulatory factor 5
IRGM	Immunity-related GTPase family, M
IS	Immune synapse
ITLN1	Intelectin 1
JAK2	Janus kinase 2
Jnk	c-Jun N-terminal kinase
KCl	Potassium Chloride
KGF	Keratinocyte growth factor
KIF21B	Kinesin family member 21B
LAMB1	Laminin, beta 1

LC3	Light chain 3
LC/MS	Liquid Chromatography/ Mass Spectrometry
LDL	Low-density lipoprotein
LiCl	Lithium chloride
LPS	Lipopolysaccharide
LRR	Leucine-rich repeat
LRRK2	Leucine-rich repeat kinase 2
LSP1	Lymphocyte-specific protein 1
LTA	Lipoteichoic acid
Lys	Lysine
MAL	MyD88 adaptor-like protein
MAPK	Mitogen-activated protein kinase
MAVS	Mitochondrial antiviral signalling
MCL-1	Myeloid cell leukaemia sequence 1
MCS	Multiple cloning site
MDDC	Monocyte-derived dendritic cell
MDS	Myelodysplastic syndrome
MDP	Muramyl dipeptide
MEKK4	Mitogen-activated protein kinase kinase kinase 4
Mg^{++}	Magnesium
$MgCl_2$	Magnesium chloride
MHC	Major histocompatibility complex
MI	Myocardial infarction
MIF	Macrophage migration inhibitory factor
miRISC	MicroRNA-induced silencing complex

miRNA/ miR	Micro ribonucleic acid
MNV	Murine norovirus
MOI	Multiplicity of infection
mRNA	Messenger ribonucleic acid
MS	Mass spectrometry
MST1	Macrophage stimulating 1
MSU	Monosodium urate
mTOR	Mammalian target of rapamycin
MUC1/ 2	Mucin 1/ 2
Myc	Myelocytomatosis viral oncogene homolog
MyD88	Myeloid differentiation primary response gene 88
NADPH	Nicotinamide adenine dinucleotide phosphate
NAV3	Neuron navigator 3
NDM	Nuffield Department of Medicine
NEB	New England Biolabs
NEC	Necrotising enterocolitis
NFκB	Nuclear Factor kappa B
NIK	NFκB-inducing kinase
NIPSNAP3A	Nipsnap homolog 3A
NKX2-3	NK2 homeobox 3
NLR	NOD-like receptor
NLRC4	NLR family CARD domain containing 4
NLRP1/ 3	NLR family pyrin domain containing 1/ 3
NOD	Nucleotide-binding Oligomerisation Domain
NOD2	Nucleotide-binding Oligomerisation Domain containing 2

NOD2-S	Short isoform of NOD2
NOX	NADPH oxidase
NP40	Nonyl phenoxypolyethoxylethanol
OAS2	2'-5'-oligoadenylate synthetase 2
ODN2216	Synthetic oligonucleotide 2216
ORMDL3	Orsomucoid-1-like gene 3
OTUD3	OTU domain containing 3
OVA	Ovalbumin
PAGE	Polyacrylamide gel electrophoresis
Pam_3CSK_4	Synthetic triacylated lipoprotein – TLR1/2 ligand
PAMP	Pathogen-associated molecular pattern
PAR-CLIP	Photoactivatable-ribonucleoside-enhanced crosslinking immunoprecipitation
PBS	Phosphate buffer saline
PBA	Phosphate buffer saline containing bovine serum albumin
PBMC	Peripheral blood mononuclear cell
PCR	Polymerase chain reaction
PDCD4	Programmed cell death 4
PDGF-B	Platelet-derived growth factor B
PERK	Pancreatic ER kinase
PGN	Peptidoglycan
PI3K	Phosphoinositide-3-kinase
PIM3	Pim-3 oncogene
PLA2G2E	Phospholipase A2, group IIE
PM	PremiR

PMC	PremiR control
PMP22	Peripheral myelin protein 22
Pol	RNA polymerase
Poly I:C	Polyinosine-polycytidylic acid
PPARγ1	Peroxisome proliferator-activated receptor γ1
PPIC	Peptidylprolyl isomerase C (cyclophilin C)
PPP5C	Protein phosphatase 5 catalytic subunit
PRDM1	PR domain containing 1, with ZNF domain
PRDX5	Peroxiredoxin 5
PRR	Pattern recognition receptor
PSA	Polysaccharide A
PTGER4	Prostaglandin E receptor 4
PTPN2 / 22	Protein tyrosine phosphatase, non-receptor type 2 / 22
PYD	Pyrin domain
qPCR	Quantitative polymerase chain reaction
Q-TOF	Quadrupole time-of-flight
R10	RPMI +10% foetal calf serum, glutamine, and penicillin/ streptomycin
Rac	Ras-related C3 botulinum toxin substrate
RACK1	Receptor of activated protein kinase C 1
RAG	Recombination activating gene
Rb	Retinoblastoma
REL	V-rel reticuloendotheliosis viral oncogene homolog
Rho	Ras homolog gene family member
RIG-I	Retinoic acid inducible gene I

RIPK-2	Receptor-interacting protein kinase 2
rIL-23	Recombinant interleukin 23
RNAi	Ribonucleic acid interference
ROS	Reactive oxygen species
RPMI	Roswell Park Memorial Hospital media
rRNA	Ribosomal ribonucleic acid
RT	Reverse transcription
RTEL1	Regulator of telomere elongation helicase 1
S	Stimulated
SCID	Severe combined immunodeficiency
SDS-PAGE	Sodium dodecyl sulphate polyacrylamide gel electrophoresis
SEB	*Staphylococcus aureus* enterotoxin B
SEM	Standard error of the mean
sFRP2	Secreted frizzled-related protein 2
SGT1	Suppressor of G2 allele of SKP1
SHIP1	Src homology-2 domain-containing inositol 5-phosphatase 1
SILAC	Stable isotope labelling with amino acids in cell culture
siRNA	Small interfering ribonucleic acid
SMAD	Mothers against decapentaplegic homolog
SNP	Single nucleotide polymorphism
SOCS1	Suppressor of cytokine signalling 1
SP1	Specificity protein 1 (transcription factor SP1)
SP140	Nuclear body protein

SS	Systemic sclerosis
ssRNA	Single-stranded Ribonucleic Acid
SSU RNA	Small subunit ribosomal Ribonucleic Acid
STAT3	Signal transducer and activator of transcription 3
SYT1	Synaptotagmin 1
TAB 1 / 2	TGF-beta activated kinase 1 / 2
TAGAP	T-cell activation RhoGTPase activating protein
TAK1	TGF-beta activated kinase 1
TAP	Transporter associated with antigen processing
TBE	Tris borate EDTA
T-bet	T-box transcription factor
TBST	Tris Buffer Saline Tween
TCF4	Transcription factor 4
TCL1	T-cell lymphoma-1A
TGFβ	Transforming growth factor beta
Th1/ 17	T helper 1/ 17
THADA	Thyroid adenoma associated
THP-1	Human acute monocytic leukaemia cell line
TIR	Toll/ interleukin-1 receptor-like protein
TLR	Toll-like receptor
TNF	Tumour necrosis factor
TNFAIP3	See A20
TNFRSF	Tumour necrosis factor receptor superfamily
TNFSF	Tumour necrosis factor (ligand) superfamily
TNIP2	TNFAIP3 interacting protein 2

TRAF	TNF receptor-associated factor
TRAPS	Tumour necrosis factor receptor-associated periodic syndrome
Treg	Regulatory T cell
TRIB2	Tribbles homolog 2
TRIF	Toll-like receptor adaptor molecule 1
TTP	Tristetraprolin
TYK2	Tyrosine kinase 2
UC	Ulcerative colitis
UPR	Unfolded protein response
US	Unstimulated
UTR	Untranslated Region
UV	Ultraviolet
VAMP3	Vesicle-associated membrane protein 3
VASP	Vasodilator-stimulated phosphoprotein
WB	Western blot
WD	Tryptophan-aspartate
Wnt	Wingless
WT	Wild-type
WTCCC	Wellcome Trust Case Control Consortium
XBP1	X-box binding protein 1
YDJC	YdjC homolog
YY1	Yin Yang 1
ZMIZ1	Zinc finger, MIZ-type containing 1
ZFP36L1	Zinc finger protein 36, C3H type-like 1

ZNF365	Zinc finger protein 365

Acknowledgements

Dr Alison Simmons supervised this work and I would like to thank her for all her support, guidance and patience. I would also like to thank Professor Derek Jewell for his encouragement and advice.

Funding for this study was supplied by Core / NACC (in association with The Barbour Trust in Memory of Simon Ash), for which I am hugely grateful.

I wish to acknowledge the members of the Human Immunology Unit who provided much support and assistance, in particular John Baker, Rachel Cooney, Tica Pichulik, Philip Allen, Alasdair Leslie, Peter Simpson, and Elham Khatamzas, and subsequently the members of the Translational Gastroenterology Unit, including all the members of Professor Powrie's Group. I would particularly like to thank Ben Owens for his assistance with the DC flow cytometry.

My thanks to Oxford Gene Technology who assisted me with the array work, and to Benedikt Kessler and his laboratory for their help and advice with the NOD2 IP.

Lastly, to my wife Laura – thank you for your love, support and understanding, without which none of this would have been possible.

For Alexander and Hugo.

1 Introduction

1.1 The Gastrointestinal tract in health and disease

The gastrointestinal tract (GIT) is an organ with multiple functions, and is in a complex symbiosis with the microbial flora that resides within. The ability of the gut to correctly carry out these functions – which include digestion, nutrient absorption, excretion of waste, maintenance of an effective barrier and a healthy immune system – is intimately linked to this microbial interaction[1]. The quantity of this flora is staggering – at its most dense the bacteria number 10^{12}/ml, making this one of the most populated bacterial niches described, and meaning that bacteria outnumber our own cells approximately 10-fold[2]. In contrast, the diversity of this flora at the level of phyla is relatively restricted, with two – Bacteroides and Firmicutes – dominating the field[3]. Immunology has been described as the 'science of self non-self discrimination'[4], and understanding how this vast bacterial load is not only tolerated but also required for health is critical for understanding the pathogenesis of diseases such as Crohn's disease (CD) and ulcerative colitis (UC).

Crohn's disease, one of the two main forms of IBD, is a chronic illness with periods of relapse and remission. Clinically it manifests with a combination of abdominal pain, weight loss and diarrhoea, although other extra-intestinal features, such as arthralgia, erythema nodosum, and iritis, can also occur. Histologically it is characterised by the inflammation being both discontinuous ('skip lesions'), and transmural (that is extending through the muscularis mucosa to the lamina propria or 'full thickness'). Although CD can affect any

part of the gut from mouth to anus, it most commonly affects the terminal ileum and colon. Current medical therapies include corticosteroids, antibiotics, monoclonal antibodies and immunomodulators, but there is a significant therapeutic gap as evidenced by the relapse of patients on therapy, and by the need for up to 70% of CD patients to undergo surgery within 3 years of diagnosis[5]. CD has a prevalence of 44-198 cases per 100,000 within a Caucasian population, although this increases 5.4-7.7 fold in Ashkenazim populations[6].

When considering the pathogenesis of CD there are currently three main branches of interest: defective immunity; disrupted mucosal barrier function; and the role of gut flora.

1.2 Defective immunity

1.2.1 Genetics

Much of our understanding of the importance of the immune system in Crohn's pathogenesis, and in particular the specific branches involved, stems from genetic studies. The clinical evidence for a genetic basis to this disease is wide-ranging and includes: the observations of familial clustering by Crohn himself[7], the monozygotic twin concordance rate of nearly 50%[8], and the high percentage of patients with a positive family history[9]. The discovery of mutations in the caspase recruitment domain family member 15 (CARD15), or nucleotide-binding oligomerisation domain containing 2 (NOD2), gene in the IBD1 locus on Chr 16[10] both highlighted the role of innate immunity in CD pathogenesis, and heralded the start of a decade of gene discoveries. A recent meta-analysis of the genome-wide association studies (GWAS) studies

that have followed has now identified 71 Crohn's susceptibility genes[11], although the relative risk from many of these newly identified polymorphisms is small. Some of these polymorphisms are specific to Crohn's disease risk, and others also have associations with Ulcerative Colitis.

The GWAS have revealed the importance of both autophagy (with two of the strongest associations in ATG16L1 and IRGM[13]) and the IL-23/Th17 (T helper 17) pathway (including IL-23R, IL-12B (IL-12p40), STAT3, JAK2 and TYK2)[11] in CD predisposition. Along with NOD2 polymorphisms (which individually contribute the greatest risk of CD in Caucasian populations), these two pathways have been amongst the most fertile areas of research into CD pathogenesis.

1.2.2 Autophagy

Autophagy is a process in which cytoplasmic components are sequestered into double membrane vacuoles, the contents of which are then degraded by fusion with lysosomes. This process is ubiquitous in eukaryotic cells, and allows for the removal of defective proteins and organelles to prevent cell damage. Autophagy can also be induced by starvation in order that nutrients are recycled, and by immune stimuli such as intracellular infection. Autophagy impinges on several aspects of immune defense[14]. These include direct capture of intracellular microbes during phagocytosis as a downstream response to pattern recognition receptor triggering, enhancement of MHC II antigen presentation, and involvement in acquired immunity as an effector of Th1/ Th2 cytokines[15]. Autophagy has also shown to be involved in thymic selection, lymphocyte development and survival[16].

1.2.3 ATG16L1

ATG16L1 encodes a key autophagy protein, which functions as part of a complex with autophagy proteins ATG5 and ATG12, and is responsible for the proper subcellular localization of the autophagy machinery[17,18]. The ATG16L1 polymorphism results in a change from A to G allele at position 300, with GG being the disease-associated genotype. In the presence of the CD-risk allele the non-conserved carboxy-terminal domain, which contains tryptophan-aspartate (WD) repeats, is subject to a threonine-to-alanine substitution (T300A) (**Fig. 1.3a**). This finding has been replicated in a number of studies across Europe and the US[19-24]. Despite this convincing evidence it should be borne in mind not only that the GG allele occurs in 51.3% of controls versus 58.1% of CD patients[23], but also that the affected domain of ATG16L1 is non-conserved, and is not required for all of its functions[25].

Figure 1.3 Domain organisation of ATG16L1 and NOD2

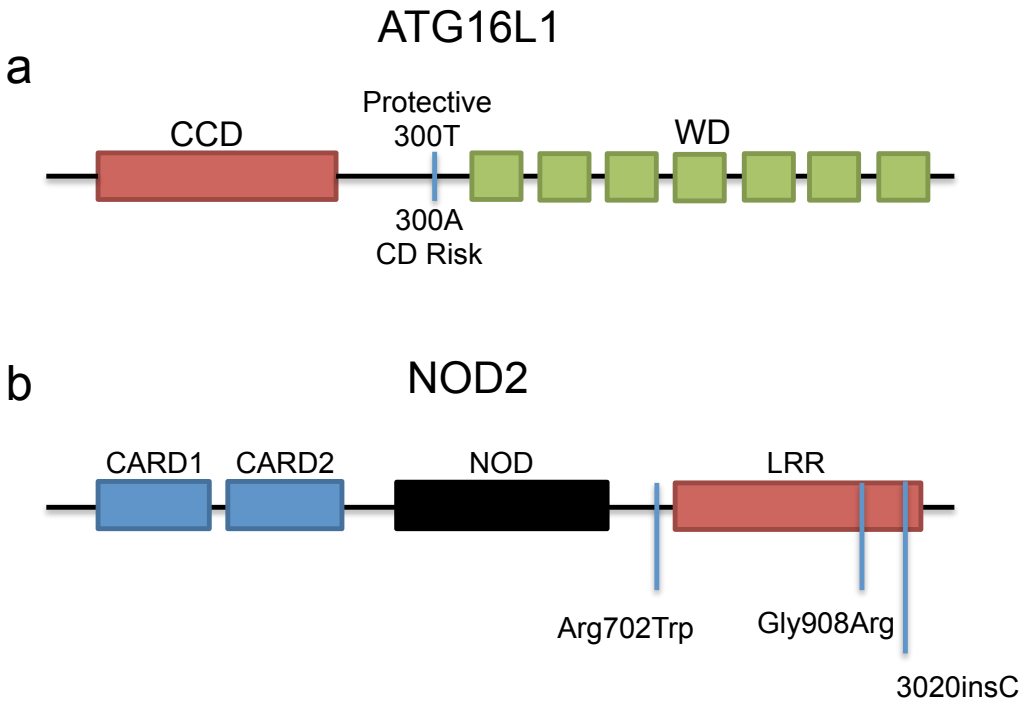


Figure 1.3 Domain organisation of **(a)** ATG16L1 and **(b)** NOD2 proteins. The approximate positions of the Crohn's associated risk alleles are shown. CCD = Coiled coil domain, WD = Tryptophan-aspartate repeat domain, CARD = Caspase activation and recruitment domain , NOD = Nucleotide-binding oligomerisation domain , LRR = Leucine rich repeat domain

Murine models in which ATG16L1 is deleted die in the first day of life, possibly as they fail to tolerate post-natal starvation[26]. (ATG5 and ATG7 knock-out mice behave in a similar fashion). One of the roles of ATG16L1 is to recruit the ATG5-ATG12 complex to the autophagy isolation membrane. However, although ATG16L1-deficient cells have an overall impairment of autophagy due to ineffective complex recruitment, the ATG16L1 domain which contains the CD-associated variant (henceforth ATG16L1 T300A) is not required for this function[25], which begs the question – What is the role of this affected domain?

One answer is that ATG16L1 T300A produces a defect in the handling of intracellular bacteria. In a knock-down/ reconstitution system in human

epithelial cell lines, followed by *S. enterica ser*. Typhimurium infection, ATG16L1 T300A is less effective at capturing bacteria within autophagosomes, although basal levels of autophagy are unaffected[25]. Autophagy and ATG16L1 (and IRGM) also play a role in the control of adherent-invasive *Escherichia coli* (AIEC)[27], a bacteria known to colonise ileal CD lesions, and this is in contrast to other strains of *E. coli* that are unaffected. Other aspects of the CD-associated ATG16L1 polymorphism, such as the impact on Paneth cells and the relationship to NOD2, are considered below.

1.2.4 IRGM

The IRGM gene, located on chromosome 5q33.1, encodes a protein belonging to the immunity-related GTPases (IRG), one of the strongest intracellular pathogen-resistance systems in mice. Interestingly although the IRG family in mice contains 21 copies, this has been reduced to only 2 copies in humans, IRGC and IRGM[28]. Highly significant associations between IRGM variants and CD were detected in the Wellcome Trust Case Control Consortium (WTCCC) GWAS and subsequent replication panel[19 29]. Although single nucleotide polymorphisms (SNP) variants in this locus are associated with CD in different populations[30-34], it remains unclear how these contribute to CD pathogenesis.

As for ATG16L1, a functional role for IRGM in bacterial handling had previously been shown, with a study demonstrating the requirement for IRGM in IFNγ-induced autophagy, and in the control of *Mycobacterium tuberculosis* in human macrophages[35]. LRG-47/ IRGM involvement in murine resistance to

mycobacteria has also been shown[36], as has its role in mice in protection from other pathogens including *L. monocytogenes* and *S. enterica ser*. Typhimurium[37 38], and AIEC already mentioned above[27].

How this may be linked to the IRGM GWAS SNPs was potentially answered when they were found to be in perfect linkage disequilibrium with a 20kb deletion polymorphism upstream of the IRGM transcriptional start site[39]. This alters the expression levels of IRGM in a cell line-dependent manner. Manipulation of the level of IRGM, either by siRNA knockdown or overexpression of IRGM in HeLa cells, affects the efficiency of anti-bacterial autophagy against *S. enterica ser*. Typhimurium[39]. This raises the hypothesis that there is a threshold level of IRGM expression that can induce autophagy, a level that is not reached in the presence of CD polymorphisms. Further evidence for this comes from other variants of the locus, independently associated with CD, that affect the IRGM promoter region (as well as the 5' untranslated region)[40]. This study also reported lower IRGM expression in lymphocytes from CD patients. Another SNP (rs9637876) that increases IRGM expression has been shown to contribute to protection from *M. tuberculosis* [41].

More recently an IRGM CD-associated polymorphism that alters a microRNA binding site (miR-196) has also been described[42]. miR-196 expression is increased in the GI epithelium during inflammation, thus contributing to the control of IRGM epithelial expression. In this context the CD-associated polymorphism would lead to inappropriately *high* IRGM levels, and although their experiments demonstrate that IRGM over-expression increases AIEC association with LC3-II (Light chain 3; a marker of autophagosome formation),

they also show reduced autophagosome acidification[42], presumably resulting in defective bacterial killing.

Another study has begun to elucidate not only the mechanism by which IRGM controls autophagy and protection against invading microbes, but has also revealed that IRGM can induce apoptosis[43]. These functions are coordinated, in part, through IRGM's affinity for the mitochondrial lipid cardiolipin, and subsequent initiation of either mitochondrial fission or membrane depolarisation. Of the four different splice isoforms expressed in human cells (denoted IRGMa/b/c/d), overexpression of IRGMa/c/d, but not IRGMb, led to mitochondrial depolarisation and cell death (in cooperation with other mitochondrial fission factors). Interestingly, IRGM-mediated cell death led to the release of HMGB1, which acts as a pro-inflammatory DAMP (damage associated molecular pattern). This is in contrast to the induction of mitochondrial fission and autophagy when IRGM is expressed at more moderate levels. This study agrees and adds to previous observations that both the level, and now isoform, of IRGM expressed affects its functions. It will be interesting to see if any of the CD-associated IRGM polymorphisms influence the expression of one or more of these isoforms preferentially.

1.2.5 IL-23/ Th17 pathway

Early experimental models of colitis in which IL-12p40 was neutralised suggested that IL-12 and an aberrant Th1 response were crucial to IBD pathogenesis[44]. However, in 2000 a new IL-12 family cytokine subunit, p19, was discovered to pair with IL-12p40 and form IL-23[45]. It is now clear that in several major animal models of colitis, IL-23 is in fact the major driver of

intestinal inflammation[46-50]. The GWAS studies identified SNPs in the IL-23 receptor that can either protect from, or increase the susceptibility to, Crohn's[51]. Although the mechanisms by which this is mediated are not fully understood, some of these SNPs are likely to encode for loss- or gain-of-function receptor changes, whilst others cause alternative mRNA splicing leading to the expression of a soluble decoy receptor[52].

IL-23 not only promotes expansion and maintenance of Th17 cells[53-55], which produce IL-17, IL-21 and IL-22[56], but also inhibits the accumulation of intestinal $Foxp3^+$ regulatory T (Treg) cells[57]. A recent study of human intestinal IL-23p19 expression in IBD patients has revealed an increase in CD, but not ulcerative colitis (UC) or normal controls, and this promotes Th17 differentiation[58]. Th17 cells and signature cytokines are also elevated in both the intestinal mucosa and serum of patients with CD[59,60].

1.2.6 Unfolded Protein Response

Another cellular mechanism, and its relationship to immune function, which is coming under increasing scrutiny is the unfolded protein response (UPR). Immune cells such as DCs and macrophages[61,62], and also gut epithelial cells[63], are particularly reliant on an intact UPR in order to deal with the endoplasmic reticulum (ER) stress that occurs with the accumulation of misfolded proteins. The UPR is governed by glucose-regulated protein 78 (GRP78), which in the resting state chaperones three proteins (pancreatic ER kinase (PERK), inositol-requiring 1 (IRE1) and activating transcription factor 6 (ATF6)) that can initiate the UPR. These proteins are released by the binding of unfolded proteins to GRP78. There are a number of genetic polymorphisms

in genes relating to the UPR that increase the risk of CD. These include orsomucoid-1-like gene 3 (ORMDL3)[64], and X-box binding protein 1 (XBP1)[63]. ORMDL3 is a membrane-spanning ER protein that regulates the uptake of Ca^{++} from the cytosol to the ER, and siRNA-mediated knockdown results in attenuated UPR activation[65].

XBP1 is IRE1-regulated, and the CD-associated variants are unable to initiate a normal transcriptional response in the face of ER stress. The importance of this response in maintaining the intestinal epithelium is hinted at by the fact that (in mice) only this epithelium expresses an additional isoform of IRE1 (IRE1β) as well as the ubiquitously expressed IRE1α[66]. Moreover, murine models in which there is partial loss of XBP1 in the intestinal epithelium demonstrate spontaneous enteritis due to two apparent defects[63]. Firstly there is increased responsiveness to microbial and inflammatory milieu, as shown through the use of TLR ligands and TNFα. Secondly, there is demonstrable Paneth cell dysfunction with reduced cryptidin expression and, like NOD2-deficient mice, an increased susceptibility to *L. monocytogenes* oral challenge.

1.3 GI Barrier Function

1.3.1 The GIT forms a large environmental interface

The GIT has an enormous surface area (approximately $300m^2$ [67]) primarily in order to facilitate nutrient absorption, but this inevitably provides opportunity for pathogen invasion. Unlike the mucosa of healthy controls, which are relatively sterile, many patients with CD have mucosa with adherent and invading bacteria[68,69]. In order to prevent this, normal mucosa is organised to

provide both mechanical and anti-microbial barriers to bacteria, viruses, and parasites.

1.3.2 Mucus Layer

Firstly a thick layer of mucus provides a physical barrier to prevent microbes coming into direct contact with the epithelium. Secreted by goblet cells, gel-forming mucins such as MUC2 (Mucin 2) provide the structure for the mucus layer. Changes in goblet cell number and MUC2 expression are more typical of ulcerative colitis (UC) than Crohn's, and MUC2 mutant mice spontaneously develop a distal colitis similar to UC[70]. Although mutations affecting the genes involved in the epithelial barrier predominantly predispose to UC not Crohn's[71], the related MUC1 is a recently described CD-susceptibility gene[11], and Muc1 knockdown mice exhibit increased small bowel damage after *C. jejuni* infection[72].

1.3.3 Epithelial Organisation

Secondly, there is a fast epithelial cell turnover, with most cells being replaced every 3-4 days in murine studies[73]. Thirdly, epithelial cells are linked by tight junctions, the importance of which becomes apparent when the mode of entry of many pathogens is examined. For example rotaviruses (that typically cause a self-limiting diarrhoeal illness in children) change the levels of occludin phosphorylation and thus its localization to tight junctions[74], and enteric bacterial pathogens can alter tight junction integrity in a number of ways, including the use of proteases to key junctional proteins[75]. Tight junctions are disrupted in active CD[76], and although it is not yet known whether this is the

cause or effect of inflammation, in some murine models abnormal tight junctions definitely precede inflammation[77]. It is likely that in a subset of patients this is also the case.

1.3.4 Anti-microbial Peptides

Lastly, secreted into the mucus are anti-microbial peptides both from epithelial cells, and from specialised cells of the intestinal crypts called Paneth cells. These peptides predominantly function by making micropores in the phospholipid bilayer of microbial membranes[78]. Defensins are a key part of this armoury, and these are both constitutively expressed in the gut to regulate commensal organisms, and inducible in the face of infection. The most abundantly expressed in the human small intestine are the α-defensins HD-5 and HD-6, whereas the β-defensins are predominantly expressed in the colon. There is evidence that defensin levels contribute to ileal Crohn's disease, and perhaps also to colonic Crohn's. For example, an association with copy number variations (CNV) in β-defensin genes and colonic Crohn's has been described, but both low[79] and high[80] CNV have been observed, and the conflicting nature of these two studies has not yet been resolved.

Ileal Crohn's is generally associated with reduced small bowel alpha defensin levels[81], and NOD2 appears to have a crucial role in this regard (see below), but other CD-polymorphisms and signalling pathways are involved. For example, a defect in the Wnt signalling pathway, specifically in the transcription factor TCF4, may account for some of the defensin reduction in both adult[82] and paediatric[83] populations.

Some of the reported functions of two other CD-susceptibility genes, ATG16L1 and XBP1, also converge on the Paneth cell. ATG16L1 encodes a key autophagy protein, which functions as part of a complex with autophagy proteins ATG5 and ATG12, and is responsible for the proper subcellular localization of the autophagy machinery[17,18]. Mice with hypomorphic ATG16L1 protein expression demonstrate defective Paneth cell function[84]. These mice have decreased lysozyme secretion, as well as decreased and disorganised secretory granules due to an apparent defect in the granule exocytosis pathway, but no defect in handling *L. monocytogenes*. Histological comparison using ileocolic resection specimens from CD patients shows the same morphological abnormalities in Paneth cells, but only in specimens from ATG16L1 T300A patients. Furthermore, microarray profiling of murine autophagy-deficient Paneth cells demonstrates an up-regulation of genes associated with an inflammatory response, including leptin and adiponectin.

It was subsequently found, when these mice were rederived into an enhanced barrier facility (as opposed to a conventional barrier), that these Paneth cell abnormalities disappeared and only returned with the (re)-introduction of a persistent murine norovirus (MNV)[85]. In the presence of this virus, these mice also display an exaggerated inflammatory response to dextran sodium sulfate (DSS), with many of the histopathological features of CD, and an associated ileal injury. These changes are dependent on TNFα and IFNγ, and are prevented by broad-spectrum antibiotics, linking a triumvirate of genetic polymorphism, commensal bacteria and, the newcomer, viral infection to disease pathogenesis for the first time.

1.4 Gastrointestinal Flora

1.4.1 The microbial flora is intimately linked with GIT inflammation

The importance of the gut flora in driving, if not definitively initiating, inflammation is based on a number of pieces of evidence. Clinically, faecal stream diversion improves Crohn's colitis[86] and ileitis[87], and antibiotic treatment ameliorates inflammation[88]. In vitro, the lamina propria T cells from CD patients are reactive to gut flora[89]. Further, murine models of colitis are nearly all dependent, to a greater or lesser degree, on the presence of gut microbes (an exception being the anti-CD40 model[47]). A T-bet and RAG2 double deficient model even demonstrates that colitis can not only be spontaneous but also transmissible to other animals[90], albeit to those lacking an adaptive immune system (RAG2 single knockouts), revealing the potential importance of an altered 'colitogenic' microflora in IBD pathogenesis. A transferable colitogenic flora was also seen in experiments using both ASC-deficient mice, and mice with a deficiency of the inflammasome activator NLRP6. Transferring their flora to wild-type mice rendered the recipients more susceptible to DSS colitis[91]. (As already discussed, the hegemony of bacteria in disease pathogenesis has recently been challenged by a murine model of colitis in ATG16L1-deficient mice, that also requires a murine norovirus to develop disease[85]. However, this finding has yet to be replicated in other mouse models or similar findings proven in humans.)

Although bacteria can be pathogenic, it is also clear that commensal bacteria shape intestinal immune system development and protect against inflammation in mouse models[92-94]. With that in mind, and as bacterial detection techniques have improved, many studies have focused on specific

components of the gut flora that may be either protective or pathogenic, and whether CD is associated with either general or localised alterations in intestinal microbiota (dysbiosis).

1.4.2 Anti-inflammatory commensals

For example, a member of clostridia species, *Faecalibacterium prausnitzii* is known to increase IL-10 and reduce IL-12 production in vitro from monocytes[95], and in murine models of colitis inflammation can be ameliorated by administration of either live *F. prausnitzii*, or the bacterial supernatant, partly through metabolite inhibition of NFκB activation[96]. Other studies have revealed that related clostridia species in murine models have anti-inflammatory effects through induction of colonic regulatory T cells[97]. Furthermore, after surgery there is an increased Crohn's recurrence rate if there are low levels of *F. prausnitzii* on the resected specimen mucosa[96]. However, thus far no clinical trial has shown efficacy of altering human gastrointestinal *F. prausnitzii* levels, and a CD clinical trial that attempted to manipulate the levels of *F. prausnitzii* with fructo-oligosaccharides was disappointing[98].

This line of inquiry concerning anti-inflammatory bacteria is being taken a step further, as the specific microbial components responsible are sought. For example, a murine study has demonstrated that the single microbial molecule polysaccharide A (PSA) can have beneficial effects in preventing gastrointestinal inflammation[99]. They found that this was the molecule conferring anti-inflammatory properties to the bacterium *B. fragilis*, in a model of gut inflammation using the bacterium *H. hepaticus*.

1.4.3 Disease-associated bacteria

Conversely there has been much interest in the pathogenic potential of certain microbes in the aetiology of CD, for example adherent-invasive *Escherichia coli* (AIEC). Several studies have reported the presence of AIEC in CD ileal mucosa[69,100,101], and this is in part related to increased CEACAM6 (carcinoembryonic antigen-related cell adhesion molecule 6) expression in the mucosa that facilitates AIEC binding via type 1 pili[102,103].

Invasive bacteria often target the follicle-associated epithelium that line Peyer's patches – this being the site of specialised M cells that are optimised for delivery of antigen and microbes to the mucosa associated lymphoid tissue beneath[104]. Interestingly the initial site of inflammation in ileal CD is often these lymphoid follicles[105]. A recent study has demonstrated that AIEC also utilise long polar fimbriae to adhere to M cells[106], in a manner that is reminiscent of *Salmonella* Typhimurium. After adhesion, AIEC are able to invade the epithelium, and survive and replicate in macrophage vacuoles, and this leads to increased production of TNFα[107].

1.4.4 Defining the normal gut microflora

Considering the gut flora on a more global scale, several studies have begun the task of defining what is 'normal', i.e. in healthy individuals, and what may be abnormal in those with CD and UC. This process is made more difficult for three main reasons – the first is that the results obtained depend on what is sampled, be that faecal or mucosa-associated bacteria[108], or be that from inflamed or non-inflamed mucosa in the context of IBD. Secondly, the results

can vary not only between individuals, but also within individuals depending on which part of the GI tract is tested[109-112]. Thirdly, the results depend on the technology used to identify the bacterial flora (most of which are not culturable), or to identify the bacterial functions. These techniques include: those based on small subunit ribosomal RNA (SSU rRNA) gene cloning to high throughput sequencing; metagenomics; and metatranscriptomics, metaproteomics and metabonomics. We are therefore some way from being able to define what 'normal' is, and therefore even further from clearly understanding how dysbiosis definitively effects, or is affected by, IBD.

Initial studies using bacterial 16S ribosomal RNA (rRNA) gene cloning and sequencing technology revealed that two phyla, the Bacteroidetes and Firmicutes, dominate the microbiota, encompassing up to 90% of species[113]. Subsequently this was shown to be a slight over-estimation, as two other phyla, Proteobacteria and Actinobacteria, also supply up to 20% and 5% respectively of the mucosa-associated resident species[112]. In contrast the diversity at the level of microbial species is estimated to be up to 1000 within a given individual, and approximately 5000 species in total across all human GI tracts[114].

This diversity appears to be at least in part host mediated. It is relatively stable within individuals over time as has been shown from faecal samples[115], and over the course of the colon demonstrated by mucosa-associated samples[116]. Furthermore, studies examining the impact of the human genotype on the microbiota, using relatives and monozygotic twins, have confirmed a significant influence of the host genome[117]. However that is not to say that environmental and disease factors are unable to alter the microbiota,

albeit some, for example antibiotics, in the short term. Dietary factors contribute to the composition[118], as does aging which changes the gut floral composition in mice[119] and man[120].

1.4.5 Dysbiosis in Crohn's disease

People with CD have more unstable microbial communities[121], and disease severity corresponds with the degree of difference from a healthy group[114]. Those with active inflammation also demonstrate a reduced epithelial microbial diversity compared with non-IBD controls[122], with a loss of anaerobic bacteria such as *Bacteroides*. A larger study examining mucosa-associated bacteria from surgical resection specimens[112] also demonstrated microflora changes, although these were most marked in a subset of patients, (which correlated with younger patients and an abscess formation phenotype). CD colon specimens had fewer Bacteroidetes and the *Lachnospiraceae* subgroup of Firmicutes, and correspondingly more of Proteobacteria and the *Bacillus* subgroup of Firmicutes, and in CD ileal specimens Proteobacteria were more abundant and *Bacillus* less abundant, although it should be noted that these colonic and ileal changes were also seen in the UC samples. This implies that they are either secondary to (end stage) gut inflammation or to treatments common to both conditions; or less likely that those CD and UC patients sampled shared disease susceptibility genes common to both diseases, and that these independently influenced the microbiota.

Although most studies thus far have demonstrated that IBD, and specifically CD, is associated with a general dysbiosis, interestingly they have provided limited evidence for a specifically enriched pathogen or aetiological agent. In

general, whether the microflora changes are causative, or occur as a result of inflammation, is not yet known, although clearly these two possibilities are not mutually exclusive. One way to answer that question lies in analysing how the major CD-risk alleles, such as NOD2, impact on the microbiota both in the presence and absence of inflammation. This is discussed in more detail below.

1.5 NOD2

1.5.1 NOD2 Introduction

NOD2 is a cytosolic innate immune receptor. Mutations in this gene predispose to CD, but why this occurs is still uncertain. Interestingly NOD2 mutations have been shown to affect all three of the major potential pathogenic mechanisms described above, often in multiple ways. For example, defects in innate immune signalling and autophagy induction; reduced defensin production; and changes to gut microflora composition.

1.5.2 NOD2 discovery and structure

Although there was epidemiological evidence that CD was at least in part genetically determined, it wasn't confirmed until 1996 and the discovery of the IBD1 susceptibility locus on chromosome 16[123]. It took another 5 years to determine that the responsible gene within this region was NOD2, when two papers were published simultaneously[10,124]. The NOD2 polymorphisms that predispose to CD occur in (or adjacent to in the case of R702W) the leucine-rich repeat (LRR) domain. Three single nucleotide polymorphisms (one frame-shift: FS1007insC, and two missense: G908R and R702W), account for over

80% of those identified within patients[125] (**Fig. 1.3b**). The frame-shift mutation results in an early stop codon and a truncated protein. Homozygosity, or compound heterozygosity, confer a 17-fold increased risk of developing CD, whilst around 40% of European CD patients carry at least one mutation[126], versus 14% of healthy controls.

NOD2 mutations result specifically in a predisposition to terminal ileal CD[126], early onset disease[125,127], and possibly a stricturing phenotype requiring surgery[128].

NOD2 encodes for an intracellular pattern-recognition receptor (PRR), one of a number of NOD-like receptors (NLRs) that also include the NLR proteins that trigger the inflammasome[129]. NOD2 has two N-terminal caspase-recruitment domains (CARDs), a central nucleotide-binding oligomerisation domain (NOD), and a C-terminal leucine-rich repeat (LRR) domain.

NOD2 responds to muramyl dipeptide (MDP)[130,131] a component of peptidoglycan (PGN) present in gram-positive and gram-negative bacterial cell walls. (NOD2 may also respond to viral ssRNA, and be involved in anti-viral responses[132], although this finding has yet to be replicated.) The mechanism by which NOD2 responds to MDP – a tiny moiety – is not yet understood, and may involve other proteins.

The crystal structure of NOD2 has not yet been elucidated, although inference has come from other NLRs (for example NOD1[133]) and from mutational analyses. An example of the latter[134] demonstrated that certain amino acid residues in the LRR domain, either in the predicted α-helix or the β-strand, are crucial for MDP recognition. On ligand recognition, NOD2 likely undergoes a conformational change, allowing the central NOD domain to facilitate self-

oligomerisation[135,136]. The LRR domain represses this change, until MDP recognition. Residues in the CARD region and NOD region are also essential for MDP response, the CARD region residues being necessary for association with, and activation of, the adaptor protein receptor-interacting serine/threonine kinase 2 (RIPK-2)[137].

1.5.3 NOD2 expression in Dendritic cells

NOD2 is expressed in myelomonocytic cells such as dendritic cells and in intestinal cells including Paneth cells and epithelial cells[137-140], and its expression can be up-regulated by pro-inflammatory stimuli[138]. Dendritic cells (DCs) are the archetypal antigen-presenting cells, and perform a crucial role in determining the nature of any acquired immune response[141]. Immature DCs express a broad range of PRRs, including NOD2 and other NLRs, toll-like receptors (TLRs), c-type lectin receptors (CLRs), complement and Fc receptors[142]. On infection these PRRs are one of the first aspects of the immune system to be triggered, and their combined signals derived from ligation direct the maturation profile of DCs, and the nature of the subsequent immune response[143]. PRRs are triggered via bacterial components expressed by both pathogens and commensals[144], and the mechanism by which they are distinguished has not yet been elucidated.

DCs are very active phagocytes, constantly sampling their microenvironment both in receptor-mediated and indiscriminate fashion[145]. Expression of certain chemokine receptors (CCR1, CCR2, and CCR5) ensures that they are attracted to areas of infection[146]. DC maturation is accompanied by down-regulation of receptors for microbial constituents and inflammatory

chemokines, and up-regulation of MHC II and MHC I expression, and of CCR7 which guides the DC to secondary lymphoid tissues for engagement with T cells[146]. Monocyte-derived DCs (MDDCs) are a subset of dendritic cells that accumulate at the site of infection, including the intestinal epithelium, to promote both innate and adaptive immune responses[147,148], and in mice E-cadherin^{+} MDDCs are a driver of T cell-mediated colitis[149].

How MDP reaches the cytosolic NOD2 in DCs is not definitively known, and the mechanism may depend on both the type of cell and bacteria. Potential mechanisms in DCs include: intracellular release during phagocytosis of whole bacteria[150]; injection of bacterial components into the cytoplasm by secretion systems or pore-forming toxins; or via clathrin-dependent endocytosis[151,152]. In intestinal epithelial cells the active transport of extracellular MDP by the peptide transporter hPepT1[153] may be the most important mechanism; alternatively invasive bacteria can induce their own phagocytosis in non-phagocytic cells, and some escape from a vacuolar compartment into the cytoplasm in order to replicate[154] and in so doing enable MDP release[155].

NOD2 is in part membrane-associated (at least in cell lines), and this may assist in signalling. This may mean that NOD2 is triggered by MDP at the point of bacterial entry and/ or phagocytosis, leading to NFκB activation[156] or autophagy induction through recruitment of ATG16L1[157]. This membrane targeting of NOD2 is dependent on six C-terminal amino acids (aa), and with FS1007insC NOD2 lacking 33 C-terminal aa, it localises instead to an alternative intracellular vesicle compartment, possibly the endoplasmic

reticulum[156]. Further, NOD2 promotes the membrane recruitment of RIPK-2, and optimal RIPK-2 activity depends on its subcellular location[158].

1.6 NOD2 and Immunity

1.6.1 NOD2 signalling

After NOD2 oligomerisation, and recruitment of RIPK-2 via a CARD-CARD interaction, the classical pathway of NFκB activation via NOD2 is set in train. The presence of RIPK-2[159], and its kinase activity[160], are critical to this process. RIPK-2 becomes ubiquitinated (with negative control by A20), with subsequent binding and ubiquitination of IKKγ, the regulatory subunit of the IKK complex[161]. Recruitment of IKKγ leads to IκBα phosphorylation and release of NFκB to the nucleus and induction of transcription[137] (**Fig. 1.4**). Although initially RIPK-2 was thought to be downstream of TLR signalling as well as NOD1 and NOD2[159], this was subsequently found not to be the case[162], and this may well reflect contamination of previously available commercial PRR ligands.

1.6.2 NOD2-signalling regulators: A20

Potential regulators of this pathway have been detected, including A20[163] (also known as TNFAIP3) that was identified as a candidate gene for CD in the Wellcome Trust GWAS. A20 is an ubiquitin-modifying protein with roles in restricting TNF-receptor and TLR-induced signals[164]. Polyubiquitin chains can be built onto target proteins via links with the seven lysine residues on ubiquitin[165]. The resultant conformation of the chain can target proteins for degradation, or for localization to subcellular compartment, and thus helps

regulate a variety of cellular processes[165]. In the case of NOD2 signalling, the E3 ubiquitin ligases cIAP1 and cIAP2 (cellular inhibitor of apoptosis proteins 1 and 2) are responsible for RIPK-2 ubiquitination and activation[166,167]. Conversely, A20 inhibits NF-kB activation in response to MDP stimulation of NOD2 via RIPK-2 de-ubiquitination. A20 deficient mice demonstrate prolonged NFκB signalling and increased pro-inflammatory cytokine production in response to MDP.

1.6.3 NOD2-signalling regulators: directly interacting proteins

Other proteins potentially involved in the NOD2-NFκB signalling pathway, and that physically interact with NOD2, include a mitogen-activated protein kinase kinase TAK1 (transforming growth factor (TGF)-beta-activated kinase 1)[168], Erbin[169], CD147[170], CARD8 (caspase activating and recruitment domain 8)[171], CENTB1 (centaurin beta1)[172], AAMP (angio-associated migratory cell protein)[173], and GRIM-19 (gene associated with retinoic and IFN-induced mortality 19 protein)[174]. There is also a short form of NOD2, NOD2-S (which is just 21kDa in weight, as opposed to 116kDa, and predominantly comprises just a single CARD), whose expression is up-regulated in epithelial cells by anti-inflammatory signals such as IL-10, and acts as an endogenous inhibitor of NOD2 signalling[175]. NOD2-S was found to be the dominant form of NOD2 expressed in colonic epithelium, and exerts its effect by preventing the oligomerisation of NOD2 and RIPK-2 recruitment.

TAK1 has been shown to interact directly with NOD2-LRR domain, and in the absence of RIPK-2, NOD2 acts to negatively regulate TAK1-mediated NF-kB activation. TAK1 was demonstrated to be a mediator of NOD2-driven NF-kB

activation, and in keratinocytes TAK1 appears essential in this regard[176]. This is discussed further below with regard to NOD2/ TLR interactions.

Erbin, which was identified as a NOD2-interacting protein via the CARD domain in a biochemical screen, can inhibit NOD2-dependent NF-kB activation[169]. This is discussed in detail in chapter 4.

The transmembrane receptor CD147, whose expression is up-regulated by inflammatory stimuli such as MDP, is a glycoprotein that can interact with the CARD domains of NOD2 in human cell lines, and again can negatively regulate NOD2-dependent NF-kB activation[170]. However the exact role of CD147 in this regard is not clear since its expression actually facilitates *L. monocytogenes* entry into epithelial cells.

CARD8, which is a component of the NLRP3 inflammasome[177], was identified by the same group as a protein that interacts with NOD2 in epithelial cells, and inhibits both NF-kB activation and *L. monocytogenes* killing[171].

CENTB1, a GTPase-activating protein, was identified in a yeast two-hybrid screen to associate with NOD2 (and NOD1), and negatively regulate NOD-driven NF-kB activation in epithelial cells[172].

Lastly AAMP, a ubiquitously expressed WD40 repeat-containing protein found both in the cytoplasm and in a membrane-bound form, was also demonstrated in a yeast two-hybrid screen to associate with NOD2[173]. No reduction in binding was observed when FS1007insC NOD2 was expressed instead. Once again the predominant functional readout used was NF-kB activation in epithelial cells, with AAMP having a negative effect.

What nearly all these interacting proteins have in common is that, with the exception of TAK1 and GRIM-19 (see 'NOD2 and epithelial intracellular

bacterial control' below), they inhibit NF-kB activation, and also they have been found to predominantly function in epithelial cells, and this likely reflects the critical importance of keeping inflammatory signalling in check in GIT cells constantly exposed to commensal flora. The flip side to this is that, apart from A20, much less is known about how NOD2 signalling is controlled in professional immune cells such as DCs.

1.6.4 NOD2-signalling: MAPK activation

NOD2 activation also induces MAPK activation, including Erk (extracellular signal-regulated protein kinase), p38, and Jnk (c-Jun N-terminal kinase)[178]. It is not clear how most of these different pathways are regulated, although the adaptor protein CARD9 (caspase recruitment domain family member 9), another Crohn's susceptibility gene in its own right, functions downstream of NOD2 leading to p38 and Jnk activation[179]. CARD9 can mediate non-TLR signalling pathways for anti-fungal immunity by mediating dectin-1 induced NF-kB activation[180]. As regards NOD2, CARD9 physically associates with it and RIPK-2, and in CARD9-deficient mice NOD2 stimulated macrophages demonstrated defective production of IL-6 and TNFα. (Also defective after TLR2, 3 and 7, but not TLR4, stimulation.) CARD9 is required for the activation of p38 and Jnk (but not NFκB)[181], and CARD9 and NOD2 co-stimulation leads to synergistic activation of p38 and Jnk.

1.7 NOD2 in context

NOD2 is just one of a broad range of innate immune receptors or PRRs which together sense pathogen-associated molecular patterns (PAMPs) or damage

associated molecular patterns (DAMPs), and contribute to immunity through signalling pathways and effector mechanisms[144,182]. The effector mechanisms include antimicrobial effectors, inflammatory mediators such as cytokines, and signals (for example via DC maturation) to induce adaptive immunity[183,184]. These receptors and their functions exist not in isolation but in the context of the other innate receptors[185], of the cell in which they are expressed, of the tissue milieu of the cell, and of the resident animal. Most pathogens can be detected by more than one PRR – for example bacteria can typically be sensed by several TLRs, NOD1 and 2, inflammasome Nod-like receptors, the complement system and so on. Understanding both how they complement each other, and the apparent redundancy that exists between them, is challenging but also crucial to discriminating their true biological function and the potential result of loss-of-function.

A recent review[186] has described these interactions as being either cooperative (essentially where two PRRs synergistically activate an effector pathway), complementary (where two PRRs have distinct effector mechanisms which together form a functional whole), or compensatory (which means loss of one PRR is adequately compensated by the function of another). Interestingly they did not include an inhibitory category, where one PRR acts in some way to regulate or negate the effects of another, as has been particularly mooted for NOD2 and TLR2 interactions[187]. However, as the authors argue, the apparent increased activation of an effector pathway, such as may be seen on TLR2 triggering in the absence of NOD2 signalling, may in fact be over-compensation of the innate immune system for the loss of important effector mechanisms, and not intrinsic negative regulation of one

pathway for another. (As an example, immunodeficiencies are often also associated with apparent 'over-compensatory' autoimmune diseases[188].)

Where compensation is apparently complete in an experimental system, this implies redundancy for the functions of two PRRs. However, this can easily be the result of the in vitro or in vivo system used, the pathogen being tested, or the question asked. True redundancy would be unlikely in the long term when subjected to evolutionary pressures.

With this in mind, over the next two sections I will summarise the main data on the interactions between NOD2 and both TLRs and NLRs.

1.7.1 NOD2 and Toll-like receptors

Toll-like receptors were the first PRRs to be described, and are probably the best characterised. They are transmembrane proteins, expressed either at the cell surface or on endosomes[189]. Like NOD2, they have an LRR region that lies external to the cell membrane (or within the endosome) and functions as the ligand-recognition domain[190]. The rest comprises a central transmembrane domain, and a cytosolic Toll-IL-1R (TIR) domain[190] that activates the downstream effector pathways, via recruitment of adaptor molecules such as MyD88 or TRIF (toll-like receptor adaptor molecule 1)[189]. There are 10 human (and 12 murine) TLRs identified thus far.

There is good reason to suspect that many of the TLRs would be co-triggered with NOD2 by bacterial PAMPs, as most bacteria will co-express peptidoglycan (PGN): TLR2; lipopolysaccharide (LPS): TLR4; flagellin: TLR5; and DNA motifs particular to microbes: TLR9.

1.7.2 NOD2: TLR2

This is never more so than for NOD2 and TLR2 which both respond to components of bacterial cell walls – lipopeptides in the case of TLR2 – and these structures are actively remodelled and released, enabling potential detection, during bacterial replication. This particular NOD2 interaction has therefore probably generated not only the most interest, but also the most contentious data. As already briefly discussed, Warren Strober's laboratory have consistently published a model in which NOD2 appears to normally function as a negative regulator of TLR2 responses[187,191,192]. In the absence of NOD2, murine splenic macrophages demonstrate enhanced PGN (but not other TLR-ligand)-driven Th1 responses, as measured by IL-12 and IFNγ production. Interestingly, these effects were predominantly observed at MDP concentrations of 100μg/ml which are far in excess of 'classical' MDP experimental concentrations. (How these relate to physiological concentrations experienced in the gut is very difficult to ascertain.) These mice are also more susceptible to a TLR2-driven colitis. These results may be due to the specific role of NOD2 in mouse splenocytes as opposed to antigen presenting cells (APCs) such as DCs and macrophages, they may relate to differences in the function of NOD2 between mice and humans (discussed further below), or they may relate to an over-compensation of TLR2 signalling in the absence of NOD2, rather than a negative regulation of TLR2 under normal circumstances.

Whatever the reason, these data are at odds with the predominant view, and much of the published data from APCs, that NOD2 cooperates or synergises with TLR responses[193-197], including TLR2. For example, the cytokine profile

both in human mononuclear cells and murine peritoneal macrophages after NOD2 and TLR2 co-stimulation, demonstrates synergy for TNF, IL-1β, and IL-10 production[193], with defective IL-10 production in the presence of FS1007insC mutation. Our lab also has DNA array data from human MDDCs, with qPCR confirmation, that for the expression of many critical inflammatory mediators NOD2 and TLR2 demonstrate synergistic effects (Simmons 2008, unpublished data).

1.7.3 NOD2: TLR4

NOD2 also cooperates with TLR4 effector functions[193,197,198], including production of pro- and anti-inflammatory cytokines in human DCs, with this synergy significant enough for MDP treatment to allow stimulation by normally sub-active doses of LPS[198]. Interestingly similar data is published for unrelated cells, such as pituitary folliculostellate cells[199], with synergy of NFκB activation and IL-6 production via NOD2 + TLR4 stimulation. In part this cooperation between NOD2 and TLR4 may be mediated by NIK (NFκB-inducing kinase), which is involved in non-canonical or alternative NFκB activation, it being critical for the processing of the NFκB subunit p100 to p52[200]. NIK has been shown to interact with NOD2 in mouse BMDMs, and to facilitate MDP-induced NFκB activation[201]. BMDMs from mice with inactive NIK, also fail to demonstrate synergy of p52 NFκB activation on MDP and LPS stimulation.

In murine enterocytes, NOD2 may provide protection from TLR4-driven necrotising enterocolitis (NEC). Specifically NOD2 stimulation protects enterocytes from TLR4-induced apoptosis, via a reduction of second

mitochondria-derived activator of caspase/ direct inhibitor of apoptosis binding protein with low PI (SMAC-DIABLO), an apoptosis mediator[202].

1.7.4 Other NOD2: TLR interactions

Cooperative interactions between NOD2 and the signalling of TLR3[193], TLR5, TLR7/8 and TLR9[196], are also published. TLR9 SNPs are probably associated with Crohn's disease susceptibility [203], and there is possible epistasis between NOD2 and TLR9[204]. Functional work carried out in human PBMCs demonstrates synergy of TNFα and IL-8 production with dual NOD2 + TLR9 stimulation, an effect that is lost in cells from Crohn's patients homozygous for NOD2 mutations[195].

1.7.5 NOD2: TLR interaction mechanisms

Which molecular mechanisms link NOD2 and TLR receptor signalling is not yet certain, and it is possible that the proteins involved have not yet been identified. The most promising candidates so far are the kinase TAK1, an important component of TLR-induced NFκB signalling[205], and TRAF(TNF receptor-associated factor)6, an E3 ubiquitin ligase (**Fig. 1.4**). TLRs activate IRAK (IL-1 receptor-associated kinase) kinases to activate TRAF6, which in turn nucleates the TAK1 complex so that it can phosphorylate the IKK signalosome, leading to NFκB activation. TRAF6 is also activated by NOD2 stimulation, and both TRAF6 and NOD2/ RIPK-2 utilise TAK1 to activate NFκB[168,206,207]. Interestingly NOD1 can up-regulate the expression of TAK1 [208], although the same has not yet been shown for NOD2.

NOD2 stimulation does up-regulate MyD88 expression[209], which may explain some of the synergy observed for TLRs that utilise that adaptor, but not for example TLR3. In a reciprocal manner, LPS also up-regulates NOD2 and RIPK-2 expression[138]. Lastly, several PRR signalling pathways are known to converge on CARD9[179,210], but this adaptor appears to be dispensable for TLR signalling[180].

Figure 1.4 NOD2 crosstalk with TLRs

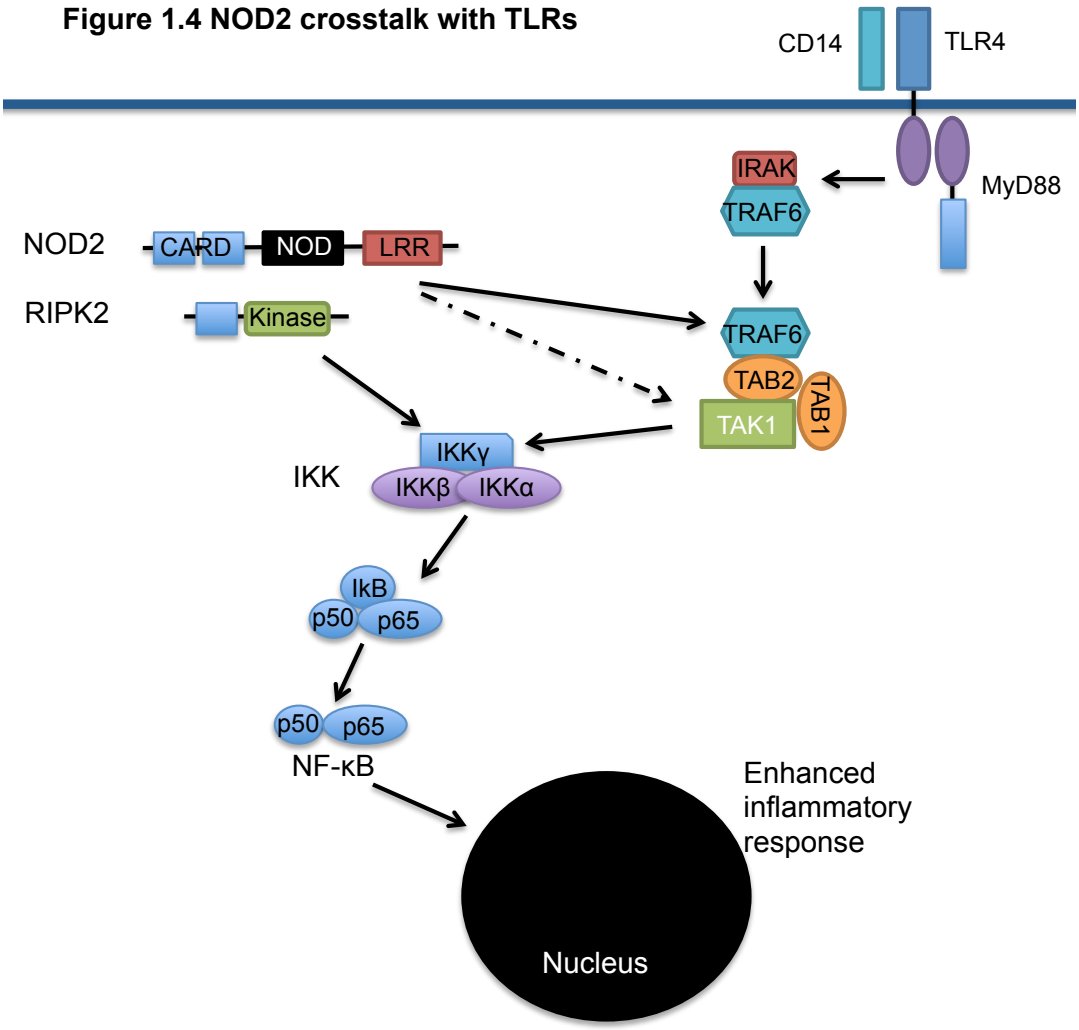


Figure 1.4 The signalling cascades downstream of NOD2 and TLR4 triggering are shown. There is enhanced expression of inflammatory mediators when co-stimulated, and this may be mediated by co-operative TRAF6 activation, or possibly by increased TAK1 expression.

1.7.6 NOD2 pre-stimulation

Some studies have explained the interaction of NOD2 and TLRs by pre-stimulating one receptor and examining the effect on the other. These experiments predominantly show that pre-treatment with MDP induces tolerance to subsequent TLR4 + NOD2 stimulation, but only for TNFα and IL-10, whereas IL-6 and IL-8 are unaffected[211]. Other studies have similar results, although only for TNFα[212]. This effect is associated with reduced phosphorylation of TAK1. In cells from CD patients who are FS1007insC homozygote, or compound heterozygote, for NOD2 mutations, pre-treatment fails to abrogate TNFα production, raising the possibility that this might explain the inflammation seen in CD. However, although this approach is interesting, there is very little reason to suppose that NOD2 might be stimulated before TLRs in a biological setting (perhaps quite the reverse given its cytosolic location). Moreover, even if this just examines the response of immune cells in general to repeated or continuous bacterial stimuli, it is already understood that repeated TLR triggering itself tolerises for further immune activation through a number of different mechanisms[213-217], so this does not in itself define anything specific for NOD2 function.

1.7.7 NOD2: TLR summary

In summary, in studies where NOD2 and TLRs are co-triggered, they are broadly co-operative, raising the possibility that CD-associated NOD2 mutations lack this synergism. Indeed we and others[193,218] have demonstrated that DCs derived from CD patients homozygous for FS1007insC mutation fail

to enhance a number of TLR-activated pro- and anti-inflammatory mediators. This fits with NOD2 mutations being broadly loss-of-function, and poses the question as to whether the loss of the pro- or anti-inflammatory components is most important in the context of combinatorial signalling and CD pathogenesis.

1.8 NOD2 and Nod-like receptors

It was the discovery of NOD1 and NOD2 that prompted the search for other homologous human proteins. This has thus far revealed more than 20 human members of the Nod-like receptor (NLR) family, and these are divided into 5 subgroups depending on their effector domain[219]. Although they have diverse functions they share similar domain architecture, which includes a leucine-rich repeat domain (LRR) and a nucleotide-binding oligomerisation domain (NOD), and these perform similar roles as those described for NOD2. The effector domains, which allow homeotypic interactions with downstream proteins, consist either of a CARD domain (as for NOD2) or a pyrin (PYD) domain, or both (as for NLRP1).

1.8.1 Inflammasome activators

The main interest in NLRs, other than NOD1 and NOD2, has centred on those that trigger the inflammasome. The best characterised function of this multi-protein complex, which includes the adaptor protein ASC (apoptosis-associated speck-like protein containing a CARD), is to activate caspase-1, enabling processing of pro-IL-1β and pro-IL-18 to their mature active forms[220]. This forms the second part, or ‘signal 2’, of the control of IL-1β and IL-18

release – signal 1 being the transcriptional regulation of pro-IL-1β and pro-IL-18 via TLR activation[220] (**Fig. 1.5**). This post-transcriptional regulation is an unusual event in most cytokine biology, and may reflect both the importance of IL-1β and / or IL-18, and the need to tightly control their expression. NLRP1, NLRP3, and NLRC4 (or IPAF) are the inflammasome activators with the most clearly defined ligands[221], but it is highly likely that many (or all) of the other NLRs also activate inflammasomes under certain circumstances.

Figure 1.5 NLR signalling

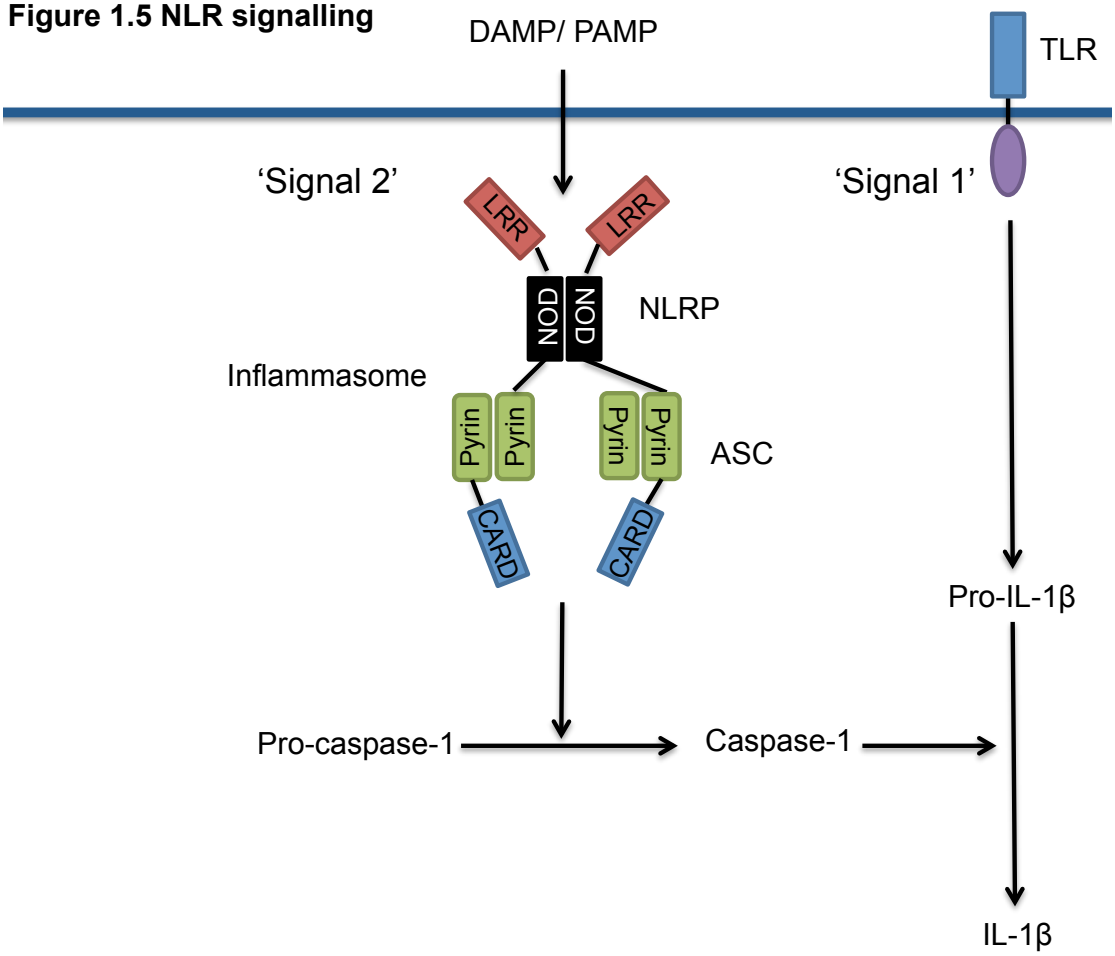


Figure 1.5 Nod-like receptors are typically triggered by DAMPs (damage associated molecular patterns) or PAMPs (pathogen-associated molecular patterns), leading to an association with ASC and the formation of the inflammasome. This facilitates the activation of caspase-1. Concomitant TLR

triggering results in increased pro-IL-1β production, which is converted to active IL-1β by caspase-1.

Evidently NOD2 and other NLRs are likely to be co-triggered during some immune responses, either directly by sensing microbial PAMPs (for instance flagellin by NLRC4) or indirectly through the detection of inflammatory damage (for example NLRP3). As with NOD2 / TLR interactions, the outcome of these interactions is of some interest in the attempt to understand the coordination of innate immune responses, however the nature of these NLR interactions is less well understood. This is in part because the triggers for NLR activation (which can be multiple for a given NLR) and the mechanisms of inflammasome assembly are still being elucidated, and these need to be well characterised before combined NLR signalling can be rigorously investigated.

1.8.2 NOD2: NLRC4

NLRC4 is expressed in myeloid cells and the gastrointestinal tract[222]. Activation is predominantly (although not exclusively[223]) by cytosolic bacterial flagellin[224], probably via type III and IV bacterial secretion systems. This can lead to IL-1β production, as described, but also to a form of cell death called pyroptosis in an ASC-independent manner[225].

NOD2 and NLRC4 have been shown to interact via their NOD domains, and this may result in reduced NFκB activation and IL-1β production[226]. The main flaw underlying this, and indeed some other NOD2/ NLR studies, is that much of the data rests on determining interactions between NLRs in over-expression systems (normally in HEK293 cells). As these proteins express

homotypic protein domains, these interactions may purely represent potential hetero-oligomerisation on biochemical grounds, and may not be relevant in the biological sense. This view is reinforced by the finding that the NOD of NLRC4 appears to bind to the NODs of NOD1, NOD2, NLRP3, ASC, NLRC4 and others[226], raising questions as to the biological validity of so many interactions.

1.8.3 NOD2: NLRP3

NLRP3 is a more promiscuous receptor, with the ability to respond to a wide variety of ligands such as asbestos, monosodium urate (MSU), silica, alum, protein aggregates, and adenosine triphosphate (ATP). It is likely that indirect mechanisms may allow this number of ligands to be detected – for example through potassium efflux, or generation of reactive oxygen species (ROS)[221]. The NLRP3 inflammasome is also activated by pathogens – for example *S. Aureus,* or *L. monocytogenes* via the pore-forming toxin listeriolysin[227]. Activating mutations in NLRP3 are associated with diseases – the cryopyrin-associated periodic syndromes (CAPS) – characterised by excessive IL-1β release and resulting in varied symptoms including rashes, fevers and arthralgia[228]. Interestingly hypofunctional NLRP3 mutations, that result in decreased expression and dampened IL-1β production, have been associated with Crohn's disease[229,230]. This is reminiscent of NOD2, with hypofunctional mutations contributing to CD, and activating mutations in the central NOD domain resulting in Blau syndrome, characterised by skin, eye and joint pathology[231].

Direct physical interactions between NOD2 and NLRP3 have been demonstrated in yeast two-hybrid experiments[232]. These also demonstrate possible novel interactions between NOD2 and NLRP1 and -12, although the immunoprecipitation in HEK293s only confirmed NLRP3. However, these interactions are relatively weak, and the experiments involve over-expression of these proteins with the caveat already described. Moreover, expression was typically of selected domains, not the complete NLRs, and therefore would be lacking the tertiary structures that may normally protect these domains from direct physical interaction.

More recently a functional analysis of NOD2 and NLRP3 co-triggering was performed in murine DCs, using cDNA gene expression arrays[233]. The cells were stimulated with MDP and MSU, and the authors found a unique transcriptional signature, with synergy for Erk1 and c-Jun, antigen presentation and co-stimulation molecules, and certain cytokines (including IL-1β, IL-6, IL-12p40 and IL-23p19). Interestingly the demonstrated synergism for cytokine genes was partially dependent on NOD2, but not on NLRP3. This is clearly context and stimulus dependent, as human PBMCs infected with *L. monocytogenes* make IL-1β via an NLRP3 inflammasome, and this is independent of NOD2 and RIPK-2 (and indeed other NLRs)[234].

MDP has been mooted as a possible ligand for both NLRP3[235] and NLRP1 (see below). However the contribution of NOD2 in the production of NLRP3-inflammasome-related IL-1β is uncertain. Clearly in the context of whole bacteria (such as *L. monocytogenes*) NOD2 appears dispensable, at least in human cells. However, stimulation with purified MDP ligands in murine experiments demonstrates a requirement for NOD2, RIPK-2, NLRP3, and

ASC in the production of IL-1β[236]. Another murine macrophage study further defined these roles, with NOD2 being required for *pro*-IL-1β production in MDP + ATP stimulated cells, but not for caspase-1 activation which required NLRP3[237]. This apparently contradictory evidence probably in part reflects that whole bacteria carry a number of potential PRR ligands and stimulate other danger signals, and that this circumvents in some way the requirement for NOD2 in that experimental system, rather than implying true redundancy in all settings. Some of the observed discrepancies may also relate to differences in the interactions of murine and human NLRs.

1.8.4 NOD2: NLRP1

NOD2 probably also has a role in the NLRP1 inflammasome via MDP stimulation, although once again this is not yet clearly defined. The NLRP1 inflammasome was the first to be described[238], and NLRP1 is expressed in a number of immune and non-immune cell types, including monocytes and DCs. In humans NLRP1 contains 5 domains: PYD, NBD, LRR, FIIND (function to find), and C-terminal CARD. In contrast mice not only have three polymorphic paralogues[129], but also murine NLRP1 lacks functional PYD and FIIND domains and may not be able to activate ASC[239], raising questions as to the validity of extrapolating data from mice to humans. As already described, NOD2 can promote pro-IL-1β (signal 1), and it was further demonstrated[239] that the CARD domain of NOD2 can also directly bind the CARD domain of, and activate, caspase-1 (signal 2) through a direct interaction with NLRP1. This leads to IL-1β secretion in MDP-stimulated murine macrophages.

How these interactions between NOD2, NLRP3 and NLRP1 (and possibly NLRC4) function in a biological (in vivo) context is not yet known. Nor is it understood whether the NOD2 mutations that predispose to CD may disturb these interactions, and whether this may contribute to pathogenesis (for example by altering IL-1β secretion, or altering the balance of pyroptosis and autophagy). A signal of their collective importance in innate immunity comes interestingly not from bacteria, but from a herpes family virus. Kaposi sarcoma virus Orf63 is a recently described homolog of human NLRP1, and interacts not only with NLRP1, blocking innate immune responses and IL-1β production, but also with NOD2 and NLRP3[240].

1.9 NOD2 and Autophagy

Signalling through TLRs has been shown to induce autophagosome formation[241,242], and the question arose as to whether this was also true of NOD2. NOD2 polymorphisms have a strong independent association with terminal ileal CD, with ATG16L1 T300A also showing this association (albeit less strongly)[20,243]. Cooney et al. observed (in human dendritic cells) that autophagy is induced through NOD2 stimulation, and that autophagy induction, antigen presentation, and bacterial handling (of both *S. enterica* and AIEC) are all defective in the presence of both ATG16L1 T300A, and/or any of the 3 most common CD-associated NOD2 polymorphisms[244]. Travassos et al. similarly demonstrated a link between NOD2 and autophagy in human cell lines and murine macrophages[157]. Here bacterial entry triggers the recruitment of ATG16L1 by NOD2 to the plasma membrane, and this is defective in cells bearing the FS1007insC mutation of the NOD2 gene.

Although there are differences in the demonstrated mechanisms, together these studies provide compelling evidence for the critical role of autophagy in bacterial handling and in CD pathogenesis, and neatly show that two significant CD polymorphisms affect the same pathway.

This functional association between ATG16L1 and NOD2 was confirmed by a further study[245] in which MDP stimulation of NOD2 enhanced autophagic bacterial killing, an effect abrogated by RNAi knockdown of ATG16L1, or of the NOD2-signalling adaptor RIPK-2. Although they failed to show an effect of the ATG16L1 T300A variant on MDP-stimulated bacterial killing in monocytic cells, these cells were derived from healthy controls (vs. CD patients in Cooney et al), which may imply that in CD patients there are further acquired or inherited defects that modulate these two pathways. (Interestingly Homer et al also demonstrated a reciprocal relationship in human epithelial cells, with autophagy and ATG16L1 being involved in the delivery of MDP to NOD2, and thus of NOD2 activation.)

It is speculated that NOD2- and/ or ATG16L1-defective autophagy ultimately leads to inflammation due to increased inflammasome activation. This idea predominantly comes from the observation that ATG16L1 also regulates lipopolysaccharide (LPS)-induced inflammasome activation in mice[26]. In this experimental setting, murine macrophages deficient in the conserved coiled-coil domain of ATG16L1 produce more IL-1β and IL-18 in response to LPS, than their wild-type counterparts. These mice also develop a more severe DSS-induced colitis, with improvement on administration of anti-IL1β and IL-18 neutralising antibodies. It should be borne in mind that the conserved

domain of ATG16L1 deleted here is not the WD-repeat domain altered by the CD-associated ATG16L1 polymorphism.

1.10 NOD2 and ER stress

The UPR has recently been linked both with autophagy and innate immune function. An example of the former is IRE1 which, via an interaction with TRAF2 under ER stress conditions, can induce Jnk activation which is directly capable of inducing autophagosome formation via LC3[246]. Impaired autophagy can also promote ER stress – ATG7 suppression in the liver leads to increased ER stress[247]. An example of the latter is the promotion of immune cell survival upon the triggering of PRRs such as TLR4 and TLR3, via TRIF-mediated suppression of the UPR effector CHOP (c/EBP-homologous protein)[248]. Prolonged exposure to CHOP is cytotoxic. The IRE1/ XBP1 axis is also required for optimal cytokine secretion from macrophages[62].

Although the direct role of NOD2 in the UPR has not been studied, it is interesting to speculate that given the above associations a defective UPR in the presence of NOD2 CD-polymorphisms is likely.

1.11 NOD2 and Adaptive Immunity

1.11.1 NOD2 in DCs

DCs are the most potent antigen-presenting cells in the immune system, with the capacity to uptake and efficiently present antigen to naïve T cells[145], and therefore the specific role of NOD2 in these cells is of interest. The mechanism of NOD2-mediated adaptive immune responses may well be through autophagy induction which, as just described, influences MHC II

presentation in DCs. NOD2 or ATG16L1 siRNA knockdown abrogate antigen-specific autologous $CD4^+$ T cell proliferation[244]. Alternatively, NOD2 signalling also enhances DC-mediated cross-priming[249], in which DCs deliver exogenous (as opposed to cytosolic) antigen to the MHC I compartment to stimulate $CD8^+$ T cell responses. This occurs through up-regulation of intracellular proteins such as TAP (transporter associated with antigen processing) which no doubt allows increased transport of cytosolic antigen into the endoplasmic reticulum. This effect is perhaps not surprising given that TLR triggering (specifically TLR9 and TLR3) is known to efficiently induce cross-priming[250], and NOD2 for the most part synergises with TLRs.

An examination of adaptive immune responses in wild-type and NOD2-deficient mice immunized with OVA and MDP, revealed that NOD2 stimulation alone appears to direct a Th2 response, and this is predominantly through NOD2 function in DCs. This was characterised by increased IL-4 and IL-5 production by T cells, and IgG1 antibodies[251]. Although IgG1 production is weak when using MDP, as opposed to LPS, as an adjuvant, NOD2 is required for optimal IgG1 and IgG2c responses in the absence of other PRR stimuli[252]. However, when using an adjuvant (complete Freund's adjuvant) that stimulates both NOD2 and NOD1, and TLRs 2, 4 and 9, and is therefore more typical of a whole (myco)bacterial stimulus, wild-type NOD2 acts to enhance both Th1 and Th2 responses[251]. In vitro experiments with BMDMs confirmed the synergism of NOD2 and TLRs for IL-6 (a Th17 polarising cytokine) and IL-12p40 subunit (a Th1 or TH17 polarising cytokine) production. These findings predominantly show that NOD2 acts in conjunction with other PRRs to enhance adaptive immune priming, and its absence may well result in

reduction in any of the T cell effector subsets depending on the co-stimuli used. I think it is hard to argue, as the authors do, that this shows NOD2 normally has a predominantly Th2 priming role.

In support of this interpretation, other studies have shown that MDP stimulation of DCs can induce the production of IL-17 from memory, but not naïve, human $CD4^+$ T cells, and enhances TLR-induced IL-23 and IL-1 production from DCs[253].

1.11.2 NOD2 T cell-intrinsic function

Under some circumstances NOD2 may also have a T cell-intrinsic function in the promotion of Th1 responses. Mice lacking NOD2 (but not RIPK-2) have increased susceptibility to *Toxplasma gondii*, an obligate intracellular protozoan pathogen which does not express MDP[254]. Interestingly this is a delayed immune impairment, with NOD2-deficient mice producing normal amounts of IL-12p40, but less IFNγ on day 7 post-infection, in an apparently T cell-intrinsic manner and due to a lack of IL-2. In T cells NOD2 interacts with c-Rel (an NFκB subunit) to enhance IL-2 production downstream of CD28 co-stimulatory signalling. In this system NOD2-T cell function is also important for Th2 differentiation, and in lymphopoenia-induced T cell proliferation. However, the argument that this is the critical defect leading to NOD2-CD predisposition is slightly undone by the finding that T cell deficient (RAG2 knockout) mice reconstituted with NOD2-deficient T cells are *protected* from small and large bowel inflammation[254].

1.12 NOD2 and Epithelial Barrier Function

1.12.1 NOD2 and epithelial extracellular bacterial control

1.12.2 Defensins

Antimicrobial peptides are a critical component of epithelial defense, not least in the GIT, and are expressed by both standard epithelial and specialist cells. These specialists - Paneth cells - are located within the crypts of Lieberkühn of the small intestine, and secrete antimicrobial peptides and lysozyme. NOD2 is highly expressed in Paneth cells[139,140], and these cells are themselves most highly expressed in the terminal ileum[255], the site of NOD2-associated CD. (Paneth cell metaplasia does occur in colonic IBD.) There has therefore been much interest as to whether NOD2 mutations functionally affect Paneth cells.

NOD2 mutations are associated with decreased alpha defensin production (HD-5 and HD-6) from Paneth cells[256-258], although interestingly this effect is seen almost exclusively with the FS1007insC mutation, and not the other common missense mutations. There is some debate as to whether this apparent reduction owes more to inflammation rather than NOD2 expression[259], and there is evidence that most ileal CD patients express lower levels of α-defensins independent of inflammation[81], possibly by defective Wnt signalling as discussed above[83]. However, murine models deficient in NOD2 also express lower levels of cryptidins (the mouse defensin equivalent) in the absence of inflammation, and are more susceptible to infection with oral *Listeria monocytogenes*[260]. Moreover, although mice with a targeted deletion of Paneth cells[261], or with an inability to make mature cryptidins[262], do not develop spontaneous inflammation, nor do NOD2 deficient mice so this does not argue against the presence, or potential importance, of this defect.

NOD2 deficient (and RIPK-2 deficient) mice do develop granulomatous inflammation if exposed to *Helicobacter Hepaticus*, a murine opportunistic pathogen[263]. These mice also expand their Th1 T cells, and enlarge their Peyer's patches and mesenteric lymph nodes. The importance of NOD2 expression in the epithelial compartment, and to defensin production specifically, in this model was implied by the rescue experiments. Transferring wild-type bone marrow did not affect the phenotype, whereas transgenic expression of α-defensins in Paneth cells alleviated the inflammation. Of course, this does not prove that NOD2-associated defensin loss is sufficient for disease (as other experiments have shown), only that over-expressing defensins artificially can abrogate existing inflammation in a NOD2 deficient model. As an inability to cope with commensal flora and/ or pathogens are mooted as likely triggers, and drivers, of inflammation, it is quite possible that increasing anti-microbial peptide expression in the face of existing inflammation, may be the most tractable way to compensate for a variety of immune defects.

1.12.3 DMTB1

DMTB1 (deleted in malignant brain tumours 1) belongs to another class of antimicrobial peptide - the secreted scavenger receptor cysteine-rich proteins. DMTB1 can bind and aggregate both Gram-positive and Gram-negative bacteria[264], and may depend on NOD2 for appropriate secretion from epithelial cells[265]. Interestingly NOD2 and TLR4 cooperate in the up-regulation of DMTB1, highlighting the integrated nature of the innate immune response. Mutant NOD2 patients express this protein at lower levels in inflamed tissue

than their wild-type counterparts. DMTB1 aggregates and inhibits invasion of *Salmonella enterica* in vitro, and may also inhibit TLR4-induced NFκB activation by neutralising the activity of PAMPs, suggesting a role in a negative feedback loop to downgrade innate immune activation.

1.13 NOD2 and epithelial intracellular bacterial control

1.13.1 GRIM-19

WT NOD2, but not FS1007insC NOD2, has also been shown to function in the control of intracellular bacteria in intestinal epithelial cells[266]. This group went on to show that this effect, and NOD2-mediated NFκB activation, depended on another protein, GRIM-19[174]. GRIM-19 is up-regulated by invasive bacteria, and both co-localises and interacts directly with NOD2 in epithelial cell lines. GRIM-19 expression inversely correlates with intracellular survival of S*. Typhimurium*, and this at least in part also depended on the presence of NOD2, although the mechanism of action is unknown. It may be that GRIM-19, which is a subunit of the mitochondrial NADPH ubiquone oxidoreductase, is responsible for the generation of reactive oxygen species (ROS), which are involved in host defense against pathogens.

1.13.2 DUOX2

A more recent study, which took plant ROS generation via NLR homologues as its starting point, identified the NADPH oxidase family member DUOX2 (dual oxidase 2) as a critical mediator of NOD2-dependent ROS production[267]. In epithelial cells DUOX2 was shown to directly interact with NOD2 (which is analogous to NOX (NAPDH oxidase) family member interactions with

TLRs[268]) via the LRR domain, which FS1007insC NOD2 failed to do, and cooperate with NOD2 in the defense of invasive *L. monocytogenes*. Interestingly this study did not investigate any potential involvement of GRIM-19 in their findings.

1.14 NOD2 and the Microbiome

PRRs are triggered by PAMPs that are conserved between pathogens and commensals, and it is not clear how the immune system differentiates these two groups on this basis. One answer would be that under normal conditions PRRs are protected from commensal bacterial interaction by the epithelial barrier, and are only triggered when the barrier is breached by pathogens. However, doubt was cast on this explanation by the finding that commensal bacteria are recognised by TLRs even under steady-state conditions, and that this interplay is crucial for intestinal homeostasis[93]. Moreover the authors found that TLR activation by commensal flora, via a Myd88-dependent pathway, was a critical component of host protection against gut injury. (This may in part be NFκB-mediated, as blocking NFκB activation in enterocytes also induces more severe damage following injury[269].)

1.14.1 NOD2 microbiota: mice

Given the associations with NOD2 mutations and CD, a legitimate question is clearly whether NOD2 also influences the microbiome. NOD2-deficient mice have an increased load of commensals in the terminal ileum, when compared with WT controls[270]. Genus-specific 16S rRNA primers used to analyse *Bacteroides* and Firmicutes demonstrated that only NOD2-deficient mice had

significant numbers in the terminal ileum, although there was no difference in a faecal analysis. Their intestinal crypts also demonstrate a diminished ability to kill bacteria, and these findings may be explained by previous studies that linked murine NOD2 to antimicrobial peptide production from Paneth cells[260]. It is possible that NOD2 is also influencing commensals via immune surveillance by myeloid cells, or as the authors speculate, via management of lymphoid tissue genesis via a mechanism similar to the related NOD1[271]. Furthermore this study demonstrated that NOD2 (and RIPK-2 but interestingly not MyD88) epithelial expression is dependent on the presence of the commensals, in keeping with in vitro studies of NOD2 epithelial induction through innate immune receptor triggering[138], and highlighting a co-regulatory mechanism between NOD2 and commensals.

A more recent study has provided similar data from NOD2 deficient mice[119], reporting elevated bacterial loads in the terminal ileum *and* the faeces, with specific changes in the ratio of *Bacteroidetes* and *Firmicutes* depending on the age of the NOD2 deficient mice. They also demonstrated that these changes are present in weaning mice, implying an influence for NOD2 on the developing microbiota.

1.14.2 NOD2 microbiota: humans

Rehman et al then examined the effect of NOD2 on human gut flora[119]. Their biopsy biobank was screened for CD patients who were also homozygous for the FS1007insC or 'SNP13' NOD2 variant, and they subsequently compared terminal ileal biopsies from 3 SNP13 homozygotes with 11 wild-type NOD2 samples who also had quiescent CD. The NOD2 homozygotes had increased

Firmicutes and *Bacteroidetes* loads in the biopsies, and the level of *F. prausnitzii* was marginally reduced. The controls here also had CD, presumably in an effort to exclude the confounding effect of inflammation on the microbiota, although interestingly the authors do not state if they genotyped all the samples for the other common NOD2 SNPs, as these may well be present in their controls that have terminal ileal CD.

Another study has also re-analysed human intestinal tissue microbiota results, obtained by 16S rRNA sequencing, in light of subsequent NOD2 and ATG16L1 genotyping[272]. These patients had undergone surgery either for UC, CD, or other un-related pathologies. The Firmicutes, particularly Clostridium Groups XIVa and IV, were decreased, and the frequencies of Actinobacteria and Proteobacteria increased in CD compared with control samples. Although both NOD2 and ATG16L1 genotypes influenced this result, these shifts in the microbiota appeared to be more dependent on the disease phenotype. However, there was some evidence both for an allele-dosage effect regarding mutated NOD2 (but not ATG16L1) and microbial changes, and for NOD2 genotype microbiotas tending to cluster together regardless of the CD phenotype. This study therefore provides some evidence for NOD2 influencing the microbiota regardless of inflammation in humans, but it is limited by: a shallow level of DNA sequence coverage; by using heterogeneous genotypes and phenotypes (the study included Crohn's colitis as well as ileitis); and by the analysis of both inflamed and non-inflamed mucosa together.

Overall the evidence that NOD2 function influences the development and composition of the GIT microflora is reasonable, especially in mice where it is

easier to control for other factors. How NOD2 effects these changes is currently less clear, and is mostly speculative based on previously described NOD2 functions.

1.15 NOD2 function: Of mice and men

The study of NOD2 function has thrown up a number of differences between mice and humans, both in the way wild-type NOD2 functions, and the way in which mutant NOD2 behaves (sometimes in murine model systems). The most obvious of these concerns the regulation of IL-10 by NOD2. NOD2 controls IL-10 through the phosphorylation of the DNA/RNA-binding protein hnRNP-A1, which acts as a physiological inducer of IL-10 through binding the promoter region[273]. hnRNP-A1 is one of approximately 30 hnRNPs, and these have diverse functions that include DNA repair; chromatin remodelling and transcription; promoting RNA stability, and mediating RNA export and translation. The FS1007insC NOD2 mutation inhibits expression of IL-10 by reducing the p38-mediated phosphorylation of hnRNP-A1. Interestingly, this occurs both on MDP stimulation and constitutively, but is only found in human monocytes and not in murine experiments.

Another example is that of IL-1β production. In a murine bone marrow-derived macrophage (BMDM) model that expressed the equivalent of the human NOD2 frame-shift mutation (termed 2939insC NOD2 in mice), it was found that this potentiates NF-kB activity and IL-1β processing[274]. MDP-induced gene-expression of several cytokine genes was increased in NOD2 mutant macrophages, but only IL-1β secretion was significantly elevated. These results suggest NOD2 mutations are gain-of-function, and induce elevated

IKK (IκB kinase) and caspase-1 activation in response to MDP. This is clearly at odds with human data, in which the frame-shift NOD2 mutation is loss-of-function and abrogates IL-1β secretion[275]. These differences may relate purely to this particular model in which an *equivalent* of the frame-shift mutation is expressed, or as already discussed in the section on NOD2 and NLRs, this might suggest a fundamental difference in the way in which murine and human NLRs behave and control IL-1β.

Lastly, the data concerning the negative regulation of TLR2 by NOD2 comes from NOD2 deficient murine models, and again is at odds with the described interaction of NOD2 and TLRs in human experiments. What all these studies demonstrate is that the mouse 2939insC NOD2 mutant is not the same as the NOD2 frame-shift mutation in humans, and that lacking NOD2 is not equivalent to expressing FS1007insC NOD2.

1.16 NOD2 Summary

Clearly much has been learnt about NOD2 in the 10 years since it was defined as the first CD-susceptibility gene. The predominant findings suggest that in myelomonocytic cells NOD2 plays a role in autophagy induction, promotion of IL-10 secretion, synergy with TLRs, and probably a role in an MDP-triggered inflammasome. In epithelial cells, NOD2 appears predominantly to effect both extra- and intra-cellular bacterial killing, and there are many described negative regulators that control excessive NOD2-driven NFκB activation. No doubt through a combination of these effects, NOD2 modulates the gut microbiome.

However many unanswered questions remain about the general function of NOD2, which include: What is the structure of NOD2?; How does a moiety as small as MDP induce a conformational change in this 116kDa protein?; How does NOD2 trigger autophagy?; What are the molecular mechanisms and signalling intermediaries that link NOD2 and TLR triggering?; Is NOD2 part of the multimolecular inflammasome complex, and under what circumstances?; Why are NOD2 polymorphisms so common? (The implication being that heterozygosity confers some selective advantage.); and so on.

Then there are questions that apply specifically to CD pathogenesis: How do loss-of-function mutations lead to a pro-inflammatory disease?; Is the loss of pro- or anti-inflammatory mediators most significant?; How do they link specifically to an aberrant Th17-mediated disease response?; Which of the many described NOD2 functions are important for CD pathogenesis?; In which cellular compartment is NOD2 function most critical?; Is the described NOD2 dysbiosis an initiator of, driver of, or predominantly secondary to, inflammation?

I aim to answer some of these questions, firstly by examining the role of microRNAs (miRNAs) in the function of NOD2 in human DCs. These short non-coding RNAs prevent the translation of messenger RNA into protein, and are important negative regulators of TLR signalling[276]. I hypothesised that NOD2 might also control miRNA expression, and that loss of these negative regulators in the presence of NOD2 polymorphisms might contribute to the pro-inflammatory state found in CD. The results from this project are described in chapters 3, 4, and 5.

Secondly, in order to more fully understand the NOD2 signalling complex in DCs, I propose to perform an immunoprecipitation of NOD2-associated proteins in a human cell line, and confirm any results in primary human DCs. The results of this project are described in chapter 6.

2 Material and Methods

2.1 Molecular Biology Methods

2.1.1 Polymerase chain reaction

A typical 25 μl reaction comprised: 1 μl template (1-100 ng of plasmid DNA or 50-250 ng of genomic DNA), 0.5 μl of forward and reverse primers (5-25 pmoles each), 0.5 μl DNTP 50 mmol, 0.5 μl enzyme (Long PCR Enzyme Mix; Fermentas K0181 – a blend of *Taq* DNA polymerase and a proofreading DNA polymerase), 2.5 μl 10x Buffer, Mg^{++} 0.0 to 1.5 mmol, distilled H_20 to final volume 25 μl. Typical PCR reaction conditions were initial denaturation 95°C for 5 min; then cycling 25-35 cycles of: denaturation 95°C for 30-60 sec, annealing (temperature dependent on primers) 30-60 sec, extension 70-75°C for 30-120 sec per kilobase; then final extension 70-75°C for 5-10 min. These methods were optimised for each PCR. The annealing temperature was determined by Tm-5°C, where the melting temperature of the primers (Tm) (the temperature at which half the hydrogen bonds in the duplex can form) = 2(A+T) + 4(G+C) of the primer content.

After PCR the products were purified using Qiagen PCR purification kit (28104) following the manufacturers instructions.

2.1.2 Mini / Maxipreps

100 μl of competent Escherichia coli (XL10 Gold Ultracompetent cells; Agilent 200314) were transformed. Firstly, 4 μl of β-Mercaptoethanol was incubated

for 10 min on ice per 100 μl of cells. Then 0.1-50ng of experimental DNA, or 2 μl of a ligation mixture, were added to the cells for 30 min on ice. The cells were then heat pulsed at 42°C for 30-45 sec, before incubation on ice for 2 min. Subsequently 0.9 ml of NZY broth was added to each tube, and incubated for 1 h at 37°C, shaking at 225 rpm. (NZY broth per litre comprises: 10 g NZ amine, 5 g yeast extract, 5 g NaCl, pH 7.5, autoclaved. Prior to use 12.5 ml 1 M $MgCl_2$, 12.5 ml 1M $MgSO_4$, 20ml of 20% glucose per litre were added.) Subsequently, 100 to 200 μl of the transformation mixture was plated on LB agar (LB agar per litre comprises: 10 g tryptone, 10 g NaCl, 5 g yeast extract, 15 g bactoagar, autoclaved) with appropriate antibiotic, and incubated 37°C overnight.

Each selected bacterial colony was expanded in 1 ml of LB broth (LB broth per litre comprises: as per LB agar without the bactoagar) without antibiotic for 1 h, 225 rpm at 37°C, before the addition of 9 ml LB broth with appropriate antibiotic, shaken 225 rpm overnight at 37°C. 3 mls LB was subsequently spun for 15 min at 5000 rpm, the supernatent removed and the DNA extracted following the standard protocol of QIAprep Spin Miniprep kit (Qiagen 27106). DNA was quantified using NanoDrop® ND-1000, and a diagnostic digest (see 2.1.3 below) performed using appropriate restriction enzymes.

For maxiprep, the remaining 7 ml LB broth was expanded in 500 ml LB broth with appropriate antibiotic, shaken 225 rpm overnight at 37°C. The LB was spun at 5000 rpm for 30 min, the supernatant discarded, and the DNA extracted using Qiagen Plasmid Maxi Kit (Cat no 12162), following the company protocol.

2.1.3 Restriction digest

1 unit of restriction enzyme was used to digest 1 µg DNA per hour (typically at 37°C), as per the manufacturers recommendation (Roche or NEB). An appropriate buffer was used as supplied by the manufacturer. The enzymes were then heat inactivated at 70°C for 2 minutes. In the case of vector linearisation prior to subsequent DNA ligation, the linearised vector ends were then dephosphorylated. Per reaction, 50 ng of vector DNA, 3 U of alkaline phosphatase (shrimp ALP; Roche 11758250001), and the supplied buffer and distilled water, were incubated at 37°C for 30 min, before heat inactivation at 65°C for 15 min.

Run down TBE 1% agarose gel (with ethidium bromide) with appropriate molecular weight marker (NEB 1 kb DNA ladder N3232L; or NEB 100 bp DNA ladder N0467L) and DNA dye (Coral Load 10x; Qiagen) was used to confirm the presence of the selected vector or PCR product fragments.

2.1.4 Western Blot

Unless otherwise stated 3 to 5 million cells were lysed in 1% NP40 lysis buffer for 30 minutes on ice, and subsequently spun for 30 min at 13,000rpm at 4 °C to remove cellular debris. 1% NP40 lysis buffer comprises per 500ml H_2O: 3.94 g TrisHCl, 4.38 g NaCl, 1 ml 0.5 M EDTA, adjusted to pH 7.45, and 5 ml NP40. Prior to use protease (Roche complete mini; 04693124001, 1 tablet per 10 ml buffer) and phosphatase inhibitors (Na Orthovanadate 200 mM pH 10, and Na Fluoride 200 mM, both added 1:200 to buffer) were added.

Cell supernatants were reduced using SDS buffer (boiled for 5 min at 100°C), before loading onto 4-12% SDS-PAGE gels. An appropriate ladder was used

(Rainbow RPN 800E, GE Healthcare). Transfer to Immobilon P membranes was achieved in a semi-dry transfer system, at 20mA for 12 hours. After blocking for 1 h room temperature, or 4°C overnight, with blocking buffer (5 ml dried milk powder added to 50 ml TBST), the membrane was washed three times for 15 min (wash buffer: TBST). TBS Tween per litre comprises 960 ml H_2O, 30 ml 5 M NaCl, 10 ml 1 M TrisHCl pH 8, 0.5 ml Tween. The membrane was then incubated with primary antibodies in blocking buffer (either 1 h at room temperature, or overnight at 4°C). Three further washes were performed before incubation for 1 h with an appropriate HRP-conjugated secondary in blocking buffer, and then three further washes. The ECL reaction was visualised on ECL-sensitive film for exposures appropriate for the target protein abundance.

2.1.5 DC Nucleofection

Nucleofection of DCs was performed as per the manufacturers protocol and electroporation unit (Lonza, VVPA-1004). Per transfection reaction 3 million MDDCs were suspended in 100 µl of DC nucleofection solution, and placed in a cuvette with 5 µl of the siRNA, or miRNA premiR, or miRNA antimiR, or appropriate control, such that the final siRNA or miRNA concentration was 50nM (unless otherwise stated). The cells were electroporated on the 'human DC' setting, and immediately placed into 5mls R10 media (RPMI supplemented with 10% Foetal Calf Serum, Glutamine, and Penicillin/ Streptomycin) warmed to 37°C, and incubated for 24 h (unless otherwise stated) before further use.

2.1.6 Preparation of Human Monocyte-derived Dendritic Cells

Buffy coats were obtained from the National Blood Service (Bristol, UK), or blood samples venesected from CARD15/ NOD2 homozygote Crohn's patients under ethical approval and patient consent (Research Ethics Committee Reference: 07/H0603/43). Samples were diluted two-fold with RPMI 1640 medium (Sigma), and separated by centrifugation over a Sodium Diatrizoate/ Polysaccharide solution (Lymphoprep, Axis-Shield, Oslo) according to standard protocols. Peripheral blood mononuclear cells (PBMCs) were harvested, and $CD14^+$ monocytes positively selected using anti-CD14 microbeads and MACS LS columns (Miltenyi Biotech), according to the manufacturers instructions. Monocytes were cultured in R10 (RPMI supplemented with 10% Foetal Calf Serum, Glutamine, and Penicillin/ Streptomycin), with IL-4 and GM-CSF. Immature dendritic cells were harvested on day 5 of culture.

2.1.7 Quantitative PCR mRNA

RNA was extracted from 1 to 3 million cells using Qiagen RNeasy kit (74124) following manufacturers instructions. Reverse transcription 20 µl reaction comprised: 9 µl RNA (at less than 250 ng/µl), 10 µl RT buffer mix, 1 µl enzyme (buffer and enzyme Applied Biosystems High Capacity RNA-to-cDNA kit, 4387406). RT PCR reaction conditions were: 37°C 60 min, 95°C 5 min.

Quantitative mRNA expression was assessed with the TaqMan system, following standard protocols (Applied Biosystems), using primers that cross an exon-exon boundary. In brief, cDNA was diluted to 5 ng/µl in distilled H_2O for use in the qPCR reaction. qPCR 20 µl reaction comprised 9 µl cDNA at 5

ng/µl, 1 µl mRNA-specific Taqman probe, 10 µl Taqman Gene Expression Master Mix (4370048) (Applied Biosystems). GAPDH (Glyceraldehyde 3-phosphate dehydrogenase) served as endogenous reference gene. Relative quantification (RQ) denotes mRNA expression relative to the constant endogenous reference gene GAPDH, calculated by the change in threshold ($\Delta\Delta C_T$) method.

2.1.8 Quantitative PCR microRNA

RNA was extracted from 1 to 3 million cells using Qiagen miRNeasy kit (217004) following manufacturers instructions. Reverse transcription 15 µl reaction comprised: 0.15 µl 100 mM DNTP, enzyme 1 µl, Buffer 1.5 µl, RNase 0.188 µl, miRNA specific primer 3 µl, RNA diluted to 2 ng/µl, H_2O 4.162 µl (reagents supplied by Applied Biosystems Taqman MicroRNA RT kit, 4366597). RT PCR reaction conditions were: 16°C 30 min, 42°C 30 min, 85°C 5 min.

Quantitative PCR was performed employing the TaqMan system, following standard protocols (Applied Biosystems). In brief, cDNA was diluted 1 in 10 in distilled H_2O for use in the qPCR reaction. qPCR 20 µl reaction comprised 1.33 µl cDNA, 7.67 µl H_2O, 1 µl miRNA specific primer, 10 µl Taqman Universal PCR Master Mix (4304437). Non-coding small RNA control RNU44, validated as having stable expression across stimulation conditions, served as an endogenous reference gene. Relative quantification (RQ) denotes miRNA expression relative to the constant non-coding small RNA control RNU44, calculated by the change in threshold ($\Delta\Delta C_T$) method.

2.2 MDDC stimulation and FACS analysis

Immature day 5 DCs were left unstimulated, or stimulated with 1 μg/ml Muramyl Dipeptide (MDP, Invivogen), or 1 μg/ml Pam_3CSK_4 (Invivogen), or both, or with 1 μg/ml lipopolysaccharide (LPS) for 24 hours in R10. DC's were washed in cold PBA (PBS plus 0.5% BSA), and resuspended at 1 million cells per ml. After washing in cold PBA, conjugated antibodies (CD86; CD80; HLA DR; CD14; CD83; Live/ dead stain Efluor 780) were applied for 30 minutes at 4°C. After appropriate washes, 1 million cells from each condition were resuspended in 400 μl of FACS fix (PBS + 1% FCS + 2% paraformaldehyde), and stored in the dark at 4°C until analysed using LSRII flow cytometer. Data were analysed using FloJo.

2.3 NOD2 homozygote Crohn's disease patient selection

Crohn's disease patients who are homozygous, or compound heterozygous, for NOD2 polymorphisms were identified from the Oxford IBD cohort. All patients in the study have predominantly terminal ileal disease (Montreal classification L1 or L3, behaviour B2), and at the time of venesection were in clinical remission; were not on immunomodulators or biological therapy; and were non-smokers.

2.4 NOD2 Genotyping

Buffy Coat and patient samples were genotyped at the major CD-associated NOD2 mutations (R702W, G908R, FS1007insC) as follows: genomic DNA was extracted from blood, or PBMCs, using a Flexigene DNA Extraction Kit (Qiagen cat no. 51206) according to the manufacturers instructions. Regions

of interest were amplified using primers: R702W forward 5'-GAA TTC CTT CAC ATC ACT TTC CAG T -3' and reverse 5'- GTC AAC TTG AGG TGC CCA ACA TT -3'; G908R forward 5'- CCC AGC TCC TCC CTC TTC -3' and reverse 5'- AAG TCT GTA ATG TAA AGC CAC -3'; FS1007insC forward 5'- CTG AGC CTT TGT TGA TGA GC -3' and reverse 5'- TCT TCA ACC ACA TCC CCA TT -3'. PCR products were purified using a PCR purification kit (Qiagen cat no. 28104) prior to sequencing with the primers described above.

2.5 MicroRNA Array

Five million DC's were left unstimulated, or stimulated with 1 μg/ml Muramyl Dipeptide (MDP, Invivogen), or 1 μg/ml Pam_3CSK_4 (Invivogen), or both, for 24 hours at 37°C, 5% CO2, in 5 ml R10. RNA was extracted using Qiagen miRNeasy kit, with a modified protocol to improve RNA quality. Modification involved performing a second separation into aqueous and organic phases by repeated addition of chloroform, prior to placing the aqueous layer on the columns. RNA was quantified using NanoDrop® ND-1000 and RNA quality checked using RNA 6000 Nano Assay on Agilent bioanalyzer 2100. Total RNA was hybridized to Agilent Human Single Colour miRNA arrays, according to standard protocols. MicroRNA expression was analysed using Genespring.

2.6 Quantitative PCR of miRNAs identified by microRNA array

RNA was prepared as for the miRNA array. (In addition experiments were performed using a panel of TLR ligands (Invivogen) including: lipopolysaccharide (LPS) 1 μg/ml; Poly I:C 10 μg/ml; ssRNA 1 μg/ml; CpG

type A ODN2216 1 μM; HKLM 10^8 cells/ ml; FSL-1 1 μg/ml; and flagellin 1 μg/ml.) Reverse transcription to cDNA and subsequent qPCR was performed as per section 2.1.8.

2.7 miRNA Target Prediction and DNA array

Potential targets were identified using TargetScan, MicroCosm, and MiRanda online algorithms. Agilent dual-colour whole human gene expression arrays were employed to identify further targets. For the array, 3 million DCs were nucleofected (section 2.1.5) for 16hrs with miR-29 mimics (either miR-29a PM12499, or miR-29b PM10103 Applied Biosystems, final concentration 50nM), or negative control (AM17110, 50 nM). Cells were subsequently stimulated for 8hrs with MDP and Pam_3CSK_4 1 μg/ml. 3 biological replicates were used. Total RNA was extracted from cell pellets with a miRNeasy Kit (Qiagen), and RNA quality validated as per miRNA array, before array hybridization. Data analysis was performed using Genespring, and genes with fold change >2 identified. In addition Crohn's disease polymorphisms were assessed for fold changes >1.2.

2.8 Quantitative PCR of potential miR-29 targets

Potential targets were validated in DCs following 48hrs nucleofection with miRNA mimic/ premiR (miR-29a PM12499; miR-29b PM10103 Applied Biosystems), or antimiR (miR-29a AM12499; miR-29b AM10103) final concentration 50nM unless otherwise stated, with appropriate negative control (premiR control AM17110; antimiR control AM17010). Where indicated cells were also stimulated with NOD2 +/- TLR ligands for 24hrs. Total RNA was

extracted (miRNeasy, Qiagen). Reverse transcription to cDNA and subsequent qPCR was performed as described in section 2.1.7.

2.9 siRNA confirmation by Western Blot

3 million DCs were transfected with siRNAs, final concentration 5nM as already described (section 2.1.5) (RIPK2 SI02758833; MyD88 SI00300909; NLRP1 SI03097619; MCL-1 SI02781205; ATF2 SI02780309; SMAD3 SI00082481; Qiagen) or non-sense control (AllStar Negative Control, Qiagen) by nucleofection (Lonza). Western blot (section 2.1.4) was used to confirm knockdown using anti-human antibodies: anti-RIPK-2, 1:1000 (4982; Cell Signaling); anti-MyD88, 1:1000 (4283; Cell Signaling); anti-NLRP1, 1:200 (sc-71641; Santa Cruz); and anti-MCL-1, 1:1000 (4572; Cell Signaling); anti-ATF2, 1:1000 (20F1; Cell Signaling); anti-SMAD3, 1:1000 (9523; Cell Signaling).

2.10 miRNA target confirmation by Western Blot

For miRNA target confirmation, 3 million DCs were transfected with miR-29 mimic (premiR) or negative control, as described (section 2.1.5), and where indicated were stimulated with NOD2 +/- TLR ligands. Anti-TBX21, 1:1000 (5214; Cell Signaling); anti-E2F1, 1:1000 (3742, Cell Signaling); anti-ATF2, 1:1000 (20F1; Cell Signaling); anti-SMAD3, 1:1000 (9523; Cell Signaling); anti-MCL1, 1:1000 (4572; Cell Signaling); anti-CDC42, 1:1000 (2466; Cell Signaling); anti-PI3 Kinase p85, 1:1000 (4292; Cell Signaling); anti-A20/TNFAIP3, 1:1000 (4625; Cell Signaling); anti-NLRC4/IPAF, 1:200 (50620; Santa Cruz); anti-TNFRSF1A, 1:100 (ABE493; Autogen); anti-B7H3,

1:2000 (66814; Santa Cruz); anti-TNFSF15, 1:1000 (HPA012948; Sigma); anti-IL-2Rα 1:1000 (5370; Cell Signaling); anti-DNMT3A, 1:1000 (3598; Cell Signaling); anti-TTP, 1:200 (14030; Santa Cruz); anti-CX3CL1, 1:500 (10108-2-AP; ProteinTech); anti-TRAF4, 1:400 (10083-2-AP; ProteinTech); anti-IL-1RAP, 1:1000 (AF676; R&D Systems); anti-Kremen2, 1:500 (ab68906; Abcam); anti-FRP-2, 1:200 (31574; Santa Cruz); anti-DKK1, 1:1000 (4687; Cell Signaling); anti-β-Catenin 1:1000 (9562; Cell Signaling); anti-phosphoβ-Catenin, 1:1000 (9561; Cell Signaling); anti-NFκB p65, 1:1000 (3034; Cell Signaling); anti-phospho-NFκB p65, 1:1000 (3033; Cell Signaling) antibodies were used to confirm change of expression by WB (see section 2.1.4).

2.11 Bacterial Killing Assay

DCs were transfected with MCL-1 siRNA or control, or miR-29a premiR or antimiR or control, for 24 hours (see section 2.1.5). Subsequently $1x10^6$ DCs were infected with AIEC MOI 25:1 for 1 hour before gentamicin was added at 50 μg/ml for 2 hours to eliminate extracellular bacteria. Cells were lysed in 100 μl 1% Triton in PBS for 10 minutes before lysates were plated in triplicate on agar (free of antibiotic) in serial dilutions. Plates were placed at 37°C for 12 hours before colonies were counted. Controls used include: plating supernatant to ensure all external bacteria killed; plating lysed and un-lysed DCs which had no bacteria added to ensure bacterial specificity; plating bacteria alone to ensure their viability; plating bacteria on gentamicin plates at 50 μg/ml to ensure adequate gentamicin concentration. The data were expressed as a ratio of colony numbers on agar plates, comparing MCL-1

siRNA plates with control siRNA plates, or miR-29a premiR or antimiR plates with their appropriate controls.

2.11 ELISA

DCs were stimulated with NOD2 +/- TLR ligands as indicated, +/- miRNA premiRs or antimiRs with appropriate negative controls (transfected as described in section 2.1.5), before supernatants were harvested and stored at -80°C. Supernatants were collected after 48 h transfection unless otherwise indicated. DCs were also transfected with IL-12p40 3'UTR miScript target protector, or negative control, (Qiagen) before stimulation with NOD2 + TLR2 ligands for 24 h. Human IL-12/IL-23p40, IL-6, IL-10, IL-12p70, IL-17, IL-19 and IFNγ Duosets, and Human IL-23 Quantikine ELISA Kit, (R&D Systems) were used following standard protocols.

2.13 Luciferase Reporter Assay

Primers were designed for IL-12/ IL-23p40 3'UTR, and for IL-23p19 3'UTR as follows in **table 2.1**:

3'UTR	Primer - forward	Primer - reverse
IL-12p40	aaacgagctcgctagtaggttctgatccaggatgaaaatttg	gcaggtcgactctagtgattacaaagaagagtttttattagttcagcc
IL-23p19	aaacgagctcgctagggcagcagctcaaggatg	gcaggtcgactctagagccacaaaaataagactttattgaa

Successful PCR was confirmed by restriction enzyme digest before insertion into pmiR-Glo dual-luciferase miRNA target expression vector (Promega), using In-Fusion Dry-Down PCR cloning (Clontech). Cloning was confirmed by restriction enzyme digest and sequencing (primers below). Mutation of the

miRNA seed target sequence in IL-12p40 3'UTR was achieved using primers, forward 5'-cca gaa aat atg gct cca tga att ttc gtc ttt taa gta atg tat gtg cgc-3' and reverse 5'- gcg cac ata cat tac tta aaa gac gaa aat tca tgg agc cat att ttc tgg-3', and QuikChange II XL Site-Directed Mutagenesis Kit (Agilent). Successful mutagenesis was confirmed by sequencing.

HEK293 cells were grown in 6-well plates to 50-60% confluency before co-transfection with 200 ng vector and 25 pmol miRNA (final concentration) mimic or negative control, in triplicate. Two different transfection reagents were tested for miR-29a premiR transfection efficiency, under conditions of co-transfection with the luciferase vector: lipofectamine 2000 (Invitrogen) and Ribojuice + Genejuice (Novagen), as per manufacturers instructions. Lipofectamine was used in subsequent experiments. Cells were harvested at 48 h before luciferase quantification using Dual-Luciferase reporter assay system (Promega), and plate reader.

2.14 3'UTR Sequence Primers, Table 2.2:

Sequence	Forward primer	Reverse primer
All 3'UTR insertions	caggttacaaccgccaagaagc	tatcatgtctgctcgaagcg
IL-12p40 1	gttgccatgggccttcatgc	ctttgcatctgtctgcttctc
IL-12p40 2	gcaatttagggccacttacac	accacaagcacgagccaccac
IL-12p40 3	gacacaggaggatgacacag	tgtacttgcagccttgcttg

2.15 DC + T-cell Co-culture

DCs were prepared as described (section 2.1.6). $CD4^+$ T-cells were negatively selected from the remaining PBMCs using $CD4^+$ T Cell Isolation Kit

II (Miltenyi Biotec). DC's were transfected with miRNA mimic or negative control, as described above, for 8 h before 16 h stimulation with 1 μg/ml MDP + Pam_3CSK_4. $1x10^5$ DCs were co-cultured with $1x10^6$ $CD4^+$ T-cells in 12 well plates, with 100 pg/ml SEB (*Staphylococcus aureus* enterotoxin B). Recombinant IL-23 (1290-IL/CF; R&D, 0.75 ng/ml or 5 ng/ml) or anti-IL23 antibody (AF1716; R&D, 1 μg/ml or 5 μg/ml) were added to selected wells. Culture media and cells were collected/ harvested for ELISA and qPCR.

2.16 CFSE Labelling and FACS analysis

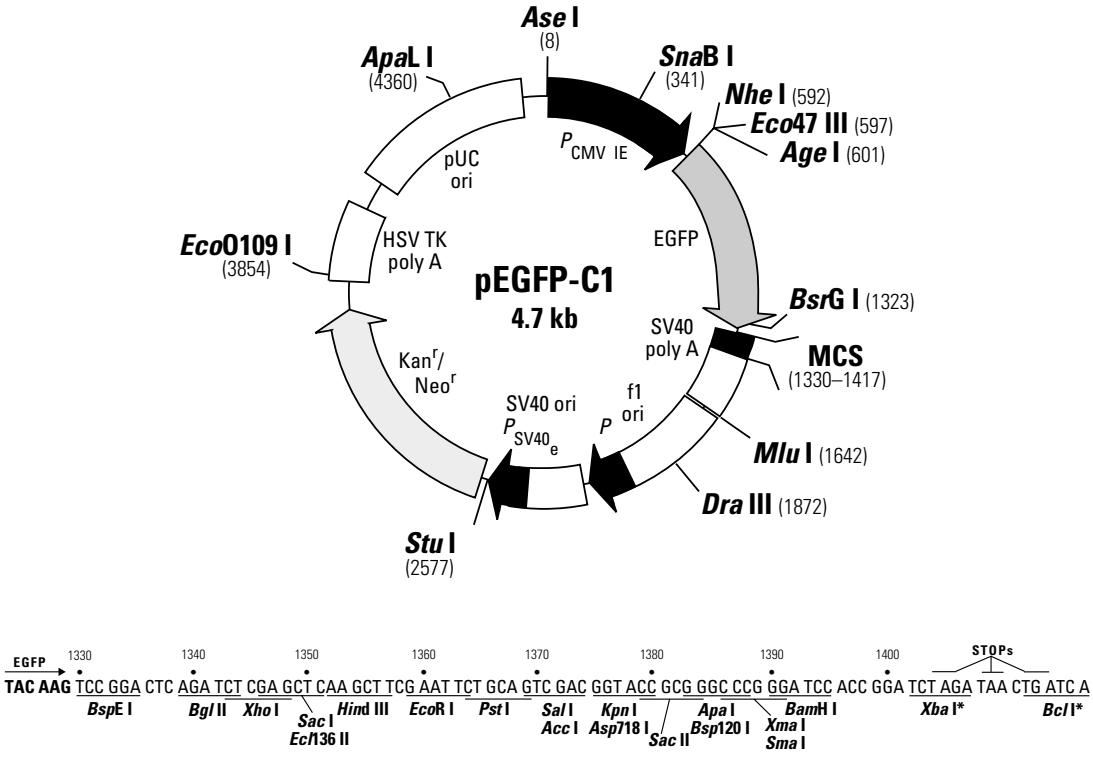
$CD4^+$ T cells were CFSE labelled at 1.25 μM prior to DC co-culture. 1.5 μL Brefeldin A (Golgiplug, BD) was added 4hrs before harvest (in cold PBS) when intra-cellular cytokine staining (ICS) was used. Cells were washed in cold PBA (PBS plus 0.5% BSA), and resuspended at 1 million cells per ml. After washing in cold PBA, cells were surface stained with anti-CD4, 1:100 (317423; Biolegend); anti-CD161, 1:100 (550968; BD Biosciences). Antibodies were applied for 30 minutes at 4°C. For ICS cells were then fixed and permeabilized (BD Cytofix/ Cytoperm) following company protocol and stained with anti-IL17, 1:10 (512306; Biolegend). If not stained intracellularly, cells were washed in cold PBA, and 1 million cells from each condition were resuspended in 400 μl of FACS fix (PBS + 1% FCS + 2% paraformaldehyde), and stored in the dark at 4°C until analysed using LSRII flow cytometer. Data were analysed using FloJo.

2.17 Maxi-prep and linearisation of EGFP-C1

75 μl of competent Escherichia coli (Invitrogen DH5α-T1 Max Efficiency) were transformed with 1 μl DNA of pLP-EGFP-C1vector (Clontech) (see section 2.1.2). A diagnostic digest (see section 2.1.3) was performed using Nhe1 and EcoRI restriction enzymes (New England Biolabs). Run down TBE 1% agarose gel (with ethidium bromide) confirmed the two correct weight fragments. Below is a vector map of EGFP-C1 (**Fig 2.1**).

BglII and Sal1 restriction sites were chosen from within the Multiple Cloning Site (MCS) of EGFP-C1. The restriction enzymes were used as per section 2.1.3, the digested vector ends were dephosphorylated (section 2.1.3), and the DNA frozen at -80°C until the ligation reaction.

Figure 2.1 EGFP-C1 vector map



2.18 PCR of NOD2 from pUNO-NOD2

pUNO-hNOD2a (Invivogen) was purchased and the DNA maxi-prepped in the usual manner (see section 2.1.2). PCR was performed initially following the method described in section 2.1.1. NOD2 PCR primers were designed as primers for Clontech 'in-fusion' method as follows: forward 5'-GTC CGG ACT CAG ATC TAC CAT GGG GGA AGA GGG T -3' and reverse 5'-CCG CGG TAC CGT CGA TCA AAG CAA GAG TCT -3', and they were reconstituted at 10 µM. The optimum PCR conditions with these oligos was 25 µl reactions of: DNTPs 0.5 µl; forward oligo 0.5 µl and reverse oligo 0.5 µl (of 10 µM solutions); enzyme 0.5 µl; buffer 2.5 µl; Mg^{++} 1 µl (to create 1 mM conc); pUNO-NOD2 0.1 µl (concentration 370 ng/µl); H_20 19.4 µl. Optimum PCR reaction was: Step 1 95°C 5minute; Step 2 95°C 30seconds; Step 3 57°C 30seconds; Step 4 72°C 5minute; Go to step 2 for 29 more cycles; Step 5 72°C 5minutes.

The resulting band was gel-purified using Qiagen QIAquick Gel Extraction Kit (cat no. 28704) following the manufacturers instructions, and digested with BstEII restriction enzyme (NEB) (see section 2.1.3).

2.19 PCR of FS1007insC NOD2 from pUNO-NOD2

The following primers were designed so that the stop-codon associated with the Crohn's disease-associated frame-shift mutation (FS1007insC) was inserted in the PCR product at the 1007 position: forward 5'- GTC CGG ACT CAG ATC TAC CAT GGG GGA AGA GGG T -3' as per wild-type NOD2; reverse 5'- CCG CGG TAC CGT CGA TCA AGG GGC CTG CAG GAG GGC

-3'. The same PCR conditions were used (see section 2.18), and the resulting band gel-purified.

2.20 Ligation of NOD2/ FS1007insC NOD2 and linearised EGFP-C1

Ligation was achieved using Clontech 'In-Fusion' 2.0 Dry-Down PCR Cloning Kit, following the manufacturers guidelines. Briefly, the linearised EGFP-C1 and NOD2 PCR-product (using the In-Fusion oligos) were combined in the In-Fusion dry-down eppendorf at molar ratios of 1:1, 2:1, and 3:1, plus a control eppendorf containing solely linearised EGFP-C1. Transformation was performed using Stratagene XL-10 Gold Ultracompetent Cells (200315). The FS1007insC NOD2 PCR-product was ligated in the same way.

2.21 Diagnostic digest and sequencing of NOD2 constructs

BspHI restriction enzyme (NEB) digest cuts both NOD2 EGFPC1 and FS1007insC NOD2 EGFPC1 in 3 places. Digestion (see section 2.1.3) and gel run (see section 2.1.3) was performed, demonstrating the appropriate fragments and negative controls.

I designed sequence oligonucleotides for NOD2 and FS1007insC NOD2 in EGFP-C1 using Primer3 and Amplify software. Sequencing of the appropriate samples was performed, and the sequences analysed using pregap4 and gap4.

2.22 HEK293 Stable Clones

2.22.1 G418 Kill Curve

6-well plates were prepared, within each well there being 5mls D10 plus a range of concentrations of G418 (0.0 mg/ml to 1.2 mg/ml). HEK293 cells were harvested and 1000 cells placed into each well of the 6-well plates. After 14 days the cells were harvested, washed in ice-cold PBS, stained with Trypan Blue Solution and counted.

2.22.2 Stable Transfection and single cell sorting

Calcium phosphate transfection of HEK293 cells was used for the EGFPC1 vector, and both the WT NOD2 and FS NOD2 constructs. In brief, HEK293 cells were grown to 40-60% confluence on 12 cm plates. 30 µg vector DNA were added to 1 ml of 250 mM $CaCl_2$, and incubated at room temperature for 10 min. This was then added drop-wise to 1ml of 2x HBS (Hepes Buffer Saline) and incubated at room temperature for 25 min, before drop-wise addition to the HEK293 cells and incubation overnight at 37°C. 2x HBS per 50 ml H_2O contains: 0.8 g NaCl, 0.596 g Hepes, 0.0106 g Na_2HPO_4, adjusted to pH 7.2.

Transfected cells were then seeded onto 6-well plates, 300,000 cells per well in 5mls D10, and left for 6 hours. G418 was then added at 1.2 mg/ml concentration, and the cells left for 14 days. Cells were filtered to avoid clumping, counted and then serially diluted to 1 cell per 10 µl D10. 10 µl of this was added to each well of 96-well plates prepared with190 µl D10 and G418 (final concentration was 1.2 mg/ml). 5x 96-well plates were prepared for each condition and the plates returned to the incubator.

2.23 Clone Testing

2.23.1 FACS Analysis of GFP expression

The HEK293 cells were harvested and washed in ice-cold PBS. 3 million cells from each condition were resuspended in 400 μl of FACS fix (PBS + 1% FCS + 4% formaldehyde), and stored in the dark at 4°C until analysis using CYAN flow cytometer. Data were analysed using Cytoscape (BD Biosciences) or FloJo.

2.23.2 Western Blot

Appropriate expression of NOD2-GFP and FS1007insC NOD2-GFP was determined by western blot (see section 2.1.4). The membrane was incubated with primary antibodies anti-NOD2 2D9 ab31488 (Abcam) or anti-GFP 11814460001 (Roche), and subsequently an appropriate HRP-conjugated secondary. The ECL reaction was visualised on ECL-sensitive film for exposures ranging from 10 to 120 seconds.

2.23.3 Confocal

HEK293s were harvested after transfection with WT NOD2/ FS NOD2 constructs, and seeded at $2x10^5$ cells/ well onto 8 well poly-D-lysine Tissue Culture Slides (BD Biosciences) and subsequently fixed with 4% paraformaldehyde (wt/vol) for 10 minutes at room temperature. With appropriate washes with PBS/PBA cells were permeabilised with 0.1% Triton X-100 for 7 minutes. HEK293s were stained with anti-NOD2 (Abcam 2D9) overnight at 4°C, and an appropriate secondary added for 2 hours at room temperature (Invitrogen Alexofluor goat anti-mouse IgG 594). To-Pro was added for 10 minutes at 0.025% (vol/vol) in 5% PBA. After staining cells were

washed and coverslips mounted using Vectashield + DAPI (Vector Laboratories). A Radiance 2000 laser-scanning confocal microscope was used for confocal microscopy, with subsequent analysis with LaserSharp 2000 software (Bio-Rad). All images were acquired in sequential scanning mode.

2.23.4 IL-8 ELISA

NOD2-GFP clones were distributed $2x10^5$ cells per well of 96-well plates, and after 12 h were stimulated with 10 μg/ml MDP for 16 h. MDP was added directly to the D10 media. IL-8 elisa was performed using IL-8 Duoset (R&D Systems) according to company protocol. Results are representative of the change in IL-8 secretion compared with unstimulated cells from 3 different experiments.

2.24 NOD2 IP

2.24.1 MAPK 44-42 Phosphoblot

Selected HEK293 cell clones were grown to confluency on 12 cm plates in D10. After stimulation cells were harvested and washed, on ice, in cold HBS (Hepes Buffer Saline) with phosphatase inhibitors (Sigma). (1x HBS per 50 ml H2O contains: 0.4 g NaCl, 0.298 g Hepes, 0.0053 g Na_2HPO_4, adjusted to pH 7.2.)

Cells were lysed in phospholysis buffer (Qiagen) with Chaps detergent for 30 minutes at 4ºC. After centrifugation a Bradford assay was performed and the supernatants adjusted to 0.3 mg/ml. Western blot (see section 2.1.4) was

performed using antibodies to phosphorylated MAPK 44-42, 1:1000 (9101; Cell Signaling), and total MAPK 44-42, 1:1000 (9102; Cell Signaling).

2.24.2 IP conditions

3 stable single cell clones were used: EGFPC1 clone 1, NOD2 EGFPC1 clone E, and FS1007insC NOD2 EGFPC1 clone II. 100 $x10^6$ cells from each condition were left unstimulated, or stimulated with 10 μg/ml MDP for either 10 or 30 minutes. The MDP was added directly to the D10 growth media. Cells were then harvested in cold PBS and lysed immediately with 0.5% NP40 lysis buffer (as per 1% NP40 lysis buffer section 2.1.4). After centrifugation the supernatant was retrieved, a Bradford Protein assay performed (Bio-Rad 500-0205), and the samples diluted to 5 mg/ml concentration. Pre-clear was with 50 μl of agarose G and 50μl of agarose A beads (Sigma-Aldrich EZview) to each sample and rolled at 4°C. Samples were spun at 4000 rpm 4°C, to remove beads. Subsequently 50 μl GFP-Trap-A beads (Chromotek) were added and rolled at 4°C. The beads were washed 3x with 0.05% NP40 plus protease and phosphatase inhibitors (see section 2.1.4), before elution of associated proteins using 200 μl 100 mM glycine pH 2.5. IP conditions were optimised against the resultant silver stains.

2.24.3 Preparation for Mass Spectrometry Analysis

Following methanol/ chloroform precipitation of each sample, in-solution digestion of NOD2-associated proteins was performed. In brief, the sample is evaporated and resuspended in 6 M urea/ 100 mM Tris Buffer, reduced in dithiothreitol (DTT) solution, and then an alkylating reagent added

(iodoacetamide solution). The sample is digested with trypsin, purified over Sep-Pak C18 columns, and finally placed in the speed-vac to dry before resuspension and storage at -20°C until analysis.

2.24.4 Immunoprecipitation Immunoblot

IP samples were prepared in the standard fashion as described above. Subsequently potential candidate members of the NOD2 signalling complex were screened by Western blot (section 2.1.4). Antibodies used were: anti-RIPK-2, 1:1000 (4982; Cell Signaling); anti-β-Arrestin, 1:1000 (4674; Cell Signaling); anti-RACK1, 1:1000 (4716; Cell Signaling); anti-Erbin, 1:500 (55930; Abcam); anti-VASP, 1:1000 (3120; Cell Signaling); anti-Alix, 1:200 (99010; Santa Cruz).

2.25 Statistical Analyses

I used Prism software (GraphPad) to determine the statistical significance in the means of experimental groups. When making multiple comparisons on a data set, analysis was by one-way Anova with Bonferroni post-test. For experiments with two sample groups (one condition, one control) and a single comparison, analysis was by paired, two-tailed Student's t-test.

3 NOD2 control of microRNA expression in human DCs

3.1 Introduction

It is important that PRR signalling pathways, which for example induce effector cytokines, are tightly regulated so that after an initial robust response to eliminate pathogens, homeostasis can be restored thus limiting bystander tissue damage. One way in which that might be achieved is via miRNAs, key regulators of gene expression whose main function is to repress target mRNA levels in mammalian cells.

3.1.1 MicroRNA discovery and function

18 years ago Lee et al[277] described the first microRNA (miRNA) in *Caenorhabditis elegans*, and since then these non-coding RNAs have been described in plants, viruses, and animals. Approximately 20-22 nucleotides in length, they are often conserved across eukaryote species[278]. (For example about 55% of *C. elegans* miRNAs have human homologues[279]). More than 1000 human miRNAs have now been described (miRBase database Version 16), and they are predicted to influence the expression of around a third of the human genome[280].

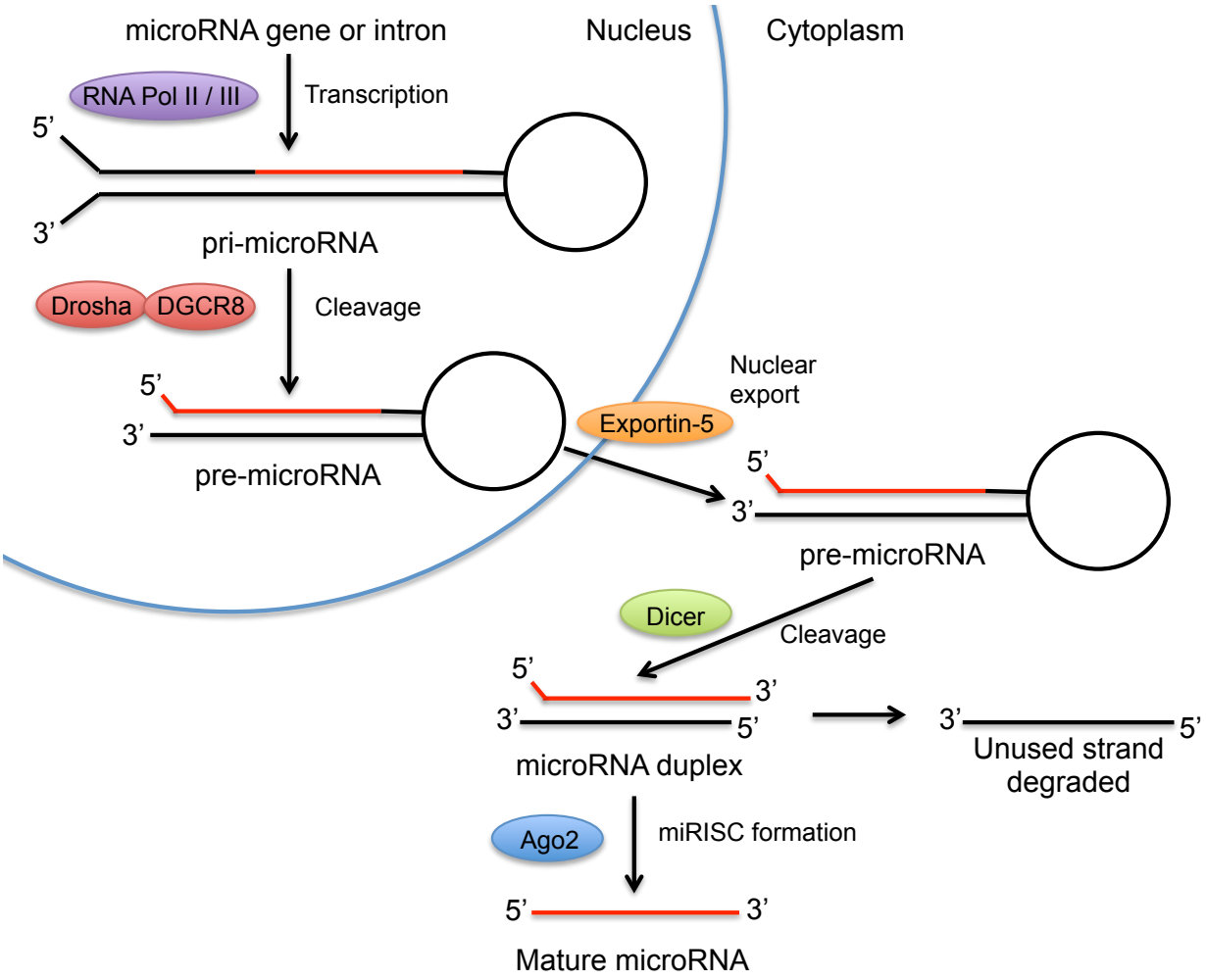
They act as post-transcriptional regulators of messenger RNA (mRNA) by binding to complementary sites in the 3' UTRs of their target gene. Imperfect binding inhibits translation[281,282], whereas perfect/ near-perfect sequence complementarity causes mRNA degradation by increasing the rate of

deadenylation of the poly(A) tail[283]. In general, microRNAs do not completely switch off, but rather fine-tune, protein expression. MicroRNAs with identified functions are predominantly involved in regulating inflammatory responses[284], in initiation or progression of cancer[285], or in cell proliferation or death[286].

3.1.2 MicroRNA genesis

MicroRNA transcription can be initiated via RNA polymerase II (Pol II), or less commonly Pol III, producing primary miRNAs (pri-miRNA) which contain both a 5' cap and poly(A) tail and are up to several kilobases in length[287-289]. The pri-miRNA is then processed by Drosha (a member of RNase III family) and its cofactor DGCR8, to release a ~70bp hairpin-shaped pre-miRNA[290-292]. This step defines the miRNA sequence within the pre-mRNA by generating one end of the molecule. The pre-miRNA is then exported into the cytoplasm by exportin-5 (a nuclear transport factor)[293-295]. Once there the pre-miRNA is processed further by Dicer, a cytoplasmic RNaseIII, to generate ~22 nt miRNA duplexes[296,297]. One strand of this remains as a mature miRNA, and is assembled, along with Ago2 (Argonaute 2), into the miRNA-induced silencing complex (miRISC)[298,299], which is guided by the miRNA through base pairing to the target mRNA. See **Figure 3.1**.

Figure 3.1 microRNA genesis (See text section 3.1.2)



3.1.3 MicroRNA Clustering

MicroRNA genes, which interestingly may reside in introns and intergenic regions, can either exist as single units, or are organised into clusters. Clustered miRNAs often have related functions and are transcribed together. For example, the miR-17-92 cluster resides on chromosome 13 and encodes 6 different miRNAs, some of which have identical seed sequences, and which together regulate components of functionally interrelated pathways involved in cell cycle progression and apoptosis[300]. It is also possible to identify families of miRNAs, which are not clustered, with similar 5' seed sequences.

Mature vertebrate miRNAs can potentially bind approximately 200 mRNAs and thus regulate a large number of genes[301]. Conversely the 3'UTRs of mRNA target genes often contain scores of binding sites for unrelated miRNAs. This obviously raises the question both of the cooperative action of miRNAs (miR-17-92 cluster example described above), and also of functional redundancy between miRNAs.

3.2 MicroRNAs and Innate Immunity

Given that microRNAs are able to post-transcriptionally regulate protein expression, it is perhaps unsurprising that these small molecules have a role in the complex control of inflammation. This is a role to which they are perhaps well suited given that significant expression is often induced many hours after any pro-inflammatory stimulus, allowing an initial robust immune response against the infective agent before any subsequent reduction in inflammation. Recent studies have indicated that stimulation of PRRs, specifically toll-like receptors, affects miRNA expression, and that this indeed aids control of innate immunity. Moreover, murine models with Dicer-specific knockouts have recently demonstrated the diverse roles of miRNAs in the intestine including in immune homeostasis via epithelium to T cell crosstalk[302], and in the development and survival of gastrointestinal smooth muscle[303].

miRNAs are therefore of interest when considering the pathogenesis of inflammatory conditions such as Crohn's disease, and the role of NOD2. Below I detail the main miRNAs described thus far that are stimulated by PRRs, and/or that modulate innate immune function.

3.2.1 miR-155

The roles of miR-155 are diverse, with involvement in haematopoiesis, T and B cell differentiation and function, and in the innate immune system. The most striking demonstration of this comes from the miR-155 null mouse, in which the miR-155-containing portion of exon 2 of the Bic gene is deleted[304]. (Mouse models of other miRNAs are more challenging, as there are often multiple miRNA gene copies, or other miRNAs share seed sequence and function.) These mice have defects in B and T cells, and DCs (which have defective antigen presentation), and this is manifest for example in a poor protective immune response to live attenuated *S. typhimurium* vaccine. Interestingly the gross phenotype of the miR-155 null mice includes not only lung fibrosis, but also intestinal inflammation.

It is not yet clear whether miR-155 predominantly behaves as a negative regulator of immune activation, because some data clearly demonstrates targets by which it may amplify inflammation, and as ever this is probably context dependent. Increased miR-155 expression in myeloid cells after TLR stimulation was described by two studies from the same group[284,305]. They demonstrate that miR-155 expression is up-regulated by TLR2, 3, 4 and 9 ligands, as well as by TNFα and IFN-β stimulation. The c-Jun N-terminal kinase (Jnk) pathway and the MAPK pathway are involved respectively in the induction, and regulation of the levels, of miR155.

As one might expect for an expression profile like this, miR-155 has been shown to target a number of TLR signalling proteins. In MDDCs, this includes TAB2 (TGF-beta activated kinase 1), an adaptor of the TLR/ IL-1 signalling cascade, and through this miR-155 functions as a negative regulator of IL-1β

production[306]. MyD88 is also a demonstrated target of miR-155 in two studies, one examining H. pylori infection in human epithelial cell lines[307], and the other the effect of LDL (low-density lipoprotein) in macrophages[308]. Furthermore, inhibition of miR-155 produces enhanced LPS-induced expression of pro-inflammatory cytokines and chemokines in murine macrophages [309].

Another study using murine macrophages, whose focus was endotoxic shock, showed up-regulation of miR-155 on LPS stimulation, and down-regulation after 30 minutes treatment with TNFα[310]. An anti-inflammatory role for miR-155 was suggested by the identification of IKKε as a potential target, this being a kinase that favours NFκB activation. Other possible targets identified were FADD and RIPK-1, proteins involved in TLR4-signalling post LPS stimulation[310]. However, mice over-expressing miR-155 were actually found to be *more* susceptible to LPS-induced endotoxic shock, highlighting that the control by miR-155 of innate immunity is not fully understood.

The temporal nature of expression may be the key factor in understanding this apparent contradiction, although miR-155 targets that would potentially increase inflammation have been described. For example, a pro-inflammatory role in macrophages has been demonstrated[311] through the miR-155 target Src homology-2 domain-containing inositol 5-phosphatase 1 (SHIP1), a negative regulator of macrophage activation. Also, miR-155 targets suppressor of cytokine signalling 1 (SOCS1)[312]. These targets no doubt contribute to the miR-155-dependent expression of pro-inflammatory cytokines such as TNFα, IL-6, IL-23 and type 1 interferons[312,313]. It may be that miR-155 helps to maintain immune activation in an optimal state, by both

enhancing activation and also ensuring it does not breach a pathogenic threshold.

Lastly, miR-155 can affect the expression of PRRs. In MDDCs, through the transcription factor PU.1, miR-155 down-regulates the expression of DC-SIGN (DC-specific intracellular adhesion molecule-3 grabbing nonintegrin)[314], a c-type lectin receptor expressed on DCs and macrophages. Low DC-SIGN expression, occurring on miR-155 up-regulation, reduces the capacity of the DCs to bind to yeasts (*C. albicans*) and gp120, an HIV envelope protein.

3.2.2 miR-146a

As with miR-155, the stimulation of monocytes/ macrophages through TLR4 and other TLRs (TLR2 and TLR5, although interestingly not intracellular TLRs), results in robust up-regulation of mature miR-146a[284]. NF-κB was shown in this and another study[315] to have a critical role in the induction of miR-146a. Two important targets for this miRNA are IRAK-1 (IL-1 receptor-associated kinase 1) and TRAF6 (TNF receptor-associated factor 6), adaptor molecules both involved in TLR and IL-1 receptor signalling. 3'UTR luciferase reporters have confirmed that miR-146a down-regulates their expression[284], and through this it is likely that miR-146a acts as a negative regulator of the innate inflammatory response. For example, a study using THP-1 cells has determined that miR-146a plays an important role in maintaining LPS-induced tolerance in relation to TNFα production[316]. Interestingly, miR-146a has also been shown to have an important role in promoting intestinal tolerance in neonatal mice[317].

IRAK-2 has also been described as a miR-146a target. miR-146a is up-regulated through RIG-I triggering by viral infection, and contributes to the down-regulation of the type I IFN response by targeting IRAK-1, IRAK-2 and TRAF6[318].

3.2.3 miR-145

MAL (MyD88 adaptor-like protein), another bridging adaptor for TLR2- and TLR4-mediated MyD88 signalling, is targeted by miR-145. miR-145 has recently been found to be one of two miRNAs, along with miR-146a, deleted in a common subtype of myelodysplastic syndrome (MDS)[319]. The loss of these miRNAs contributes to the phenotype seen in 5q-syndrome, although it has not yet been demonstrated that miR-145 (like miR-146a) is up-regulated by PRR triggering.

3.2.4 miR-9

miR-9 is the only identified miRNA up-regulated in both human neutrophils and monocytes in response to LPS. Expression is also elicited in response to TLR2, and 7/8 ligands, as well as TNFα and IL-1β[320]. LPS induced expression of miR-9 is dependent on MyD88 and NFκB, and appears to target NFκB1, suggesting that this miRNA also operates negative feedback control on the TLR4-induced, NFκB-dependent, innate immune response. As this miRNA targets a transcription factor, rather than a specific signalling molecule, it will potentially have a more global mediating effect on the immune response.

3.2.5 miR-27b

Transcription factor targeting has also been observed for this miRNA. PPARγ1 (peroxisome proliferator-activated receptor γ1) is expressed in macrophages and has anti-inflammatory effects, such as suppressing nitric oxide synthase and NFκB-driven pro-inflammatory cytokines[321,322]. LPS-induced suppression of PPARγ1 is partly driven by early (from 2 to 6h) up-regulation of miR-27b[323], and thus this miRNA has a role in *amplifying* the initial immune response. This again highlights the importance of understanding the temporal nature of miRNA expression, and its relation to control of the immune response.

3.2.6 miR-147

In murine macrophages there is increased expression of this miRNA after TLR2, 3 and 4 stimulation, with the latter being the most potent, and induction being both MyD88 and TRIF dependent[324]. An inverse relationship between miR-147 expression and inflammatory cytokine production (IL-6 and TNF-α) suggests that this miRNA also forms part of the negative feedback on TLR-induced inflammatory response.

3.2.7 miR-21

Expression of this miRNA is induced by LPS treatment of human mononuclear cells, and targets the protein PDCD4 (programmed cell death 4) [325]. PDCD4, which has an NFκB-binding site in its promoter, acts as a pro-inflammatory protein partly through suppressing IL-10, and partly through enhancing TNFα-induced NFκB activation. miR-21 up-regulation therefore results in reduced NFκB activity and increased IL-10 production.

miR-21 is also predicted to directly target the 3'UTR of IL-12p35 subunit, and shown in luciferase assays to do so[326].

3.2.8 Let-7

The Let-7 family of miRNAs are highly conserved across species and were the first human miRNAs to be discovered. They have a role in regulating the expression of PRRs, specifically TLR4, as was demonstrated using cultured human cholangiocytes[327]. Infection of these cells with a parasite that causes biliary and intestinal disease (*Cryptosporidium parvum*) results in decreased expression of mature let-7 in a MyD88/ NFκB dependent manner, and subsequent up-regulation of TLR4. The role of Let-7 as a regulator of TLR4 was also in part demonstrated in experiments on LPS-treated macrophages from $Akt1^{-/-}$ mice[328]. Akt1 is a serine threonine kinase activated by PI3K, with the ability to suppress MAPK and NFκB activation in macrophages and dendritic cells. $Akt1^{-/-}$ LPS-treated macrophages fail to induce Let-7e, and have increased expression of miR-155, which leads to an inability to down-regulate TLR4, and decreased expression of SOCS1, respectively. These cells are thus hyper-responsive to LPS with an inability to tolerise.

These two studies demonstrate a cell-specific difference in miRNA expression. Epithelial cells would likely need to enhance their pro-inflammatory potential during an infection by down-regulating Let-7i, whereas macrophages that constitutively express high levels of TLR4 would need to induce Let-7e in order to dampen and control the immune response. Let-7 is also predicted to directly target the 3'UTR of IL-6, and has been shown to down-regulate IL-6 in a study on breast cancer transformation[329]. Since Let-7

can be down-regulated by TLR triggering in epithelial cells, this raises the possibility that this is an important amplification step in TLR-induced IL-6 secretion, and a mode of IL-6 control in macrophages, but again this may well be cell-specific.

3.2.9 miR-125b

Endotoxic shock was the main focus of a study using mice and murine macrophages[310]. They found that in response to LPS, macrophages in vitro, and splenocytes in vivo, down-regulate miR-125b. In contrast, 30 minutes of TNFα stimulation up-regulated miR-125b, with expression returning to pre-stimulation levels after 1 hour. Their results suggest that miR-125b directly targets TNFα, with adequate TNFα production dependent on initial miR-125b down-regulation.

3.2.10 miR-132

Vagal secretion of acetylcholine can suppress peripheral inflammation by abrogating cytokine production as part of the post-inflammatory response. Shaked et al[330] demonstrated that LPS treatment of murine splenocytes down-regulates acetylcholinesterase (AChE). LPS also induces miR-132 expression[284]. This miRNA targets the mRNA encoding AChE, potentiating the anti-inflammatory effects of acetylcholine, and this identifies miR-132 as a regulator of the neuro-immune axis. Transgenic mice that express AChE devoid of its 3'UTR are impaired in their cholinergic anti-inflammatory regulation, and have both higher basal levels of circulating IL-1β and IL-6, and excessive pro-inflammatory production on LPS challenge[330].

3.2.11 Summary

The induction of innate immunity needs to be tightly controlled so that pathogens are detected and destroyed, and so that there is limited bystander damage to local tissues.

Although the mechanisms described by which microRNAs contribute to this innate immune control are varied, there are some common themes. For example, many of those miRNAs identified thus far predominantly appear to be negative regulators of inflammation, and are often induced some hours after PRR triggering. Notable exceptions include miRNAs such as miR-27b, and in certain cells Let-7, which are rapidly up- or down-regulated respectively in order to enhance an initial immune response. miRNA induction through TLR4 stimulation with LPS is also a frequent finding, no doubt reflecting both that this strong immune stimulant produces changes in miRNA expression that are more easily detectable by current methods, and that the pro-inflammatory pathways induced require powerful counterbalancing.

These microRNAs are likely to be only a proportion of those involved in immune function, and many questions remain largely unanswered. Some of these questions surround the governance of miRNA expression and function, and the mechanisms involved. Further we don't know if, once expressed, microRNAs inhibit protein expression of all of their potential mRNA targets equally, or if some targets predominate depending on the stimulus, timing, or cell type. Although we have begun to identify miRNAs elicited through single TLR stimulation, we have yet to understand expression through multiple PRR

triggering, for example in combination with NLRs, and the overall effect of miRNA co-expression.

We hypothesized NOD2 might modulate miRNA expression to down-regulate inflammatory responses induced following receptor stimulation, and that NOD2 variants associated with Crohn's might be deficient in this process, leading to inadequate arrest of anti-microbial effectors at the end of an immune response. In this chapter I demonstrate that NOD2 can regulate miRNA expression in human DCs. Of particular interest, NOD2 is required for induction of the miRNA family 29a, 29b, 29c and induces this family alone and synergistically with TLR2 or TLR5. This induction requires RIPK-2 but not MyD88, and is lost in the presence of CD-associated NOD2 polymorphisms.

3.3 Aims

The aim of this chapter is to determine:

- Whether NOD2 stimulation induces miRNA expression in human DCs.
- The degree to which NOD2+TLR co-triggering is involved in miRNA induction.
- Whether wild-type NOD2 function is required for miRNA expression.

3.4 Results

3.5 Genotyping

Figure 3.2 gives an overview of the miRNA experiment in human DCs. To ensure that the healthy donor monocyte-derived dendritic cells (MDDCs) do not carry NOD2 polymorphisms the samples are genotyped **(Fig. 3.3)**. PCR is used to amplify and sequence samples at the three major NOD2 CD-

associated single nucleotide polymorphisms (SNPs). Where cells are used from CD-patients in the Oxford IBD Cohort, the results of my genotyping has matched that previously obtained.

Figure 3.2: miRNA Experiment Protocol

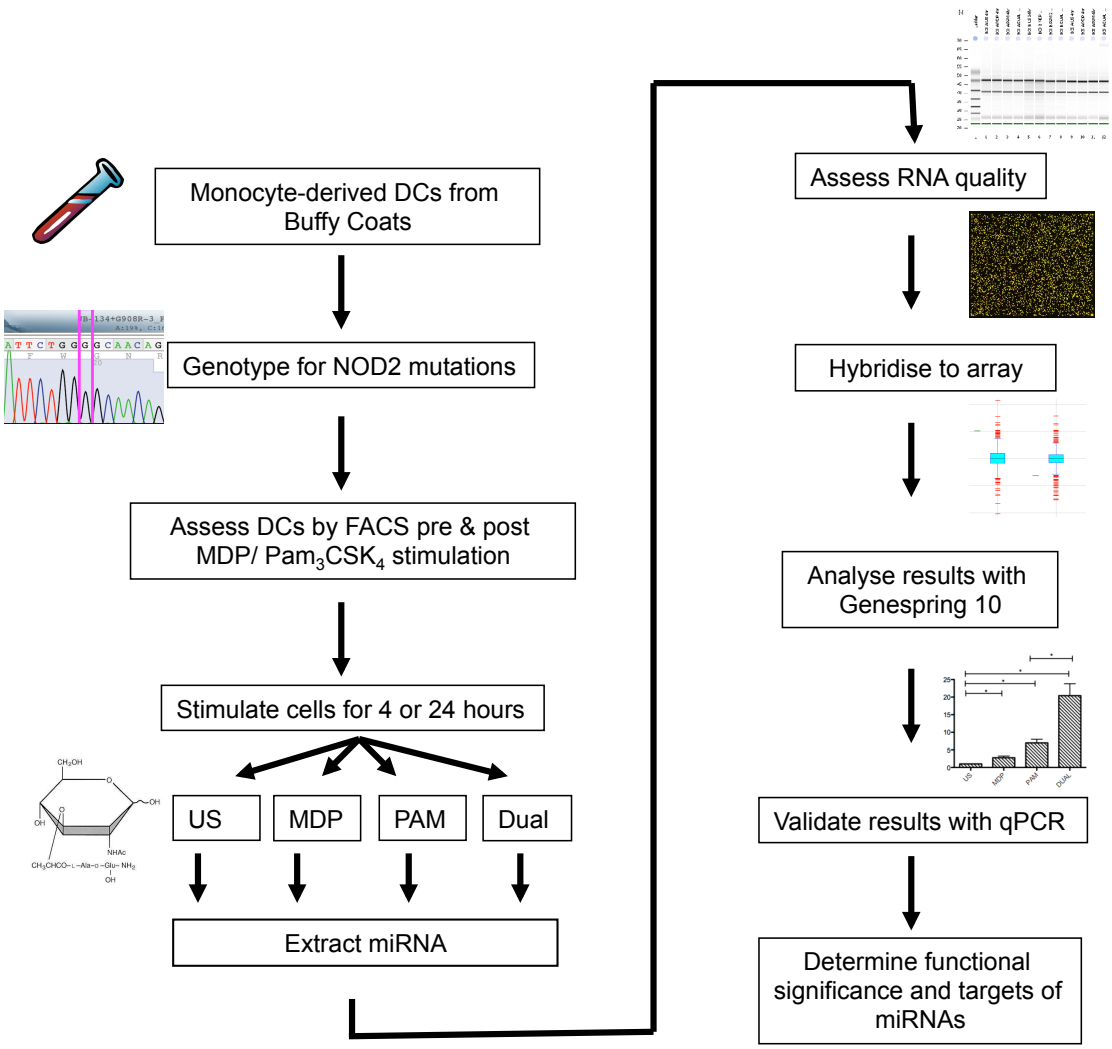


Figure 3.3: NOD2 Genotyping

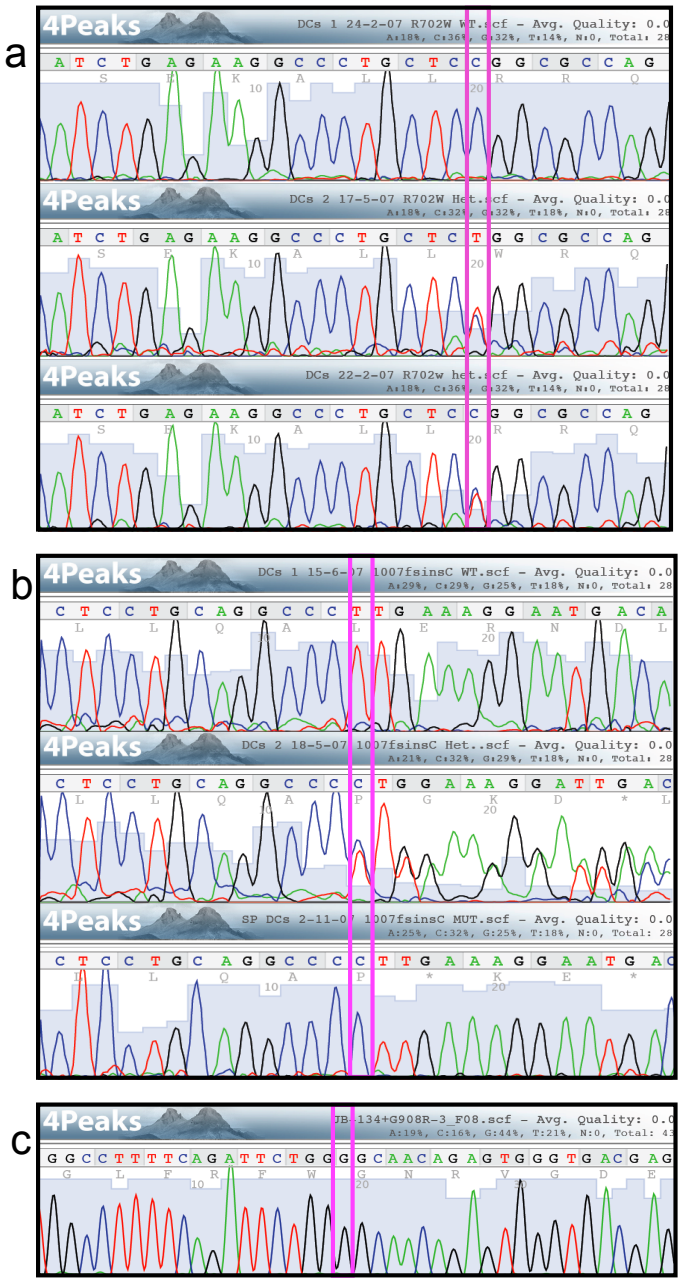


Figure 3.3 Conventional Genotyping of NOD2 mutations

Genomic DNA was extracted from 1ml buffy coat, using Flexigene DNA extraction kit (Qiagen). Regions of interest containing the three major CD-associated NOD2 mutations, R702W, G908R, and 1007fsinsC, were amplified by PCR . The results were PCR purified and sequenced bi-directionally. Typical results are shown: **a) R702W** from top to botttom: wild-type (C) homozygote, and two heterozygotes (C/T). **b) 1007fsinsC** from top to bottom: Wild-type homozygote (T), heterozygote cytosine frame-shift insertion, and homozygote frame-shift insertion. **c) G908R** homozygote (G instead of C).

3.6 Initial Stimulation of Dendritic Cells, and Validation of Conditions

MDDCs were stimulated with MDP, TLR2 ligand Pam_3CSK_4, MDP plus Pam_3CSK_4, or TLR4 ligand LPS, and FACS analysis used to confirm appropriate up-regulation of DC activation markers CD83, CD86 and HLA-DR **(Fig. 3.4)**. A 27-plex cytometric bead array to measure cytokine production by

human MDDCs under the same stimulation conditions has also been performed in our lab (J Baker). This demonstrated broadly synergistic responses in cytokines through NOD2+TLR2, including TNFα and IFN-γ, in keeping with published data (data not shown).

Figure 3.4: DC characterisation by FACS

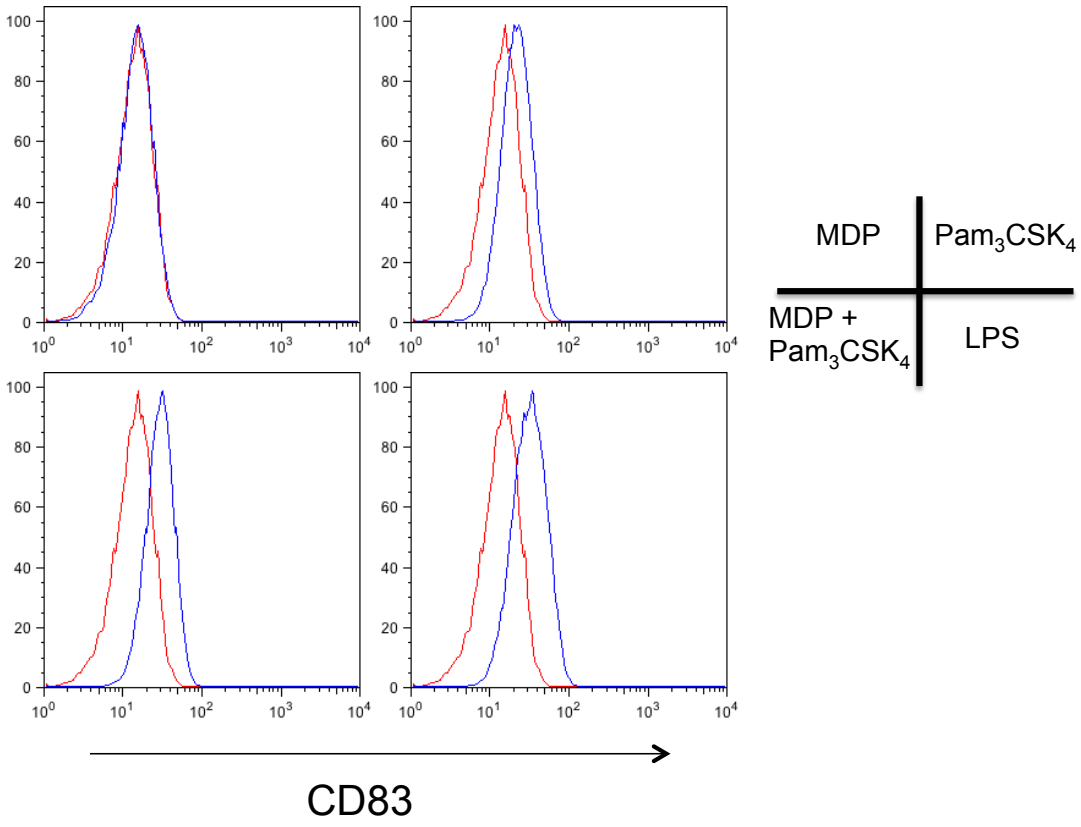


Figure 3.4 One million DCs were left unstimulated (blue), or stimulated (red) with Muramyl Dipeptide (MDP), Pam_3CSK_4, MDP plus Pam_3CSK_4 or lipopolysaccharide (LPS) all at 1 µg/ml for 24 h before harvest. DC's were washed in cold PBA, and stained with conjugated antibodies (CD86; CD80; HLA DR; CD14; CD83; Live/ dead stain) applied for 30 minutes at 4°C. After appropriate washes, and fixation, data were collected using LSRII flow cytometer and analysed using FloJo software. After gating on live CD14 positive cells, CD83 is shown (representative of both CD83 and CD86 up-regulation).

3.7 microRNA Microarray: NOD2 affects miRNA expression in DCs

Five million immature MDDCs from healthy donors were left unstimulated or stimulated for 4 or 24 hours with MDP, Pam_3CSK_4, or dual stimulation. mRNA was extracted using miRNeasy (Qiagen). Here the protocol was modified to improve mRNA quality. RNA was quantified and initial quality checked by nanodrop **(Fig. 3.5a)**, and subsequently RNA quality was checked using RNA 6000 Nano Assay on Agilent bioanalyzer 2100 **(Fig. 3.5b)**.

Figure 3.5: mRNA Preparation for miRNA Array

a

User ID	Date	Time	Conc.	Units	260/280	260/230	SDV	RIN
BC2 B US 4hr	29/5/09	13:49	147.9	ng/ul	2.05	1.69	1.3	9.5
BC2 B MDP 4hr	29/5/09	13:49	158.4	ng/ul	2.05	1.85	1.5	8
BC2 B PAM 4hr	29/5/09	13:49	151	ng/ul	2.07	1.9	2.1	7.6
BC2 B DUAL 4hr	29/5/09	13:49	161.9	ng/ul	2.08	1.72	2.3	9.7
BC2 A US 24hr	29/5/09	13:49	154.5	ng/ul	2.06	1.62	2.8	9.4
BC2 A MDP 24hr	29/5/09	13:49	170.4	ng/ul	2.06	1.88	2.8	9.3
BC2 A PAM 24hr	29/5/09	13:49	152.8	ng/ul	2.07	1.65	3.6	9.4
BC2 A DUAL 24hr	29/5/09	13:49	162.2	ng/ul	2.05	1.85	3.4	9.4
BC3 A US 4hr	29/5/09	13:50	265.8	ng/ul	2.08	1.98	3.7	9.5
BC3 A MDP 4hr	29/5/09	13:50	263.1	ng/ul	2.1	1.9	3.5	8.2
BC3 A PAM 4hr	29/5/09	13:50	241.8	ng/ul	2.1	1.93	3.4	9.7
BC3 A DUAL 4hr	29/5/09	13:50	243.3	ng/ul	2.1	1.83	3.7	9.7
BC3 A US 24hr	29/5/09	13:50	277.4	ng/ul	2.09	1.78	3.7	8.8
BC3 A MDP 24hr	29/5/09	13:50	324.9	ng/ul	2.09	1.93	4.5	9.7
BC3 A PAM 24hr	29/5/09	13:50	294.6	ng/ul	2.09	1.99	3.2	8.5
BC3 A DUAL 24hr	29/5/09	13:50	316.9	ng/ul	2.08	2.05		9.6
BC6 B US 4hr	29/5/09	13:51	312.1	ng/ul	2.08	1.97	2.7	9.6
BC6 B MDP 4hr	29/5/09	13:51	208	ng/ul	2.06	1.85	2.7	9.4
BC6 B PAM 4hr	29/5/09	13:51	202.4	ng/ul	2.08	1.95	2.9	9.6
BC6 B DUAL 4hr	29/5/09	13:51	226.3	ng/ul	2.08	1.78	2.6	9.7
BC6 B US 24hr	29/5/09	13:51	232.6	ng/ul	2.09	2.03	6.1	8.8
BC6 B MDP 24hr	29/5/09	13:51	285.5	ng/ul	2.1	1.93	3.5	8.4
BC6 B PAM 24hr	29/5/09	13:51	290.8	ng/ul	2.09	2.1		9.2
BC6 B DUAL 24hr	29/5/09	13:51	297.9	ng/ul	2.09	2.02	2.9	9
BC8 A US 4hr	29/5/09	13:51	198.4	ng/ul	2.08	1.98	1.8	9.4
BC8 A MDP 4hr	29/5/09	13:51	173	ng/ul	2.07	1.61	3.1	9.2
BC8 A PAM 4hr	29/5/09	13:51	205.9	ng/ul	2.08	1.84	3.5	9.3
BC8 A DUAL 4hr	29/5/09	13:51	212.9	ng/ul	2.09	2.06	2.8	9.4
BC8 B US 24hr	29/5/09	13:51	137.7	ng/ul	2.06	1.78	4.7	8.8
BC8 B MDP 24hr	29/5/09	13:51	169.2	ng/ul	2.07	1.85	4.2	8.6
BC8 B PAM 24hr	29/5/09	13:51	243.1	ng/ul	2.09	1.99	2.2	9.5
BC8 B DUAL 24hr	29/5/09	13:51	226.9	ng/ul	2.09	1.94	1.8	9.2

b

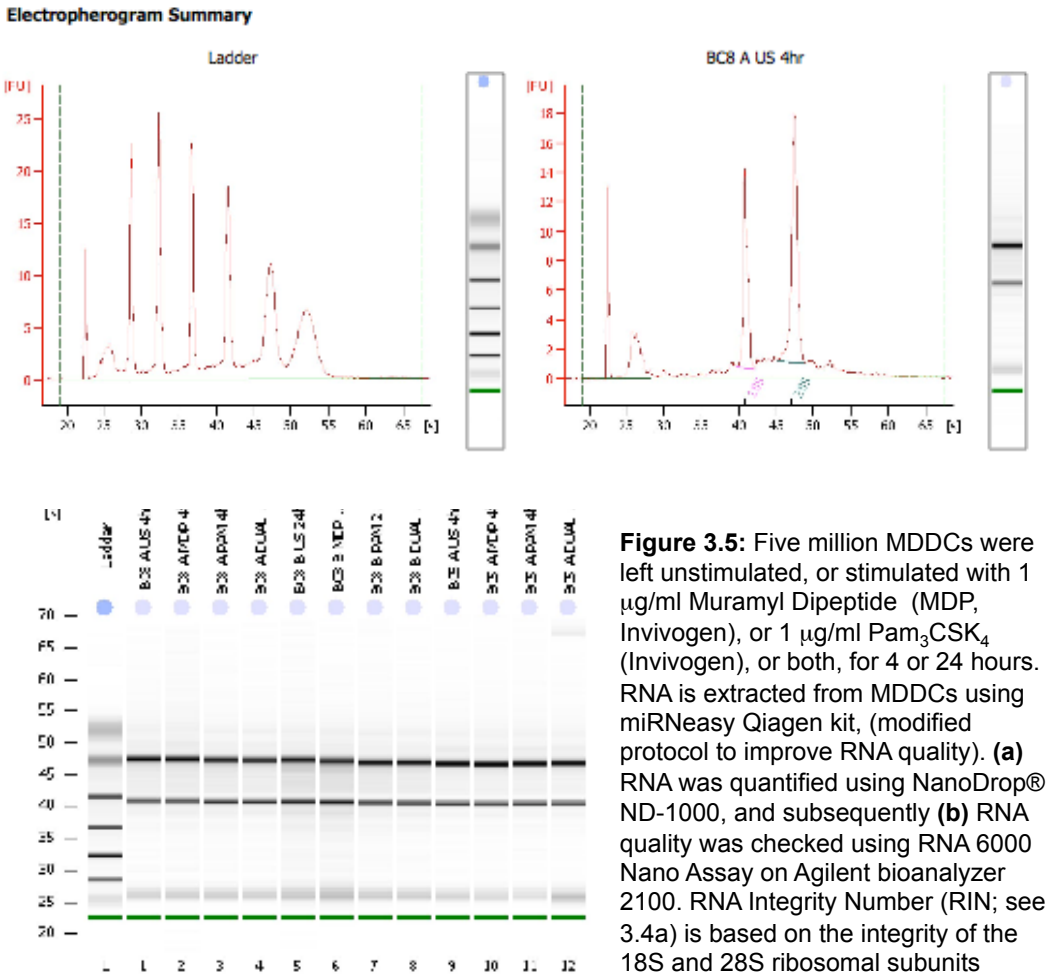


Figure 3.5: Five million MDDCs were left unstimulated, or stimulated with 1 μg/ml Muramyl Dipeptide (MDP, Invivogen), or 1 μg/ml Pam_3CSK_4 (Invivogen), or both, for 4 or 24 hours. RNA is extracted from MDDCs using miRNeasy Qiagen kit, (modified protocol to improve RNA quality). **(a)** RNA was quantified using NanoDrop® ND-1000, and subsequently **(b)** RNA quality was checked using RNA 6000 Nano Assay on Agilent bioanalyzer 2100. RNA Integrity Number (RIN; see 3.4a) is based on the integrity of the 18S and 28S ribosomal subunits demonstrated on the bioanalyzer, and the absence of degraded RNA 'noise'. It is calculated using the Agilent bioanalyzer 2100 software. A value of 8 or above (maximum is 10) denotes RNA of sufficient quality for the array.

The highest quality mRNA was hybridised to Agilent Human Single Colour miRNA arrays (four biological replicates in all). miRNA microarrays represented 866 human and 89 human viral miRNAs sourced from Sanger miRBase (release 12.0). On NOD2 triggering alone I observed very little differential regulation of miRNAs; only miR-29 was induced **(Table 3.1)**. By comparison, stimulation of TLR2 with Pam_3CSK_4 led to robust differential

regulation of miRNAs with strong induction of miR-155 and miR-146 previously described as being induced on TLR triggering[284,305] and DC maturation[306] **(Table 3.1)**. NOD2 has previously been shown to cross talk with TLR2, and as both these PRRs recognize different components of peptidoglycan it is likely they would normally be co-triggered on bacterial recognition. I compared the results of single triggering of either NOD2 or TLR2 with that occurring on dual stimulation with MDP and Pam_3CSK_4. This led to increased (synergistic) differential regulation of a number of miRNAs regulated by TLR2 alone and in addition greatly increased induction of miR-29 induced by NOD2 **(Table 3.1)**. Furthermore I observed differential expression of a number of new miRNAs not observed with single TLR2 or NOD2 activation **(Table 3.1)** emphasizing the ability of NOD2 to cross-talk with other PRRs.

Figure 3.6: miRNA Array Results

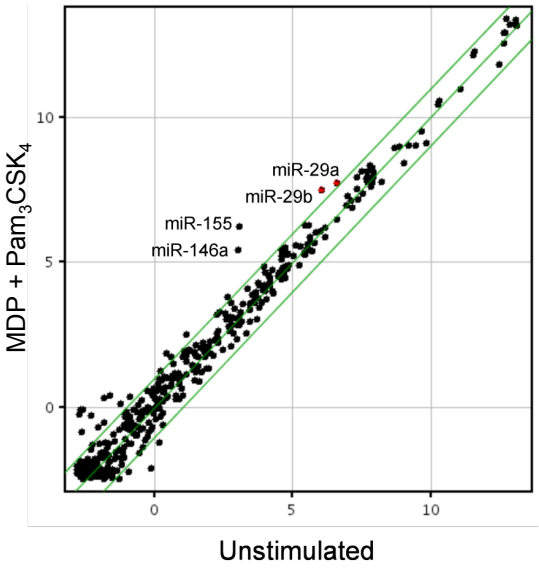


Figure 3.6: Total RNA was hybridized to Agilent Human Single Colour miRNA arrays, and microRNA expression was analysed using Genespring.
Dot plot shows miRNAs more than 2 fold up-regulated by dual stimulation, compared with unstimulated DCs.

Table 3.1 Table of all miRNAs > 1.5 fold differentially regulated at 24 h compared with unstimulated DCs, after single ligand or dual (MDP + Pam_3CSK_4) ligand stimulation. Statistical analysis $p<0.05$ by T-test vs unstimulated condition. Data are from 4 biological replicates for array.

Table 3.1

Stimulation Conditions					
MDP		**Pam3CSK4**		**MDP + Pam3CSK4**	
Up-regulated	**Fold**	**Up-regulated**	**Fold**	**Up-regulated**	**Fold**
hsa-miR-29b-1*	1.81	hsa-miR-146a	7.01	hsa-miR-155	15.1
		hsa-miR-155	6.68	hsa-miR-146a	8.70
		hsa-miR-505	1.84	hsa-miR-155*	5.76
				hsa-let-7e	4.28
				hsa-miR-29b-1*	3.46
				hsa-miR-147b	2.85
				hsa-miR-34a	2.66
				hsa-miR-505	2.64
				hsa-miR-29b	2.61
				hsa-miR-29a	2.56
				hsa-let-7i	2.34
				hsa-miR-193a-3p	2.25
				hsa-miR-132	2.20
				hsa-miR-16	2.08
				hsa-miR-151-5p	1.90
				hsa-miR-652	1.82
				hsa-miR-34b*	1.64
Down-regulated	**Fold**	**Down-regulated**	**Fold**	**Down-regulated**	**Fold**
		hsa-miR-629	6.30	hsa-miR-513b	3.61
		hsa-miR-202	2.33	hsa-miR-1181	2.59
		hsa-miR-513b	2.37	hsa-miR-572	2.52
		hsa-miR-663	2.00	hsa-miR-1207-5p	2.40
		hsa-miR-630	1.90	hsa-miR-1915	1.87

3.8 qPCR Analysis of miRNA Results

RNA was generated from human MDDCs stimulated as per array conditions. MicroRNA-specific primers were used (Applied Biosystems) for both the reverse transcription (RT) and quantitative PCR (qPCR) reactions. The expression of the non-coding small RNA controls (RNU6b and RNU44) were first validated as being unchanged by the stimulation conditions **(Fig. 3.7)**.

Figure 3.7 qPCR Reference Control Assessment

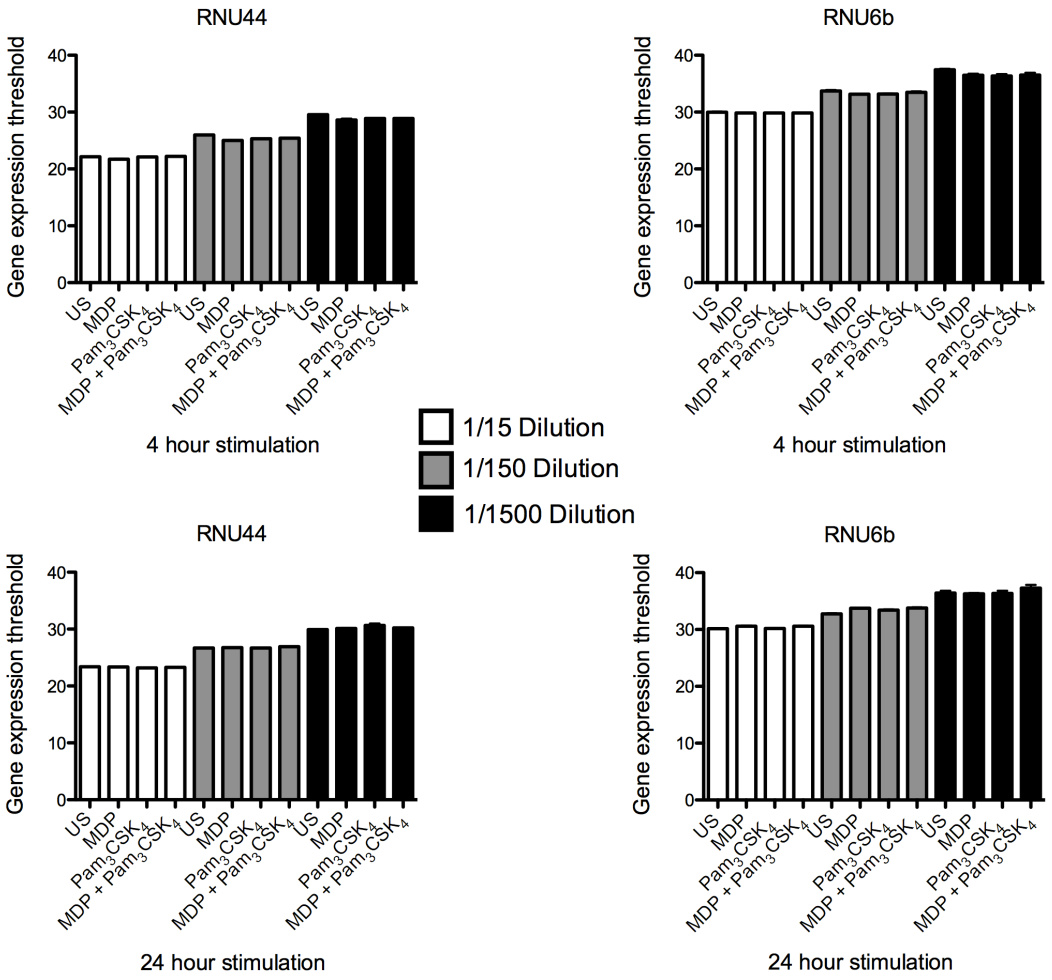


Figure 3.7 Short non-coding RNAs RNU6b and RNU44 were selected as potential qPCR reference controls. The cDNA template was tested at 3 different dilutions, with the expression of the controls remaining static across the DC stimulation conditions. 'Gene expression threshold' refers to the cycle threshold (Ct) at which the short non-coding control became detectable at qPCR. RNU44 was used in subsequent qPCR experiments.

To confirm the accuracy of the results obtained by microarray analysis I undertook quantitative PCR (qPCR) of the most strongly induced microRNAs on NOD2+TLR2 co-triggering and confirmed strong synergy between NOD2 and TLR2 in up-regulation of miR-155 **(Fig. 3.8a)**. miR-155 is the most well characterized miRNA utilised by the immune system and it is well known to be induced on PRR signalling. I used a panel of PRR ligands to compare the effect of NOD2 on miR-155 induction in comparison with other PRRs. Activation of TLR4 by lipopolysaccharide (LPS) dwarfed the effect of NOD2+TLR2 triggering on miR-155 expression, suggesting NOD2 is unlikely to play a major role in miR-155 in physiological circumstances when DCs encounter microbes **(Fig. 3.8b)**.

Although miR-146a was strongly up-regulated by TLR2 stimulation I found that, unlike miR-155, co-stimulating with MDP produced no synergy of response **(Fig. 3.8c)**, demonstrating that NOD2 contributes little to overall miR-146a induction.

Figure 3.8: qPCR Assessment of miR-155 and miR-146a

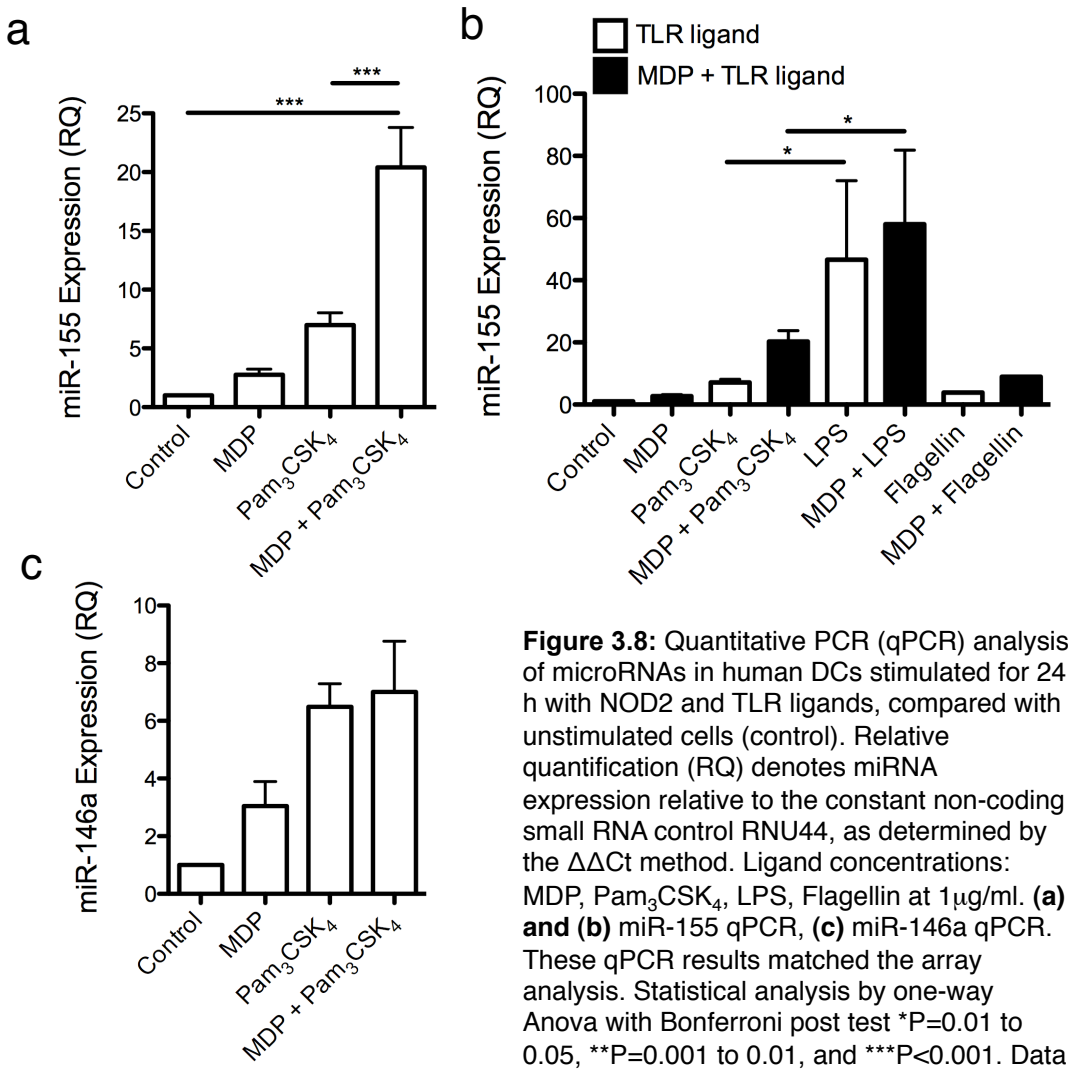


Figure 3.8: Quantitative PCR (qPCR) analysis of microRNAs in human DCs stimulated for 24 h with NOD2 and TLR ligands, compared with unstimulated cells (control). Relative quantification (RQ) denotes miRNA expression relative to the constant non-coding small RNA control RNU44, as determined by the ΔΔCt method. Ligand concentrations: MDP, Pam_3CSK_4, LPS, Flagellin at 1μg/ml. **(a) and (b)** miR-155 qPCR, **(c)** miR-146a qPCR. These qPCR results matched the array analysis. Statistical analysis by one-way Anova with Bonferroni post test *P=0.01 to 0.05, **P=0.001 to 0.01, and ***P<0.001. Data are pooled changes from 3 donors assayed independently; error bars, s.e.m.

qPCR analysis of Let-7, miR-572, and miR-16 revealed that there was very little induction through either NOD2 or TLR2 stimulation, and certainly no demonstrable synergy **(Fig. 3.9)**, highlighting the limitations of array technology and the need to carefully assess array data.

Figure 3.9: qPCR assessment of Let-7i, Let-7e, miR-572, miR-16.

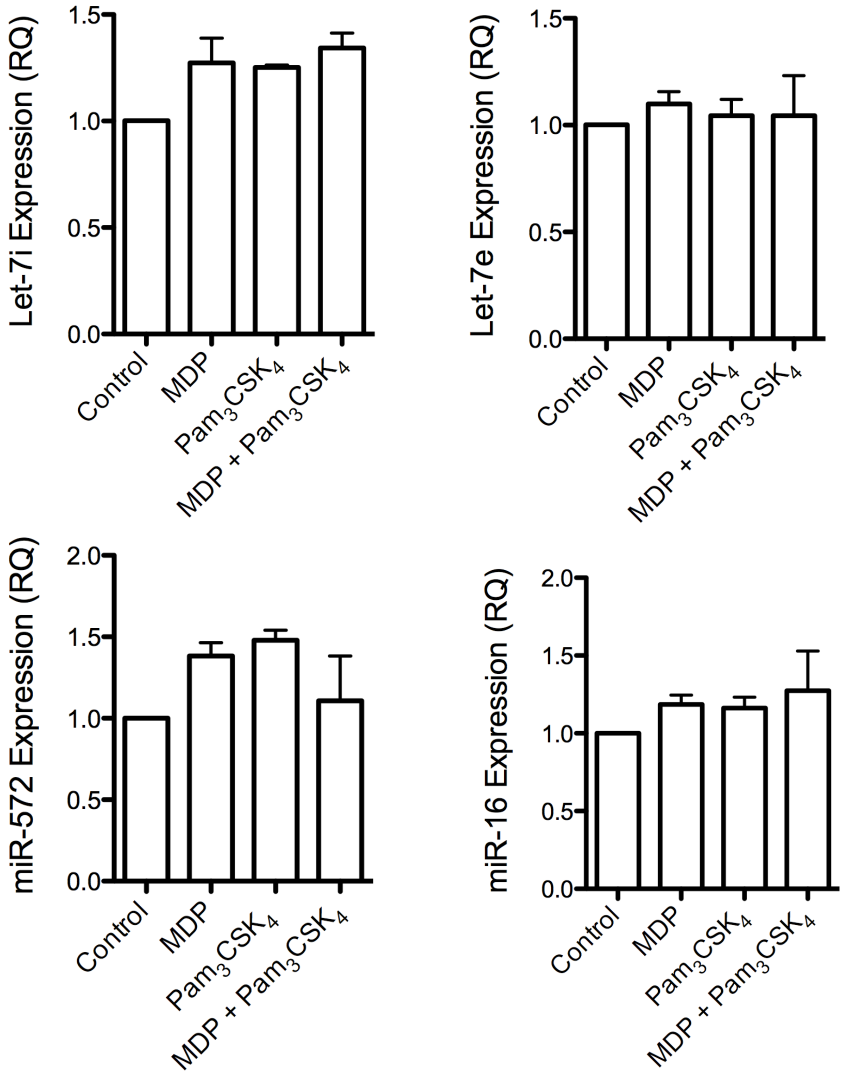


Figure 3.9: Quantitative PCR (qPCR) analysis of microRNAs in human DCs stimulated for 24 h with NOD2 and TLR2 ligands, compared with unstimulated cells (control), and relative to non-coding small RNA control RNU44. Ligand concentrations: MDP and Pam_3CSK_4 1 μg/ml. The qPCR contradicted the array results in the case of these miRNAs. Data are from: 2 independent experiments; error bars, s.e.m.

3.9 NOD2 induces miR-29a and 29b in human DCs

In contrast NOD2 played a dominant role in the induction of miR-29, where greatest up-regulation was observed with NOD2+TLR2 triggering (**Fig. 3.10a**). A panel of TLR ligands was employed, with and without MDP, to investigate the role of other PRRs in the induction of miR-29. I found that only the combined stimulation of NOD2 with TLR2 or TLR5 produced a significant (and greater than 2 fold) change in miR-29 up-regulation **(Fig. 3.10b)**.

NOD2 was absolutely required for this effect as combined TLR2+TLR5 triggering did not result in miR-29 up-regulation (**Fig. 3.10c**). These experiments revealed an exclusive role for NOD2, in comparison with other PRRs in inducing miR-29 in DCs.

Figure 3.10: NOD2 induces miR-29a and 29b in human MDDCs

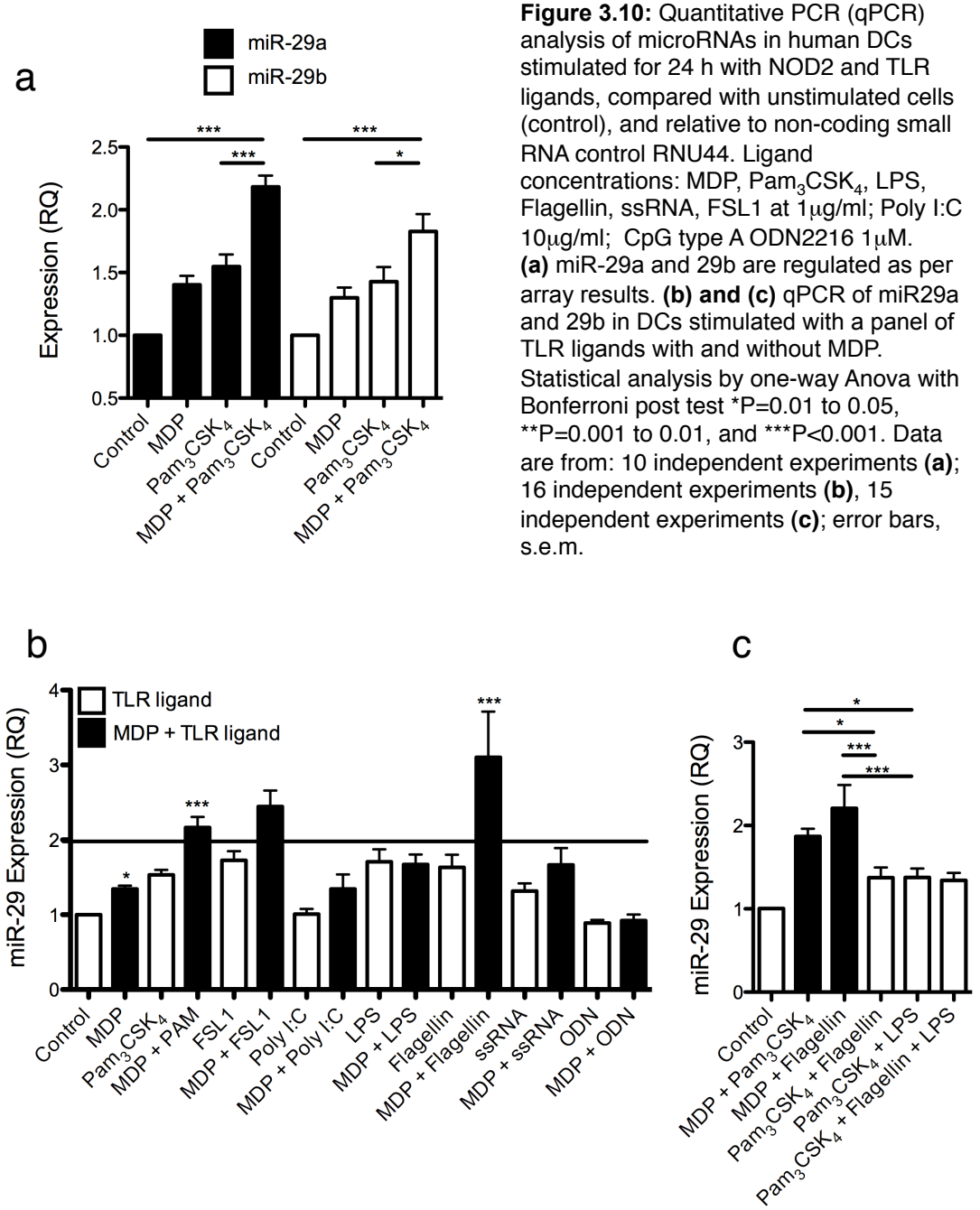


Figure 3.10: Quantitative PCR (qPCR) analysis of microRNAs in human DCs stimulated for 24 h with NOD2 and TLR ligands, compared with unstimulated cells (control), and relative to non-coding small RNA control RNU44. Ligand concentrations: MDP, Pam_3CSK_4, LPS, Flagellin, ssRNA, FSL1 at 1μg/ml; Poly I:C 10μg/ml; CpG type A ODN2216 1μM. **(a)** miR-29a and 29b are regulated as per array results. **(b) and (c)** qPCR of miR29a and 29b in DCs stimulated with a panel of TLR ligands with and without MDP. Statistical analysis by one-way Anova with Bonferroni post test *P=0.01 to 0.05, **P=0.001 to 0.01, and ***P<0.001. Data are from: 10 independent experiments **(a)**; 16 independent experiments **(b)**, 15 independent experiments **(c)**; error bars, s.e.m.

3.10 NOD2 induces miRNA family 29a, 29b, 29c in DCs

miR-29 forms part of a miRNA family expressed from two clusters on chromosomes 1 and 7, and possessing identical seed regions (nucleotides 2 to 8 relative to the 5' end of the miRNA), therefore targeting the same endogenous mRNAs (**Fig. 3.11a**). Clustering and co-expression provides the ability to influence complex cell signalling networks. (For example the miR-16 family regulates a series of cell cycle related genes, and can effectively arrest cell cycle division[331].) miR-29a and miR-29b-1 are transcribed within the same pri-miRNA from an intron of a spliced expressed sequence tag (EST) on chromosome 7 (chromosome 6 in mice). miR-29c and 29b-2, also from the same pri-miRNA, are found within the last exon of an EST on chromosome 1[332].

I tested whether in addition to 29a and 29b the other member of the family, miR-29c was also induced on NOD2 or NOD2+TLR2 dual triggering. I found induction of miR-29c to similar levels as miR-29a or 29b following combined NOD2+TLR2 stimulation (**Fig. 3.11b)**. Induction of the miR-29 family increased over time after NOD2+TLR2 dual stimulation, being detectable from 8 h post-stimulation and peaking around day 3 (**Fig. 3.11c**).

Figure 3.11: NOD2 induces both of the miR-29 clusters in DCs

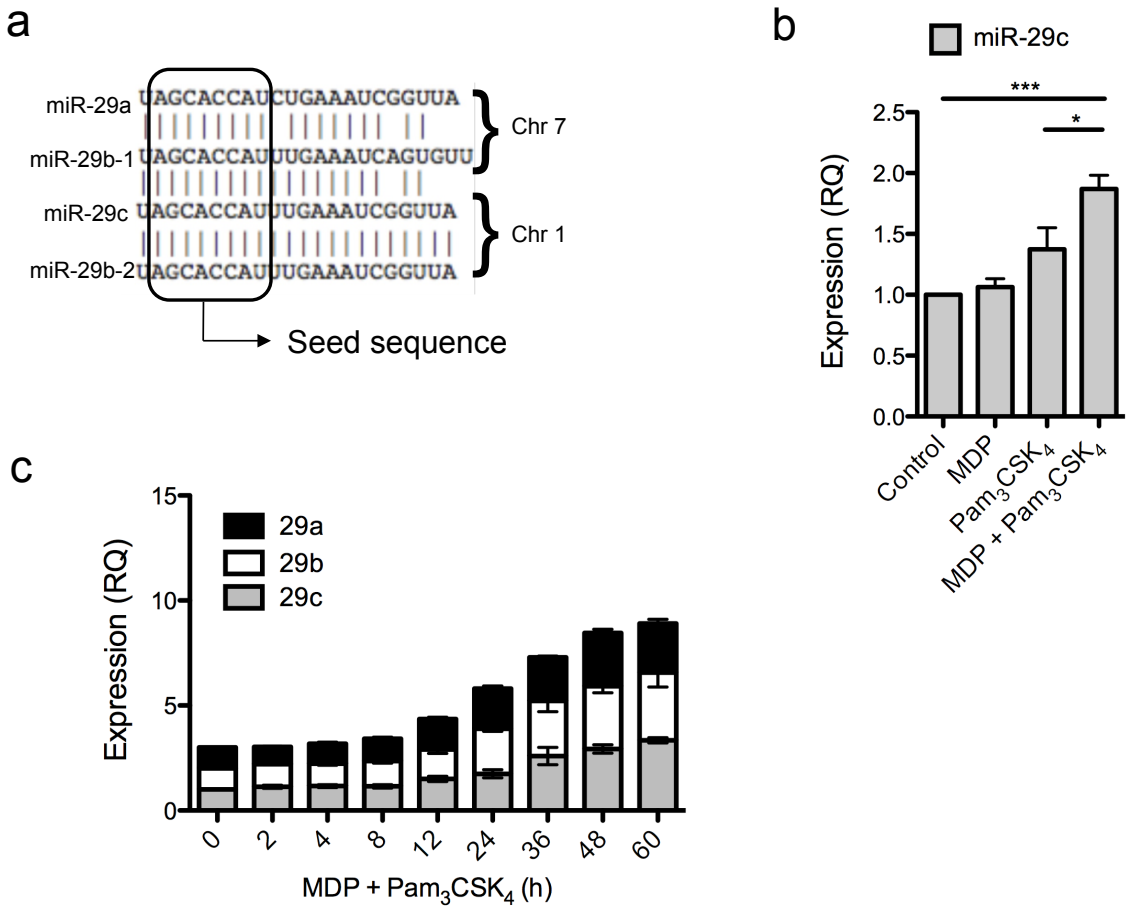


Figure 3.11: miR-29a/b/c are part of two clusters on chromosomes 7 and 1. They have an identical seed sequence, and thus target the same mRNAs. **(b)** qPCR analysis of miR-29c in human DCs stimulated for 24hrs with MDP and/ or Pam_3CSK_4 (1 μg/ml). **(c)** qPCR analysis of miR-29a/b/c in MDP + Pam_3CSK_4 1 μg/ml stimulated DCs over time. Statistical analysis by one-way Anova with Bonferroni post test *P=0.01 to 0.05 and ***P<0.001. Data are from 3 independent experiments **(b)**, 5 independent experiments **(c)**; error bars, s.e.m.

3.11 miR-29 expression is dependent on RIPK-2 and wild-type NOD2

NOD2 signalling requires RIPK-2 but not the TLR adaptor MyD88. I tested whether miR-29 expression required either of these signalling mediators for its up-regulation on MDP+Pam_3CSK_4 treatment of DCs. I knocked down MyD88 or RIPK-2 in DCs using siRNAs (**Fig. 3.12a**). I then undertook qPCR analysis of miR-29 expression following MDP+Pam_3CSK_4 exposure and demonstrated a requirement for RIPK-2 but not MyD88 in miR-29 induction (**Fig. 3.12b**).

I next investigated whether Crohn's patient DCs expressing variants of NOD2 associated with the disease exhibited defects in miR-29 up-regulation on either NOD2, or NOD2+TLR, triggering. I obtained DCs from donors who had previous histological diagnosis of Crohn's, and who were in remission and off immunotherapy at the time of sampling. **Figure 3.12c and d** show that these donors DCs fail to induce miR-29 on stimulation of NOD2, or NOD2+TLR2, or NOD2+TLR5 combined stimulation.

These data demonstrate that NOD2 induces expression of the miR-29 family over time after MDP treatment of DCs; that strongest expression is seen when both NOD2 and TLR2/ 5 are stimulated; that NOD2 stimulation, and normal NOD2 and RIPK-2 function, are critical to exert this effect.

Figure 3.12: miR-29 expression is dependent on RIPK-2 and wild-type NOD2

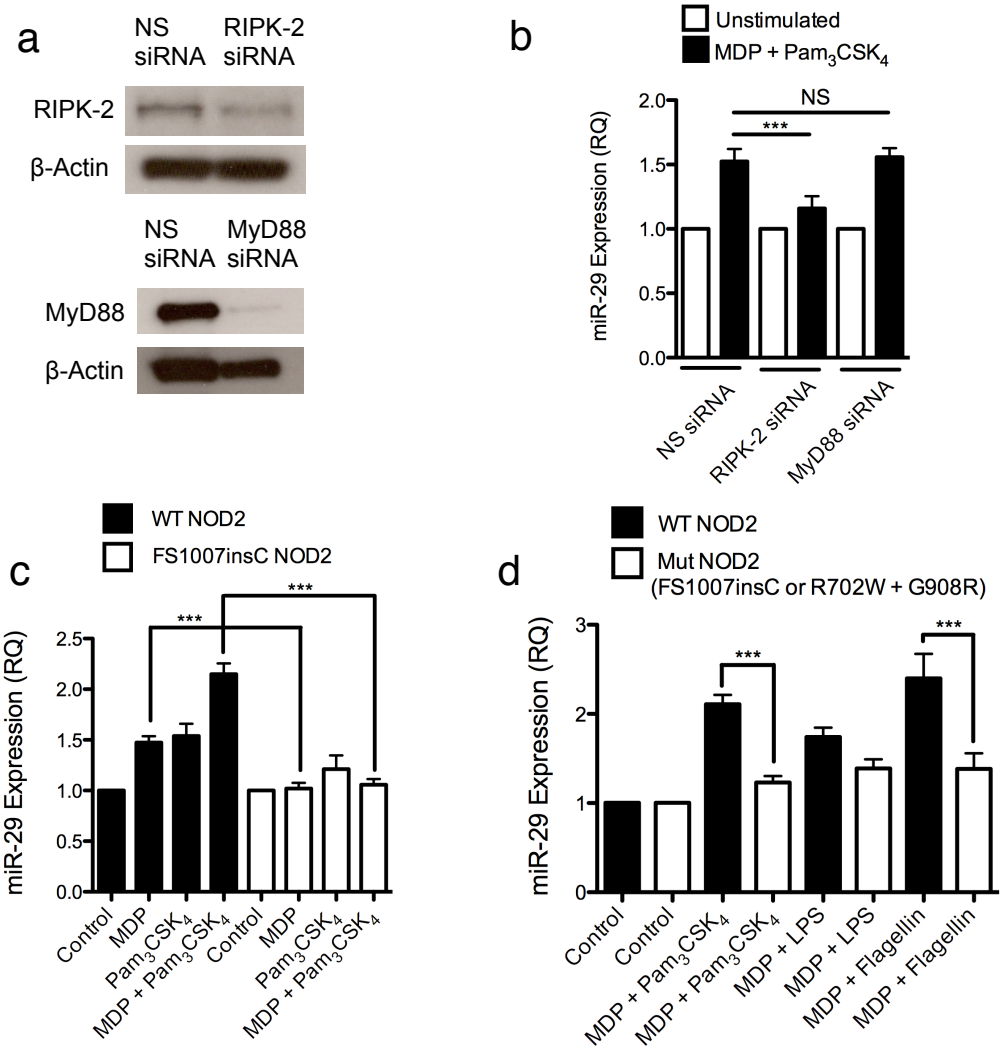


Figure 3.12: (a) RIPK-2 and MyD88 siRNAs, or control non-sense siRNA (NS siRNA), were transiently transfected into DCs, and the effect confirmed by Western blot. **(b)** Subsequently cells were left unstimulated or stimulated for 24hr with MDP + Pam_3CSK_4 1μg/ml, and miR-29 expression determined by qPCR.
(c) and (d) DCs were derived from CD patients homozygous for FS1007insC NOD2 (10 patients), or R702W + G908R NOD2 compound heterozygotes (5 patients). qPCR analysis of miR-29 expression in NOD2 mutated DCs, or wild-type (WT) NOD2 DCs, after MDP and/or Pam_3CSK_4, or MDP + Flagellin, or MDP + LPS stimulation (1μg/ml). Statistical analysis by one-way Anova with Bonferroni post test ***P<0.001. Western blots are representative of 3 independent experiments **(a)**; qPCR data are from: 6 independent experiments **(b)**, 8 independent experiments **(c)**, 14 independent patient experiments **(d)**; error bars, s.e.m.

3.12 Discussion

In this chapter I demonstrate for the first time that NOD2 can control miRNA expression: that it induces miR-155, and is critical for the expression of the miR-29 family through innate immune triggering in DCs. The latter requires

the key NOD2 signal transducer RIPK-2, and can be augmented by co-triggering NOD2 with either TLR2 or TLR5.

Understanding the transcriptional regulation of these miRNAs in DCs will be more challenging. Indeed, control of miRNA expression has been described not only through transcriptional enhancer and repressor elements[333,334], but also via: epigenetic control (for example the miR-203 locus is often methylated causing loss of expression in T cell lymphoma, but not normal T cells[335]); through regulated processing (for example pri-miR-21 conversion to pre-miR-21 by the DROSHA complex is increased by TGFβ and bone morphogenic proteins[336]); and through regulated transport (for example precursors of miR-31, miR-128b and miR-105 are retained in the nucleus in certain cell types, thus blocking cytoplasmic processing[337].)

Some transcription factors, such as NFκB and AP-1 member cJun[338], have been shown to regulate miRNA promoter activity. NOD2 and TLR dual stimulation increase NFκB activation, but although miR-146a has an NFκB-binding site in the promoter region[284], my data show that adding MDP to TLR2 stimulation has no effect on mir-146a expression, so clearly miRNA transcriptional control is multifaceted. In contrast it is possible that the observed synergistic effect on miR-155 expression after NOD2 + TLR2 stimulation, directly reflects increased AP-1 and/ or NFκB activation, as miR-155 has binding sites for both these in the promoter region[305]. This seems a reasonable hypothesis since LPS, known to be a powerful NFκB activator, is also the strongest inducer of miR-155 for the stimuli I tested.

In general the transcriptional regulation of miRNAs is not yet well described, and this is the case for the miR-29 family. An analysis of miR-29b-1 and 29a

promoter region identified two putative Myc binding sites, a Gli binding site (part of the developmental hedgehog signalling pathway), and three NFκB binding sites[339]. Both Myc and Gli binding repress miR-29 expression in this study.

Clearly, in the context of NOD2 and TLR triggering, the NFκB binding sites are of most potential interest in DCs. It is worth bearing in mind however that, even if NFκB is involved in miR-29 induction, my data suggest there is not a direct linear relationship since LPS does not significantly induce miR-29. Interestingly in this study of cholangiocyte and cholangiocarcinoma cell lines, TLR4 and 5 triggering with LPS and flagellin actually *reduce* miR-29 expression, although Pam_3CSK_4 equivocally increased expression[339]. Although the TLR ligands clearly activate NFκB, it is not demonstrated that the observed effects on miR-29 expression in cholangiocarcinoma cells are NFκB-driven. Moreover, despite the fact that this discrepancy between my data and theirs at first glance seems odd, it is known that TLR signalling has *cell-specific* effects on miRNA expression (reviewed in [276]), and what was observed in cholangiocytes may not hold true for DCs.

A separate analysis of the 29a/ b-1 promoter revealed a number of TCF/LEF sites - transcription factors that are activated by nuclear β-catenin during Wnt signalling. This study also found that canonical Wnt signalling up-regulates miR-29 in human osteoblasts[340]. Interestingly treatment of the cells with Wnt3a, or LiCl a known Wnt activator, up-regulated miR-29 fairly rapidly (within 3 h) suggesting this perhaps is not the mechanism of NOD2-miR-29 regulation in DCs.

Wnt signalling is highly conserved through different species, although this family of glycoprotein ligands and receptors is diverse. The final common pathway in Wnt signalling is the activation and nuclear translocation of β-catenin. The role of Wnt signalling is well defined in processes such as embryogenesis, and cell differentiation, but Wnt activation downstream of innate immune PRRs has in general not been well studied. In intestinal epithelial cells (IECs) TLR9 can be expressed on the cell membrane. Apical (luminal) but not basolateral TLR9 triggering by bacterial DNA results in the up-regulation of Wnt receptors, specifically Frizzled 5 (Fzd5), that regulates the maturation of Paneth cells and results in increased defensin production[341]. Clearly this Wnt up-regulation is likely to be different in DCs where TLR9 is endosomal.

Perhaps more relevant to my data is the observation that Wnt5A expression is up-regulated by TLR-induced NFκB activation in human monocyte-derived macrophages and DCs, specifically through mycobacterial, or TLR2 or 4, stimulation[342]. The receptor for Wnt5A, Fzd5, is also expressed on human mononuclear cells by these stimuli, leading to increased IL-12p40 release via this pathway. It is possible that NOD2 also stimulates Wnt signalling, and that this is what leads to the observed miR-29 up-regulation in human DCs.

Another study in human myoblasts identified a transcriptional repressor site for YY1 (Yin Yang 1) in the 29b-2/ 29c locus, but not the 29b-1/ 29a locus[343]. YY1 is also an NFκB-driven factor, and is important in muscle differentiation. Although the study shows transcriptional repression of miR-29b and c in myoblasts by YY1, (and YY1 may in turn be dependent on NFκB expression), it fails to explain why similar patterns of expression are seen for miR-29a

during myogenesis, suggesting that this mode of control may not sufficiently explain miR-29 transcriptional control, since all three mir-29 miRNAs can strongly enhance muscle differentiation. Once again, this method of miR-29 control may be redundant in DCs.

The miR-29 family is also up-regulated in Hela cells during induced cellular senescence, through activation of the retinoblastoma (Rb) tumour suppressor pathway[344]. Although the exact mechanism inducing miR-29 expression was not examined, the authors speculated that it may be through c-Myc repression upon Rb induction, as Myc has been shown to repress miR-29[332] (and interestingly miR-146a), presumably through the described binding sites in the promoter region.

In fibroblasts and myocytes, miR-29 expression appears to be down-regulated by transforming growth factor beta (TGFβ1)[345-347], platelet-derived growth factor B (PDGF-B) and IL-4[348], which are known to be pro-fibrotic cytokines and growth factors. Interestingly I found that MDP + Pam_3CSK_4 stimulation of DCs significantly down-regulates TGFβ1 expression (data not shown), and it is possible that this contributes to the demonstrated up-regulation of miR-29.

Lastly, it is interesting to note that for miR-18 it was recently shown that hnRNP A1, an RNA-binding protein, is required for Drosha processing from the primary precursor[349]. Since wild-type NOD2 function has been implicated in the appropriate activation of hnRNP A1[273], this raises the intriguing possibility that activated hnRNP A1 is also required for miR-29 processing and that this accounts for the loss of miR-29 expression in NOD2 mutant DCs.

Another process to consider when determining mature miRNA expression is the rate of destruction. miRNAs are mostly tightly packaged by RISC[350], and a

member of the RISC complex AGO2 also protects the resident miRNA from degradation[351], but the mechanisms guiding miRNA stability outside of this in general have not been clearly defined. One example is miR-122 which, in a manner similar to messenger RNA, modifies its 3' end with an additional adenosine to provide some protection from degradative nucleases[352].

Specifically related to my data and the miR-29 family, miR-29b has been shown to have a relatively accelerated turnover (declining from 4 hours post expression, half-life 7.4 h) which depends on the presence of uracils at positions 9, 10 and 11 of its mature miRNA sequence[353]. This is in contrast to miR-29a that lacks the uracil at position 10, and is more stable in its expression (stable up to 12 hours, half-life 12 h). miR-29c, which like 29b contains the 3 uracils in these positions, has an intermediate half-life (10.6 h). My data shows that there is little difference between the expression levels of miR-29, 29b and 29c at 24 h stimulation. At first glance this would lead one to conclude that this mechanism is not significantly contributing to the determined expression, although it should remembered that there are two identical copies of miR-29b (b-1 and b-2 on chromosomes 7 and 1 respectively), implying that without this increased turnover one might expect miR-29b expression to be roughly twice that of miR-29a. However, over the time-course experiment, both mir-29b and 29c expression is increased over that of 29a, suggesting that if this mechanism is active in DCs, there must be continued active transcription of the miR-29 clusters, especially on chromosome 7.

The delay in miR-29 expression is also of some interest, although not atypical of miRNAs. For example, both miR-21 and miR-146a are detectable on LPS

stimulation at 4-8 h, and have rising expression at 24 h[325]. It is not yet clear how this delay in expression is controlled, particularly as the pro-inflammatory response is determined through transcription factors and RNA Pol II-sensitive genes – the same factors that probably control miR-29 induction. It may be that the miRNA promoters have protective elements whose removal or degradation is delayed, but at present this is entirely speculative.

In summary, this chapter demonstrates the novel finding that NOD2 stimulation is critical for the up-regulation of the miR-29 family in human DCs. The fact that this expression is lost in cells homozygous for the CD-associated NOD2 mutations raises the intriguing possibility that their absence contributes to disease pathogenesis. The next two chapters therefore focus on determining the targets and functional effects of these microRNAs in human DCs.

4 MicroRNA-29 targets and functional effects in DCs

4.1 Introduction

4.1.1 MicroRNA Targeting

There is no perfect way to detect miRNA targets, not least because the biology of how the mRNAs are targeted is incompletely understood. The most important part of the miRNA for targeting are the 5' nucleotides from 2-8[354], known as the seed sequence, and this is correspondingly the most evolutionarily conserved region[355]. However, in some cases the seed region is not enough to determine mRNA targeting, with the 3' miRNA sequence, and features of the mRNA 3'UTR, contributing to the strength of binding in a number of ways[356]. There are some targets with no complete 6mer seed match, and others still have no complete seed sequence pairing and instead rely on 11-12 continuous base pairs in the central region[357]. Furthermore, although the 3'UTR of mRNA is the most common target area, target sites have also been observed in the 5'UTR, and indeed the protein coding region, of mRNA[358].

4.1.2 Predicted targeting: Algorithms

The algorithms available to predict miRNA targeting (for example the most commonly used: Targetscan, miRanda, and PicTar) are for the most part focused to detect miRNA-seed sequence to mRNA-3'UTR binding. The targets they predict differ not least because some algorithms use different

3'UTR sequence databases (e.g. Targetscan uses Ensembl, and miRanda uses University of California Santa Cruz), but even using the same database the degree of predicted target overlap between two algorithms is a relatively small 40%[359]. Not surprisingly therefore, many predicted targets are false positives (approximately 24-70%)[360], and there are also many false negatives. Thus although these algorithms are useful, they are far from perfect.

4.1.3 Detecting miRNA: mRNA targeting

In terms of experimental techniques, these can essentially be split into those that detect miRNA targets on a gene-by-gene basis, and those that attempt to define miRNA effects and potential targets on a more global scale. Nearly all of the approaches use expression of either a miRNA mimic (premiR) or a modified antisense oligonucleotide that binds and thus blocks miRNA activity (antimiR). The main problem with the latter is that antimiRs may sequester miRNAs without triggering their decay, and therefore measuring their appropriate transfection (which for the miRNA mimics is done by quantitative PCR) is difficult. The main problem with premiR use are the supraphysiological levels of expression that can be achieved, which potentially could have unwanted effects such as out-competing and displacing other miRNAs from the RISC complex[361]. However this over-expression is also useful as it allows one to experimentally amplify the miRNA effect, and therefore presumably to identify targets more easily.

4.1.4 Individual miRNA target identification

In terms of defining individual miRNA targets, this is usually done with quantitative PCR (qPCR) and western blot, with target confirmation using a 3'UTR luciferase construct. Luciferase assays are relatively labour intensive, and prone to variable results depending on the exact methodology used.

4.1.5 Screening methods for miRNA targets

Global screening methods have the advantage of detecting a network of effects and targets. Gene microarray analysis following miRNA over-expression or blocking is well described[362], and although some targeting of mRNAs predominantly causes translational repression[363], as much as 84% of miRNA-mediated repression is detectable as decreased mRNA expression[364]. Another technique is to tag and then immunoprecipitate RISC components such as Argonaute (Ago)[365], and this has the advantage of being able to detect mRNAs regulated at the level of translational repression as well as mRNA degradation. However this method relies on a very stable miRNA: mRNA interaction, and since the cells are lysed before immunoprecipitation, the interactions detected may be artefactual as cell compartments that are normally separate are allowed to coalesce[366]. To avoid this problem it is possible to crosslink the RNA to binding proteins with UV (ultraviolet) radiation before lysis, using HITS-CLIP (high-throughput sequencing of RNA isolated by crosslinking immunoprecipitation)[367], or PAR-CLIP (photoactivatable-ribonucleoside-enhanced crosslinking immunoprecipitation)[368].

Approaches to directly examine miRNA effects on protein expression include SILAC (stable isotope labelling with amino acids in cell culture)[369] and 2D-DIGE (two-dimensional differentiation in-gel electrophoresis)[370]. SILAC, which

measures protein abundance in samples labelled with different isotopes, requires actively dividing cells so would not have been appropriate for finding miR-29 targets in primary DCs. 2D-DIGE, which involves labelling two samples with different fluorescent dyes and separating the proteins by isoelectric focusing before mass spectrometry identification, has already been applied to miR-29[371]. Although this study in lung cancer cells identified over 100 proteins differentially regulated by manipulating miR-29, only 14 of the corresponding mRNAs include a miR-29 target sequence, suggesting this technique is not as adept as gene-expression analyses at identifying bona fide targets.

4.2 Methods undertaken to detect miR-29 targets

I initially undertook a search for targets on an individual or case-by-case basis, with mRNA or protein changes detected by qPCR and western blot respectively. These potential targets were identified by a careful search of online algorithms, and of course from published targets of miR-29, with this last group growing considerably during my project. These targets are the focus of this chapter, and their varied nature by necessity makes the subject matter of this chapter somewhat disjointed. I subsequently performed a more global analysis employing a whole human genome DNA array, and this, along with the resulting experiments on IL-23 expression, form the subject of Chapter 5.

4.3 miR-29 published targets

The first paper directly concerning miR-29 was published in December 2006[372], and there are now approximately sixty publications, forty-five of which have been published in the last two years (since August 2009), reflecting the growth of interest in miRNAs in general, and in miR-29 specifically. Although published miR-29 targets are clearly multiple, many of them can be grouped into those that affect either cancer biology, or the extracellular matrix. Most of these have no clear relationship to PRR or immune function in DCs, and were not experimentally assessed, but are detailed in the chapter introduction below. I did experimentally assess those published targets, such as MCL-1 and the Wnt negative regulators, that were more likely to influence DC function, and these are predominantly discussed in the results section of the chapter.

4.3.1 miR-29 and malignancy

In general there is much interest in the relationship between miRNAs and cancer, not least because an analysis of 186 human miRNAs revealed that almost half are located in fragile sites of genomic regions, and these are often altered in various malignancies[373]. The first miR-29 target described was TCL1 in B cells, an oncogene that relates to the development of B cell chronic lymphocytic leukaemia (CLL), and lower levels of miR-29 expression are associated with poorer prognosis in aggressive CLL[372]. However over-expression of miR-29 in mouse B cells also leads to CLL, albeit an indolent form that is not dependent on TCL1, possibly through the targeting of tumour suppressor peroxidasin[374]. Higher miR-29 expression also correlates with a form of acute myeloid leukaemia[375]. It is clear from this data that although

miR-29 levels affect cancer biology, a clear anti- or pro-oncogenic role in leukaemia has not yet been determined.

Continuing on the lymphoproliferative malignancy theme, in mantle cell lymphoma (an aggressive B cell lymphoma) the miR-29 family is one of the most frequently down-regulated miRNAs[376]. Mantle cell lymphoma is associated with a chromosomal translocation, t(11;14)(q13;q32), which causes over-expression of cyclin D1, and this exerts effects on cell proliferation through binding to CDK4 and CDK6 (cyclin-dependent kinase 4 and 6). This study shows that miR-29 can target CDK6 3'UTR, and interestingly the degree of miR-29 down-regulation in lymphomas correlates with decreased patient survival.

MCL1, an anti-apoptotic BCL-2 family member, is also targeted in cholangiocytes by miR-29. miR-29 is down-regulated in malignant cholangiocytes, allowing MCL-1 expression and providing the cancer cells with a mechanism to avoid apoptosis[377]. This is discussed further below.

Another miR-29 effect that has been linked to cancer biology is the up-regulation of the tumour suppressor p53[378] which regulates anti-proliferative responses such as cellular senescence and apoptosis. This may occur indirectly in cell lines through miR-29 targeting the regulatory subunit of PI3 kinase p85α, and CDC42 (a Rho family GTPase), both of which can negatively regulate p53. Furthermore B-Myb, an oncogene transcription factor that controls cell cycle progression and loss of which can lead to cellular senescence, is also targeted by miR-29[344]. Cellular senescence is an important mechanism of tumour suppression, via irreversible growth arrest. Perhaps in part reflecting the importance of these two pathways, lower levels

of miR-29 in malignant tissue, compared with healthy tissue, have been reported for malignancies as varied as prostate[379], rhabdomyosarcoma[343], cholangiocarcinoma[377], CLL[372], lung and melanoma (these latter two in part through altered methylation, as miR-29 targets DNA methyltransferases DNMT3A and B)[380,381]. However, *higher* miR-29 levels were reported in breast cancer in a study examining epithelial to mesenchymal transition and metastasis[382]. Here miR-29 appears to affect epithelial polarity and increase metastasis, partly through targeting tristetraprolin (TTP), a protein involved in the degradation of mRNAs with AU-rich 3'UTRs, and which is known to contribute to cytokine homeostasis[383]. Again this apparent contradiction highlights not only that (in part because miRNAs have many different potential targets) target detection depends on the methodology and question posed, but also that miRNA function is very likely cell and tissue specific.

4.3.2 miR-29 and the extracellular matrix

Disordered miR-29 expression is associated with a number of fibrotic physiological and pathological processes, and this appears to be because many extracellular matrix (ECM) proteins (e.g. type I and III collagens, elastin and fibrillin) are targeted by miR-29 in certain cells, particularly fibroblasts. For example, cardiac fibrosis often occurs after a myocardial infarction (MI), and in murine post-MI models miR-29 is down-regulated in fibroblasts by TGFβ1, leading to increased collagen production and scarring[346]. Interestingly, in animal models investigating the role of aerobic training on cardiac function, miR-29 is up-regulated in the hearts of exercised rats, correlating with reduced collagen expression and an improved ventricular compliance[372].

miR-29 down-regulation also contributes to hepatic fibrosis in murine models[345], and to pulmonary fibrosis in bleomycin treated mice[384,385], both via an increase in collagen and other ECM proteins. In systemic sclerosis (SS), miR-29 is again down-regulated in human SS fibroblasts and skin sections, allowing unregulated collagen production[348]. Lastly, mir-29 expression also controls the ECM synthesis in the ocular trabecular meshwork[386].

4.3.3 Other miR-29 published targets

B7-H3 (also known as CD276), a transmembrane member of the B7/ CD28 immunoglobulin superfamily, is induced on DCs as they differentiate from monocytes, and has been described in both two-Ig and four-Ig forms[387]. Interestingly B7-H3 has been shown to provide stimulatory signals to T cells[388], although other studies have demonstrated no significant effect[387], and so a consensus on its main role has not yet been reached. A study using human tumour cell lines demonstrated that miR-29 targets B7-H3[389], and the authors suggested that the general down-regulation of miR-29 in tumours increases cancer immune-evasion, but this conclusion only holds if B7-H3s main role is immune-inhibitory.

In neurons, miR-29 targets peripheral myelin protein 22 (PMP22), a protein primarily expressed in myelinating Schwann cells[390]. In muscle cells miR-29, and miR-206, regulate differentiation by targeting histone deacetylase 4 (HDAC4)[347]. HDAC4, whose expression is stimulated by TGFβ via SMAD3, normally acts as an inhibitor of muscle differentiation, and miR-29 targeting of this protein antagonises the inhibitory role of TGFβ on muscle differentiation.

The negative regulators of Wnt signalling discovered in osteoblasts are discussed below.

4.4 Aims

The aims of this chapter are:

- To identify targets of miR-29 in human DCs from predicted and published data
- To determine which of these are regulated by miR-29 expression in human DCs

4.5 Potential miR-29 Targets

Potential miRNA targets were identified from published data, and by using TargetScan, miRBase MicroCosm Version v5, and miRanda online algorithms. **Table 4.1** details 16 possible targets that were initially chosen for assessment based on their potential influence on DC immune function, and on their predicted target scores according to online algorithms.

Table 4.1 Potential miR-29 Targets

Target	29a	29b	29c	Ref
MCL1	✓	✓	✓	377
CDC42	✓	✓	✓	378
B7H3	✓	✓	✓	389
TTP/ ZFP36	✓	✓	✓	382
PIK3R1	✓	✓	✓	378
TNFRSF1A	✓	✓	✓	N/A
CNOT8	✓	✓	✓	N/A
TNFAIP3	✓	✓	✓	N/A
HBP1	✓	✓	✓	N/A
TNIP2	✓	✓	✓	N/A
TRAF4	✓	✓	✓	N/A
CX3CL1	✓	✓	✓	N/A
IL-1RAP	✓	✓	✓	N/A
IL-1F9	✓	✓	✓	N/A

Figure 4.1 miR-29 antimiR and premiR assessment by qPCR

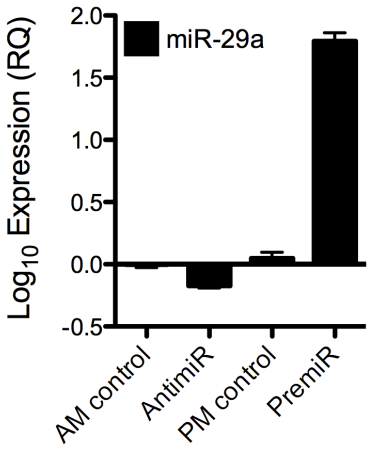


Table 4.1: miR-29 Cluster Predicted Targets

The table illustrates potential targets of the miR-29 cluster based on Targetscan online algorithm. These targets were selected as they are published targets of miR-29 in other cell types (reference supplied), or as they are predicted targets with functions that could impact on immunity.

Figure 4.1 demonstrates quantification of miR-29a in DCs after transfection of miR-29a antimiR or control, or of miR-29a premiR or control.

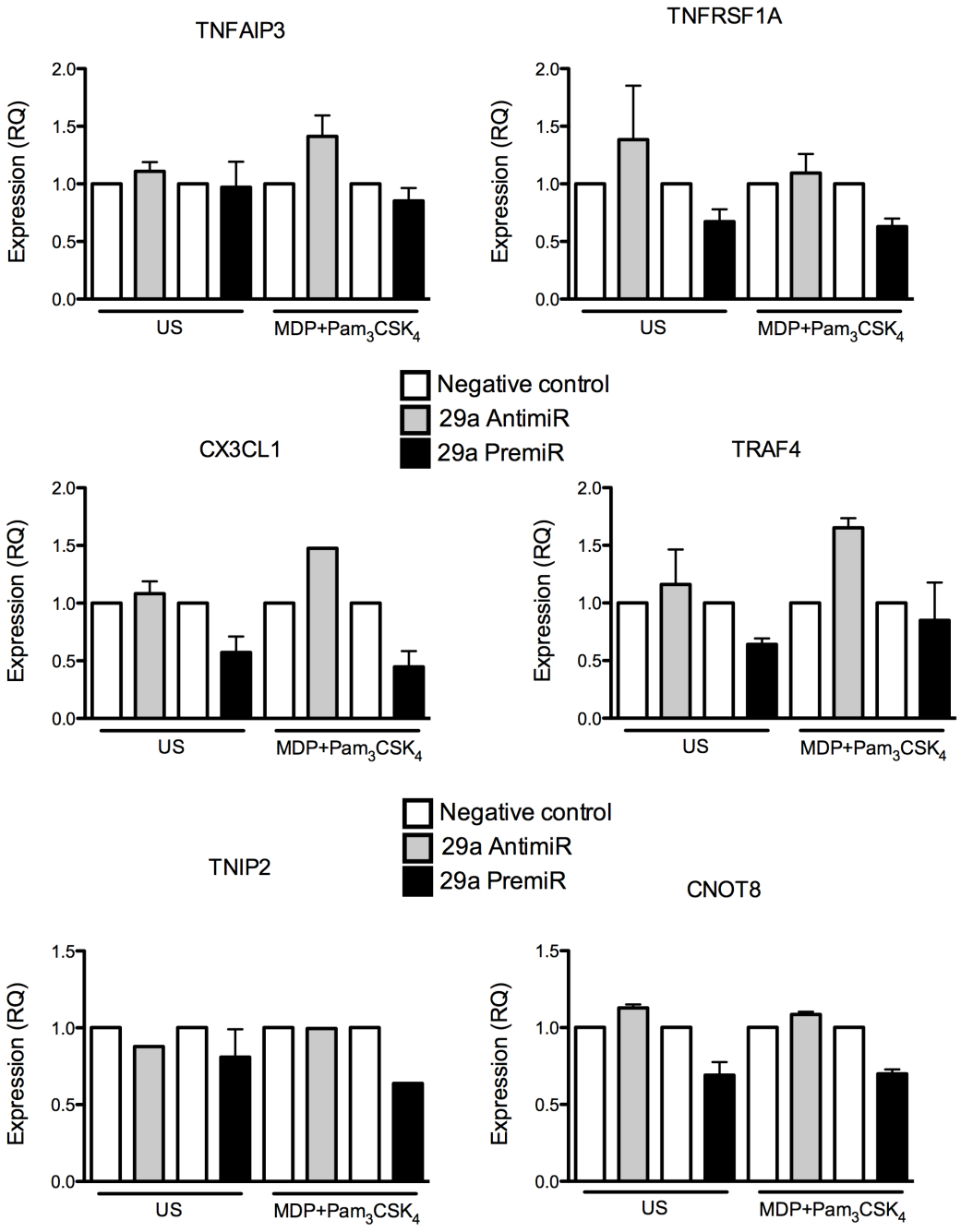
4.6 qPCR assessment of potential miR-29 targets in DCs

I transfected DCs with miR-29 premiR or antimiR, to artificially increase miR-29 expression or block miR-29 action respectively. Transfection of miR-29 premiR resulted in robust up-regulation of miR-29 sequence detected by qPCR **(Fig. 4.1)**.

Subsequently, DCs were transfected with miR-29a premiR or antimiR, and then left unstimulated or stimulated with MDP+Pam_3CSK_4, and potential miR-

29 targets screened using qPCR. This approach was used as previously it has been shown that miRNAs may act to down-regulate mRNA of target genes, rather than at the translational level in mammalian cells[362]. Of those tested, MCL-1, CX3CL1 and TRAF4 demonstrated a pattern of expression in response to the miR-29 premiR and antimiR that was most promising **(Fig. 4.2)**. However, many of those tested by qPCR demonstrated a possible response to miR-29 over-expression.

Figure 4.2 qPCR assessment of potential miR-29 targets in DCs



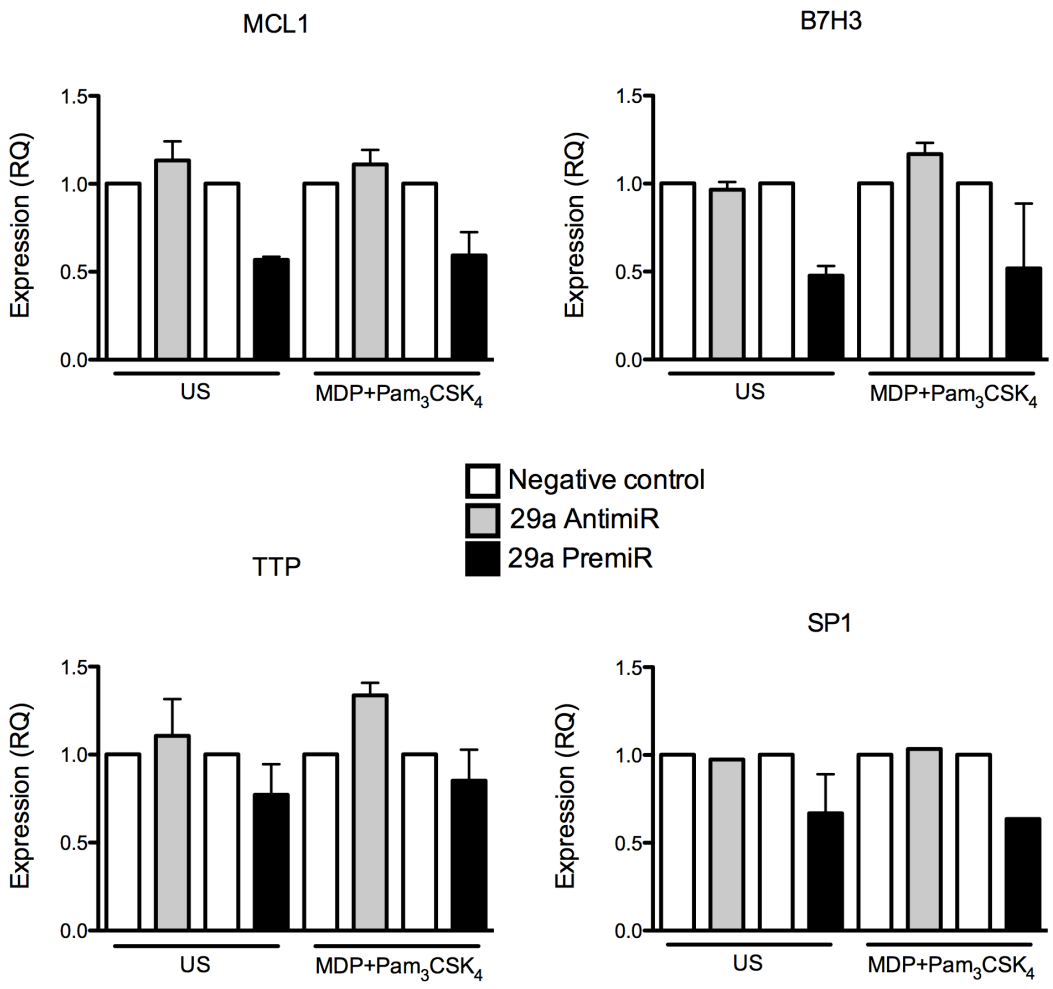


Figure 4.2 DCs were transfected with a miR-29 premiR or antimiR before subsequently being left unstimulated (US) or stimulated with MDP + Pam_3CSK_4 (1µg/ml). Potential miR-29 targets were assessed by qPCR versus GAPDH control, calculated by the change in threshold ($\Delta\Delta C_T$) method. Negative controls were set at 1 for both US and stimulated experiments. Data are from 2 independent experiments; error bars, s.e.m.

Although this approach is relatively quick and 'high throughput', it unfortunately does not negate the need to test any potential targets at the protein level, where miRNA effects may primarily be seen. However, I did find in my experiments that those targets that were significantly affected by miR-29 at protein level in DCs (see Figures 4.3a, 4.8b, 4.8c, 5.4b, 5.5b) also had

detectable changes on qPCR (see Figures 4.2, 5.3, 5.5a), in keeping with published observations of mRNA and protein levels[363].

4.7 miR-29 published targets

4.7.1 MCL-1 is a miR-29 target in DCs

MCL-1 is an anti-apoptotic protein of the BCL-2 family. The BCL-2 family play a major role in controlling apoptosis by regulating the integrity of the outer mitochondrial membrane. This family is divided into three subgroups: the multi-domain anti-apoptotic proteins (which include MCL-1[391], BCL-2[392,393] and A1[394]); the multi-domain directly apoptotic proteins that mediate mitochondrial membrane permeabilisation (BAX and BAK)[395]; and the BH3(BCL-2 homology domain 3)-only domain pro-apoptotic proteins (which include BID, BIM, BAD and BIK) which initiate apoptosis indirectly[396].

The multi-domain pro-apoptotic members BAX and BAK possess a bundle of amphipathic α-helices, facilitating different protein conformations that confer function[397]. Apoptotic stimuli induce a conformational change allowing these proteins to oligomerise and then probably to form mitochondrial pores releasing cytochrome *c*. The BH3-only members respond to upstream death and survival signals, but can only induce apoptosis through activation of BAX and BAK. The multi-domain anti-apoptotic members, such as MCL-1, serve to bind and sequester BH3-only proteins, in order to prevent BAX and BAK activation[398]. Evidence suggests that, at least following some stimuli, MCL-1 degradation is required for initiation of cytochrome *c* release[399], and that it serves as a critical checkpoint in the apoptotic pathway.

Insufficient MCL-1 can lead to, for example, B and T lymphocyte loss due to inappropriate apoptosis[400], whereas in murine models with constitutive MCL-1 expression haematological malignancies occur due to lack of apoptosis[401]. MCL-1 levels are therefore tightly regulated but the control is complex, with degradation in part via the proteasome and determined by ubiquitination levels[402].

A further mechanism of degradation was determined when MCL-1 became the second miR-29 target to be described[377] in a study using cholangiocyte and cholangiocarcinoma cell lines, (Targetscan 8mer; aggregate P_{CT} 0.92).

I found that miR-29a over-expression in human primary DCs also consistently down-regulates MCL-1 **(Fig. 4.3a)**. This was most apparent when the cells were stimulated with MDP+Pam_3CSK_4 as this up-regulated MCL-1 expression. A timecourse of MCL-1 expression in DCs following MDP+Pam_3CSK_4 stimulation reveals that MCL-1 levels drop at 18-24 h **(Fig. 4.3b)**, and this correlates with the increase in miR-29 expression over time already described **(Fig. 3.11c).** Although I performed the MCL-1 timecourse only once, and therefore I have not established that this is a reliable pattern in human MDDCs, this pattern of expression is also seen in human monocyte-derived macrophages after *Streptococcus pneumoniae* infection[403].

Figure 4.3 MCL-1 is a miR-29 target in DCs

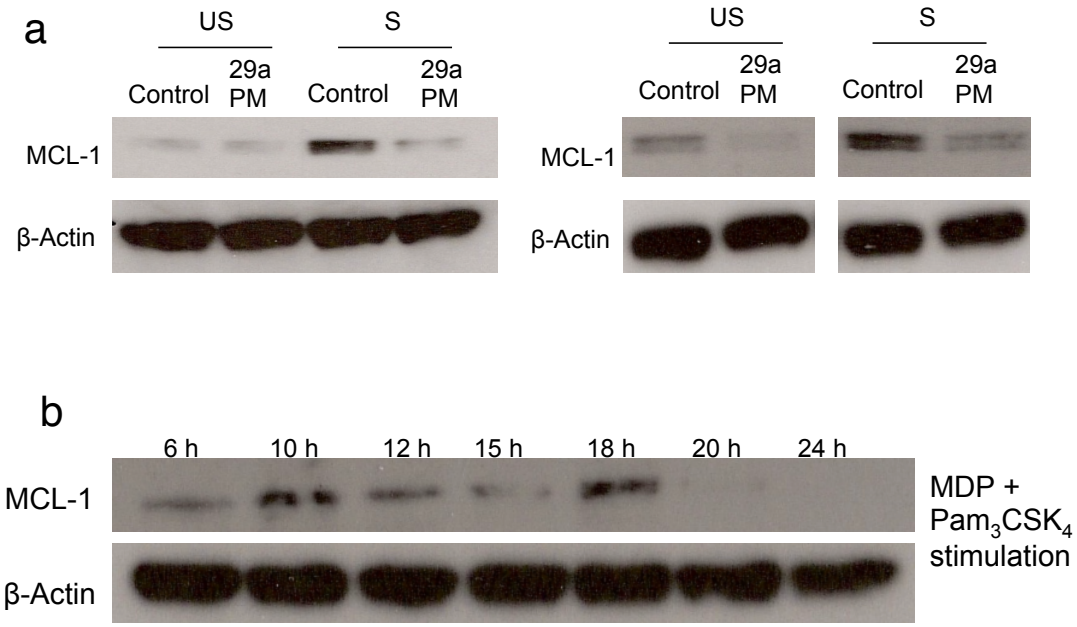


Figure 4.3 (a) DCs were transfected with miR-29a premiR (29a PM) or negative control, before being left unstimulated (US), or stimulated with MDP + Pam_3CSK_4 (1μg/ml) for 24 h, and subsequent lysis and WB for MCL-1. Two example WBs are shown. **(b)** WB for MCL-1 in DCs stimulated over time (h) with MDP + Pam_3CSK_4 1μg/ml. Data is representative of 4 WB for **(a)**, or shows the sole experiment performed **(b)**.

4.7.2 MCL-1 and miR-29 modulate AIEC handling in DCs

MCL-1 expression has been shown to influence intracellular bacterial handling, for example in a macrophage model where timely apoptosis is thought to facilitate bacterial clearance[403]. When macrophages encounter bacteria, they may initially need to resist apoptosis in the face of strong pro-apoptotic signals[404], with subsequent apoptosis allowing resolution of infection while minimising inflammation[405]. Macrophages constitutively expressing MCL-1 demonstrate delayed apoptosis and pneumococcal killing, and a MCL-

1 transgenic mouse model showed less efficient clearance of pneumococci from the lung[403].

I postulated that miR-29, by manipulating MCL-1 in human DCs, may affect bacterial clearance and that the lack of this control in NOD2-mutant DCs may contribute to the impaired immunity seen in CD. I manipulated MCL-1 levels using an siRNA, and confirmed the effect by Western blot **(Fig. 4.4a)**. Subsequently, DCs were transfected with MCL-1 siRNA, or control, before exposure to live AIEC (adherent invasive *Escherichia coli*) derived from Crohn's patients. Reducing MCL-1 expression facilitated bacterial clearance, as measured by a standard killing assay **(Fig. 4.4b)**, a trend that was replicated by manipulation of miR-29 levels, where the antimiR reduced killing, and the premiR increased it in line with the MCL-1 siRNA**(Fig. 4.4c)**.

Despite this I found no significant difference in rates of cell death when miR-29 expression was modulated either by trypan blue staining or FACS analysis **(Fig. 4.4d and e)**. This may be because miR-29 also targets pro-apoptotic members of the BCL-2 family in DCs, for example BAK, a predicted target (Targetscan 8mer, aggregate P_{CT} 0.82). BAK interacts with MCL-1[406-408], and it is in part through this interaction that MCL-1 exerts its anti-apoptotic effect. Specifically reducing MCL-1 expression using an siRNA did result in a reduction in the rate of cell death when compared with a non-sense siRNA **(Fig. 4.4f)**.

Figure 4.4 MCL-1 and miR-29 modulate bacterial killing in DCs

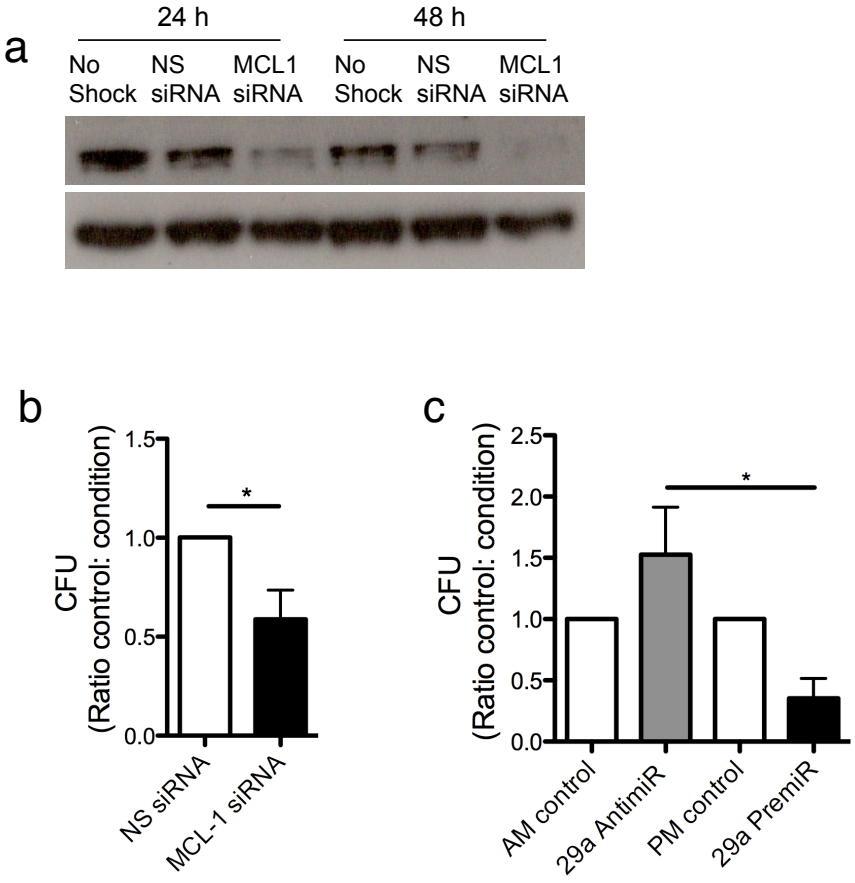


Figure 4.4 (a) DCs were left untransfected (no shock), or transfected with non-sense siRNA (NS), or MCL-1 siRNA for 24 or 48 hours (h). Cell lysates were subsequently blotted for MCL-1. **(b)** DCs were transfected with MCL-1 siRNA or control, and subsequently infected with AIEC for 2 hours before extracellular AIEC were killed with gentamicin. Cells were lysed and plated on agar plates, and placed at 37°C for 12 h. The graph expresses a ratio of colony numbers on agar plates, comparing control siRNA plates with MCL-1 siRNA plates. **(c)** Cells were transfected with miR-29a premiR or antimiR, or appropriate controls. The AIEC killing assay was performed as per MCL-1 siRNA experiment. The graph expresses a ratio of colony numbers on agar plates, comparing control plates with 29a antimiR or premiR plates. Significant results shown: analysis by two-tailed paired t-test **(b)**, or by one-way Anova with Bonferroni post test (*P=0.01 to 0.05) **(c)**. Data from 6 independent experiments **(b)**, 3 independent experiments **(c)**; error bars, s.e.m.

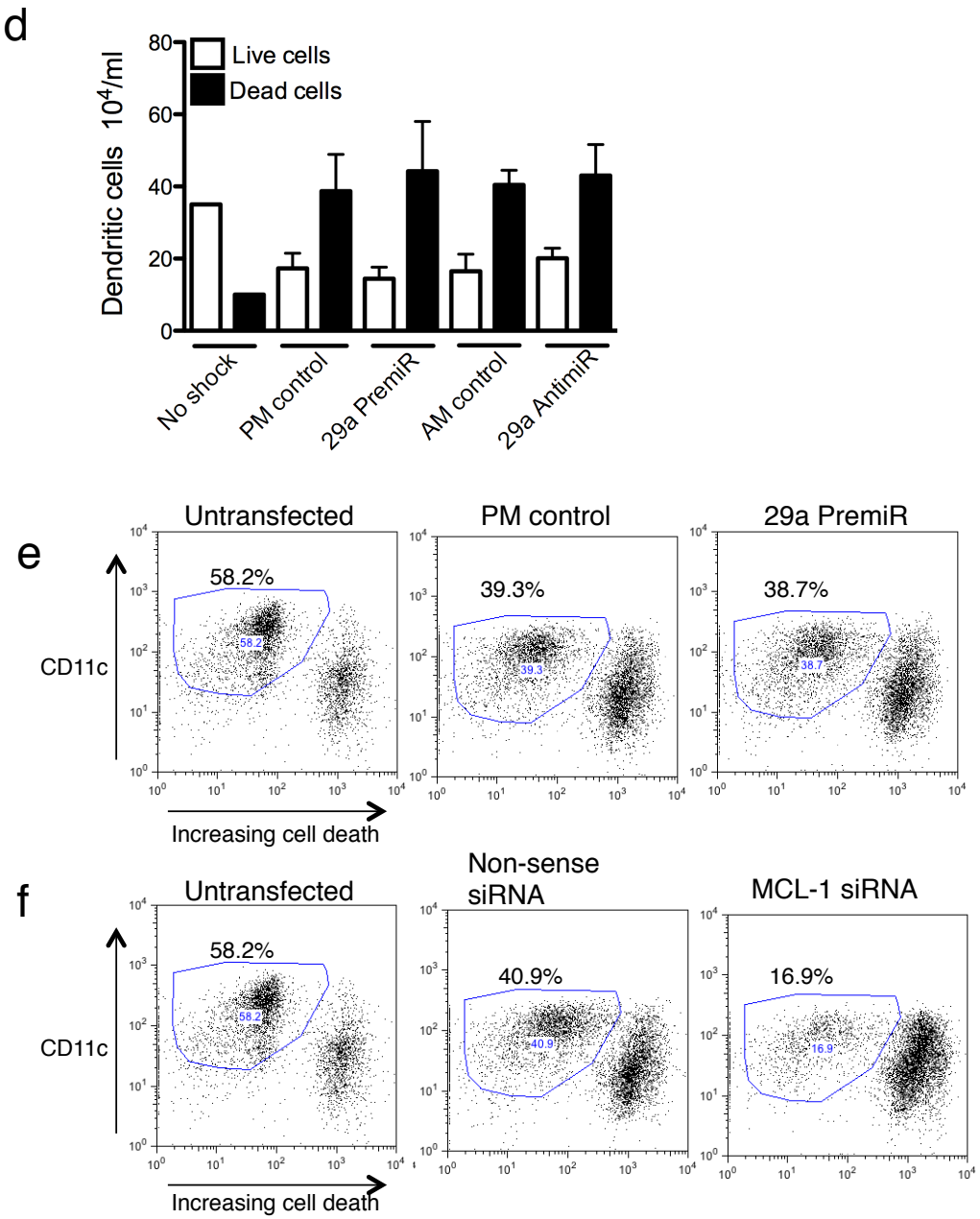


Figure 4.4 (continued) Live: dead cell ratio, assessed with trypan blue **(d)** staining and FACS analysis **(e)**, in DCs transfected with miR-29 premiR or antimiR for 24hrs before stimulation for 24hrs with MDP + Pam_3CSK_4 1μg/ml. **(f)** FACS analysis of live: dead cells in DCs transfected with MCL-1 siRNA, or control. Data from 4 independent experiments **(d)**; or representative of 3 independent experiments **(e) and (f)**; error bars, s.e.m.

This data raised the question as to whether the observed effect of both miR-29 and MCL-1 expression on bacterial handling could be attributed to apoptosis. As previously stated, NOD2 has been found to induce autophagy[157,244] and this induction is critical to MHC II induction, antigen presentation, and bacterial handling. However, the mechanism by which PRRs, such as NOD2, induce autophagy is not yet understood. The induction of autophagy is tightly regulated and requires the coordination of multiple proteins, with recent data providing a role for BCL-2 in preventing autophagy by inhibiting Beclin1 (also known as autophagy related gene-6 (ATG6))[409,410]. Beclin1 is a component of the class III phosphoinositide 3-kinase (PI3K) complex that is involved in autophagosome formation[411].

I postulated that MCL-1 may have a similar role to the related BCL-2 in preventing autophagy as well as apoptosis (indeed it has also been shown to interact with Beclin1[412]), and that the up-regulation of miR-29 through NOD2 with subsequent down-regulation of MCL-1, might lead to autophagy induction. It has subsequently been shown that MCL-1 does indeed regulate autophagy and apoptosis[413]. After MCL-1 degradation, autophagy was the favoured outcome unless it was specifically inhibited, or unless BAX was activated, in which case apoptosis ensued. Their results also suggest that loss of MCL-1, at least up to 8 h starvation, is not in itself sufficient to induce apoptosis. They went on to show that MCL-1 and Beclin1 interact at the mitochondria, the cellular location of MCL-1[414], (as opposed to the endoplasmic reticulum where BCL-2 resides and interacts with Beclin1[409]).

4.7.3 miR-29 and Wnt signalling

Two studies of osteoblast differentiation and function raised a connection between Wnt signalling and miR-29. As already discussed in Chapter 1, the first study demonstrated that the expression of miR-29 was increased by Wnt signalling[415]. The second developed this theme to provide evidence that a positive feedback loop exists between miR-29 and Wnt, via miR-29 targeting negative regulators of the Wnt pathway[340]. Wnt signalling can be inhibited by several classes of negative regulator, including DKK1 (Dikkopf-1)(a soluble factor) that acts in conjunction with Kremen2 (a decoy receptor), to prevent the binding of Wnt proteins to the LRP5/6 co-receptor. sFRP2 (secreted frizzled-related protein 2) binds extracellular Wnts to prevent their binding and activation of Wnt receptors. This study provided evidence that miR-29 directly targets all of these negative regulators to enhance Wnt signalling.

Wnt signalling is a fundamental pathway in the development and function of many tissues, not least the GIT, but an interesting immune-regulatory role specifically in GIT DCs was also recently published[416]. This demonstrated a critical role for Wnt-β-catenin signalling in DC production of anti-inflammatory mediators, such as IL-10, TGFβ, and enzymes of the retinoic acid pathway, and therefore the stimulation of regulatory T cells. This evidently raised the question as to whether NOD2 may control Wnt signalling in DCs via miR-29 expression, and that loss of this pro-regulatory signal might lead to the inflammation that occurs in the presence of NOD2 mutations.

I tested whether over-expression of miR-29, or blocking its effect with an antimiR, could alter Kremen2, DKK1 or FRP-2 levels in DCs **(Figure 4.5)**. Although the first results suggested a possible down-regulation of Kremen2 **(Fig. 4.5a)**, subsequent Western blots failed to recapitulate this result **(Fig.**

4.5b). Moreover, manipulation of miR-29 levels did not appear to affect either total β-catenin levels **(Fig. 4.5c)** or activated β-catenin, as measured by phosphorylation **(Fig. 4.5d)**. These results do not completely exclude the possibility that miR-29 regulates Wnt in DCs, however the fact that I could demonstrate no clear link between NOD2 and Wnt concurs with the original paper, which demonstrated that gut DC-Wnt signalling is constitutive and does not depend on gut commensals[416].

Figure 4.5 miR-29 and WNT signalling in DCs

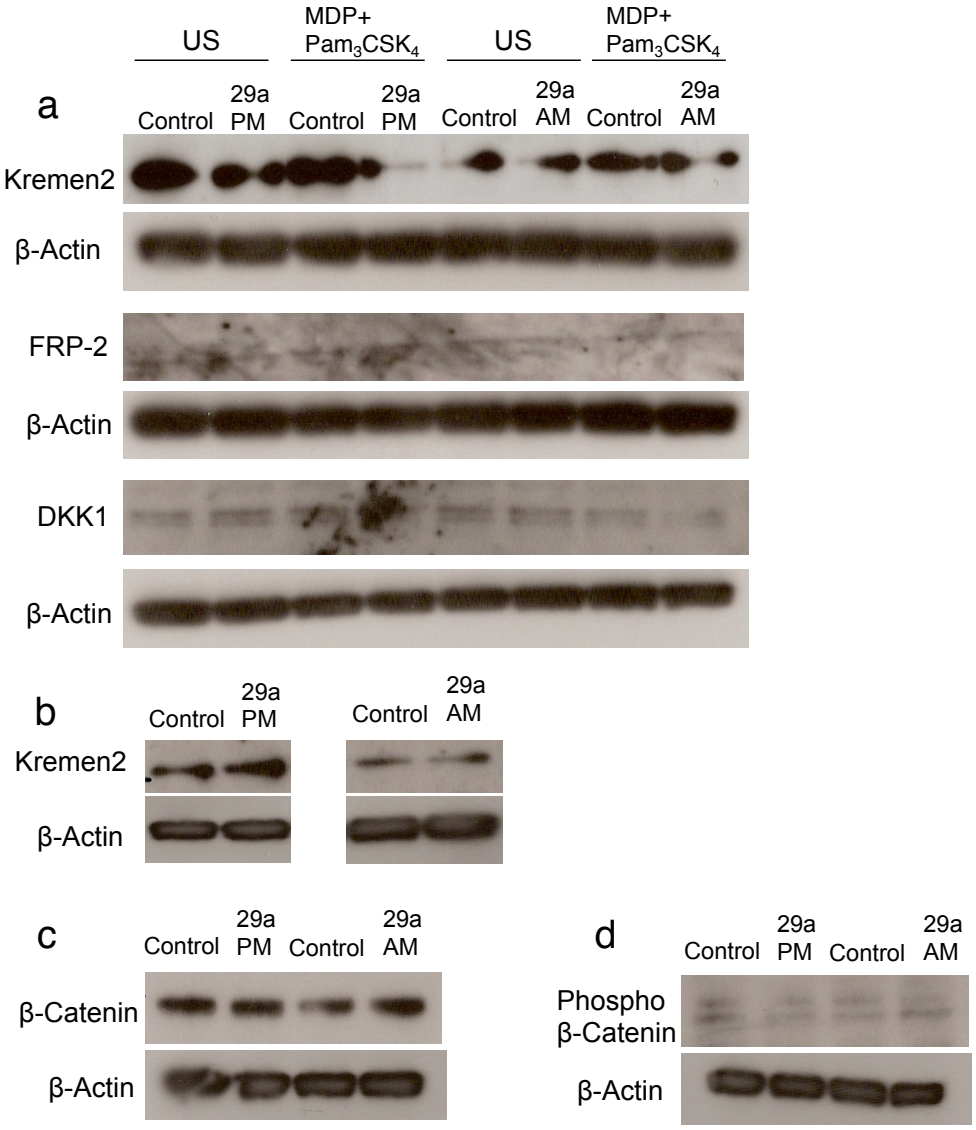


Figure 4.5 DCs were transfected with miR-29a premiR or antimiR, or appropriate controls, before being left unstimulated (US), or stimulated with MDP + Pam_3CSK_4 1μg/ml for 24 h. (All samples MDP + Pam_3CSK_4 1μg/ml stimulated for WB **(b), (c), and (d)**.) Cells were lysed and blotted for potential WNT signalling targets of miR-29 **(a) and (b)**, or for the effect on β-Catenin activation **(c) and (d)**. Data is representative of 2 WB **(a, b, c and d)**.

4.8 Other miR-29 published targets

Other than MCL-1 and Wnt signalling regulators, there were a number of published miR-29 targets that I assessed initially by qPCR, and subsequently by Western blot. Of the miR-29 targets published at that time, those in **Figure 4.6** were potentially the most interesting in terms of the possibility of affecting DC function.

Figure 4.6 miR-29 targets in DCs by WB: Published Targets

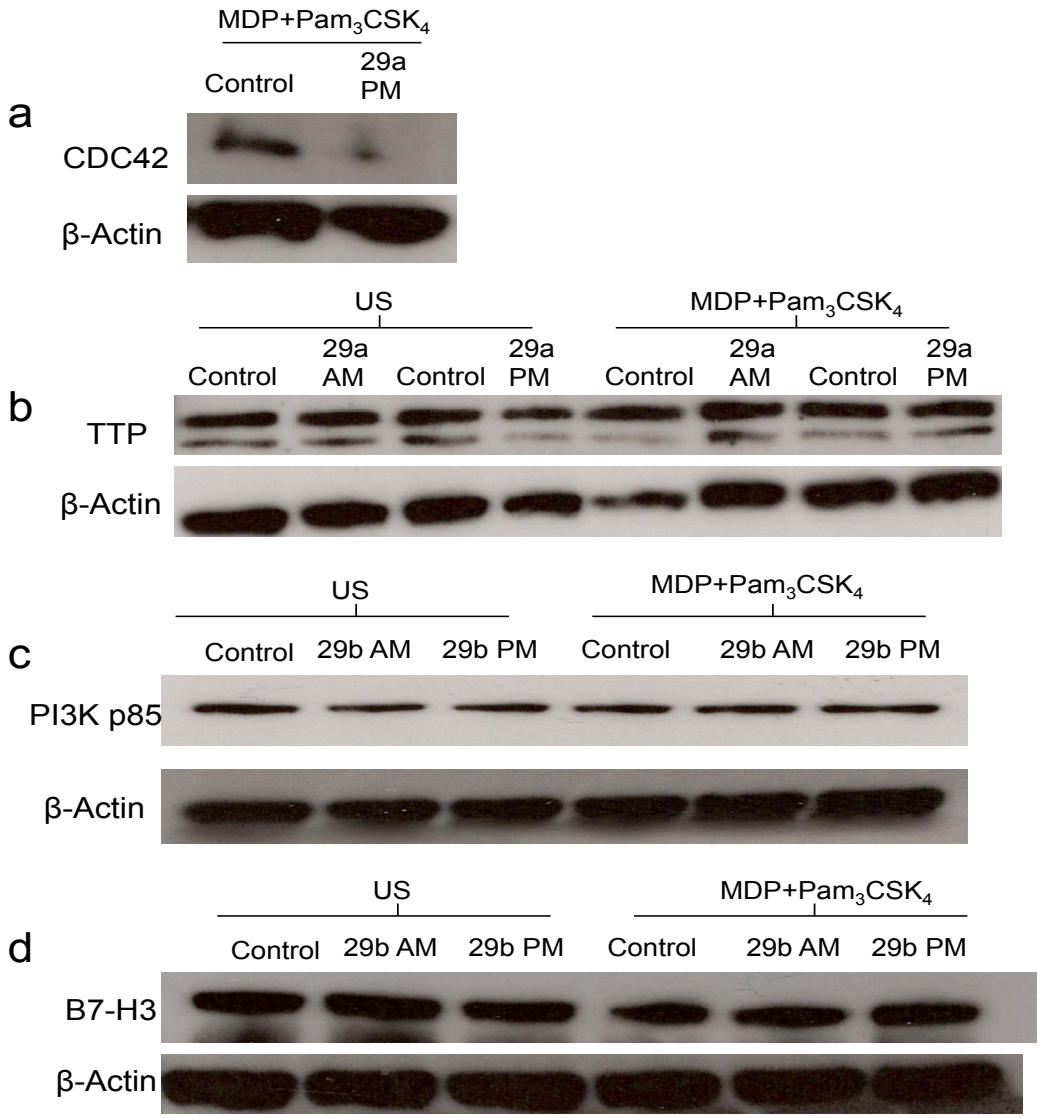


Figure 4.6 DCs were transfected with miR-29a premiR or antimiR, or appropriate controls, before being left unstimulated (US), or stimulated with MDP + Pam_3CSK_4 1μg/ml. Cells were lysed and blotted for potential targets of miR-29. Data is representative of 2 WB **(a, b, c and d)**.

4.8.1 CDC42

CDC42 (cell division cycle 42) is a member of the Rho family of small GTPases. Along with Rho and Rac, CDC42 performs a crucial function overseeing actin polymerization and depolymerisation[417]. The actin

cytoskeleton is dynamic, and control of this is important for modulating many aspects of cellular behaviour. CDC42 contains two miR-29 target sites (Targetscan 8mer and 7mer; P_{CT} <0.1 and 0.76), and was first described as a miR-29 target, along with PI3K p85α, in a study describing mechanisms of p53 activation[378]. I was initially interested in CDC42 because of its numerous roles in membrane trafficking and cell polarity[418], and in particular in phagocytosis and vesicle trafficking. DCs regulate their endocytic capacity depending on their state of maturity and activation – when immature they actively sample their environment and internalise antigen, but maturation coincides with a down-regulation of endocytosis as they concentrate on antigen presentation. Reduced levels of activated (although not total) CDC42 have been associated with this change[419], raising the question as to whether miR-29 control of CDC42 could facilitate this change in DC function.

A more recent study has also identified CDC42 as a mediator of the DC: T cell immune synapse (IS)[420], specifically of the microtubule cytoskeleton (the microtubule organizing centre) that regulates delivery of cytokines and secretory organelles to the IS. This data suggests that loss of CDC42 blocks the flow of cytokines, for example IL-12, to the IS, thus altering T cell effector function.

I was able to confirm CDC42 as a protein down-regulated in DCs by miR-29 **(Fig. 4.6a)**, but unfortunately due to work on other miR-29 targets I was unable to further investigate how this affects DC function.

4.8.2 TTP, PI3K p85, B7-H3

Figure 4.6 (b), (c) and (d) demonstrate Western blots of published miR-29 targets that I was unable to verify in DCs. Tristetraprolin (Targetscan 7mer; P_{CT} 0.83), PI3K p85 (Targetscan 7mer; P_{CT} 0.83), and B7-H3 (Targetscan 8mer; P_{CT} 0.88) all have predicted miR-29 target sites in their 3'UTRs. These proteins and some of their functions have already been discussed in the introduction to this chapter. The lack of a response in human DCs to miR-29 demonstrates either the cell-specificity of miRNA effects, or perhaps that the published data and my methodology differ to such a degree that our results are inconsistent.

4.9 Predicted miR-29 targets

4.9.1 A20/ TNFAIP3

A20 (also known as TNFAIP3) is an inhibitor of NFκB activation. As a key transcription factor that regulates a vast number of immune and inflammatory genes[421], NFκB must be tightly regulated. Several autoregulatory feedback loops for NFκB have been described, with A20 playing a critical role. A20 is an intracellular zinc finger[422] ubiquitin editing protein that was originally described as a TNF-inducible protein[423], and subsequently as under the control of NFκB[424], as well as a number of other stimuli (reviewed in[425]). Ubiquitination is a post-translational modification that influences the fate of proteins – for example polyubiqutin chain formation through Lys48 directs proteins to proteosomal degradation; alternatively Lys63-linked polyubiquitination can lead to stabilisation of protein-protein interactions, such as those seen in NFκB signalling[426,427]. Enzymes control the process of ubiquitination – E1 activating enzymes, E2 conjugating enzymes, and E3

ubiquitin ligases. A20 has both N-terminal deubiquitinating enzyme activity, and C-terminal E3 ligase activity[428], and through these negatively regulates NFκB activation.

A20-deficient mice develop severe (fatal) multi-organ inflammation and cachexia[429]. This phenotype appears to be predominantly due to myeloid cell lineage dysfunction, as the absence of lymphocytes in RAG1/ A20-deficient double knockout mice does not affect the outcome[429], whereas bone marrow transfer from A20-deficient to wild-type mice gives a similar phenotype[430].

In the specific context of my project A20 is interesting firstly as it has been described as a negative regulator of both TLR-mediated NFκB activation by restricting TRAF6 (TNF receptor-associated 6) ubiquitination[430], and also of NOD2-mediated NFκB activation through restricting RIPK-2 ubiquitination[163]. Secondly, a GWAS identified A20 polymorphisms as being associated with Crohn's disease[19]. Thirdly, as well as other features, A20-deficient mice develop severe intestinal inflammation, demonstrating the importance of this protein in intestinal homeostasis.

A20 is a strongly predicted target of miR-29 (Targetscan 8mer; P_{CT} 0.92). It was an ideal candidate to assess as a miR-29 target, especially given that miR-29 expression depends on NOD2 and is most significant on TLR co-stimulation. The working hypothesis was that over-expression of A20 in the absence of miR-29 control could ultimately lead to defective NFκB activation and immuneparesis.

Human DCs were transfected with miR-29 premiR or control as before and, after 24 or 48 h, a Western blot was performed using an anti-A20 antibody **(Fig 4.7a)**. Initial results suggested that there was reduction in A20 expression

after 48 h overexpression of miR-29. I did produce some other encouraging results including: an inverse correlation between A20 expression and miR-29 expression levels **(Fig 4.7b)**; and an apparent increase in A20 expression in FS1007insC DCs derived from CD patients when stimulated with MDP+Pam_3CSK_4, as compared with wild-type NOD2 (WT) controls **(Fig. 4.7c)**.

Figure 4.7 Analysis of miR-29 potential target A20 in DCs

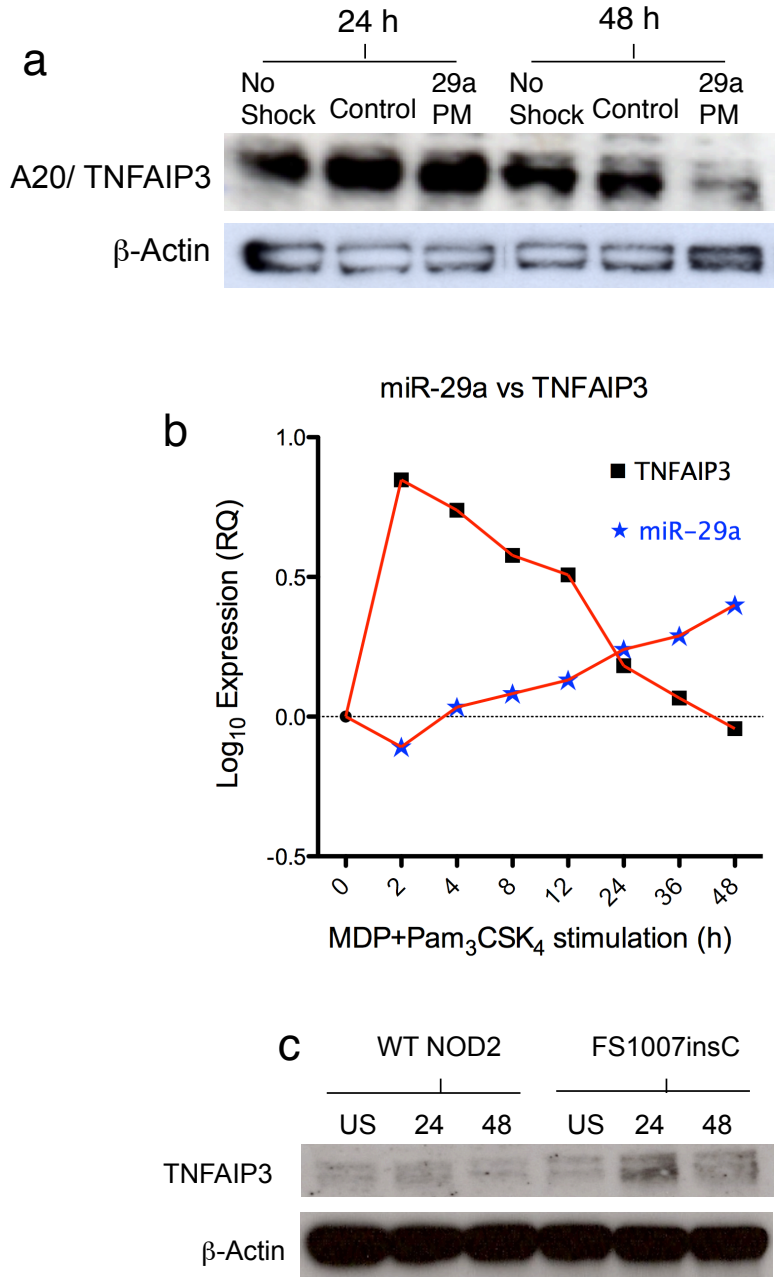


Figure 4.7 (a) DCs were left untransfected (no shock), or transfected with miR-29 premiR (29a PM) or negative control (control) for 24 or 48 hours (h). Cell lysates were subsequently blotted for A20/ TNFAIP3. **(b)** A20/ TNFAIP3 and miR-29 qPCR in DCs stimulated with MDP + Pam_3CSK_4 1μg/ml, over time. **(c)** WB for A20/ TNFAIP3 in wild-type (WT) NOD2 DCs, or FS1007insC NOD2 DCs, left unstimulated (US), or MDP + Pam_3CSK_4 1μg/ml stimulated for 24 or 48hrs.

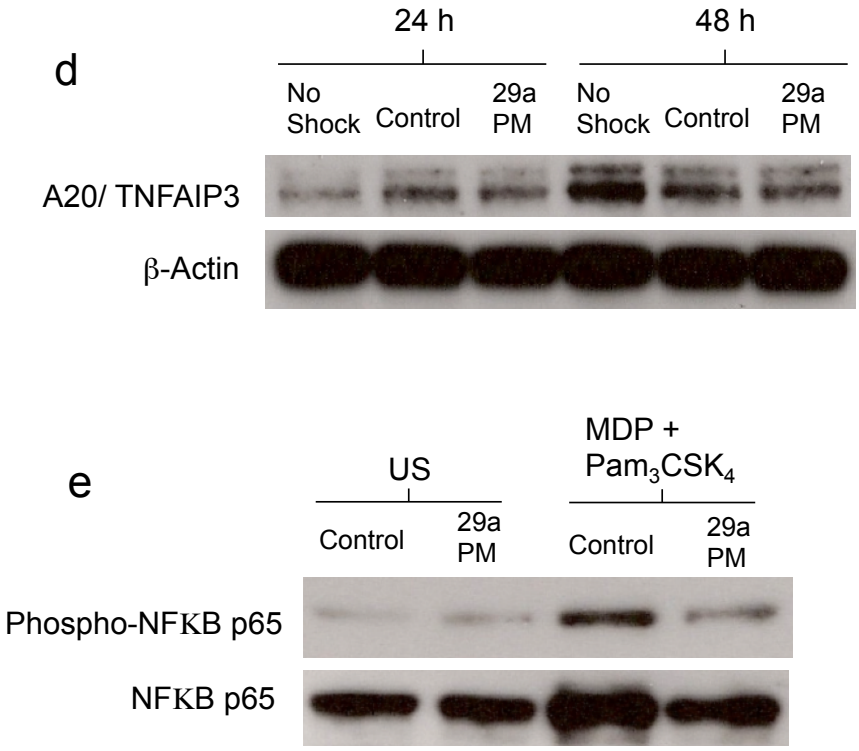


Figure 4.7 (continued) (d) DCs were treated as per figure (a). **(e)** DCs were transfected with miR-29 premiR or control, and then left unstimulated (US) or stimulated with NOD2 and TLR2 ligands for 24 h, before cell lysates were blotted for phosphorylated NFκB, and NFκB control.

However, the reduction in A20 on miR-29 over-expression was not reliably reproducible **(Fig. 4.7d),** (as opposed to the highly reproducible effect on MCL-1 expression, or indeed IL-12p40 and IL-23p19 (see chapter 5), that occurred consistently on miR-29 premiR transfection). Moreover, an analysis of NFκB activation provided no evidence that NFκB phosphorylation was increased on miR-29 over-expression, as you might expect if the expression of negative regulator A20 was reduced **(Fig. 4.7e)**. (Indeed if anything phosphorylation might be reduced although the loading was clearly not equal in this case, as shown by the total NFκB control). Lastly, I was also unable to reproduce the patient data (not shown). On reflection the negative finding of

this project is not surprising. Firstly the pattern of miR-29 expression in relation to A20 may be a little odd in this context, given that miR-29 expression is seen from 8-12 h and peaks around day 3 **(Fig. 3.10c)**. As A20 is a negative regulator of NFκB, a transcription factor that is activated within minutes of TLR and NOD2 triggering, a microRNA appearing this late in order to control A20, and by implication NFκB, would have missed the opportunity to influence the system by many hours. Secondly, mucosal biopsies from 69 CD patients demonstrated consistent *down*-regulation of A20[431], which would be at odds with the loss of miR-29 seen in NOD2 mutants **(Fig. 3.11c and d)**.

4.10 Other miR-29 predicted targets

4.10.1 TNFRSF1A (Targetscan 8mer; P_{CT} 0.79)

Tumour necrosis factor receptor superfamily 1A (TNFRSF1A) is one of two major receptors for TNFα, and therefore is an important mediator of the inflammatory response and apoptosis. Genetic polymorphisms in TNFRSF1A are associated with the autosomal dominant tumour necrosis factor receptor-associated periodic syndrome (TRAPS)[432], and with Crohn's disease[433,434]. Despite an 8mer predicted miR-29 seed target sequence there is no demonstrable reduction in TNFRSF1A protein expression in DCs after transfection of a miR-29 premiR **(Fig. 4.8a)**.

Figure 4.8 miR-29 targets in DCs by WB: Predicted Targets

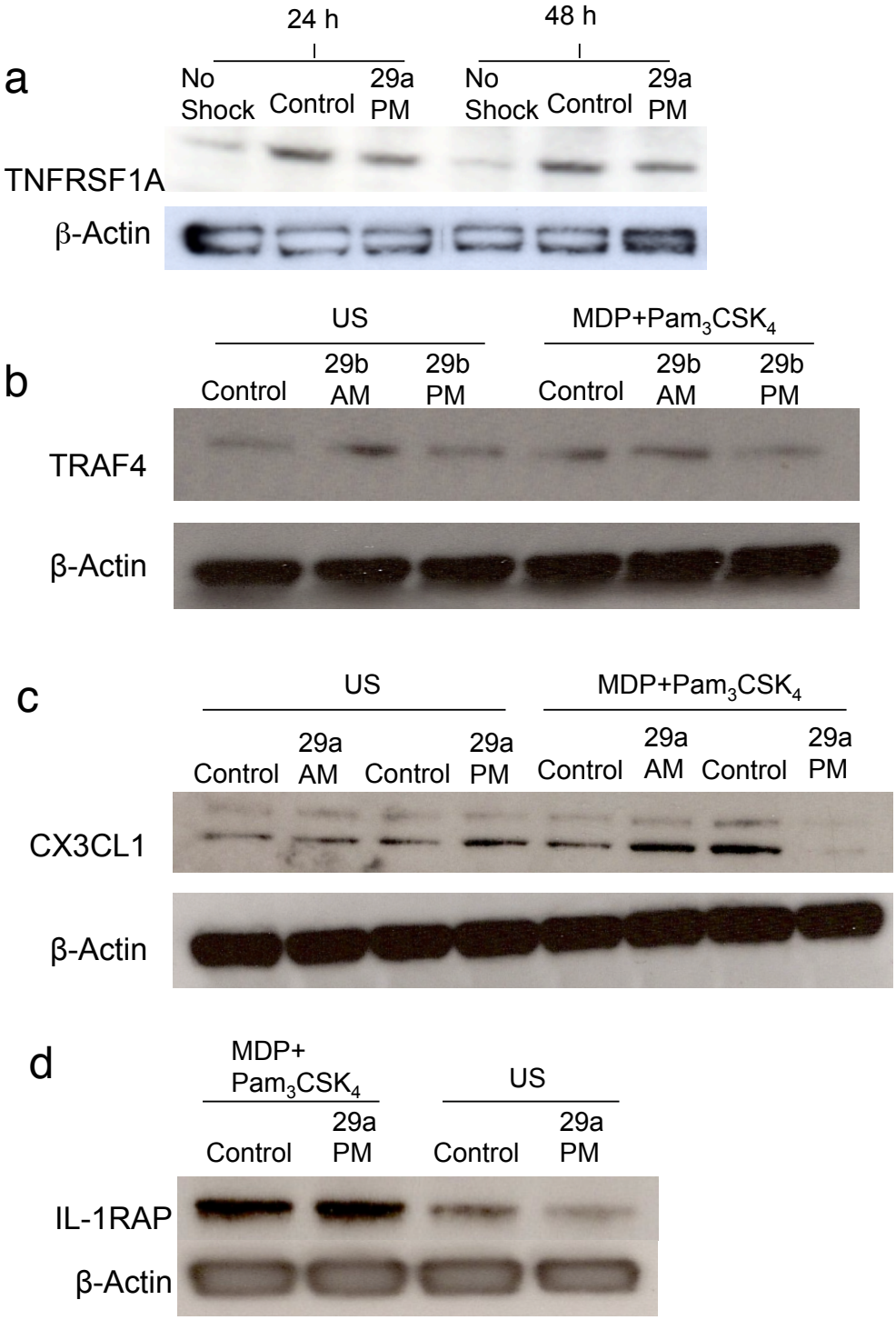


Figure 4.8 DCs were transfected with miR-29a premiR or antimiR, or appropriate controls, before being left unstimulated (US), or stimulated with MDP + Pam_3CSK_4 1µg/ml. Cells were lysed and blotted for potential targets of miR-29. Data is representative of 2 WB **(a, b, c and d)**.

4.10.2 TRAF4 (Targetscan 7mer x2; P_{CT} 0.83)

Tumour necrosis factor-associated factor 4 (TRAF4) is a largely uncharacterised member of this family of proteins that include TRAF6, already discussed as critical mediator of PRR signalling. Consistent with other TRAFs, TRAF4 has an N-terminal RING domain that confers E3 ubiquitin ligase function, followed by a series of zinc fingers, and a C-terminal TRAF domain that facilitates heterotypic protein-protein interactions. Although TRAF4 binding partners and its potential role in immune function are less well characterised than other family members, it has been shown to interact with p47, a component of cytosolic NADPH (nicotinamide adenine dinucleotide phosphate) oxidase, and with TRAF6 and TRIF (Toll-IL-1 receptor domain-containing adaptor-inducing IFN-beta) molecules to negatively regulate TLR-induced NFκB activation and IFNβ production[435]. I therefore thought it would be interesting to determine if miR-29 regulated TRAF4 expression in DCs. TRAF4 has a low level of expression in DCs, but I could detect a possible reduction in expression by western blot **(Fig. 4.8b)**. If this is a bona fide miR-29 target, it raises the possibility that NOD2 stimulation leads to amplification of the immune response through miR-29 expression. However, this result was difficult to replicate, in part because of the low expression, and I did not analyse its potential ramifications further.

Subsequently a study has identified TRAF4 as a protein that can interact with NOD2 and MEKK4, and negatively regulate MDP-induced NFκB activation[436]. However, the interaction data was only produced from protein over-expression experiments in cell lines, and the NOD2-TRAF4 interaction may be an artefact as the structurally similar TRAF6 also interacts with NOD2[436].

Moreover, any specific relation to CD pathogenesis is unlikely since direct binding of NOD2 and TRAF4 was required for inhibition of NOD2 function (for example bacterial killing), but constructs expressing NOD2 mutations also co-precipitate with TRAF4.

4.10.3 CX3CL1 (Targetscan 7mer; P_{CT} 0.93)

The chemokine CX3CL1, or Fractalkine, exists in a membrane-bound form and a soluble form, and can function as an adhesion molecule and chemoattractant respectively[437]. It is predominantly expressed on/ by epithelial and vascular endothelial cells[438], resulting in the attraction of CX3CL1-receptor (CX3CR1) positive lymphocytes, macrophages and DCs, after infectious/ inflammatory triggers. CX3CR1 expression also has a critical role in the formation of DC transepithelial dendrites in the gut, allowing efficient sampling of GI bacteria[439].

CX3CL1 expression is increased in the mucosa and vascular endothelium of actively inflamed CD patients[440], and CX3CR1-deficient mice are protected from DSS colitis[441]. CXC3L1 expression has also been observed in lymphoid tissue resident mature DCs[442], and the authors postulate that this may improve DC to T cell interactions. However DC expression of CX3CL1 has not been replicated in every study[438], and the role of CX3CL1 (as opposed to its receptor) in DCs remains uncertain.

I was able to confirm that CX3CL1 is expressed in both unstimulated and MDP+Pam_3CSK_4 stimulated DCs, and that CX3CL1 expression is down-regulated in stimulated cells by miR-29 over-expression, as assessed by WB **(Fig. 4.8c)**.

4.10.4 IL-1RAP (Targetscan 8mer; P_{CT} 0.87)

Interleukin-1 receptor accessory protein (IL-1RAP) is an essential component of the IL-1 receptor complex. Absence of IL-1RAP leads to an inability to respond to IL-1 in both murine and human cell line models[443-445]. IL-1RAP interacts with IL-1RI (interleukin 1 receptor, type I) only after IL-1 binding has caused a conformational change in the latter[446], and although IL-1RAP does not itself bind IL-1 directly, it increases the avidity of IL-1 for IL-1RI about 5-fold. A soluble form of IL-1RAP also exists, and may act as an inhibitor of IL-1 signal transduction[447].

I detected a subtle down-regulation of IL1-RAP in unstimulated DCs over-expressing miR-29, but no appreciable change in DCs stimulated with MDP+Pam_3CSK_4 **(Fig. 4.8d)**. This raises the possibility that NOD2-driven miR-29 knockdown of IL-1RAP normally functions to repress IL-1 signalling at the termination of an immune response.

4.11 Discussion

In this chapter I confirmed a number of published miR-29 targets in human DCs (MCL-1, CDC42) and identified some novel targets (CX3CL1, and possibly TRAF4 and IL-1RAP). I also investigated the possibility of miR-29 controlling A20 and Wnt signalling, although I was unable to confirm these.

MCL-1 levels influence intracellular bacterial handling in a basic bacterial killing assay, as do miR-29 levels. I did not determine the exact mechanism for this, but it is most likely linked to the control of bacterial autophagy (or xenophagy) in which MCL-1 plays a part. This link from NOD2 function, to

miR-29 expression, via MCL-1 to autophagy may be a significant mechanism in the previously described NOD2-mediated autophagy.

miR-29 control of CDC42 also raises interesting, but as yet unexplored, possibilities that NOD2 may control both a down-regulation of endocytosis on DC activation, and the down-regulation of the delivery of cytokines to the immune synapse. This latter function may augment the reduction in IL-23 by miR-29 described in chapter 5, and contribute to the cessation of an active immune response in order to limit tissue damage.

miR-29 control of CX3CL1 is an interesting finding, not least as DC expression of this chemokine (rather than its receptor) is somewhat controversial. In the context of DC function, it raises the possibility that NOD2 could modulate transepithelial dendrite formation, and since this would also affect microbial sampling this may be a mechanism through which NOD2 affects the microbiome. If miR-29 expression is also induced in gut epithelial cells via NOD2, then control of CX3CL1 could be an important mechanism to reduce immune cell recruitment, and again a way in which the immune response could be appropriately terminated.

The question as to whether NOD2 controls miR-29 expression in other cells is important, not least if this occurred in Paneth cells. The way in which NOD2 signalling induces the secretion of α-defensins is not fully understood, but as described defensin production in general appears to be responsive to Wnt signalling. Although I was unable to demonstrate miR-29 control of the Wnt pathway in DCs, it is interesting to speculate that if the increased Wnt signalling via miR-29 described in osteoblasts also occurs in Paneth cells, this could be the NOD2-mediated mechanism of defensin production.

Overall in this chapter the confirmed miR-29 targets suggest that it functions not only to improve intracellular bacterial handling (possibly via autophagy induction), but that it also probably assists in the down-regulation of the immune response. This chapter no doubt demonstrates the potential gains that can be achieved by a target-selective approach to miRNA studies, but it also ably demonstrates some problems. The most obvious of these is the significant amount of time and effort involved in essentially screening the targets this way, as many of them turn out to be negative. Also by taking a 'candidate' approach although you isolate functionally interesting proteins, you also bias the results and do not allow the opportunity for surprise findings. In the next chapter I rectify this fault by using a DNA array to screen for miR-29 targets in an unbiased manner.

5 MicroRNA-29 controls IL-23 in human DCs

5.1 Introduction

As already described, the functional role of NOD2 is not completely defined, in particular the mechanism by which it signals in dendritic cells (DCs). Like other PRRs, it can induce NFκB activation[137] but in comparison with PRRs such as the Toll-like receptors (TLRs) this effect is rather weak[194]. Large-scale gene expression studies have shown NOD2 can synergize with other PRRs in differential gene regulation and that this synergy is lost in cells expressing Crohn's variant NOD2[194,195,197].

NOD2 plays a key role in amplifying release of certain pro-inflammatory cytokines in this context, particularly IL-1β, IL-6 and IL-23 from DCs and macrophages[253,260]. IL-6 and IL-23 are required for induction of Th17 $CD4^+$ T cells, a response important for anti-microbial immunity at mucosal surfaces and a hallmark of the inflammatory response in Crohn's.

The significance of the IL-23/ Th17 pathway for Crohn's pathogenesis was highlighted by genetics studies, with polymorphisms in IL23R, IL12B (IL-12p40), STAT3, JAK2 and TYK2 all contributing to disease predisposition[11]. A key role for IL-23 in intestinal inflammation has been demonstrated in both innate and T cell-dependent experimental models of colitis[46,47]. IL-23R signalling in T cells leads to enhanced Th17 accumulation, reduced differentiation of FoxP3(+) T cells and reduced T cell IL-10 production[57]. In innate colitis IL-23 directs expression of IL-17 and induction of pathology via

innate lymphoid cells (ILCs)[448]. IL-23 is increased in mucosa of IBD patients[58] and increased ILCs are present[449], emphasizing the importance of this axis in controlling inflammation in colitis.

IL-23 is produced by dendritic cells and macrophages, and its release is mediated by NOD2 in combination with TLRs. It is important that PRR signalling pathways inducing effector cytokines such as IL-23 are tightly regulated so that homeostasis can be restored at the termination of an immune response. In this chapter I present results of a DNA array using DCs over-expressing miR-29. By undertaking large scale gene expression profiling I identify a number of miR-29 target genes within inflammatory/immune pathways, and within genes that have previously been described as containing Crohn's disease susceptibility polymorphisms. This screen for miR-29 targets also highlights IL-12p40. Subsequent experiments demonstrate that miR-29 controls expression of both IL-23 cytokine subunits, and that this is defective in the presence of CD-associated NOD2 polymorphisms.

5.2 Aims

The aims of this chapter are:

- To identify miR-29 targets in human DCs using a DNA array
- To investigate miR-29 control of IL-12p40 and IL-23p19
- To establish the effect of NOD2 mutations on IL-23 regulation

5.3 Results

5.3.1 miRNA 29 influences the expression of multiple inflammatory genes in DCs including IL-12p40

It has been shown that miRNAs mostly act to down-regulate mRNA of target genes, rather than at the translational level in mammalian cells[362], and that for those targets with significant protein repression this usually occurs predominantly via mRNA destabilisation[363]. I therefore decided to assess miR-29 function in DCs on a more global scale using a DNA array. I transfected NOD2+TLR2 stimulated DCs with miR-29 premiR to artificially increase miR-29 expression and determined, by microarray analysis, potential target genes among mRNAs that were differentially regulated. RNA quality was first assessed by nanodrop and then by bioanalyzer **(Table 5.1)**. Three biological replicates were chosen from five samples prepared, and large scale gene expression profiling was undertaken.

Amongst the differentially regulated mRNAs I observed a bias in genes previously described as functioning in immune or inflammatory pathways or as IBD susceptibility genes **(Fig. 5.1a and b; Fig. 5.2a, b and c)**. Other genes involved in protein and endoplasmic reticulum regulation **(Fig. 5.1c)** and proteins integral to the cell membrane **(Fig. 5.1d)** are also shown. I confirmed a number of these putative targets as being differentially regulated by miR-29 by qPCR **(Fig. 5.3)**. One of the most strongly down-regulated genes identified by this methodology was IL-12p40, a subunit of IL-12 and IL-23 and a known IBD susceptibility gene. Thus miR-29 exerts broad control over a number of inflammatory and immune pathway genes including known IBD susceptibility genes such as IL-12p40.

Table 5.1 RNA preparation for DNA array

a

Sample ID	Conc.	260/280	260/230	Volume	Conc.	260/280	260/230	Volume	Yield	RIN:
BC2 PMC	347	2.03	2.13	50	456.6	2.04	2.02	44	20.1	RIN:7.2
BC2 29a PM	313	2.03	2.14	50	391.7	2.04	2	47	18.4	RIN:6.9
BC2 29b PM	313	2.03	2.09	50	380.8	2.04	1.98	43.5	16.6	RIN:6.6
BC1 PMC	611	2.04	2.04	50	750.6	2.03	2	44	33.0	RIN:7.6
BC1 29a PM	623	2.05	2.08	50	723	1.98	2.07	45	32.5	RIN:8
BC1 29b PM	617	2.04	2.11	50	678	2.03	2.11	42	28.5	RIN:7.9
BC6 PMC	235	2.04	2.07	50	240.2	2.02	1.89	42	10.1	RIN:4.6
BC6 29a PM	197	2.04	2.11	50	197.4	2.03	2	46	9.1	RIN:7
BC6 29b PM	237	2.04	2.1	50	279.9	2.04	2.03	44	12.3	RIN:6.7

b

Sample ID	Conc.	260/280	260/230	Volume	260/280	260/230	Volume	Yield	RIN
BC38 PMC	181	2.06	2.15	50	2.06	1.96	42	9.56	RIN:7.8
BC38 29a PM	143	2.06	2.05	50	2.03	1.86	42	7.46	RIN:8.1
BC38 29b PM	149	2.07	2.15	50	2.02	1.96	43.5	7.50	RIN:8.3
BC42 PMC	254	2.02	1.65	50	2.04	1.46	42.5	12.07	RIN:7.5
BC42 29a PM	302	2.02	2.04	50	2.06	2.04	41.5	12.82	RIN:7.2
BC42 29b PM	281	2.04	2.19	50	2.06	2.06	42	11.87	RIN:7.4

OriginalNanodrop	Fail
OGT QC	Borderline Fail

Table 5.1 miR-29 premiRs (PM), or negative control (PMC), were transfected into DCs for 16hrs, then stimulated for 8hrs with MDP + Pam_3CSK_4 1μg/ml. RNA was quantified using NanoDrop® ND-1000 (green background), and subsequently RNA quality checked using RNA 6000 Nano Assay on Agilent bioanalyzer 2100 (blue background). **(a)** Of the original three biological replicates, two were of substandard quality, and therefore **(b)** two further replicates were generated. cDNA was hybridised to Agilent whole human gene expression arrays, and the results analysed using Genespring.

Figure 5.1 DNA Array results

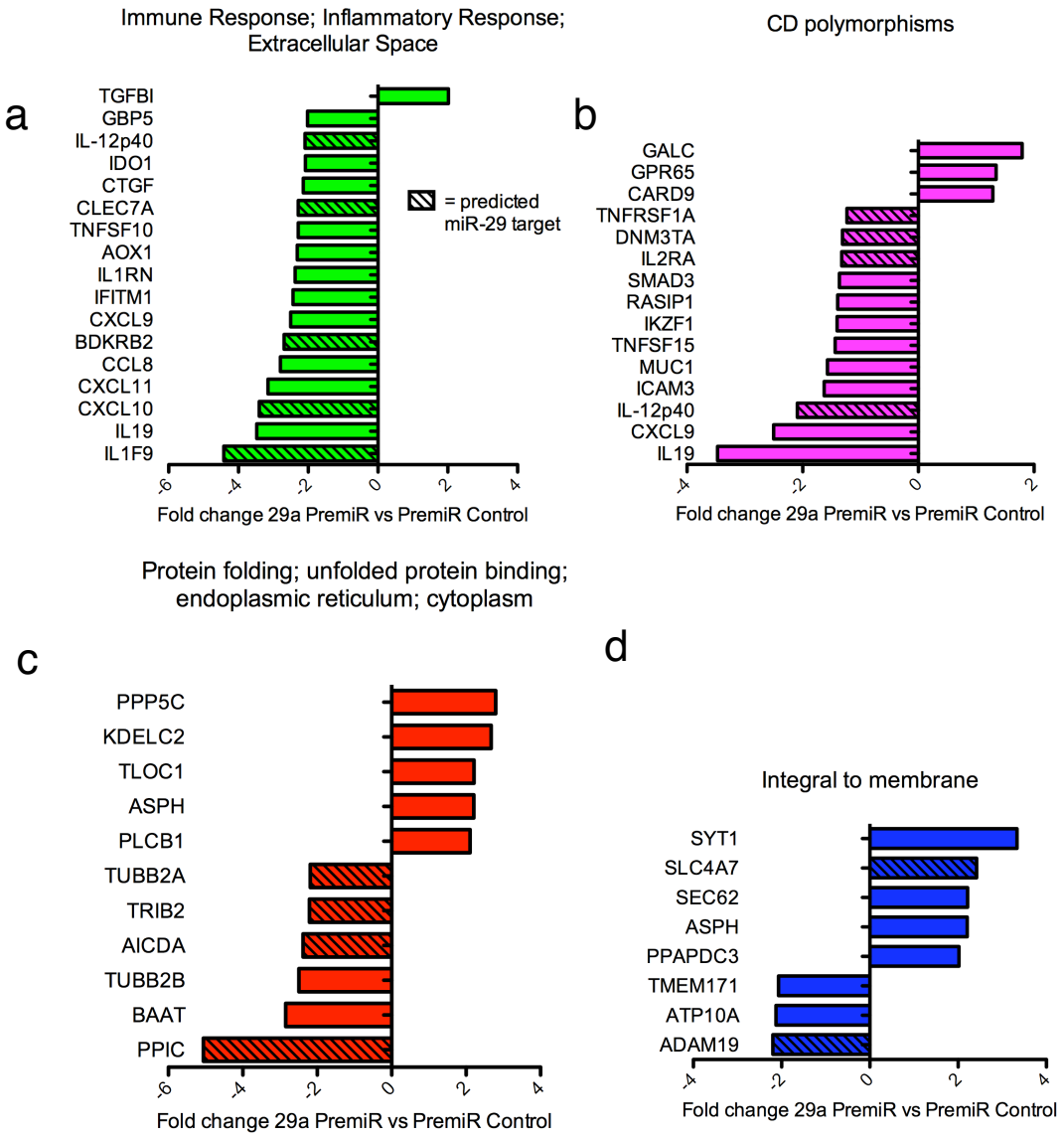
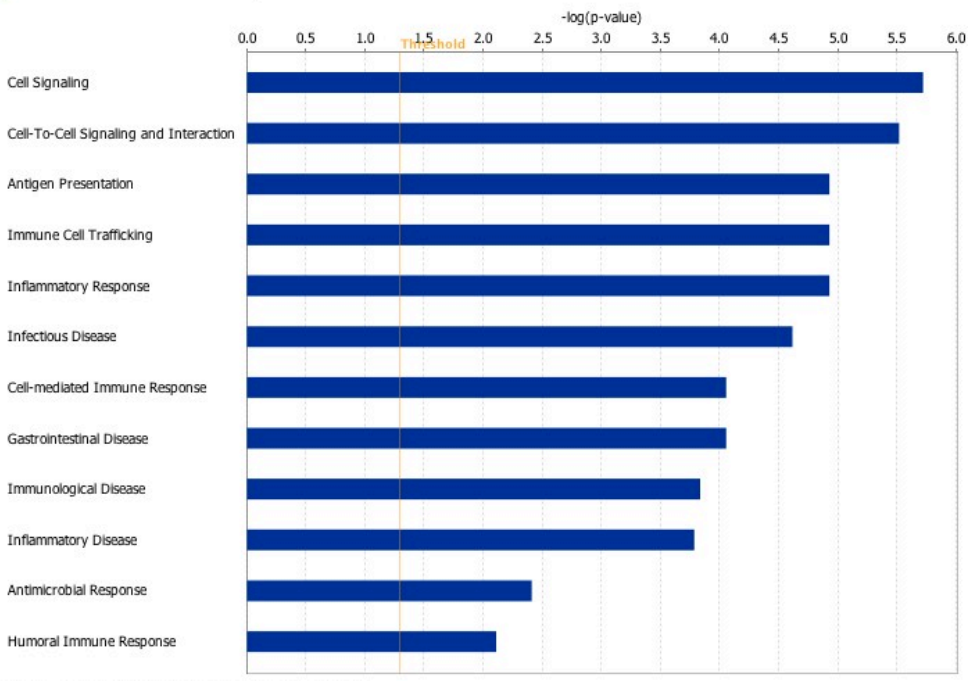


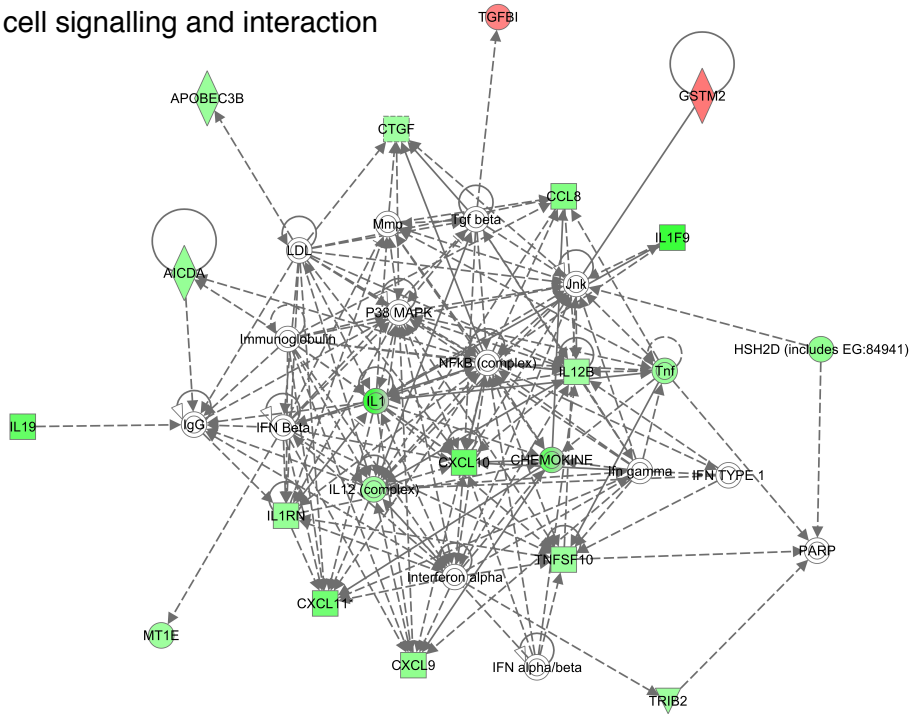
Figure 5.1 DNA array results analysed by Genespring. **(a), (c), and (d)** Results presented as per GO terms for genes more than 2 fold up- or down-regulated when comparing miR-29a premiR with negative control (PMC); or **(b)** Crohn's disease (CD) susceptibility genes more than 1.2 fold up- or down-regulated for the same analysis.

Figure 5.2 DNA Array results: Ingenuity analysis

a



b Cell to cell signalling and interaction



C Inflammatory response, cardiovascular system development and function, cell-mediated immune response

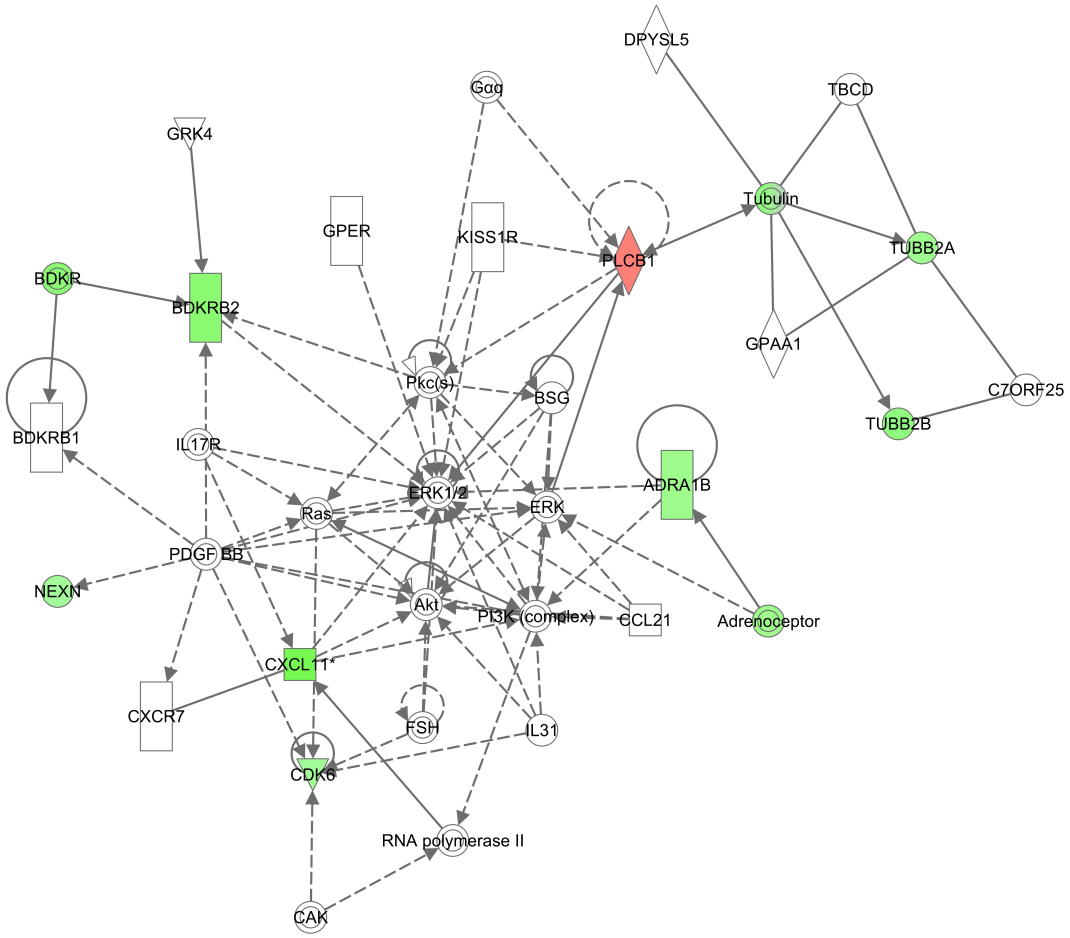


Figure 5.2 (a) Ingenuity analysis of DNA array data. Bar chart shows a biological function analysis of the DNA array data, performed in Ingenuity.
Ingenuity pathway analysis of DNA array: **(b)** Cell-to-cell signalling and interaction, and **(c)** Inflammatory response, cardiovascular system development and function, cell-mediated immune response. These figures display the known and putative interactions between mediators of cell signalling etc, that were shown by the DNA array to be regulated by miR-29 expression. They provide a visual representation of the array data and the cellular pathways and networks that miR-29 modifies within DCs.
Green= down-regulated by miR-29 expression on DNA array, Red= up-regulated by miR-29 expression on DNA array.

Figure 5.3 qPCR assessment of DNA Array Results

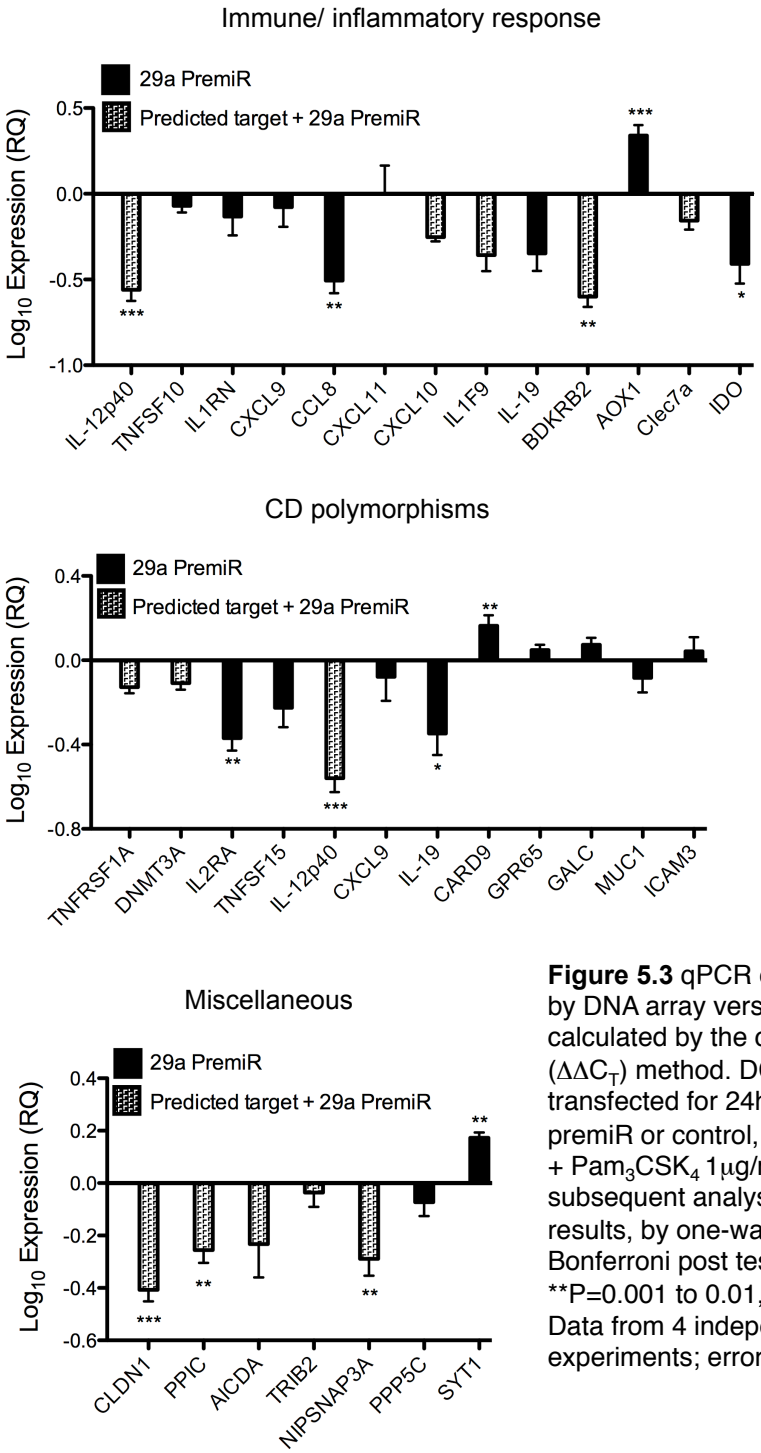
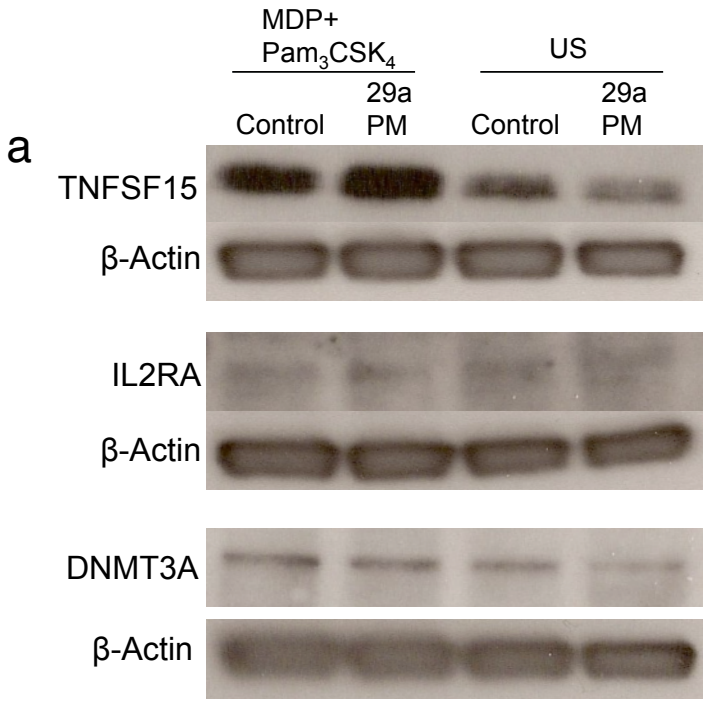


Figure 5.3 qPCR of genes identified by DNA array versus GAPDH control, calculated by the change in threshold ($\Delta\Delta C_T$) method. DCs were transfected for 24hrs with miR-29 premiR or control, before 24hrs MDP + Pam_3CSK_4 1μg/ml stimulation, and subsequent analysis. Significant results, by one-way Anova with Bonferroni post test (*P=0.01 to 0.05, **P=0.001 to 0.01, and ***P<0.001). Data from 4 independent experiments; error bars, s.e.m.

5.4 Other miR-29 targets

As well as IL-12p40, I assessed the effect of miR-29 on the expression of other genes/ proteins identified by the array – predominantly I chose those that also straddled both the immune/ inflammatory and CD-susceptibility gene groups. Before moving on to the IL-12/23 data that are the main findings of this chapter, I will discuss some of these other effects and their potential relevance to NOD2 variants and Crohn's. As previously, DCs were transfected with miR-29 premiR, and then left unstimulated or MDP+Pam_3CSK_4 stimulated, before cell lysates were analysed by WB **(Fig. 5.4a)**. DNMT3A and TNFSF15 (Tumour necrosis factor (ligand) superfamily, member 15) both demonstrated some down-regulation of expression, particularly in unstimulated cells, although these differences were relatively small. IL2RA, a component of the IL-2 receptor complex, is apparently expressed at very low levels in monocyte-derived DCs, and is unaffected by miR-29 expression as assessed by WB **(Fig. 5.4a)**. IL-19 ELISA demonstrated consistent down-regulation by miR-29 premiR, and up-regulation by the anti-miR, from MDP+Pam_3CSK_4 stimulated cells **(Fig. 5.4b)**.

Figure 5.4 WB and Elisa assessment of DNA Array Results



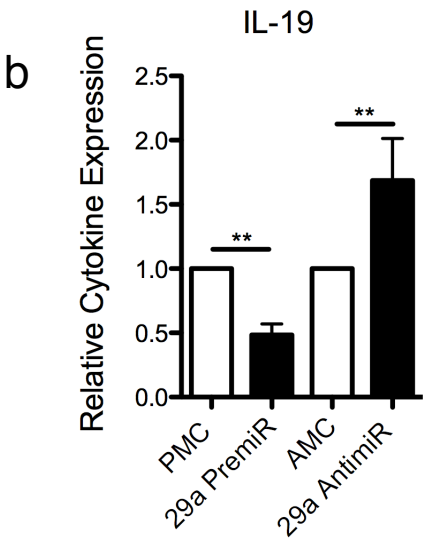


Figure 5.4 (a) DCs were transfected with miR-29a premiR (29a PM), or negative control (control), before being left unstimulated (US), or stimulated with MDP + Pam_3CSK_4 1µg/ml. Cells were lysed and blotted for potential miR-29 targets identified by array.
(b) IL-19 production from DCs was assessed by ELISA, following transfection of 29a premiR or antimiR, or control, and MDP + Pam_3CSK_4 1µg/ml stimulation. Significant results, by one-way Anova with Bonferroni post test (**P=0.001 to 0.01). Data from 6 independent experiments (premiR) and 3 independent experiments (antimiR) **(b)**; error bars, s.e.m. Western blots are representative of 2 independent experiments **(a)**.

5.4.1 DNMT3A

DNMT3A (DNA methyl transferase 3A) is one of three catalytically active DNMTs identified in mammals, and they facilitate the transfer of a methyl groups from S-adenosyl-L-methionine to cytosine or adenine in DNA[450]. This methylation has a number of functions including contributing to the control of gene expression, and maintaining genome integrity. DNMT3A 3'UTR contains a miR-29 target site (Targetscan; 7mer), and has already been identified as a miR-29 target[380] in a study investigating the effects of aberrant microRNA expression in lung cancer. The authors were interested particularly as hypermethylation is responsible for silencing of tumour suppressor genes in lung cancer pathogenesis. The importance of appropriate methylation control in CD pathogenesis has also recently been highlighted as DNMT3A was identified as a CD-susceptibility gene[11]. In the immune system, DNMT3A has been shown to influence the polarization of T cells[451], and in monocytes DNMT3A has a role in the hypermethylation of the TNFα promoter, and this contributes to endotoxin tolerance[452]. This raises the question as to whether NOD2-variant DCs that do not up-regulate miR-29 may in this way contribute to an immune paresis, as continued bacterial infection would lead to increased DNMT3A expression, and a tolerised, rather than an appropriately active, immune response.

5.4.2 TNFSF15

TNF superfamily member TNFSF15 (also known as TL1A) is a strong co-stimulator of T cells via its receptor DR3 (death domain receptor 3). This leads to proliferation and increased IFNγ production, but not apoptosis, via NFκB

and cIAP-2 activation[453]. There are several interesting links with Crohn's disease. Firstly, this co-activation is most significant for $CD4^{+}CCR9^{+}$ T cells[454], sharing many of the characteristics of small bowel lamina propria T cells which are mostly CCR9+[455]. Secondly, TNFSF15 is a CD-susceptibility gene[456,457]. The IBD-associated polymorphisms result in increased expression of the TNFSF15 protein in CD14+ monocytes, in response to FcgammaR stimulation[458], (immune complexes are known to induce TNFSF15 expression in monocytes and DCs[459]). Thirdly, in murine models there is an association between increased TNFSF15 and DR3 expression in ileitis[460], evidence that TNFSF15 neutralisation attenuates murine colitis[461], and constitutive TNFSF15 expression in lymphoid or myeloid cells leads to mild small bowel inflammation and fibrosis[462]. Lastly, there is also increased TNFSF15 expression in intestinal tissue specimens from human CD patients[463].

A functional link between NOD2 mutations and over-expression of TNFSF15 in DCs, via miR-29, would therefore be of great interest, not least as it could potentially link variant NOD2 to an aberrant Th1 response and bowel fibrosis, this last being typical of NOD2 mutations. However, I have not pursued this further for two main reasons: TNFSF15 3'UTR contains no putative miR-29 target site, so the effect is unlikely to be direct; and although the qPCR data showing TNFSF15 down-regulation on miR-29 over-expression is consistent, the effect is small as is any potential effect on protein expression levels seen at WB.

5.4.3 IL-19

Despite being discovered just over 10 years ago[464], currently very little is known about the function of IL-19, a member of the IL-10 family of cytokines. It was initially found to be produced by activated monocytes and to a lesser extent keratinocytes[465], and subsequently also shown to be induced by IL-17 and IL-13 in bronchial epithelial cells[466] via NFκB and STAT6 promoter elements. Although it shares 21% amino acid identity with, and is structurally related to, IL-10, it does not bind through the IL-10 receptor, but through a receptor made up of IL-20Rα and IL-20Rβ (reviewed in[467]), triggering STAT3 phosphorylation. This complex is also used by IL-20 and IL-24 that, with IL-19, form an IL-10 cytokine subfamily. Interestingly, although IL-19 has been ascribed immune functions, the alpha chain receptor is absent from immune cells, with some evidence suggesting IL-19 does not act directly on immune cells[465]. However, murine IL-19 (which shares sequence homology with human) can induce IL-6 and TNFα from mouse monocytes[468], but only when applied at significant concentrations.

IL-19 may play a pathogenic role in other chronic inflammatory conditions such as psoriasis, but currently most of the evidence is circumstantial rather than direct. IL-19 and the IL-20Rα/ IL-20Rβ receptor complex are expressed in psoriatic skin[469]. The IL-19 promoter contains keratinocyte growth factor (KGF) responsive elements[468], and KGF has been shown to induce IL-19 production from $CD8^+$ T cells[470], raising the possibility of a pathogenic positive feedback loop.

Regarding Crohn's, IL-19 polymorphisms may predispose to CD[11], however IL-19 lies in a cluster on chromosome 1 with three other IL-10 family members, including IL-10, and at present it is not clear which of these

cytokines the identified SNPs affect. IL-19 deficient mice are more susceptible to DSS colitis[471], and this is associated with macrophage accumulation and increased production of pro-inflammatory cytokines. However, human data from other conditions raise the possibility that IL-19 is in fact pro-inflammatory. For example, patients suffering from septic shock display elevated IL-19, and in vitro it induces neutrophil chemotaxis and the production of pro-inflammatory cytokines[472]. Furthermore in a murine model administration of a soluble IL-19 receptor improved endotoxic shock.

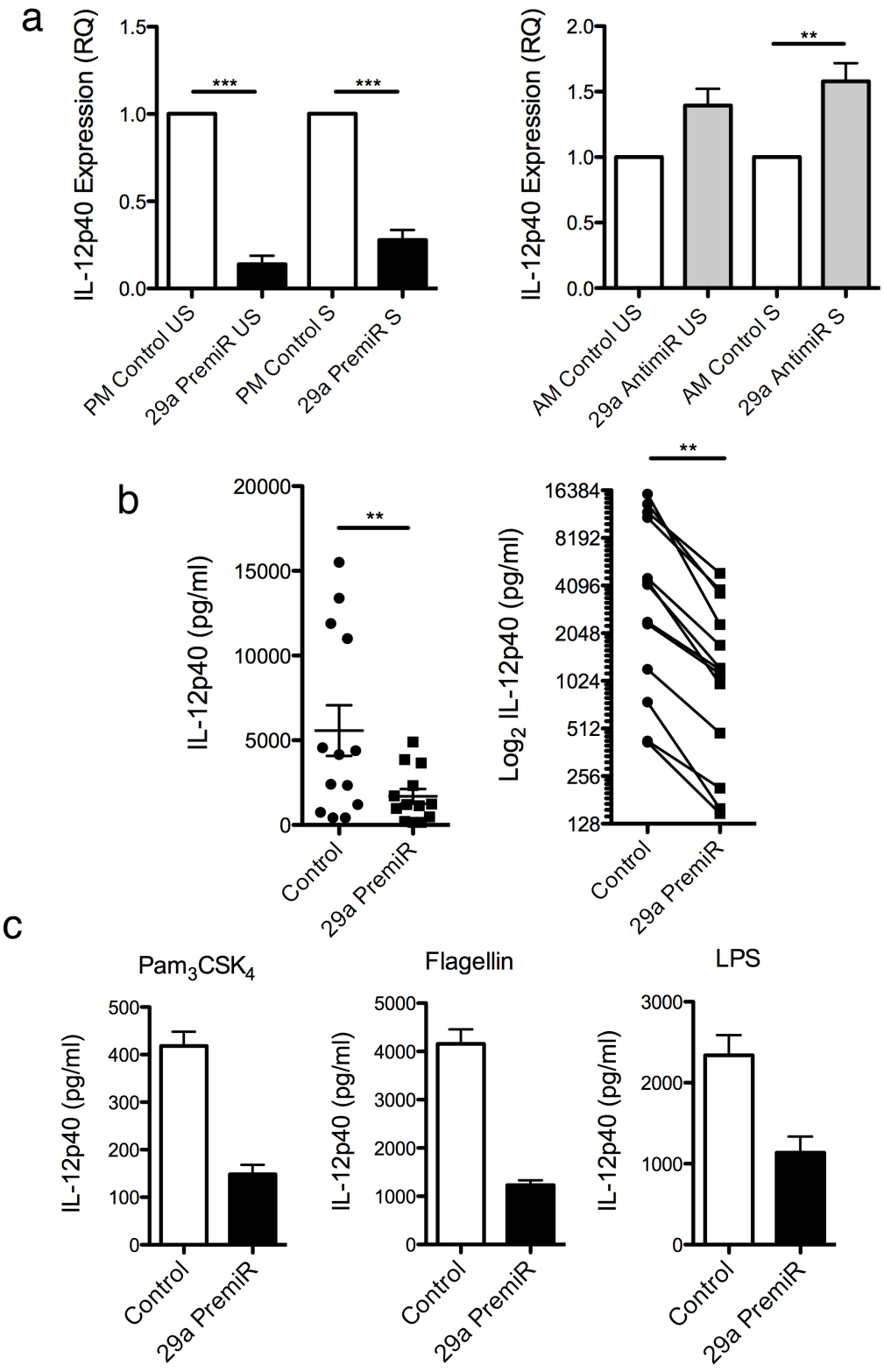
In summary, there is as yet no consensus on the function of IL-19, either in physiological or pathogenic settings. Although my data suggest that IL-19 expression is affected by miR-29 in DCs, it is difficult to interpret in the light of current knowledge. As there is no predicted miR-29 target site in IL-19 3'UTR, these observed changes are likely indirect.

5.5 miR-29 down-regulates IL-12p40

As IL-12p40 was the most strongly down-regulated gene observed following overexpression of miR-29 premiR, and as it is predicted to be directly targeted by miR-29 by computation algorithms, I investigated the role of miR-29 in control of IL-12p40 expression further. I assessed the effect of miR-29 on IL-12p40 expression by transfecting miR-29 premiR and performing qPCR for IL-12p40, or ELISA for IL-12p40 release, from DCs after NOD2+TLR2 stimulation. Overexpression of miR-29 led to marked down-regulation of both IL-12p40 mRNA levels and cytokine release from DCs **(Fig. 5.5a and b)**, and this was irrespective of the PRR stimulus used to induce IL-12p40 **(Fig. 5.5c)**. Moreover, blocking the effect of miR-29 with an antimiR, in MDP+ Pam_3CSK_4

treated DCs, increased IL-12p40 expression **(Fig. 5.5a)**. The kinetics of IL-12p40 down-regulation over time post NOD2+TLR2 triggering inversely correlates with the kinetics of miR-29 induction, with the most exaggerated effect observed at 3 days, consistent with miR-29 acting to repress IL-12p40 physiologically **(Fig. 5.5d)**. As miR-155 is also up-regulated by NOD2 + TLR2 co-triggering I assessed the effect of miR-155 antimiR and premiR alongside the effects of miR-29. There was no demonstrable effect on IL-12p40 production by DCs on manipulation of miR-155 levels, in contrast to the observed effects of miR-29 **(Fig 5.5e)**.

Figure 5.5 miR-29 down-regulates IL-12p40



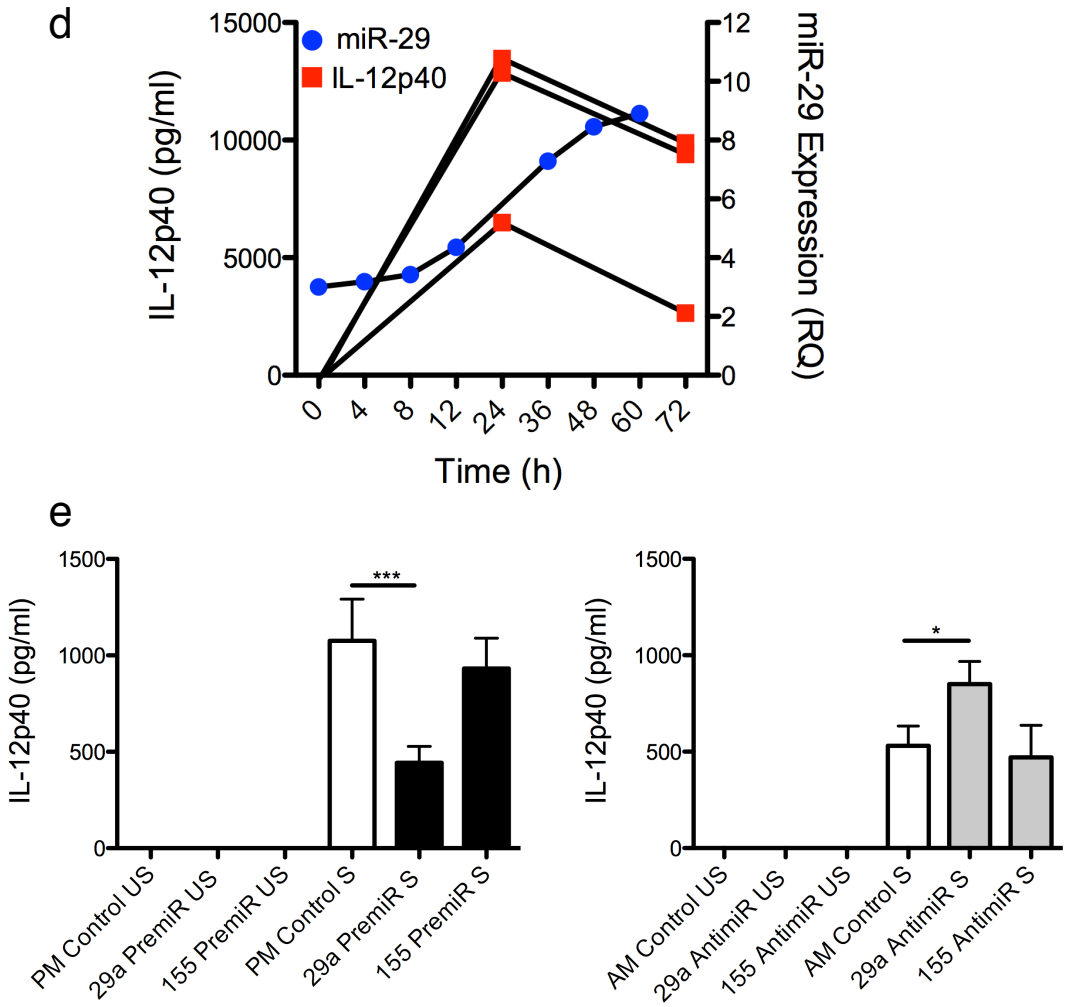
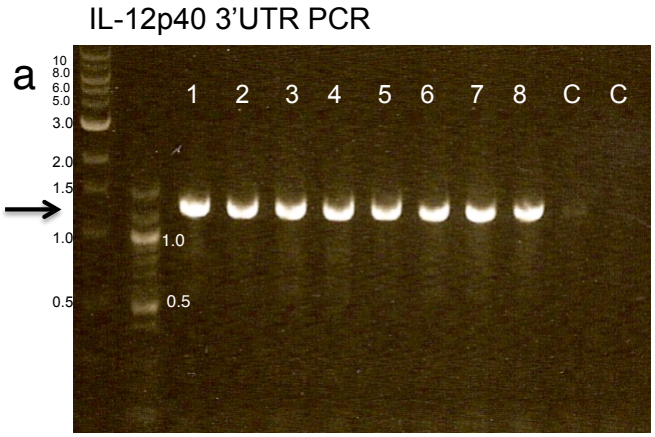


Figure 5.5 (a) IL-12p40 qPCR in DCs following miR-29 premiR or antimiR transfection, and MDP + Pam_3CSK_4 1μg/ml stimulation, expressed as relative fold change to control. Statistical analysis by one-way Anova with Bonferroni post test **P=0.001 to 0.01, and ***P<0.001. **(b)** IL-12p40 ELISA in DCs stimulated with MDP + Pam_3CSK_4 1μg/ml, or **(c)** TLR2/ 4/ 5 ligands 1μg/ml, transfected with miR-29 premiR or control. (Analysis by two-tailed paired t-test **P=0.001 to 0.01). ELISA data are represented both on a standard and log scale to demonstrate the effect of miR-29 on IL-12p40 expression more clearly. **(d)** IL-12p40 ELISA (left axis) and miR-29 qPCR (right axis) in DCs stimulated with MDP + Pam_3CSK_4 1μg/ml, over time. **(e)** IL-12p40 ELISA following DC transfection with miR-29 antimiR or premiR, or miR-155 antimiR or premiR, or relevant controls. Cells were left unstimulated (US) or stimulated with MDP + Pam_3CSK_4 1μg/ml (S). Statistical analysis by one-way Anova with Bonferroni post test *P=0.01 to 0.05, and ***P<0.001. Data from **(a)** 4 independent experiments**;** **(b)** 13 independent experiments; **(c)** 2 independent experiments; **(d)** 3 independent experiments; **(e)** 8 and 4 independent experiments respectively; error bars, s.e.m.

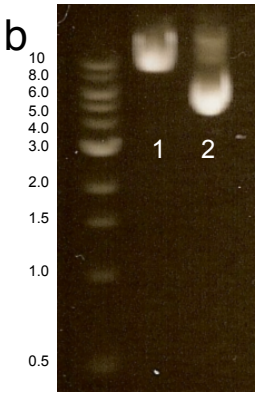
5.5.1 miR-29 directly targets IL-12p40 3'UTR

miR-29 is predicted to directly target the IL-12p40 3' UTR, (Targetscan 7mer-1A; P_{CT} <0.1) **(Fig. 5.7a)**. Although not as potent as an 8mer seed-to-target mRNA match, the miR-29-IL-12p40 seed target site has features that would increase its effectiveness including: an AU-rich seed flanking area (40 out of 60 flanking nucleotides, including 8 out of 10 in the important immediate flanking area); and a position within the 3'UTR which is not in the centre, and placed well away from the mRNA stop codon[356]. I cloned the 3' UTR (> 3,000 nucleotides) of IL-12p40 mRNA into a vector downstream of a reporter gene encoding luciferase. Firstly, primers were designed and the IL-12p40 3'UTR PCR conditions were optimised **(Fig. 5.6a)**. In order to avoid a significant problem of luciferase assays (that is ensuring consistent and equal co-transfection of two vectors), a vector that expressed both the reporter firefly luciferase and the control renilla luciferase, under the control of separate promoters, was chosen. This pmiR-Glo (Promega) vector was linearised **(Fig. 5.6b)** prior to cloning. Cloning was checked initially by digesting the vector with BspEI, and compared with the digested empty vector on a TBE gel (with ethidium bromide) **(Fig. 5.6c)**. Subsequently, the IL-12p40 3'UTR insertion was fully sequenced **(Fig. 5.6d)** using primers I designed (see methods). Finally, the miR-29 seed target sequence in the IL-12p40 3'UTR-pmiRGlo vector was mutated using a site-directed mutagenesis kit (QuikChange II XL; Agilent) and the change confirmed by further sequencing **(Fig. 5.6e)**.

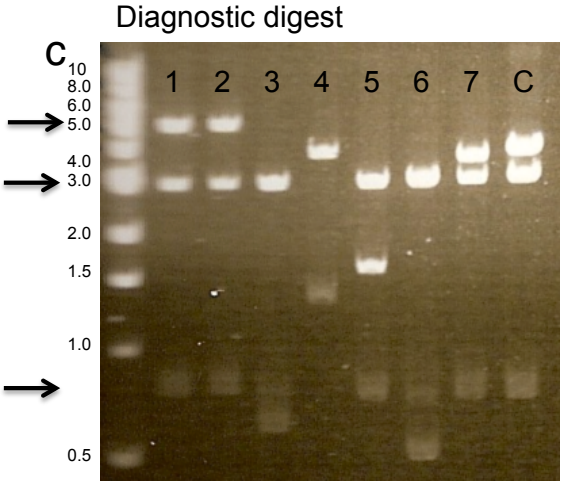
Figure 5.6 IL-12p40 3'UTR PCR and cloning into luciferase vector



1-8 = 55-68°C
C = negative controls



1 = Linearised pmiR-Glo
2 = Uncut pmiR-Glo



1-7 = Colony digest
C = pmiR-Glo digest

Figure 5.6 (a) Primers were designed to amplify IL-12p40 3'UTR by PCR. Human genomic DNA was used as the template and a temperature ramp employed to identify optimum conditions. The arrow marks the expected size of IL-12p40 3'UTR (1.3 kb). **(b)** pmiR-Glo dual luciferase vector was linearised with NheI and XbaI prior to cloning. **(c)** IL-12p40 3'UTR was cloned into pmiR-Glo dual luciferase vector. Ligation was performed using Clontech In-Fusion method, and subsequently used to transform *Escherichia coli* (DH5a-T1; Invitrogen). DNA was extracted from isolated colonies after mini-prep, and digested with BspEI (NEB). The arrows mark the expected locations for the digested IL-12p40 3'UTR luciferase vector (5 kb, 2.9 kb, and 760 bp). Colonies 1 and 2 were sent for sequencing.

Figure 5.6 IL-12p40 sequence data

d

3'UTR IL12p40

taggttctgatccaggatgaaaatttggaggaaaagtggaagatattaa
gcaaaatgtttaaagacacaacggaatagacccaaaaagataatttcta
tctgatttgctttaaaacgtttttttaggatcacaatgatatctttgct
gtatttgtatagttagatgctaaatgctcattgaaacaatcagctaatt
tatgtatagattttccagctctcaagttgccatgggccttcatgctatt
taaatatttaagtaatttatgtatttattagtatattactgttatttaa
cgtttgtctgccaggatgtatggaatgtttcatactcttatgacctgat
ccatcaggatcagtccctattatgcaaaatgtgaatttaattttatttg
tactgacaacttttcaagcaaggctgcaagtacatcagttttatgacaa
tcaggaagaatgcagtgttctgataccagtgccatcatacacttgtgat
ggatgggaacgcaagagatacttacatggaaacctgacaatgcaaacct
gttgagaagatccaggagaacaagatgctagttcccatgtctgtgaaga
cttcctggagatggtgttgataaagcaatttagggccacttacacttct
aagcaagtttaatctttggatgcctgaattttaaaagggctagaaaaaa
atgattgaccagcctgggaaacataacaagaccccgtctctacaaaaaa
aatttaaaattagccaggcgtggtggctcatgcttgtggtcccagctgt
tcaggaggatgaggcaggaggatctcttgagcccaggaggtcaaggcta
tggtgagccgtgattgtgccactgcataccagcctaggtgacagaatga
gaccctgtctcaaaaaaaaaaatgattgaaattaaaattcagctttagc
ttccatggcagtcctcacccccacctctctaaaagacacaggaggatga
cacagaaacaccgtaagtgtctggaaggcaaaaagatcttaagattcaa
gagagaggacaagtagttatggctaaggacatgaaattgtcagaatggc
aggtggcttcttaacagccatgtgagaagcagacagatgcaaagaaaat
ctggaatccctttctcattagcatgaatgaacctgatacacaattatga
ccagaaaatatggctccatgaaggtgctactttaagtaatgtatgtgc
gctccgtaaagtgattacatttgtttcctgtttgtttatttatttattt
attttgcattctgaggctgaactaataaaaactcttctttgtaatc

(d) Sequence data for IL-12p40 3'UTR cloned into pmiR-Glo dual luciferase vector. In red is the miR-29 seed target sequence.

Figure 5.6 IL-12p40 Δ seed sequence data

e

3'UTR IL12p40 Δseed

taggttctgatccaggatgaaaatttggaggaaaagtggaagatattaa
gcaaaatgtttaaagacacaacggaatagacccaaaaagataatttcta
tctgatttgctttaaaacgtttttttaggatcacaatgatatctttgct
gtatttgtatagttagatgctaaatgctcattgaaacaatcagctaatt
tatgtatagattttccagctctcaagttgccatgggccttcatgctatt
taaatatttaagtaatttatgtatttattagtatattactgttatttaa
cgtttgtctgccaggatgtatggaatgtttcatactcttatgacctgat
ccatcaggatcagtccctattatgcaaaatgtgaatttaattttatttg
tactgacaacttttcaagcaaggctgcaagtacatcagttttatgacaa
tcaggaagaatgcagtgttctgataccagtgccatcatacacttgtgat
ggatgggaacgcaagagatacttacatggaaacctgacaatgcaaacct
gttgagaagatccaggagaacaagatgctagttcccatgtctgtgaaga
cttcctggagatggtgttgataaagcaatttagggccacttacacttct
aagcaagtttaatctttggatgcctgaattttaaaagggctagaaaaaa
atgattgaccagcctgggaaacataacaagaccccgtctctacaaaaaa
aatttaaaattagccaggcgtggtggctcatgcttgtggtcccagctgt
tcaggaggatgaggcaggaggatctcttgagcccaggaggtcaaggcta
tggtgagccgtgattgtgccactgcataccagcctaggtgacagaatga
gaccctgtctcaaaaaaaaaaatgattgaaattaaaattcagctttagc
ttccatggcagtcctcacccccacctctctaaaagacacaggaggatga
cacagaaacaccgtaagtgtctggaaggcaaaaagatcttaagattcaa
gagagaggacaagtagttatggctaaggacatgaaattgtcagaatggc
aggtggcttcttaacagccatgtgagaagcagacagatgcaaagaaaat
ctggaatccctttctcattagcatgaatgaacctgatacacaattatga
ccagaaaatatggctccatgaatttcgactttaagtaatgtatgtgc
gctccgtaaagtgattacatttgtttcctgtttgtttatttatttattt
attttgcattctgaggctgaactaataaaaactcttctttgtaatc

(e) Mutagenesis primers were designed to mutate the miR-29 seed target sequence in IL-12p40 3'UTR. The sequence data after site-directed mutagenesis of the miR-29 seed target sequence is shown. The un-mutated nucleotides of the seed target sequence remain in red font.

I transfected HEK293 cells with the IL-12p40 3'UTR-containing vector, or control empty vector, along with miR-29 premiR for 48 h. I assessed by qPCR the efficiency of miR-29 transfection using two different commercially available reagents and found lipofectamine to be the most effective **(Fig 5.7b)**. Reporter gene expression was suppressed by 25% in cells carrying the vector containing the predicted binding site for the miR-29 family **(Fig. 5.7c)**. In contrast, co-transfection of a vector containing a mutated IL-12p40 3' UTR seed sequence (IL-12p40 Δ seed) with miR-29 premiR produced no suppression of reporter gene expression.

I further examined this relationship by designing a miR-29 seed target protector specific for the IL-12p40 3'UTR. This is designed to prevent miR-29 binding to IL-12p40 3'UTR, and thus hinder down-regulation of this cytokine. The protector, or negative control, was transfected into DCs before the cells were left unstimulated, or stimulated for 24 h with MDP + Pam_3CSK_4. The seed target protector resulted in an increase in IL-12p40 production as measured by ELISA **(Fig 5.7d)**, suggesting that miR-29 up-regulation is an important physiological mechanism for IL-12p40 control in DCs.

These experiments identify IL-12p40 as a direct target of miR-29 in DCs, and show an inverse correlation between expression of miR-29 and IL-12p40 induced over time post-PRR stimulation. This regulation of IL-12p40 expression is consistent with miR-29 functioning as a late induced miRNA, acting to switch off expression of this inflammatory mediator.

Figure 5.7 miR-29 directly targets IL-12p40 3'UTR

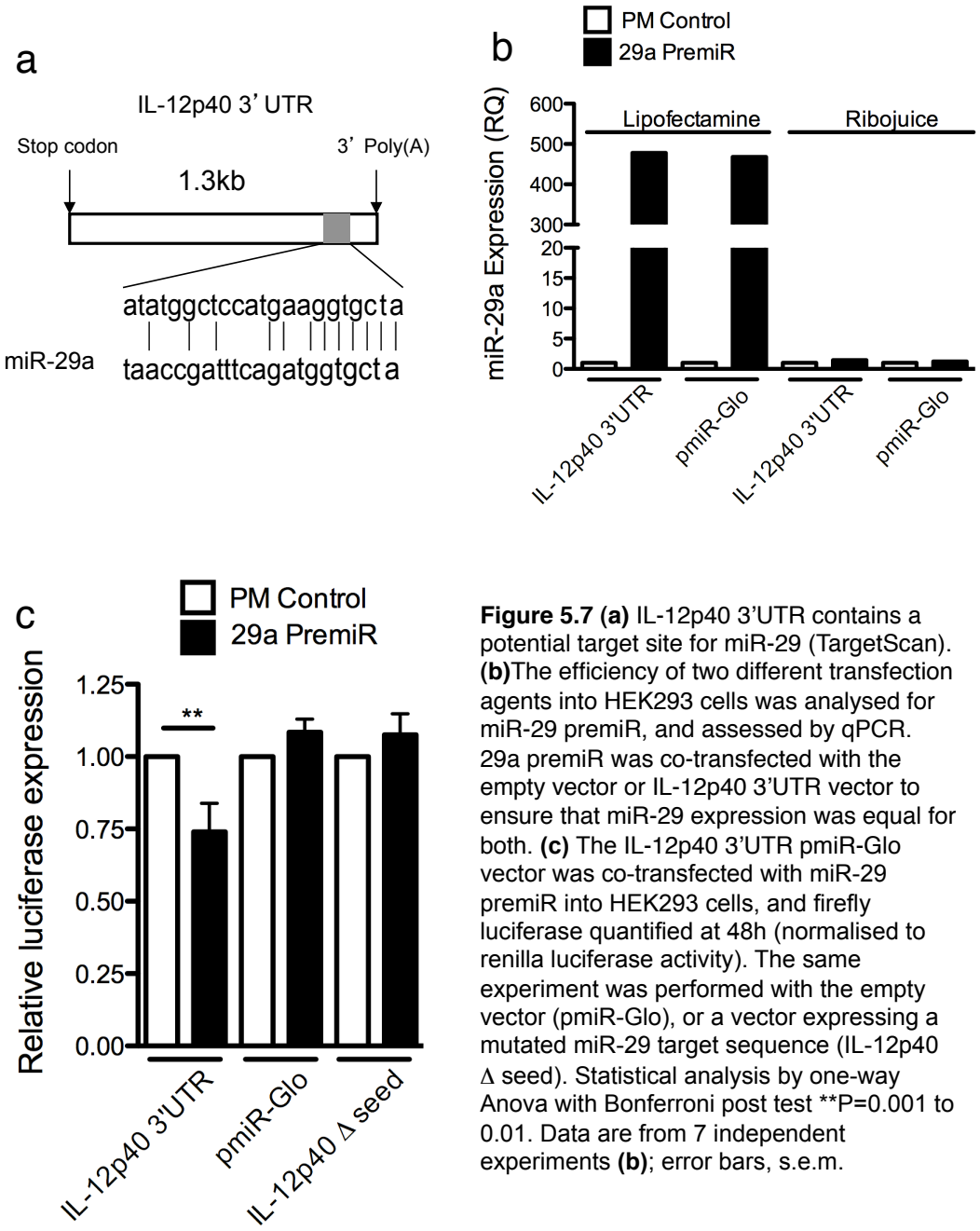


Figure 5.7 (a) IL-12p40 3'UTR contains a potential target site for miR-29 (TargetScan). **(b)**The efficiency of two different transfection agents into HEK293 cells was analysed for miR-29 premiR, and assessed by qPCR. 29a premiR was co-transfected with the empty vector or IL-12p40 3'UTR vector to ensure that miR-29 expression was equal for both. **(c)** The IL-12p40 3'UTR pmiR-Glo vector was co-transfected with miR-29 premiR into HEK293 cells, and firefly luciferase quantified at 48h (normalised to renilla luciferase activity). The same experiment was performed with the empty vector (pmiR-Glo), or a vector expressing a mutated miR-29 target sequence (IL-12p40 Δ seed). Statistical analysis by one-way Anova with Bonferroni post test **P=0.001 to 0.01. Data are from 7 independent experiments **(b)**; error bars, s.e.m.

d

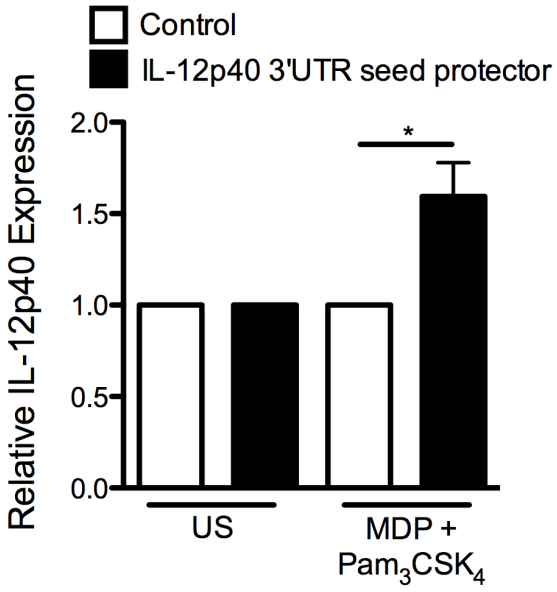
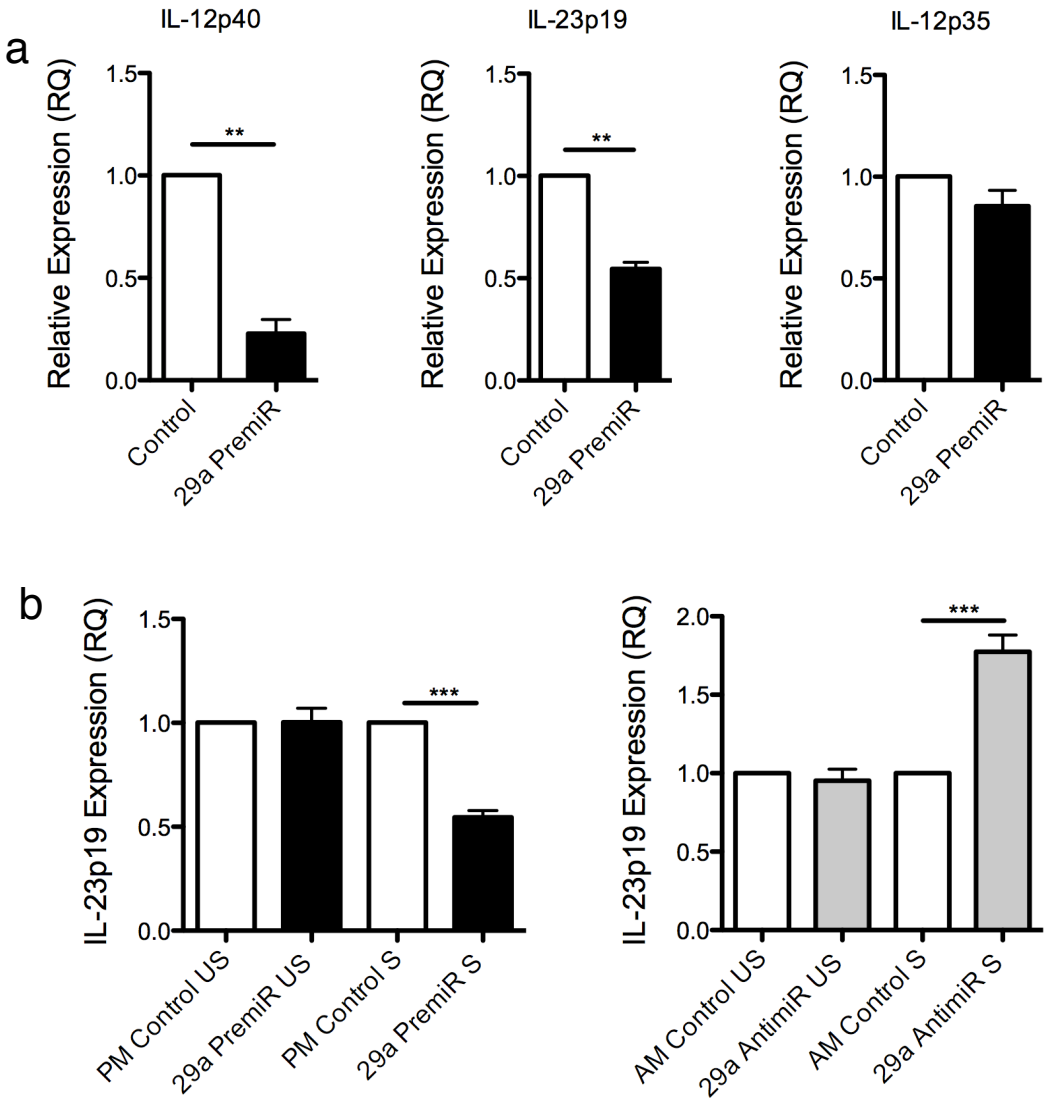


Figure 5.7d A miR-29 seed target protector for the IL-12p40 3'UTR was designed and transfected into human DCs before cells were left unstimulated (US) or stimulated for 24 h with MDP + Pam_3CSK_4. ELISA analysis of IL-12p40 production was performed. The graph shows relative IL-12p40 production comparing control with seed-protected cells. Statistical analysis by one-way Anova with Bonferroni post test *P=0.01 to 0.05. Data are from 2 independent experiments **(d)**; error bars, s.e.m.

5.6 miR-29 down-regulates IL-23

IL-12p40 is both a subunit of IL-12 and IL-23, the other subunits being IL-12p35 and IL-23p19 respectively. I investigated whether miR-29 controlled expression of either of these other two subunits that act in concert with IL-12p40 by transfecting DCs with miR-29 premiR or control and performing qPCR for their expression. **Figure 5.8a** shows that miR-29 premiR strongly down-regulates expression of IL-12p40 and IL-23p19, but not IL-12p35. The miR-29 antimiR has the opposite effect (increasing IL-23p19 expression) although the effects of both premiR and antimiR are only apparent in stimulated cells **(Fig. 5.8b)** (unlike the effect on IL-12p40 which is detectable in unstimulated cells also, see **Fig. 5.5a**). This may suggest that control of IL-23p19 by miR-29 is indirect, rather than the direct targeting observed of IL-12p40 3'UTR. miR-29 also robustly down-regulates IL-23p19 protein released from DCs on NOD2+TLR2 triggering **(Fig. 5.8c)**.

Figure 5.8 miR-29 preferentially regulates IL-23



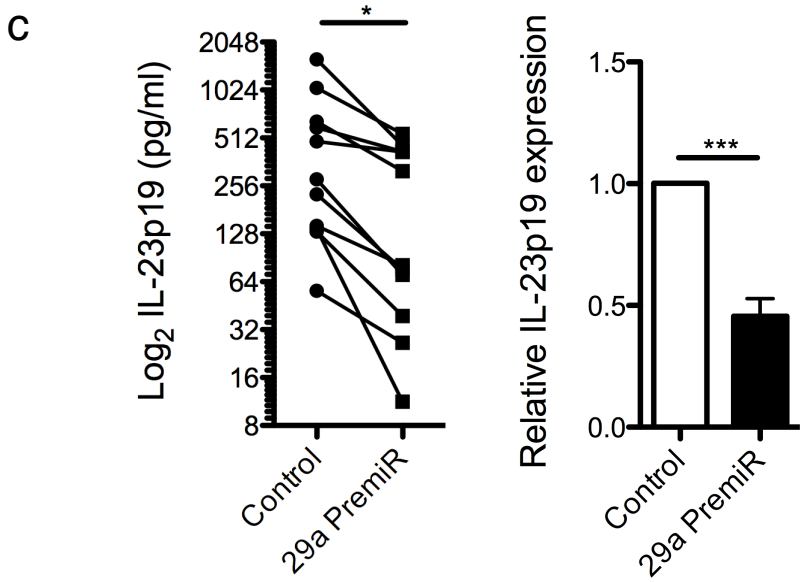
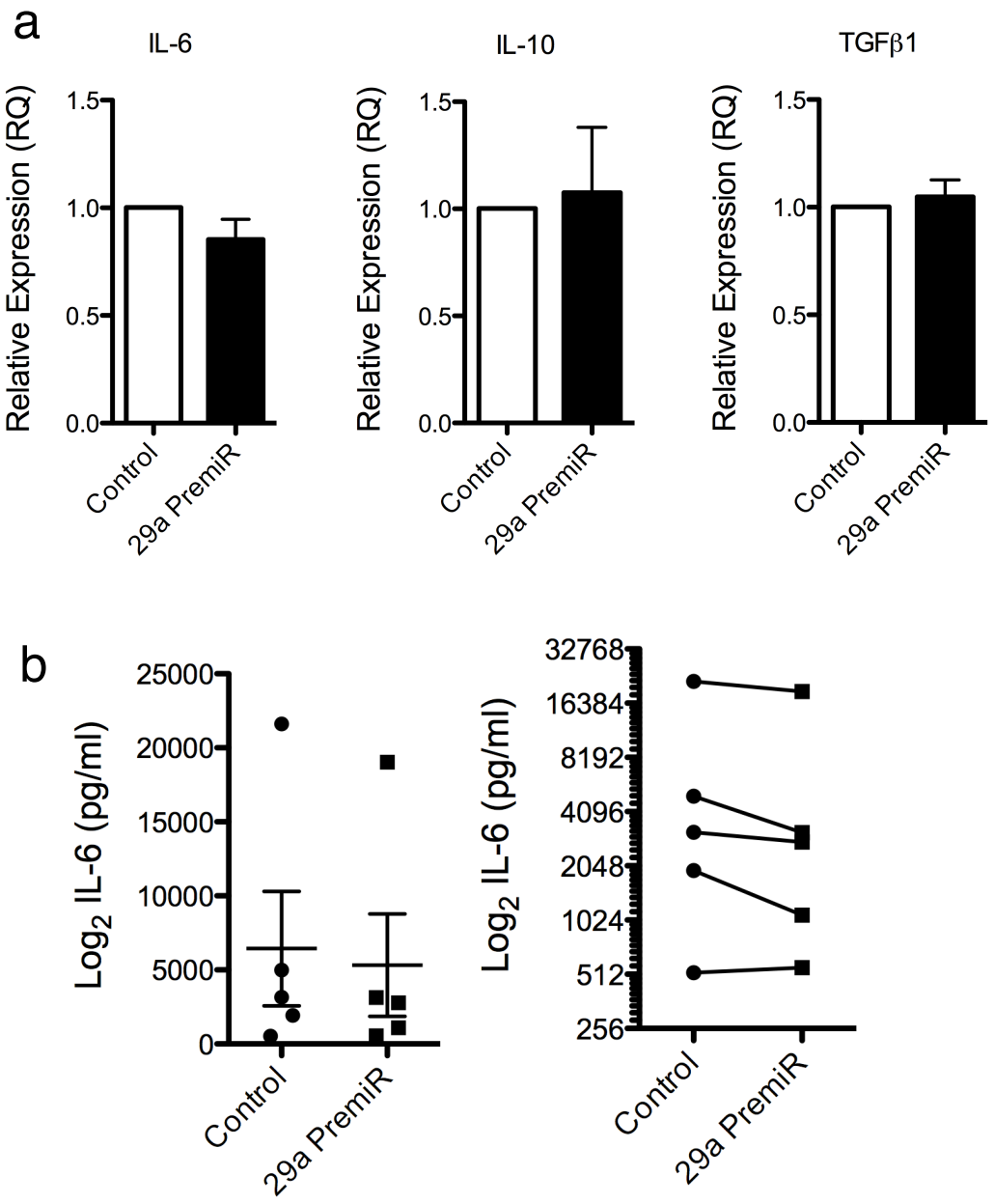


Figure 5.8 (a) DCs were transfected with miR-29 premiR, or control, and MDP + Pam_3CSK_4 1μg/ml stimulated as before. Graphs show qPCR analysis of the IL-12p40, IL-23p19 and the IL-12p35 subunits. **(b)** DCs transfected with either miR-29 premiR or antimiR, or relevant control, before being left unstimulated (US) or MDP + Pam_3CSK_4 1μg/ml stimulation (S). Graph shows qPCR analysis of IL-23p19 expression. **(c)** IL-23p19 ELISA from DCs transfected with miR-29 premiR, or control, and MDP + Pam_3CSK_4 1μg/ml stimulated. Significant differences by two-tailed paired t-test *P=0.01 to 0.05, **P=0.001 to 0.01 and ***P<0.001. Data are from 3 independent experiments **(a)** and **(b)**, 11 independent experiments **(c)**; error bars, s.e.m.

I tested the specificity of our results by analysing whether miR-29 overexpression affected the levels of other cytokines involved in Th17 or immunoregulatory responses. I found miR-29 did not affect expression of either IL-6 or TGFβ or IL-10 by qPCR **(Fig. 5.9a)**, or of IL-6 and IL-10 by ELISA **(Fig. 5.9b and c)** demonstrating a polarised role for miR-29 in regulation of IL-12p40 and IL-23p19, the subunits of IL-23.

Figure 5.9 miR-29 does not affect IL-6, TGFβ1, or IL-10



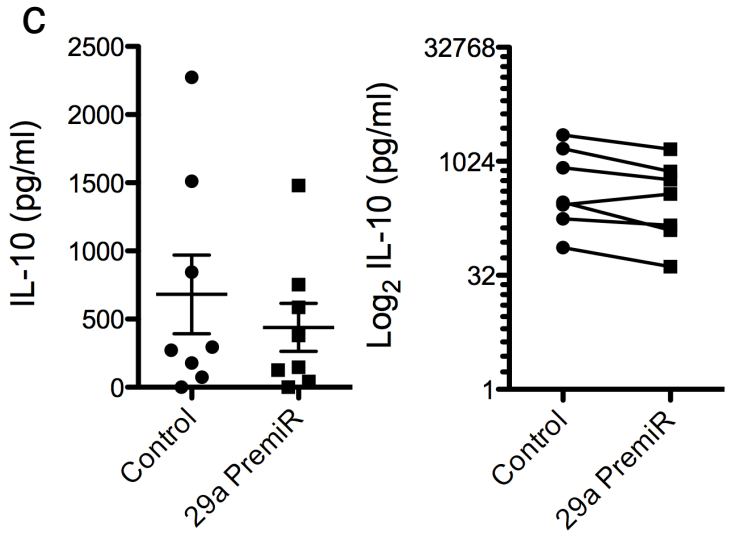


Figure 5.9 (a) qPCR and ELISA **(b and c)** analysis of DCs transfected with miR-29 premiR, or control, and MDP + Pam_3CSK_4 1μg/ml stimulated. IL-6. IL-10 and TGFβ were assessed by qPCR, and IL-6 and IL-10 by ELISA. The IL-6 and IL-10 ELISA data are represented both on a standard and log scale to demonstrate the effect of miR-29 on expression more clearly. Data are from 3 independent experiments **(a)**, 5 independent experiments **(b)**, 8 independent experiments **(c)**; error bars, s.e.m.

5.6.1 miR-29 down-regulates IL-12p40 and IL-23p19 in a dose-responsive manner

The effect of miR-29 on IL-23 was further assessed by examining the effect of the absolute level of miR-29 in DCs, by transfecting variable concentrations of the premiR and measuring the fold-change by qPCR **(Fig. 5.10a)**. A dose-response effect on both IL-12p40 and IL-23p19 was observed by ELISA **(Fig. 5.10b and c)**. These results also demonstrate that the down-regulation of the IL-23 cytokine subunits occurs at physiological levels of miR-29 – that is after transfection of miR-29 to induce an up-regulation consistent with the expression observed after MDP + Pam_3CSK_4 (or MDP + Flagellin) stimulation.

Figure 5.10 miR-29 dose-response

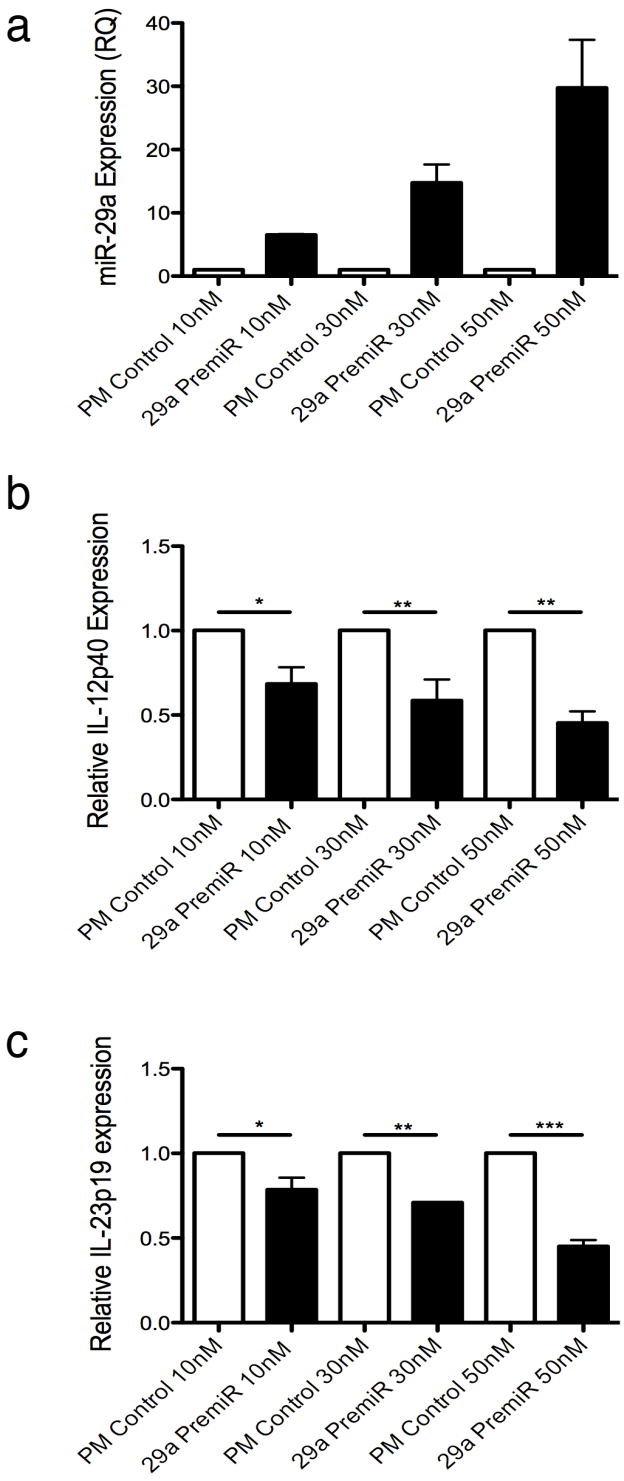


Figure 5.10
(a) DCs were transfected with varying concentrations of miR-29 premiR, or control, and the up-regulation of miR-29 assessed by qPCR. **(b) and (c)** Cells were stimulated with MDP + Pam_3CSK_4 1μg/ml and IL-12p40 and IL-23p19 production measured by ELISA. Statistical analysis by one-way Anova with Bonferroni post test *P=0.01 to 0.05, **P=0.001 to 0.01 and ***P<0.001. Data are from 3 independent experiments; error bars, s.e.m.

5.6.2 IL-23p19 is indirectly targeted by miR-29 via ATF2

I then investigated the mechanism by which miR-29 down-regulates IL-23p19 expression in DCs. miR-29 is predicted to directly target IL-23p19 3' UTR (MicroCosm), although only via a weak seed sequence pairing **(Fig. 5.11c)** and therefore unlikely to be biologically valid. To test this I cloned IL-23p19 3' UTR (>300 nucleotides) into the pmiR-Glo vector downstream of a reporter gene encoding luciferase, using the same method as for IL-12p40 3'UTR. Initially I designed PCR primers and optimised the IL-23p19 3'UTR PCR **(Fig. 5.11a)**. After cloning the resultant optimised PCR product into pmiR-Glo vector, the success of cloning was checked as before, first by digestion **(Fig. 5.11b)** and then by sequencing. Co-transfection of the IL-23p19 3'UTR-containing vector, or empty vector control, with miR-29 premiR into HEK293 cells produced no demonstrable effect on luciferase expression **(Fig. 5.11d)** in keeping with the seed pairing analysis, and suggesting miR-29 targets IL-23p19 indirectly.

Figure 5.11 miR-29 controls IL-23p19 indirectly

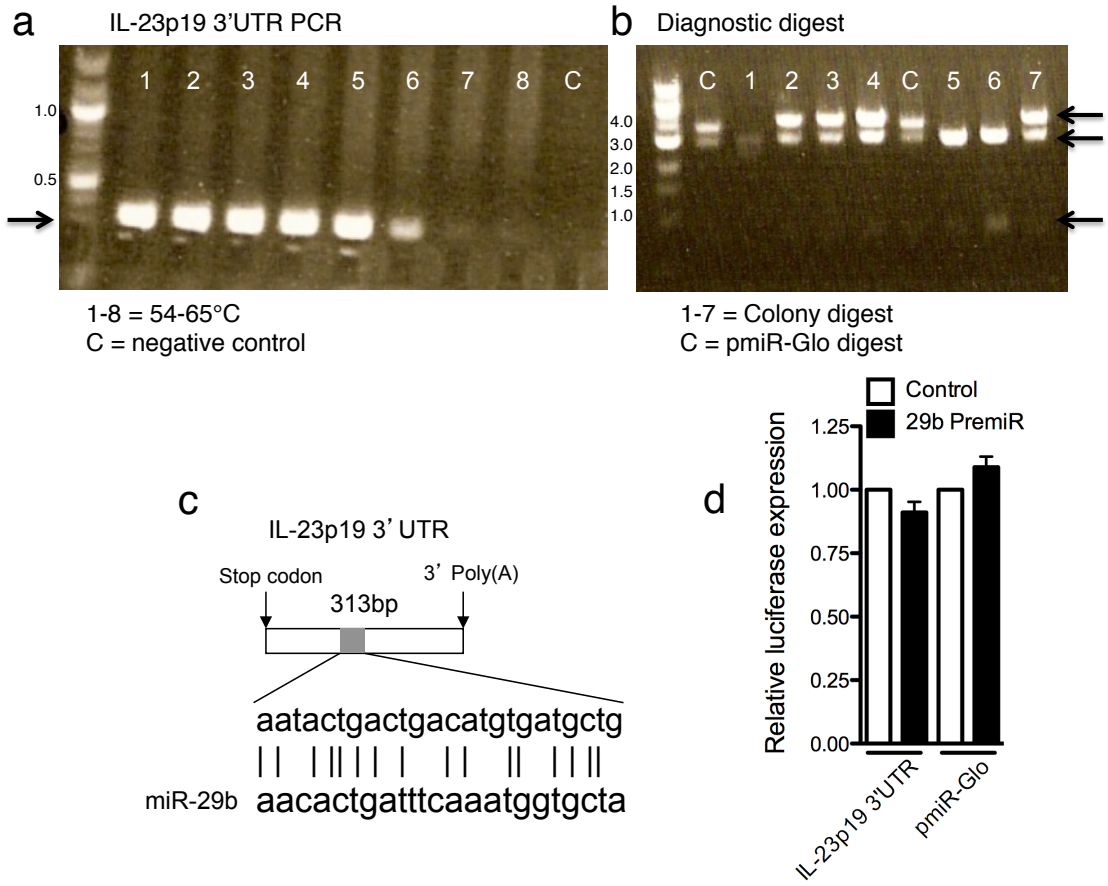


Figure 5.11 (a) Primers were designed to amplify IL-23p19 3'UTR by PCR. Human genomic DNA was used as the template and a temperature ramp employed to identify optimum conditions. The arrow marks the expected weight for IL-23p19 3'UTR (300 bp). **(b)** IL-23p19 3'UTR was cloned into pmiR-Glo dual luciferase vector. Ligation was performed using Clontech In-Fusion method, and subsequently used to transform *Escherichia coli* (DH5a-T1; Invitrogen). DNA was extracted from isolated colonies after mini-prep, and digested with BspEI (NEB). The arrows mark the expected locations for the digested IL-23p19 3'UTR and luciferase vector (4 kb, 2.9 kb, 760 bp). Colonies 2,3,4 and 7 were sent for sequencing. **(c)** IL-23p19 3'UTR contains a potential miR-29 target site (MicroCosm). **(d)** The IL-23p19 3'UTR pmiR-Glo vector was co-transfected with miR-29 premiR into HEK293 cells, and firefly luciferase quantified at 48h (normalised to renilla luciferase activity). Data are from 3 independent experiments **(d).**

I next examined the microarray data obtained when miR-29 was overexpressed in DCs to find potential mechanisms for indirect targeting of IL-23p19 by miR-29. ATF2 and SMAD3 mRNAs were both down-regulated following overexpression of miR-29 premiR in DCs and have both been shown to act as transcriptional activators of IL-23p19 in macrophages[473]. Computational analysis revealed ATF2 has a 3' UTR with miR-29 seed target sequences. Transfection of miR-29 premiR or control into DCs resulted in down-regulation of ATF2 and SMAD3 protein expression, as assessed by Western blot **(Fig. 5.12a and b)**. This correlates with recently published data demonstrating the down-regulation of SMAD3 by miR-29 in muscle cells[347]. I next transfected siRNAs specific for ATF2 and SMAD3 into DCs, and validated their effect by Western blot **(Fig. 5.12c and d)**. Analysis of IL-23p19 production after ATF2 or SMAD3 siRNA transfection into DCs stimulated with MDP + Pam_3CSK_4 demonstrated reduced expression after ATF2 knockdown only **(Fig. 5.12e)**. These results indicate that miR-29 down-regulates IL-23p19 indirectly and likely via down-regulation of its key transcriptional activator ATF2.

Figure 5.12 miR-29 controls IL-23p19 by down-regulating ATF2

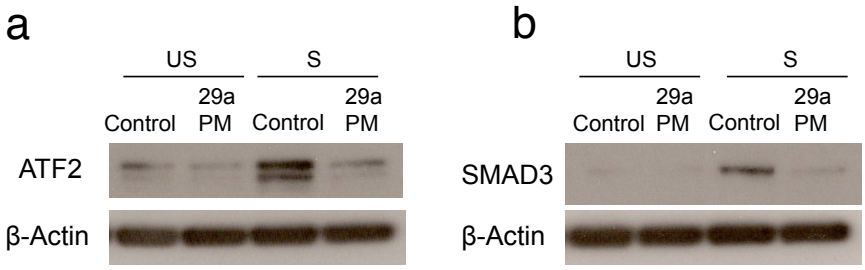


Figure 5.12 (a) and (b) DCs were transfected with miR-29 premiR (29a PM) or control (PMC), and subsequently left unstimulated (US) or stimulated with MDP + Pam_3CSK_4 1μg/ml (S). Western blot for ATF2 **(c)** and SMAD3 **(d)** were performed on the cell lysates. Data are representative of 3 independent experiments.

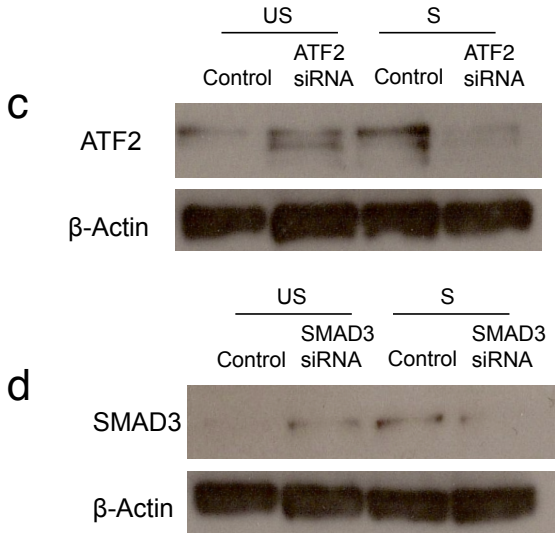
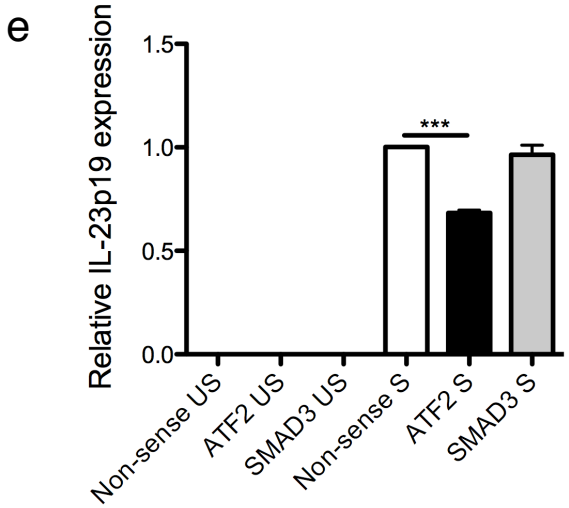


Figure 5.12
siRNAs specific for ATF2 and SMAD3 were transfected into DCs and the cells left unstimulated (US) or stimulated with MDP + Pam_3CSK_4. **(c) and (d)** Western blot assessment of siRNA knockdown. **(e)** ELISA for IL-23p19 from the same DCs. Graph shows relative cytokine production. Statistical analysis by one-way Anova and Bonferroni post test ***P<0.001. Data are representative of 3 independent experiments **(c, d),** or from 3 independent experiments **(e)**; error bars, s.e.m



5.7 Crohn's patients DCs expressing NOD2 variants are defective in miR-29 expression and down-regulation of IL-12p40 expression at the end of an immune response

I have already demonstrated that Crohn's patient DCs expressing variants of NOD2 associated with the disease exhibit defects in miR-29 up-regulation on either NOD2, or NOD2+TLR, triggering **(Fig 3.11c and d)**. The possible functional consequence for this absence in miR-29 expression, with regard to IL-23, was then investigated. It has already been established that NOD2 variants show defects in induction of IL-23 on ligand stimulation, such that there is absence of induction on NOD2 triggering alone and on dual NOD2+TLR2 triggering the levels of IL-23 produced are reduced[253]. Our experiments recapitulated this result at 24 h stimulation **(Fig. 5.13a)**.

I tested whether, despite the reduced levels of IL-12p40 initially induced in the presence of Crohn's associated NOD2 variants, the absence of miR-29 induction by NOD2 could affect return of IL-12p40 levels to background, following PRR activation. **Figure 5.13a** demonstrates that Crohn's patient DCs expressing NOD2 variants display defects in reduction of IL-12p40 at 72 h post PRR triggering. Transfection of miR-29 into NOD2 FS1007insC DCs can reduce IL-12p40 expression **(Fig. 5.13b)**, whereas blocking miR-29 effects in WT NOD2 DCs with an antimiR to miR-29 causes an increase in IL-12p40 expression **(Fig. 5.13c)**. These experiments demonstrate Crohn's DCs expressing variant NOD2 fail to induce miR-29 following PRR stimulation, and that this may lead to impaired reduction of IL-12p40 expression following combination PRR stimulation.

Figure 5.13 NOD2 mutant DCs fail to control IL-12/23p40

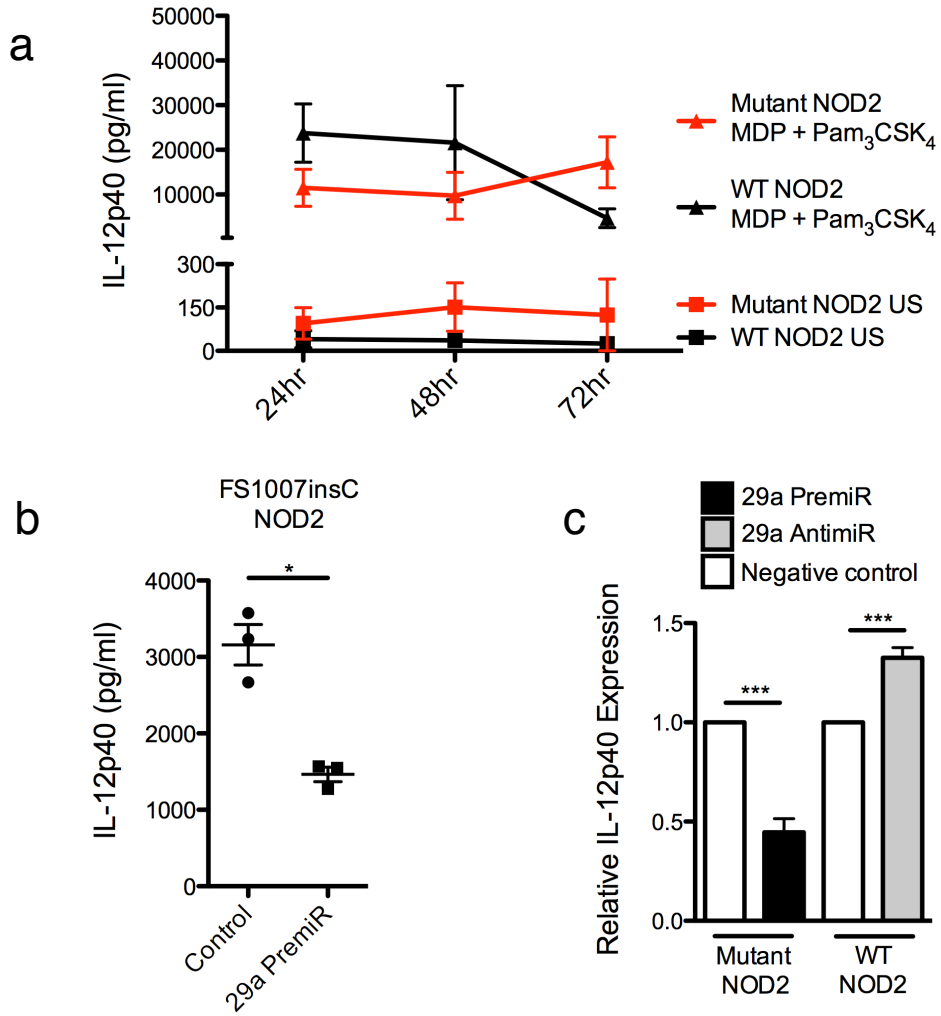


Figure 5.13 DCs were derived from CD patients homozygous for FS1007insC NOD2 (10 patients), or R702W + G908R NOD2 compound heterozygotes (5 patients). All patients have terminal ileal disease, were in clinical remission and off all immunomodulators/ biological therapy. **(a)** IL-12p40 ELISA from WT NOD2, or homozygous mutant NOD2, DCs over time. **(b)** IL-12p40 ELISA following MDP + Pam_3CSK_4 1μg/ml stimulation in FS1007insC NOD2 DCs, after transfection of miR-29 premiR or control. Significant differences by two-tailed paired t-test (*P=0.01 to 0.05). **(c)** WT NOD2 DCs transfected with miR-29 antimiR or control, and mutant NOD2 DCs transfected with miR-29 premiR, or control, before MDP + Pam_3CSK 1μg/ml stimulation. IL-12p40 expression by ELISA is shown relative to control. Statistical analysis by one-way Anova and Bonferroni post test ***P<0.001. Data are from 5 independent experiments **(a)**, 3 independent experiments **(b, c)**; error bars, s.e.m.

5.8 miR-29 decreases IL-17 expression by regulating IL-23, in DC + T cell co-culture

The functional relevance of miR-29 repression of IL-12p40/IL-23p19 on the magnitude of Th17 responses was then explored. DCs were transfected with miR-29 premiR or control before DC co-culture with $CD4^+$ T cells. IL-17 production by T cells was then assessed at 72 h. This revealed significant reduction in IL-17 production from co-cultures where DCs over-expressed miR-29 as assessed by ELISA and qPCR **(Fig. 5.14a and f** respectively**)**. I then used blocking antibodies to IL-23 and recombinant IL-23 (rIL-23) to demonstrate this effect was indeed mediated by IL-23 **(Fig. 5.14b, c and g).** The effect of DCs over-expressing miR-29 can be reversed and overcome by adding rIL-23 to these co-cultures **(Fig. 5.14d)**. IFNγ expression from T cell co-cultures is unaffected by miR-29 expression in DCs **(Fig. 5.14e)**. These results demonstrate miR-29 mediated control of IL-23 expression is functionally relevant in terms of magnitude of Th17 responses generated in its presence and absence.

Figure 5.14 miR-29 in DCs regulates IL-17 production from T cells via IL-23: ELISA

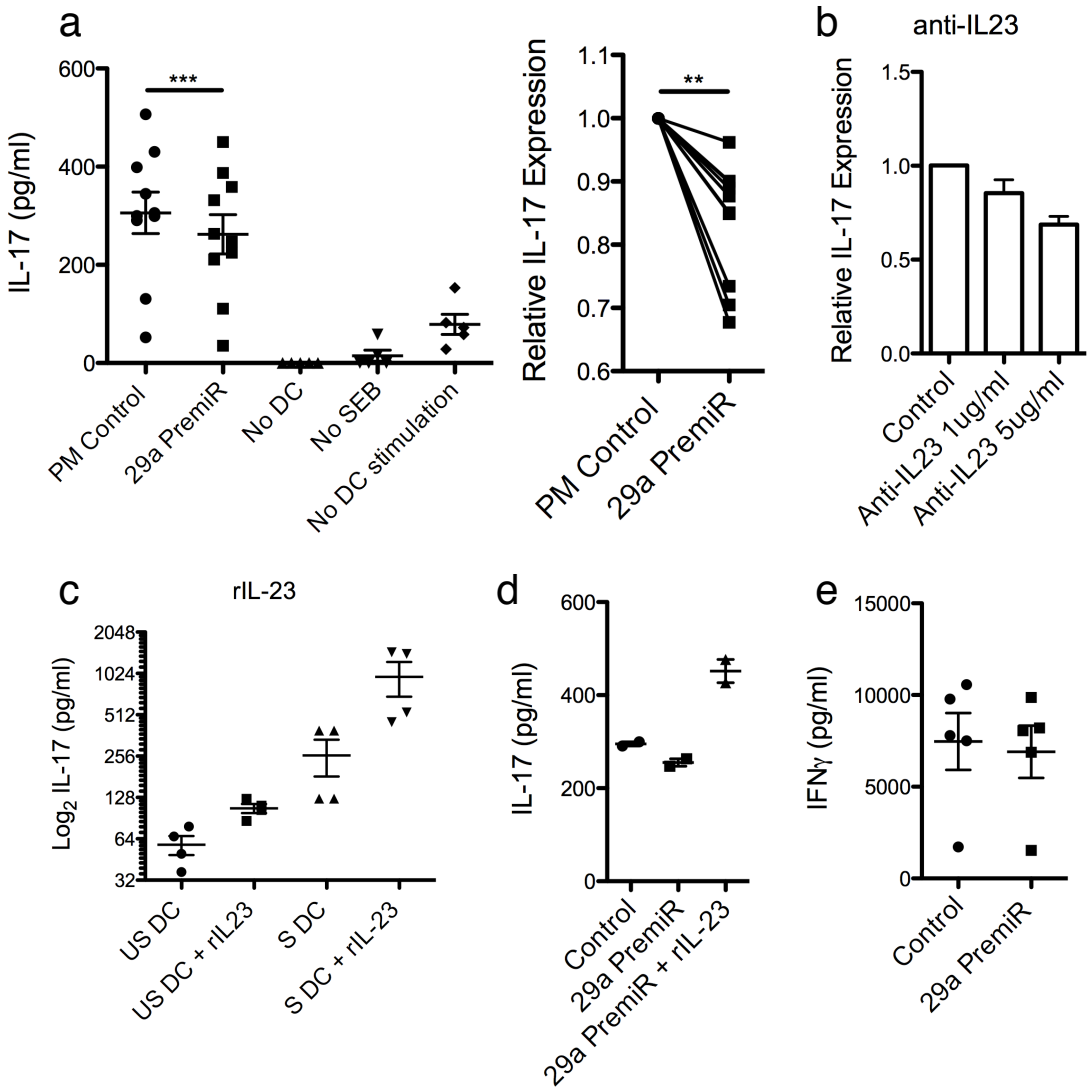


Figure 5.14 miR-29 in DCs regulates IL-17 production from T cells via IL-23: qPCR

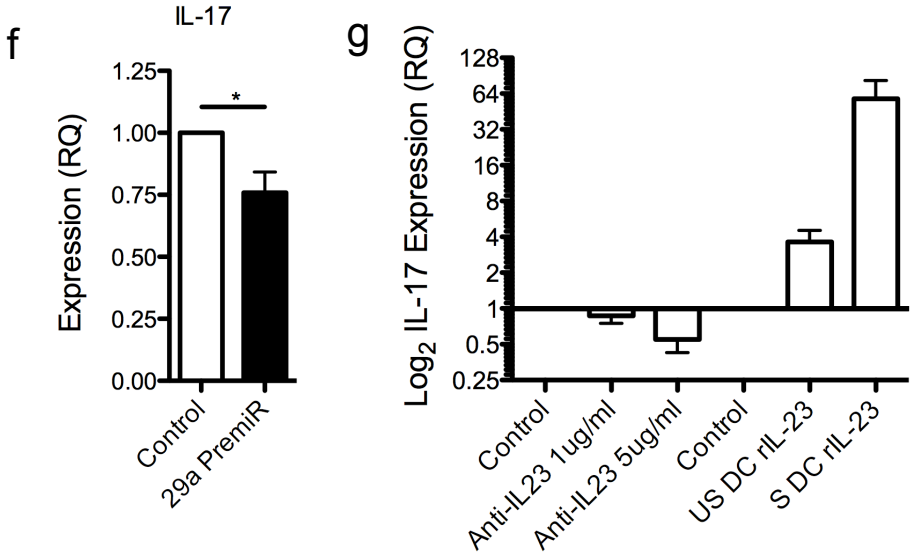


Figure 5.14 1x10^6 CD4$^+$ T cells were co-cultured with 1x10^5 DCs, with 100pg/ml SEB. DCs were transfected with miR-29 premiR, or control, for 8hrs and stimulated with MDP + Pam_3CSK_4 1μg/ml for 16hrs, before co-culture. IL-17 production after 72h co-culture was measured by ELISA **(a)** and qPCR **(f)** . Significant differences by two-tailed paired t-test **P=0.001 to 0.01 and ***P<0.001. **(b) and (g)** Anti-IL23 antibody was added to co-cultures at 1μg/ml or 5μg/ml, and IL-17 production assessed at 72h. **(c) and (g)** Recombinant IL-23 (rIL-23) was added at 0.75ng/ml to co-cultures, and IL-17 production assessed at 72h by ELISA, and by qPCR (US= unstimulated DCs; S= MDP+Pam_3CSK_4 stimulated DCs.) **(d)** DCs were transfected with miR-29 premiR, or control, prior to CD4$^+$ T cell co-culture as before. rIL-23 was added at 0.75ng/ml to co-cultures with DCs expressing the miR-29 premiR. **(e)** IFNγ production from DC + T cell co-culture, following DC transfection with miR-29 premiR or control. Data from 5 independent experiments **(a, e, f)**, 2 independent experiments **(b, d, g),** 4 independent experiments **(c)**; error bars, s.e.m.

5.9 Discussion

In this study I demonstrate for the first time that NOD2 can control miRNA expression and that it induces the miR-29 family in DCs. This induction requires the key NOD2 signal transducer RIPK-2 and can be augmented by co-triggering NOD2 with either TLR2 or TLR5. This chapter demonstrates a new series of targets for miR-29: IL-12p40, and ATF2 whose down-regulation

by this miRNA leads to down-regulation of IL-23 release from DCs. miR-29 down-regulation of IL-23 from DCs attenuates Th17 $CD4^+$ T cell responses.

MicroRNA control of cytokines, either directly or indirectly, is well described. For example, direct targeting of the 3'UTR has been shown for IL-6 mRNA by let-7[329], IL-12p35 by miR-21[326], and TNFα by miR-125b[310]. Examples of cooperative targeting include miR-221 and TTP. As already discussed, TTP targets AU-rich elements (AREs) in mRNA, many of which are found in cytokine mRNAs. miR-221 associates with TTP and together they destabilise TNFα mRNA[474]. Conversely, miRNAs are also able to protect mRNA from TTP-mediated destruction by competing for the binding sites – for example miR-4661, which contains a seed sequence complementary to the canonical ARE AUUUA sequence[475]. Transfection of miR-4661 into an LPS-stimulated macrophage cell line results in increased IL-10 expression.

Like most miRNAs miR-29a is predominantly cytosolic, whereas due to its 3' terminal motif a significant proportion of miR-29b is located in the nucleus[476]. It may be that due to this localisation this miRNA family operate a 'division of labour' with regard to IL-23 control, with miR-29a predominantly targeting cytosolic IL-12p40, whereas miR-29b would predominantly target the nuclear transcription factor ATF2.

NOD2 and TLRs are key regulators of IL-23 production by cells of the innate immune system such as DCs and macrophages[477], so induction of miR-29 controlled by NOD2 represents a key intrinsic homeostatic mechanism to switch off this critical driver of Th17 responses. IL-23 can also be induced in DCs by endogenous signals such as prostaglandin E2[478] and stimulation via CD40L[47], demonstrating a potential role for T cells in reinforcing the IL-23

response. It remains to be seen if CD40L and prostaglandin E2 also employ miR-29 as a mechanism for controlling IL-23 expression from these cells.

I found Crohn's patient DCs homozygous or compound heterozygous for NOD2 variants associated with the disease failed to induce miR-29 to any significant level on NOD2 or NOD2+TLR triggering. Although these cells also fail to induce IL-23 to the levels of WT NOD2 expressing cells on combined PRR stimulation, they exhibited defects in returning IL-12p40 to baseline levels some days after receptor stimulation. Increased basal levels of IL-23 could be important in driving inflammation in combination with other defects in NOD2 function observed in Crohn's, such as defects in autophagy induction[244] where bacterial persistence could provide an on-going trigger for IL-23 production, in the absence of intrinsic control mediated by miR-29. It is also possible these effects would be compounded in patients with co-existing IL-23R polymorphisms that might require lower levels of IL-23 to result in pro-inflammatory signalling. In addition the balance of pro- and anti-inflammatory cytokines may be upset further via Crohn's-associated NOD2 variants' active suppression of immunoregulatory IL-10 production via inhibition of hnRNP-A1 activity[273].

miR-29 is a key miRNA in a number of cellular processes and it is possible that NOD2 may function via its expression in a number of other areas. For example miR-29 has been found to regulate methylation of target genes via controlling expression of DNMT3A[380], which is also a recently described Crohn's-susceptibility gene[11]. My data suggests that this control may also occur in DCs. Alteration of methylation via this pathway could modulate

epigenetic pathways, maturation of DCs and thus influence the nature of the adaptive immune response.

NOD2 mutations are also strongly associated with disease of the terminal ileum[126], and my data are compatible with this phenotype as IL-12p40 and IL-23p19 are most highly constitutively expressed in the terminal ileum[479], increasing the need for effective regulatory mechanisms in this mucosa.

NOD2 has also been shown to influence composition of the microbiome[119]. While some of this effect might be explained by reduced expression of Paneth cell alpha defensins[256] observed in the presence of Crohn's variant NOD2, it is possible increased basal levels of IL-23 in the mucosa mediated by loss of miR-29 might facilitate this effect. It will be interesting to see the effect of NOD2 expression on miRNAs in epithelial cells and Paneth cells, where expression levels of factors affecting barrier function may be controlled.

In summary, I have shown NOD2 is critical for induction of miR-29 in DCs and assigned a number of new targets for miR-29 including those affecting IL-23 expression. Simultaneous expression by NOD2 of the key immune effector IL-23 and a molecular switch to arrest its induction illustrates the elegant ability of innate immune receptors to activate timely defence mechanisms whilst shutting off harmful immune responses. It is likely other PRRs will operate such paradigms and that these may be disrupted in inflammatory diseases, an important area for future study.

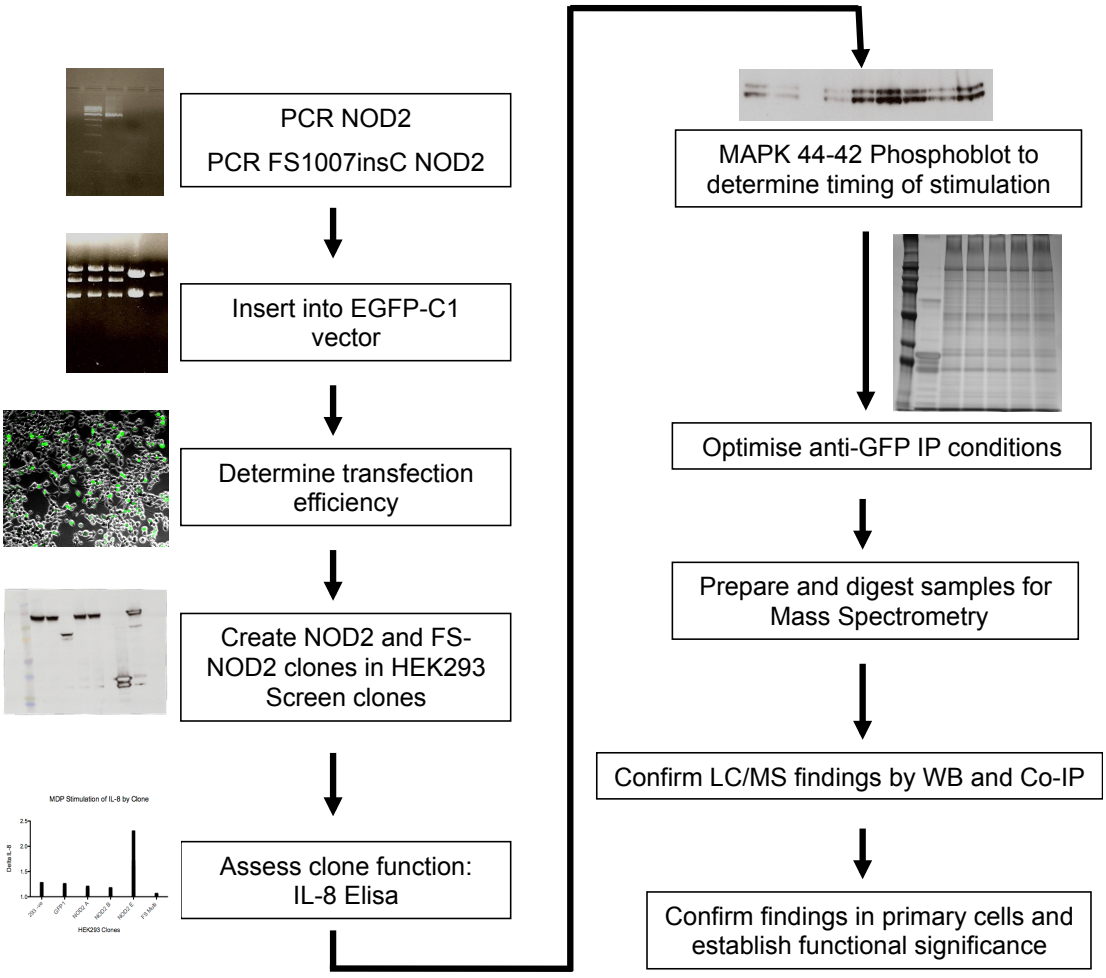
6 NOD2 Immunoprecipitation

6.1 Introduction

Although the signalling pathways downstream of NOD2 activation (outlined in the thesis introduction) have been characterised in a basic sense many questions remain unanswered. These include: Does NOD2 act in a multimolecular complex, in a similar fashion to the NLRs that activate the inflammasome?; Is NOD2 part of an MDP-stimulated inflammasome?; How are the different effector arms of NOD2 signalling – such as autophagy induction, NFκB and MAPK activation – mediated?; Which signalling proteins contribute to the observed synergy with TLR signalling pathways?

I aim to address the answers to some of these questions by performing a 'classical' immunoprecipitation of NOD2 and any associated proteins in a model system. The basic experimental protocol, which is outlined in **Figure 6.1**, involved GFP(green fluorescence protein)-tagging NOD2 and stably expressing the tagged protein in HEK293 cells. Tagging of NOD2 avoids problems with available NOD2 antibody quality, but can potentially influence NOD2 protein function. I chose HEK293 cells for tagged NOD2 expression as they are well characterised, easy to transfect, and do not express endogenous NOD2, (but do express endogenous NOD1, TLR3 and 5)[137]. I planned to compare the results obtained with wild-type NOD2 to the NOD2 frame-shift mutation, and to validate any findings in primary human cells.

Figure 6.1 NOD2 IP Experiment Design



One of the ways to validate my experimental system is to immunoprecipitate proteins that have already been shown to interact with NOD2. Most of these have been detailed in the thesis introduction and preceding chapters (including RIPK-2[137], CARD9[179], GRIM-19[174], DUOX2[267], TRAF4[436], TAK1[168], Erbin[169], CARD8[171], CD147[170], NOD2-S[175], CENTB1[172], AAMP[173], NLRP1[239], NLRP3[232], NLRC4[226] and, post ssRNA stimulation, MAVS(mitochondrial antiviral signalling)[132]). Amongst these proteins there are those that contribute

positively to NOD2-immune activation (RIPK-2, CARD9, TAK1, GRIM-19, MAVS), those whose function with regard to NOD2 is less certain (NLRP1, NLRP3), and many that are negative regulators of NOD2 signalling (DUOX2, TRAF4, Erbin, CARD8, CD147, NOD2-S, CENTB1, AAMP, NLRC4). This no doubt reflects the importance of keeping immune activation in general, and NOD2 activation specifically, under tight control.

It is also worth bearing in mind three points regarding these proteins already identified. Firstly, that most of these interacting proteins (with notable exception Erbin) have not been validated by repeat publications. Secondly, many of the interactions have been demonstrated in epithelial cell lines, and it is highly likely that different modes of signalling control will occur in DCs. (The studies of CARD8, DUOX2, TAK1, GRIM-19, TRAF4, AAMP, and CENTB1 did not test these NOD2 interactions in DCs or other myelomonocytic cells.) As an example, NOD2-S is the dominant form of NOD2 in colonic epithelial cells but not in the THP1 monocytic cell line (although expression is inducible here)[175]. This may reflect the different locations and roles of these cell types, with the epithelial cells constantly exposed to commensal gut flora and requiring many robust systems to prevent immune activation in the steady state, whereas monocytic cells are predominantly activated when the mucosa is breached and are required for active immune surveillance, and thus may not need to constitutively express NOD2 negative regulators.

Thirdly, that caveats remain concerning protein interactions demonstrated when both proteins are artificially over-expressed. This was the predominant method used to identify Erbin, CARD8, CD147, TAK1, DUOX2, GRIM-19, TRAF4, CENTB1, AAMP, NLRP1, NLRP3, and NLRC4, and in many of these

studies (e.g. CARD8, CD147, TRAF4, AAMP, NLRP3, NLRC4) the interaction was *only* shown when at least one protein was overexpressed.

Despite this plethora of potential NOD2-interactors, an unbiased IP of the NOD2 signalling complex, sometimes termed the 'nodosome' or 'signalosome', had not been performed at the time I planned this experiment. CARD domains are known to promote protein-protein interactions, so it is likely that all of the NOD2 binding partners have not been fully described. HEK293 cells had been used in a previous proteomic screen of NOD2 function, but this analysed whole-cell lysates not the NOD2 signalosome[480]. Here, HEK293 cells stably transfected with either wild-type NOD2, FS1007insC NOD2, or a control vector were stimulated with MDP for 4hours or 24hours, and global protein expression changes were analysed using two-dimensional PAGE, with differentially regulated proteins identified using mass-spectrometry. Following MDP exposure 198 proteins changed expression level between the wild-type and mutant NOD2 stimulated cells, demonstrating that these model approaches can successfully identify proteomic changes even in cell lines.

Subsequently, a NOD2 immunoprecipitation in THP1 cells using tandem affinity purification was published[481]. In this model cells were stably transfected with wild-type NOD2, and also a NOD2 mutant form associated with Blau syndrome (NOD2-R334Q). OAS2 (2'-5'-oligoadenylate synthetase 2) was identified as associating with NOD2, and this was unchanged by the presence of the Blau mutation. OAS2 is one of four human OAS genes, and expression of these antiviral proteins is interferon-induced. OAS enzymatic activity is turned on when this protein family bind to viral double-stranded

(ds)RNA, and this leads to activation of RNase-L, an endoribonuclease, resulting in single-stranded (ss)RNA cleavage and RIG-I activation[482]. Over-expression of NOD2 increases RNase-L activity when THP-1 cells are treated with poly(I:C), and along with the recent data showing that NOD2 responds to ssRNA[132], this raises interesting questions about the role of NOD2 in viral defense. Otherwise this paper gave limited information about the other proteins identified by the IP, except to confirm that in all 5 of their independent experiments they identified Erbin[481].

In summary, NOD2 has many known and putative functions, and many potential interacting partners, but a clear understanding of how these different effector arms are coordinated, particularly in myelomonocytic cells, has not been achieved. Moreover the influence of CD-associated NOD2 mutations has not been rigorously explored. I propose to screen, in an unbiased manner, potential interacting proteins of the NOD2 signalosome by mass spectrometry, and to confirm these findings and their functional significance in DCs.

6.2 Aims

The aims of this project are:

- To identify components of the NOD2 signalosome in a model system
- To determine if these interactions are altered in the presence of FS1007insC NOD2
- To validate these findings and their functional significance in primary human DCs

6.3 Results

6.3.1 PCR of NOD2 from pUNO-NOD2

pUNO-hNOD2a (Invivogen) was purchased and the DNA maxi-prepped in the usual manner, and then used as a template for PCR of NOD2 prior to cloning into a GFP vector. High fidelity PCR enzyme mix was used (Fermentas) containing both a high processive Taq DNA polymerase and a Pfu DNA polymerase. I initially designed PCR primers in order that the product be used in a 'standard' cloning reaction with DNA ligase. However, despite an optimum NOD2 PCR product, ligation was unsuccessful.

This prompted redesigning the primers for use with the Clontech 'in-fusion' method. As before the primers were designed for an in-frame fusion with the GFP vector, such that NOD2 lies at the C-terminal end of the GFP protein, thus leaving the LRR ligand-recognition domain untagged. The in-fusion method involves adding fifteen base pairs to the 5'-end of the PCR primers, such that they are homologous to the ends of the linearised vector. An endonuclease in the ligation enzyme mix exposes these 15bp on the vector to aid appropriate ligation.

Magnesium and temperature ramps were employed to optimise the PCR conditions with the new primers **(Figure 6.2)**. The optimum PCR conditions with these oligos was 25μl reactions of: DNTPs 0.5μl; forward oligo 0.5μl and reverse oligo 0.5μl (of 10μM solutions); enzyme 0.5μl; buffer 2.5μl; Mg^{++} 1μl (to create 1mM conc); pUNO-NOD2 0.1μl (concentration 370ng/μl); H_20 19.4μl. Optimum PCR reaction was: Step 1 95°C 5minute; Step2 95°C 30seconds; Step 3 57°C 30seconds; Step 4 72°C 5minute; Go to step 2 for 29 more cycles; Step 5 72°C 5minutes.

Figure 6.2 NOD2 PCR: Optimising PCR conditions

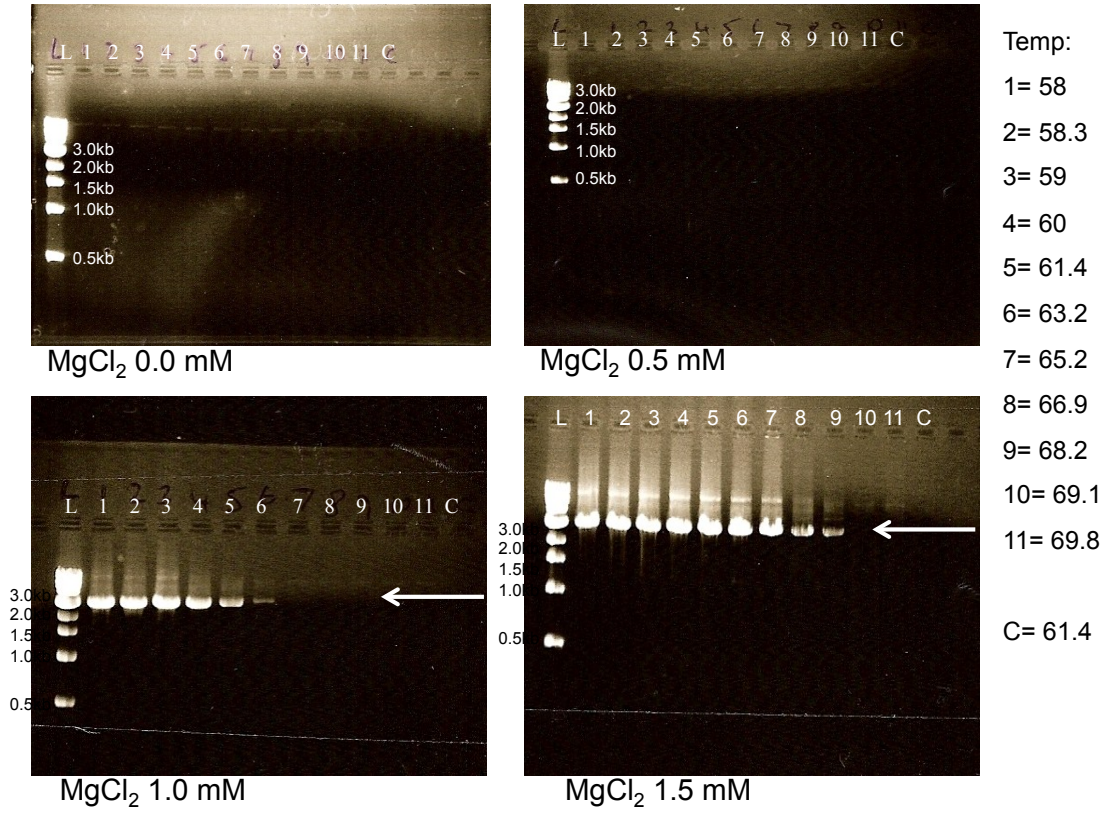


Figure 6.2 pUNO-hNOD2a (Invivogen) DNA was used as PCR template. High fidelity PCR enzyme mix was used (Fermentas) containing both a high processive Taq DNA polymerase and a Pfu DNA polymerase. The following primers were designed and used: forward 5'-GTC CGG ACT CAG ATC TAC CAT GGG GGA AGA GGG T -3' and reverse 5'-CCG CGG TAC CGT CGA TCA AAG CAA GAG TCT -3'. Temperature and Mg^{++} ramps were employed to optimise the conditions, as shown. The arrows mark the expected 3 kb weight of NOD2. Ladder: NEB 1 kb DNA ladder, N3232L.

The resulting band **(Fig. 6.3a)** was gel-purified using Qiagen QIAquick Gel Extraction Kit following the manufacturers instructions. A diagnostic digest was performed using BstEII restriction enzyme (NEB), the gel showed appropriate weight bands of 1.8kb and 1.3kb **(Fig. 6.3b)** and I proceeded with the ligation.

Figure 6.3 NOD2 PCR and Diagnostic Digest

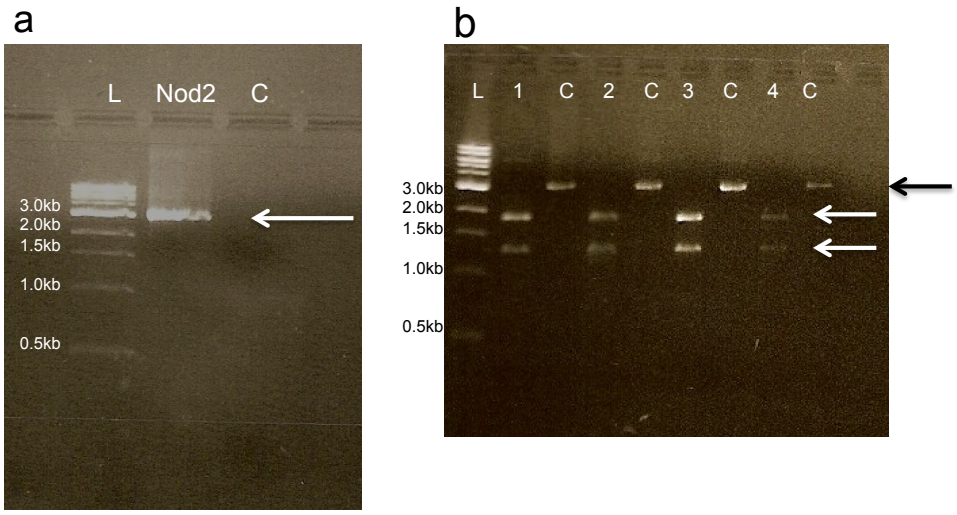


Figure 6.3 (a) Optimal NOD2 PCR. 25 μl reaction of: DNTPs 0.5 μl; 0.5 μl of 10 μM 5' and 3' oligos; 0.5 μl enzyme; 2.5 μl buffer; Mg^{++} 1 mM; template 0.1 μl of 370 ng/μl; H_2O 19.4 μl. Conditions: 95ºC for 5mins then: denature 95ºC 30sec, anneal 60.5ºC 30sec, extend 72ºC 5 min for 30 cycles, with final 5minute 72ºC extension step. Gel demonstrates a band at 3kb, the weight of NOD2 (arrow).

Figure (b) Diagnostic Digest PCR Products PCR products (1-4; black arrow) digested with BstEII (NEB) to produce two fragments 1.2kb and 1.8kb in size (white arrows), shown with undigested controls (C).

FS1007insC NOD2 PCR. The following primers were designed so that the stop-codon associated with the Crohn's disease-associated frame-shift mutation was inserted in the PCR product at the 1007 position: forward 5' - GTC CGG ACT CAG ATC TAC CAT GGG GGA AGA GGG T -3' as per wild-type NOD2; reverse 5' - CCG CGG TAC CGT CGA TCA AGG GGC CTG CAG GAG GGC -3'. The same PCR conditions were used.

6.3.2 FS1007insC NOD2 PCR

The reverse PCR primer was altered to insert a cytosine, and thus an early stop codon, into NOD2 during the PCR reaction. The same forward primer and NOD2 template was used, and the PCR reaction conditions were unchanged. The PCR product corresponds with the FS1007insC NOD2 that is associated with Crohn's disease.

6.3.3 EGFP-C1 vector

A green fluorescence protein (GFP)-expressing vector was chosen in which to express NOD2. This tag was selected so that the NOD2 constructs could be used not only in the IP experiment, but also in confocal analysis of the distribution of NOD2 both in resting and in stimulated conditions. The EGFP-C1 vector (Clontech) was selected as the multiple cloning site (MCS) is C-terminal to the GFP tag. As the ligand recognition (LRR) domain of NOD2 is the C-terminal domain, I wanted to avoid the possibility of disrupting NOD2-MDP interactions. This arrangement is also in keeping with published NOD2-tagged experiments. EGFP-C1 also contains a neomycin resistance cassette, allowing G418 selection in eukaryotic cells.

After transforming competent *Escherichia coli* with EGFP-C1, the DNA was extracted using a maxi-prep kit (Qiagen). NHEI and EcoRI restriction enzymes were used to digest the DNA, and ensure that there were appropriate weight fragments **(Fig. 6.4a)**. Subsequently the vector was linearised using two enzymes in the MCS, BglII and SalI, and the free ends dephosphorylated to prevent re-ligation **(Fig. 6.4b)**.

Figure 6.4 EGFP-C1 Vector Maxi-Prep and Linearisation

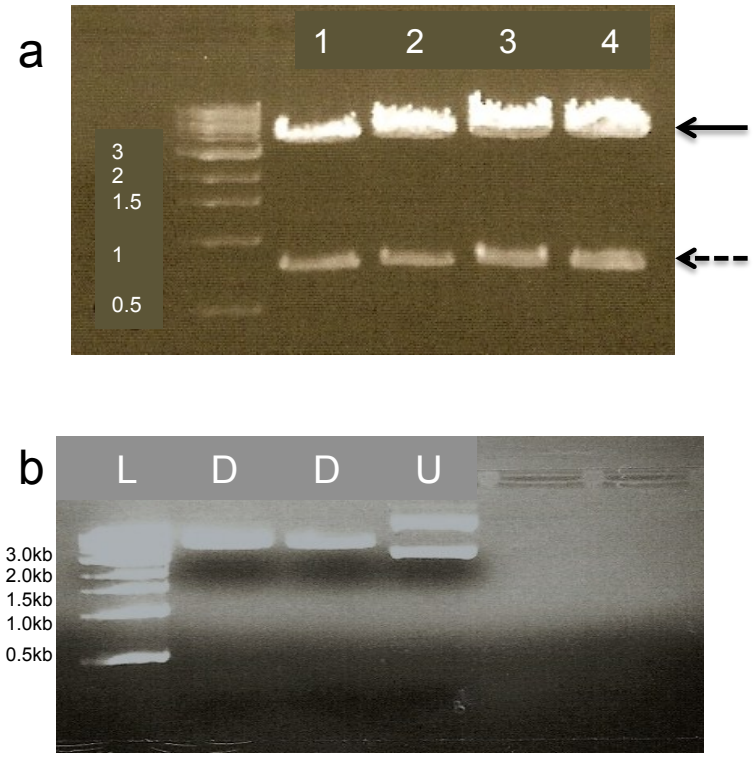


Figure 6.4 (a) EGFP-C1 Maxi-prep and Digestion
Escherichia coli (Invitrogen DH5a-T1 Max Efficiency) were transformed with 1 μl DNA of pLP-EGFP-C1 vector (Clontech; 4.7kb). Four colonies (1-4) were expanded, and DNA was extracted using Qiagen Plasmid Maxi Kit. DNA was quantified using NanoDrop® ND-1000, and a diagnostic digest performed using Nhe1 and EcoRI restriction enzymes (NEB). Run down TBE 1% agarose gel (with ethidium bromide) confirmed the correct weight fragments (0.8kb broken arrow and 3.9kb black arrow).

(b) EGFP-C1 Linearisation BglII and Sal1 restriction sites were chosen from within the Multiple Cloning Site (MCS) of EGFP-C1. 1.5 μl of each enzyme (Roche) digested 6μl EGFP-C1 DNA over 3 hours at 37°C. After heat-inactivation, dephosphorylation with alkaline phosphatase (Roche, shrimp ALP 1 U/μl) was performed. Digested samples (D) were analysed on a TBE 1% gel alongside undigested vector (U) as a control

6.3.4 NOD2 and FS1007insC NOD2 cloning into EGFP-C1

C-terminal cloning of the NOD2 PCR product and linearised EGFP-C1 was performed with the Clontech in-fusion dry down method, as per manufacturers instructions. *E. coli* were subsequently transformed, isolated colonies mini-prepped, and the resulting DNA digested with BspHI restriction enzyme to ensure correct insertion **(Fig. 6.5a)**. The FS1007insC NOD2 PCR product was also cloned into EGFP-C1 using the same method.

I subsequently designed PCR sequencing primers in order to ensure that polymorphisms had not been introduced in the cloning process. Only vectors containing exact NOD2 or FS1007insC NOD2 sequences were used in further experiments **(Table 6.1)**.

Figure 6.5 NOD2 cloning into EGFPC1 vector

a

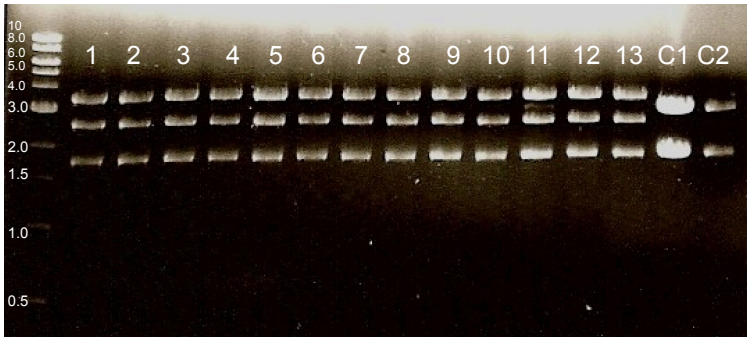


Figure 6.5 (a) Ligation of NOD2 PCR product and linearised EGFPC1 Ligation was performed using Clontech In-Fusion method, and subsequently used to transform *Escherichia coli* (Stratagene XL-10 Gold Ultracompetent Cells). DNA was extracted from isolated colonies, and digested with BspHI (NEB).

Gel shows digested ligation products (1-13) with correct weight bands (1.7 kb, 2.5 kb, 3.5 kb). Controls: C1= unlinearised, untransformed EGFPC1; C2 = linearised EGFPC1, ligated in absence NOD2, demonstrate bands of 1.7 kb and 3 kb.

NOD2-GFP	**Sequence**	**FSNOD2-GFP**	**Sequence**
Colony 1	3 nucleotide changes	Colony 1	1 nucleotide change
Colony 2	**Sequence intact**	Colony 3	**Sequence intact**
Colony 7	2 nucleotide changes	Colony 5	1 nucleotide change
		Colony 6	1 nucleotide change - synonymous
		Colony 9	1 nucleotide change - synonymous

Table 6.1 Sequencing of constructs

8x forward and 8x reverse primers were designed, using Primer3 and Amplify software, for sequencing of successfully ligated constructs. The results were analysed using Pregap4 and Gap4 software.

The table shows examples of sequencing results obtained. Only constructs with fully intact sequences were used in further experiments.

6.4 HEK293 cell transfection and clonal selection

HEK293 cells were transfected using the calcium phosphate method with EGFP-C1, NOD2-GFP, and FS1007insC NOD2-GFP vectors. Transfection efficiency was determined by flow cytometry analysis of GFP expression **(Fig. 6.6)**. EGFP-C1 transfection was much more efficient than transfection of the NOD2-expressing vectors, which may be a reflection of the size difference of the vectors (4.7kb vs 7.7kb), or it may reflect that there is a fitness cost to cells over-expressing NOD2. In part because of this difference in transfection rates, but predominantly because I wanted to standardise the IP experiment, I elected to select and expand clonal populations of HEK293 cells stably expressing each of the three vectors.

Figure 6.6 FACS Analysis Transfection Efficiency

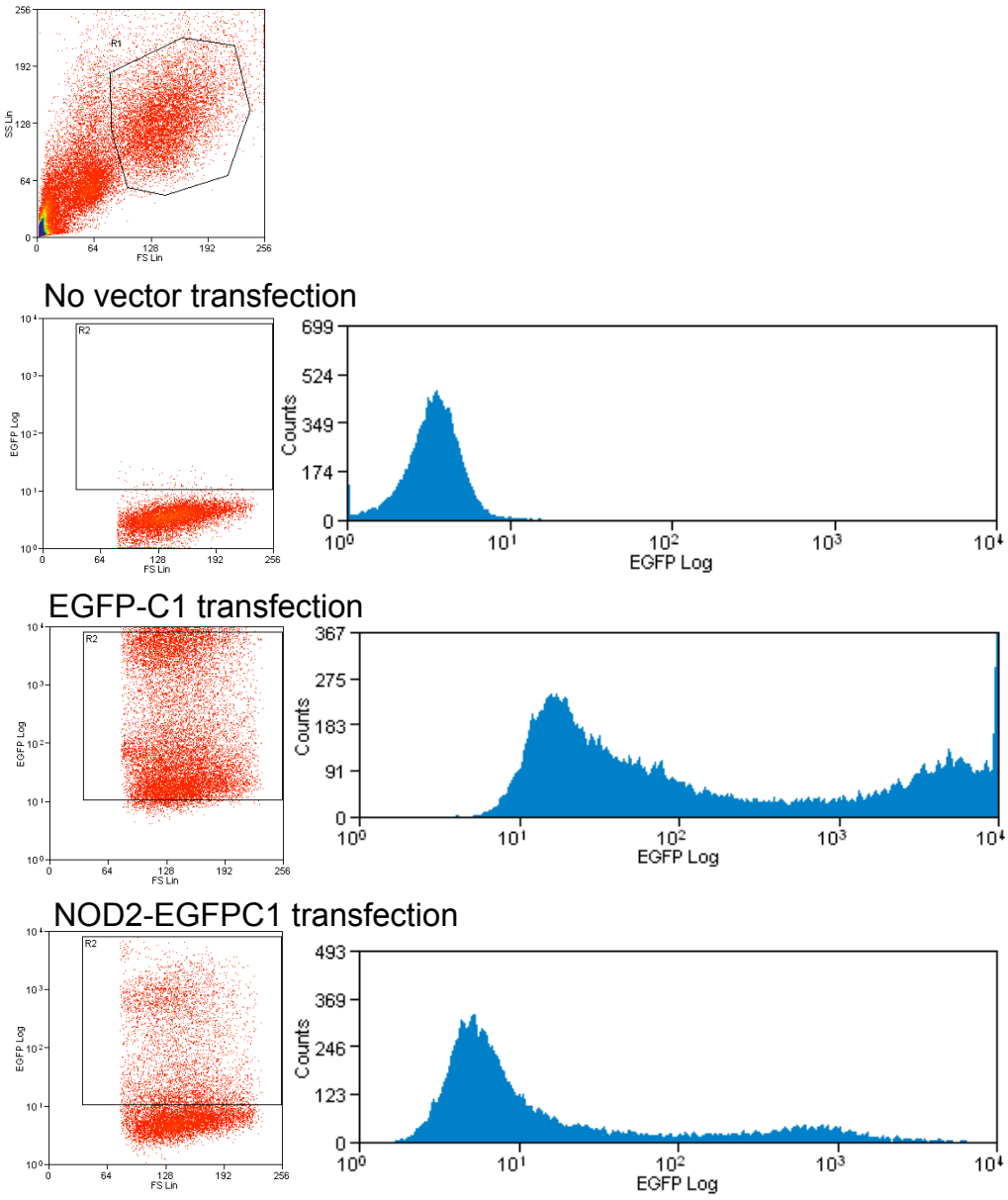


Figure 6.6 Calcium phosphate transfection of HEK293 cells was used for the empty EGFP-C1 vector, and both the wild-type NOD2 and FS1007insC NOD2-EGFP constructs. Transfection efficiency was assessed by flow cytometry as shown.

Firstly I determined, using trypan blue staining and a range of G418 media concentrations, the minimum concentration of G418 necessary to kill all HEK293 cells **(Fig. 6.7a)**. I then transfected the HEK293 cells with each vector, and grew the cells in 1.2 mg/ml of G418 in D10 for 2 weeks. The surviving stably transfected cells were single cell sorted by serial dilution into 96-well plates. Viable 96-well plate colonies were assessed initially for GFP expression by fluorescence microscopy, and subsequently by western blot for appropriate NOD2 or FS1007insC NOD2 **(Fig. 6.7b)**. A surprising number of apparent NOD2-GFP colonies were actually only expressing GFP, presumably because the NOD2 component of the vector had been silenced or spliced out, again raising the question as to whether NOD2 overexpression delivers a fitness cost.

Figure 6.7 NOD2-GFP and FS1007insC NOD2-GFP Clones

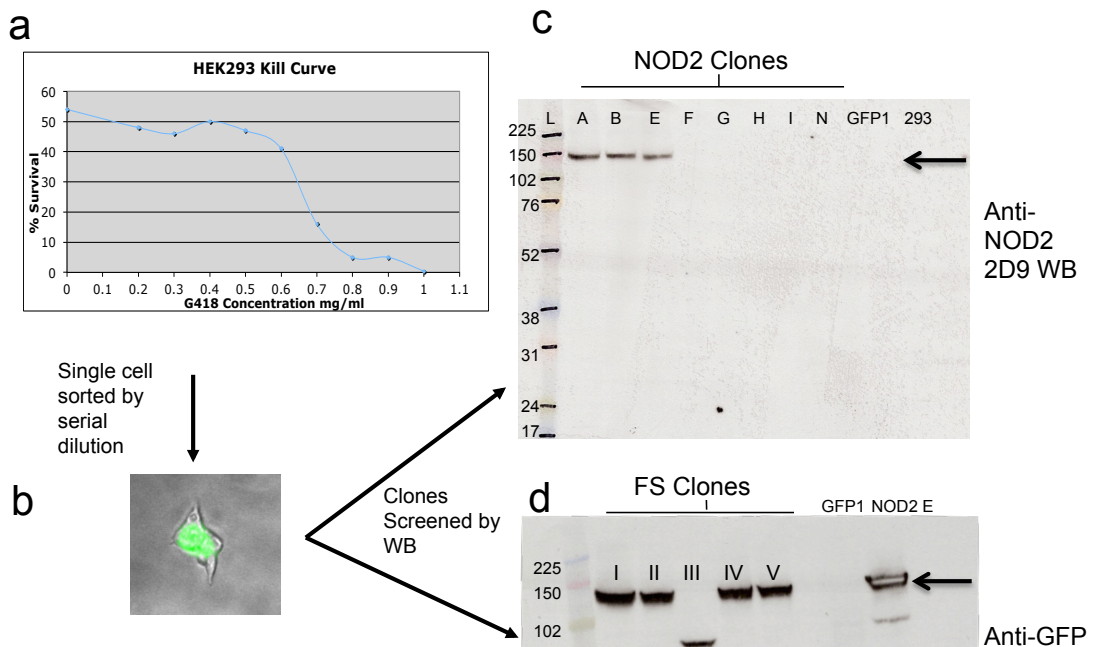


Figure 6.7 NOD2-GFP and FS1007insC NOD2-GFP Clone
(a) Concentration of G418 was determined by performing a dose-response experiment on untransformed HEK293 cells. Transformed cells were grown in D10 + 1.2 mg/ml G418 for 2 weeks, and then single cell sorted by serial dilution into 96-well plates. Clonal populations expressing GFP by fluorescence microscopy **(b)** were subsequently screened for appropriate NOD2/ FS1007insC NOD2 expression using western blot. **(c)** NOD2 clones A-N: western blot using anti-NOD2 antibody. Arrow shows the expected NOD2-GFP band at 145kDa. **(d)** FS-NOD2 clones I-V: western blot using anti-GFP antibody. Black arrow shows the expected NOD2-GFP band weight (145 kDa), the broken arrow the expected GFP weight (30 kDa).

6.5 NOD2-GFP and FS1007insC NOD2-GFP distribution

Previous NOD2 over-expression experiments have determined that NOD2 is localised to both the cytoplasm and the cell membrane, whereas FS1007insC NOD2 is only located in the cytoplasm[156]. I determined the distribution of NOD2 in my experiments by confocal microscopy, and found that this tallied with published data **(Fig. 6.8)**. I also assessed by confocal if re-distribution

occurred after MDP stimulation, but found no consistent differences with the unstimulated state (data not shown).

Figure 6.8 Distribution of NOD2-GFP and FS1007insCNOD2-GFP

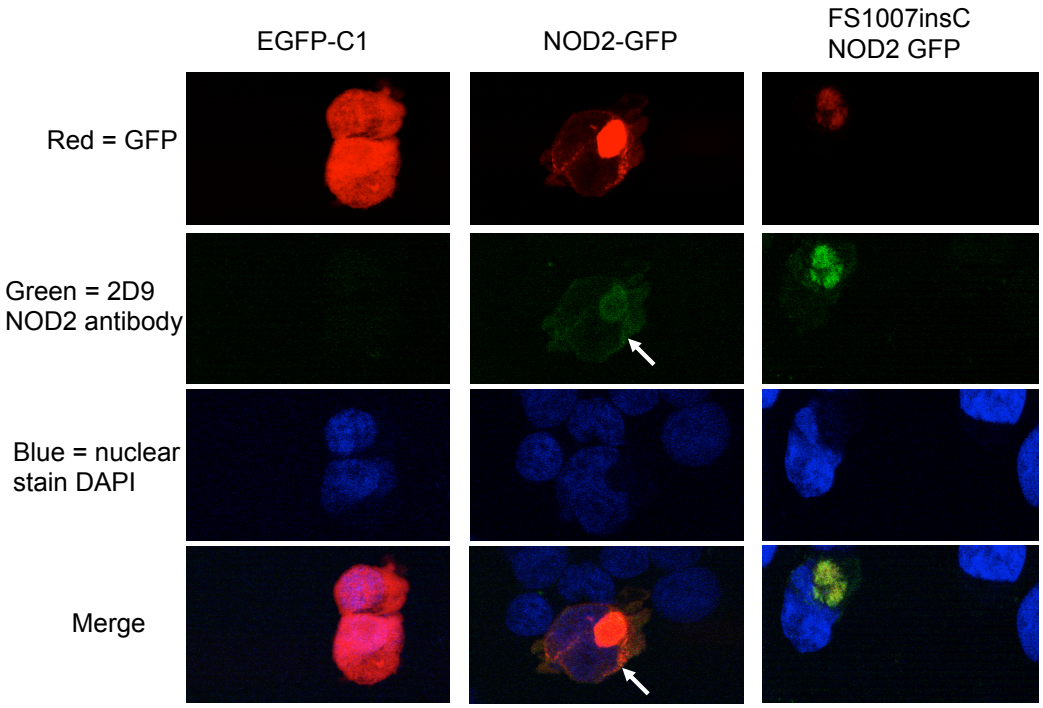


Figure 6.8 Distribution of NOD2-GFP and FS1007insCNOD2-GFP

Transfected HEK293 cells were seeded at $1x10^5$ cells/ well onto 8 well poly-D-lysine slides. After fixation and permeabilisation, cells were stained with anti-NOD2 antibody overnight at 4°C, and then Alexofluor 594 secondary antibody. To-Pro nuclear stain was added for 10 minutes. Coverslips were mounted using Vectashield + DAPI. Representative confocal images are shown.

The arrow highlights the membrane-bound form of wild-type NOD2, whereas FS1007insC NOD2 is only detectable in the cytosol.

6.6 NOD2-GFP and FS1007insC NOD2-GFP function

The NOD2 vectors and clones were then assessed for appropriate function using an IL-8 ELISA. HEK293 cells expressing no vector, and each of the three GFP-expressing vectors, were stimulated for 16 h with MDP before supernatants were harvested and IL-8 expression analysed. I demonstrated a significant difference in IL-8 production from the NOD2-expressing cells

compared with native cells or cells expressing the EGFP-C1 empty vector. As expected the FS1007insC NOD2 was loss-of-function in this assay **(Fig. 6.9a)**. The NOD2 clones A, B, and E were also assessed, with surprisingly only the 'E' clone demonstrating an IL-8 response to MDP **(Fig. 6.9b)**.

Figure 6.9 NOD2 Clone Function: IL-8 Elisa

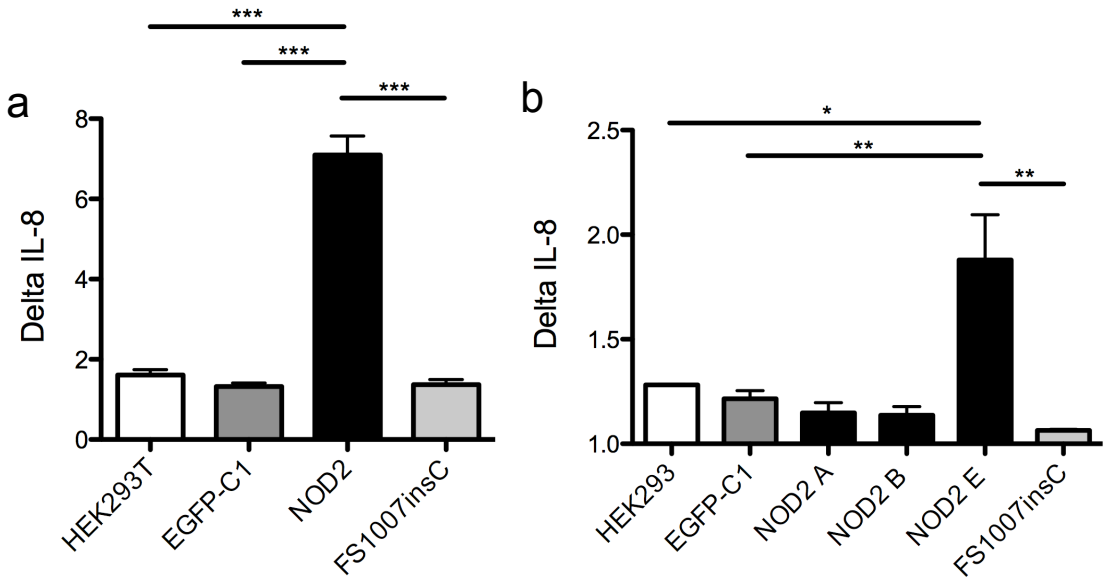


Figure 6.9 IL-8 Elisa
(a) HEK293 T cells were transiently transfected with EGFP-C1, or wild-type or frame-shift NOD2-EGFP vectors, and stimulated for 16 h with 10 μg/ml MDP. IL-8 elisa was performed using IL-8 Duoset (R&D Systems). Results are represented as the change in IL-8 secretion compared with unstimulated cells.
(b) IL-8 Elisa of NOD2-EGFP clones A, B and E, compared with native HEK293 cells, or EGFP-C1 or FS1007insC NOD2-expressing HEK293 cells, after MDP stimulation for 16 h.
Significant results, by one-way Anova with Bonferroni post test (*P=0.01 to 0.05, **P=0.001 to 0.01, and ***P<0.001). Data are from: **(a)** 2 separate experiments, and **(b)** 3 separate experiments; error bars, s.e.m.

6.7 Timing of NOD2 stimulation

MDP stimulation of NOD2 results in phosphorylation of MAP kinases[260]. To determine the most appropriate timing of NOD2 stimulation for the IP, I examined changes to MAPK 44-42 (Erk 1/2) phosphorylation by western blot.

As MDP has been shown to activate the inflammasome through both NLRP1 and NLRP3, I stimulated the clones with MDP both in the presence and absence of KCl (130 mmol) in the medium. Blocking potassium efflux by raising extracellular potassium concentration is a method of preventing inflammasome activation[483]. In this first experiment I was surprised to see that all of the cells, including native HEK293 and those expressing the empty EGFP-C1 vector, demonstrated MAPK 44-42 activation after MDP stimulation **(Fig. 6.10)**. However this was presumably not through MDP stimulation of NLRP1 or 3, as extracellular KCl produced no reduction in phosphorylation.

Figure 6.10 MAPK 44-42 Western Blot

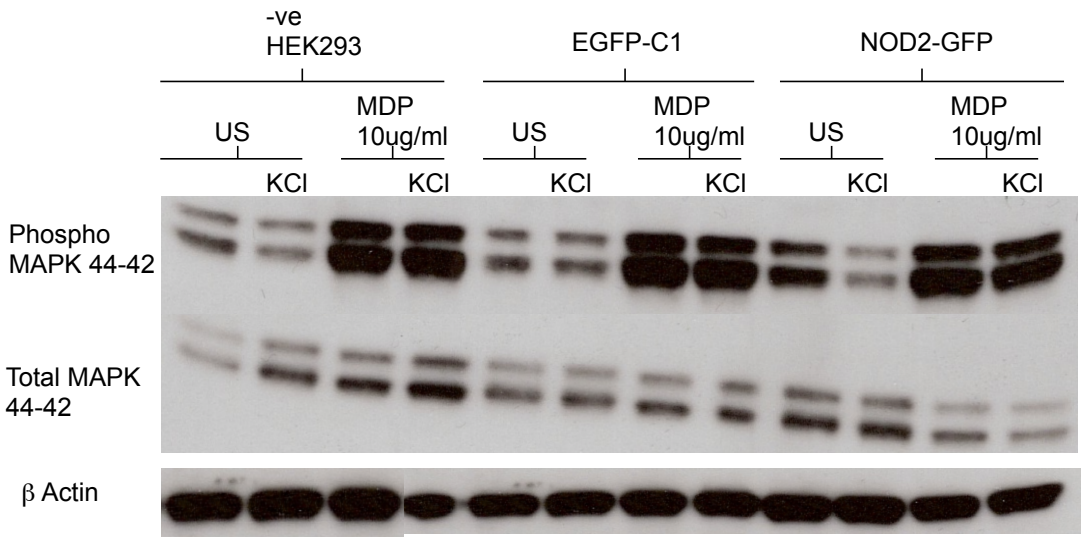


Figure 6.10 MAPK 44-42 WB
Native or transfected HEK293 cells were left unstimulated, or stimulated with MDP 10 µg/ml**.** On stimulation some cells were also treated with KCl 130mmol to prevent inflammasome activation. Cells were lysed before western blot for phosphorylated and total MAPK 42-44.

In that experiment I had not controlled for stimulation appropriately, as I had not placed fresh media on the unstimulated cells for the stimulation period. I suspected that the MAPK phosphorylation might in part reflect that the MDP-stimulated cells were also responding to the fresh media. This proved to be the case, as cells starved with D0.2 (2% foetal calf serum (FCS) media) overnight and then given standard D10 (10% FCS) media for 1 h, strongly up-regulate their MAPK phosphorylation **(Fig. 6.11a)**. I also determined that other non-specific stimuli, such as harvesting the cells at room temperature, rather than on ice, also leads to phosphorylation of MAPK 44-42 **(Fig. 6.11b)**. In subsequent experiments I ensured that the stimulation of the cells with MDP, or mock stimulation, was performed with D0.2, and that handling of the cells during lysis was quick, with all reagents chilled and the harvest and lysis performed on ice. With these safeguards in place I next determined that blocking inflammasome activation did not prevent MDP-induced MAPK phosphorylation in NOD2-expressing cells **(Fig. 6.11c and 6.12a)**.

Figure 6.11 Mechanisms of HEK293 MAPK 44-42 activation

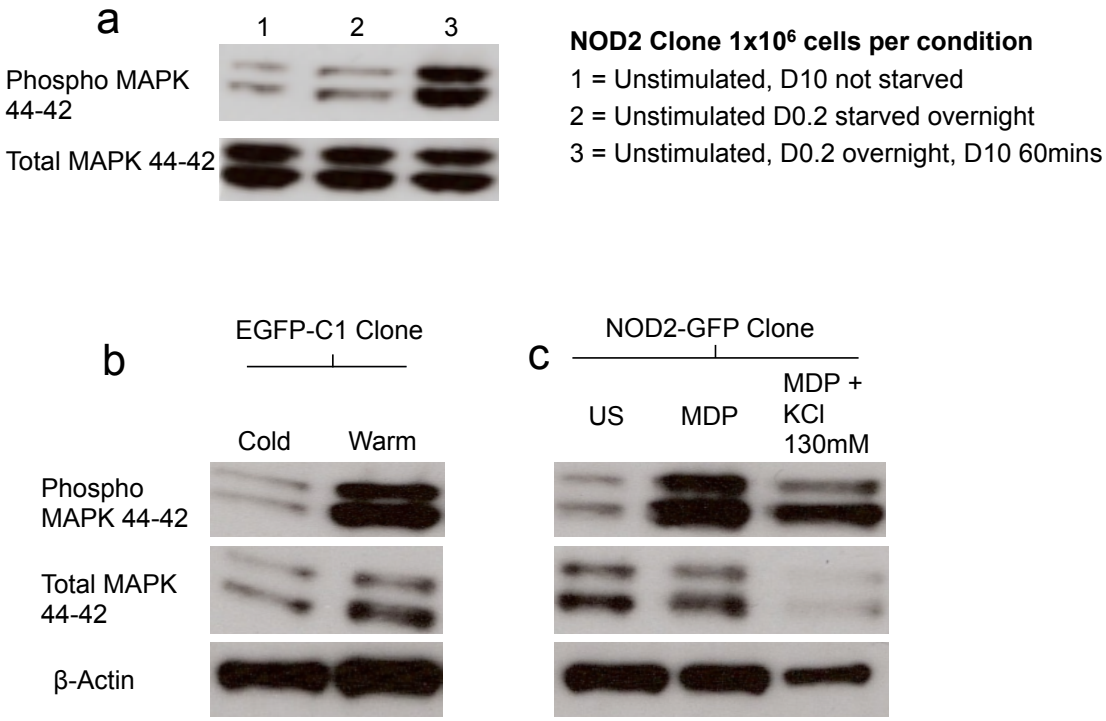
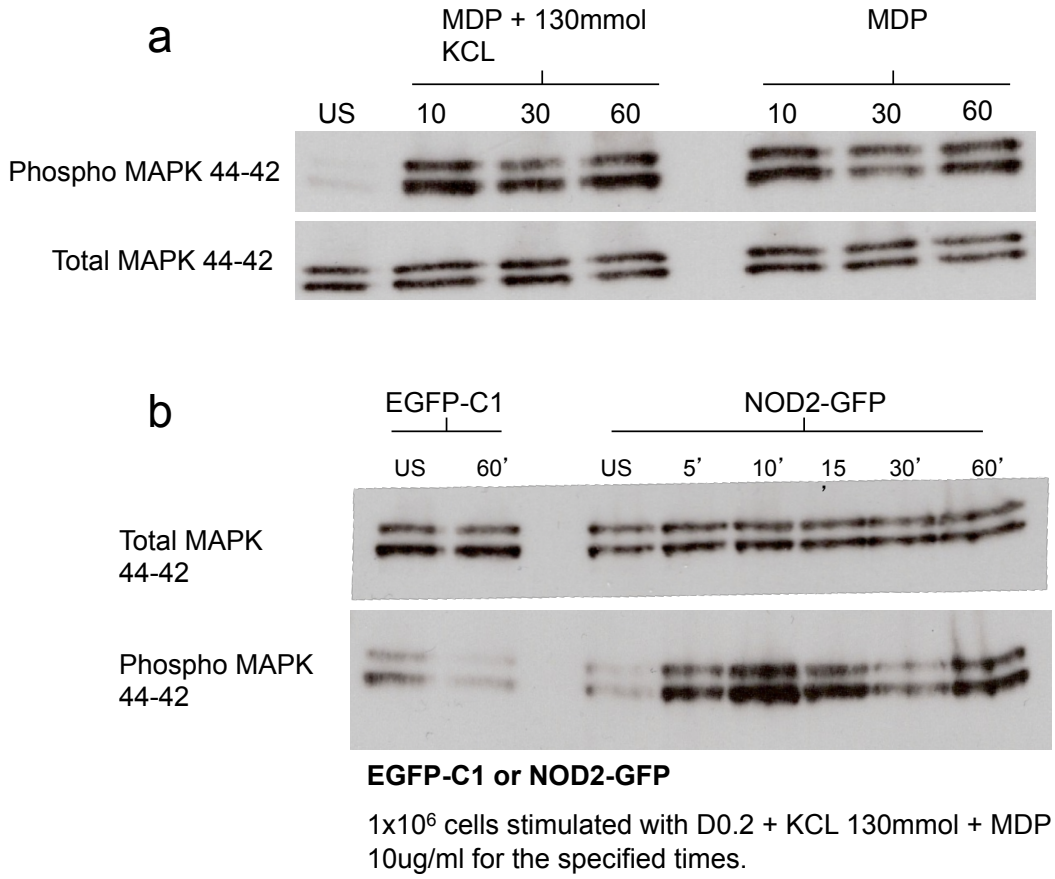


Figure 6.11 MAPK 44-42 WB
(a) NOD2-GFP clones were treated with media with restricted (2%) foetal calf serum (D0.2), before addition of standard D10 media (containing 10% FCS) for 1 h, before lysis and MAPK 44-42 WB.
(b) EGFP-C1 HEK293 cells were harvested either on ice with chilled PBS (cold), or at room temperature with chilled PBS (warm) before WB.
(c) NOD2-GFP HEK293 cells were left unstimulated, or stimulated with MDP in D0.2, with or without KCL 130mmol, before lysis on ice and WB.

Finally, whilst controlling for these other activating stimuli, I determined that MAPK 44-42 phosphorylation was apparent as early as 5 minutes post MDP stimulation, with maximal phosphorylation at 10 minutes, and possibly a degree of de-phosphorylation at 30 minutes **(Fig. 6.12b)**. I elected to perform the IP experiment after 10 minutes and 30 minutes of MDP stimulation.

Figure 6.12 Optimum MDP stimulation times



EGFP-C1 or NOD2-GFP

1x10^6 cells stimulated with D0.2 + KCL 130mmol + MDP 10ug/ml for the specified times.

Figure 6.12 MAPK 44-42 WB

(a) NOD2-GFP and **(b)** both NOD2-GFP and EGFP-C1 HEK293 cell clones were stimulated in D0.2, with or without KCL 130mmol, for the shown times (min). Cells were lysed on ice before WB. MAPK activation was observed as early as 5min, with possible maximal phosphorylation at 10min.

6.8 Immunoprecipitation

HEK293 clones were left unstimulated or stimulated with MDP before lysis in 0.5% NP40 lysis buffer, containing protease and phosphatase inhibitors as usual. A Bradford assay was performed and the lysates adjusted to 5mg/ml. To avoid non-specific binding of proteins to the agarose of anti-GFP beads, a preclear step using unlabelled agarose beads was performed overnight.

Subsequently anti-GFP beads were used to extract GFP and associated proteins from the lysates. The beads were washed twice in 0.5% NP40 before adherent proteins were eluted using pH 2.5 glycine, and then boiling the beads in PBS. Protein retrieval and differences between the experimental conditions were assessed by silver stain **(Fig. 6.13)**. This demonstrates that the original IP conditions were not specific enough and retrieved far too many proteins, such that it was impossible to see the 'bait' proteins (i.e. NOD2-GFP or GFP alone), or any differences between conditions on the silver stain.

Figure 6.13 Original IP result: Silver Stain

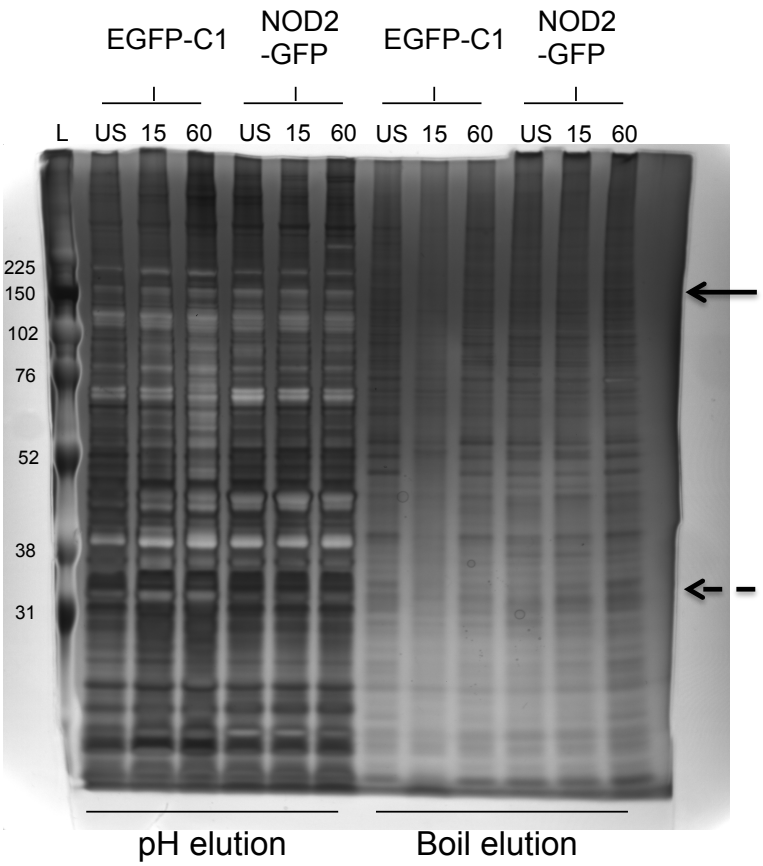


Figure 6.13 Immunoprecipitation Silver Stain
100x10^6 cells were left unstimulated (US) or MDP 10 µg/ml stimulated for 15 or 60 minutes. Cells were then harvested and lysed immediately with 0.5% NP40 lysis buffer. After centrifugation the supernatent was retrieved, a Bradford Protein assay performed, and the samples diluted to 5 mg/ml concentration. Pre-clear was with 100µl of protein A/G agarose beads (2003; Santa Cruz) to each sample and rolled at 4°C overnight. Subsequently 100 µl anti-GFP beads (9996; Santa Cruz) were added and rolled at 4°C. Proteins adherent to the GFP beads were eluted with pH 2.5 glycine, and then boiled in PBS. The black arrow marks the weight of GFP-NOD2 (145 kDa) and the broken arrow of GFP (30 kDA).

6.9 IP Optimisation

In order to optimise the IP I initially assessed the degree of protein loss in general, and specifically of NOD2-GFP, at each stage in the protocol **(Fig. 6.14)**. The silver stain demonstrates that the preclear beads were removing a considerable quantity of proteins that bind non-specifically to agarose, and little NOD2 was lost as demonstrated by the anti-GFP western blot for these samples. Moreover, washes one and two of the anti-GFP IP beads removed most of the weakly or non-specifically bound proteins, with no loss of NOD2. However, although the western blot demonstrated excellent recovery of NOD2-GFP, the silver stain of the IP elution was still not clear enough to demonstrate an obvious ‘bait’ band.

Figure 6.14 IP conditions: Protein loss assessment

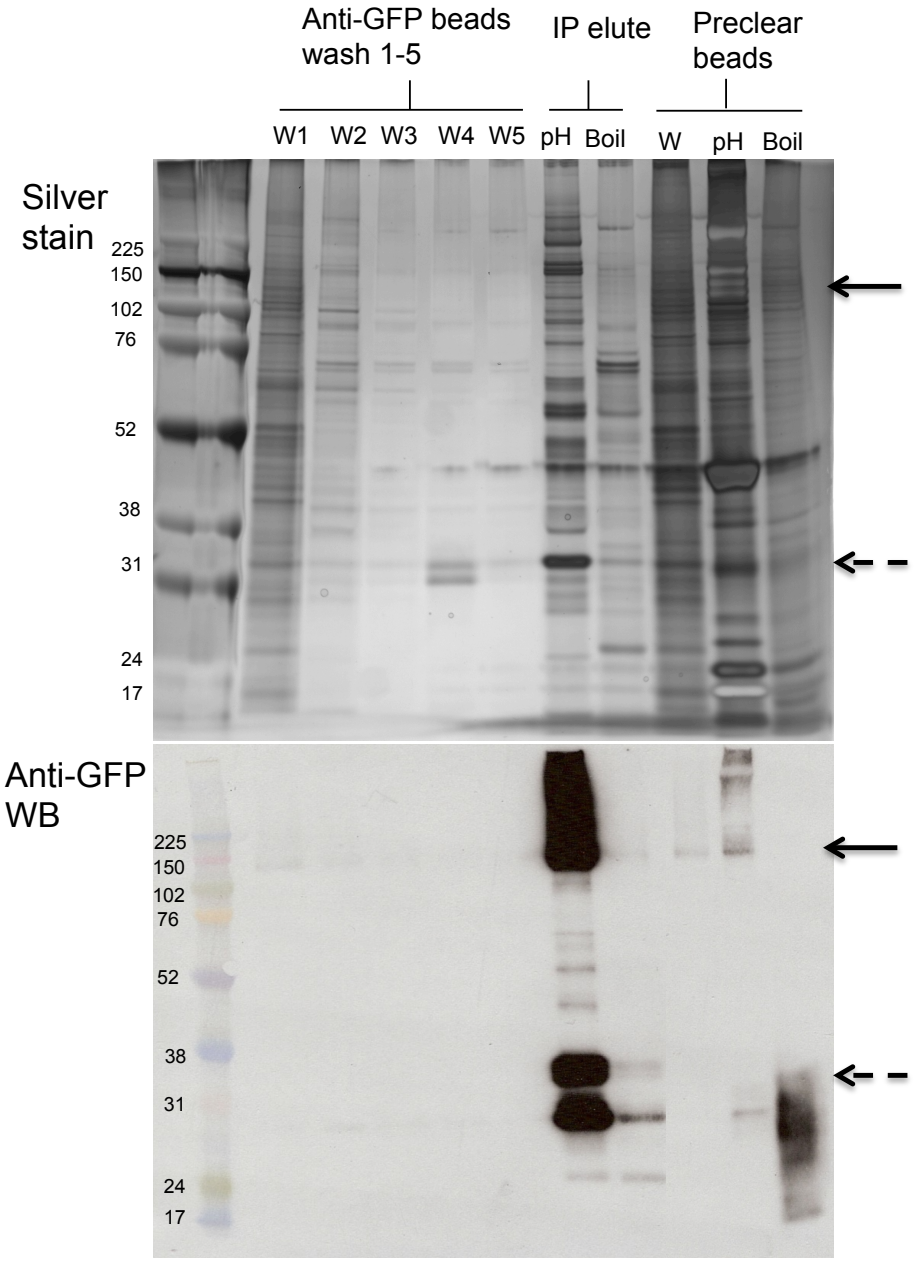


Figure 6.14 NOD2-GFP cells were lysed and rolled with the immunoprecipitation preclear and anti-GFP IP beads. At each step beads were washed (W), or proteins eluted with pH 2.5 glycine (pH) or boil eluted (boil).
Protein loss for each step was assessed using silver stain, and specific loss of NOD2 by anti-GFP western blot. The black arrow marks the weight of GFP-NOD2 (145 kDa) and the broken arrow of GFP (30 kDA).

It was clear from an analysis of the IP elution method that the majority of NOD2-GFP was retrieved by the pH elution step **(Fig. 6.15a and b),** and that this did not need to be altered. I determined to improve the stringency of the IP by altering the protein concentration and the preclear method. I changed the preclear beads to agarose that is dyed red (Ezview; Sigma) in order to improve bead retrieval without loss of lysate. I compared the IP result when using a lower concentration lysate (2.5mg/ml) and different numbers and timings of the preclear steps **(Fig. 6.16)**. The best result as per the silver stain occurred when using 2.5mg/ml lysate, one overnight preclear step, and a one-hour IP. However, once again the NOD2 'bait' band was not distinct enough when compared with the EGFP-C1 clone IP.

Figure 6.15 Determination of elution method

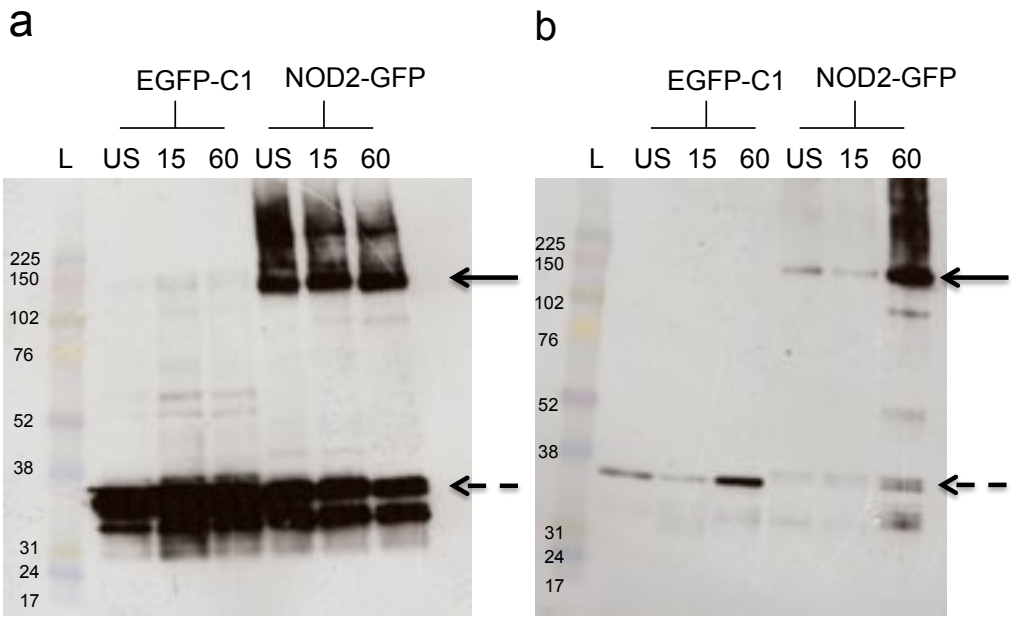


Figure 6.15 EGFP-C1 and NOD2-GFP cells were left unstimulated (US) or MDP stimulated (10 µg/ml) for 15 or 60 minutes. After preclear with agarose beads, IP was performed with anti-GFP beads.

Proteins were eluted with pH 2.5 glycine **(a)** or boiling in PBS **(b)**. Elution of NOD2-GFP was assessed by anti-GFP western blot. The black arrow marks the weight of GFP-NOD2 (145 kDa) and the broken arrow of GFP (30 kDA).

Figure 6.16 Preclear steps and lysate concentration

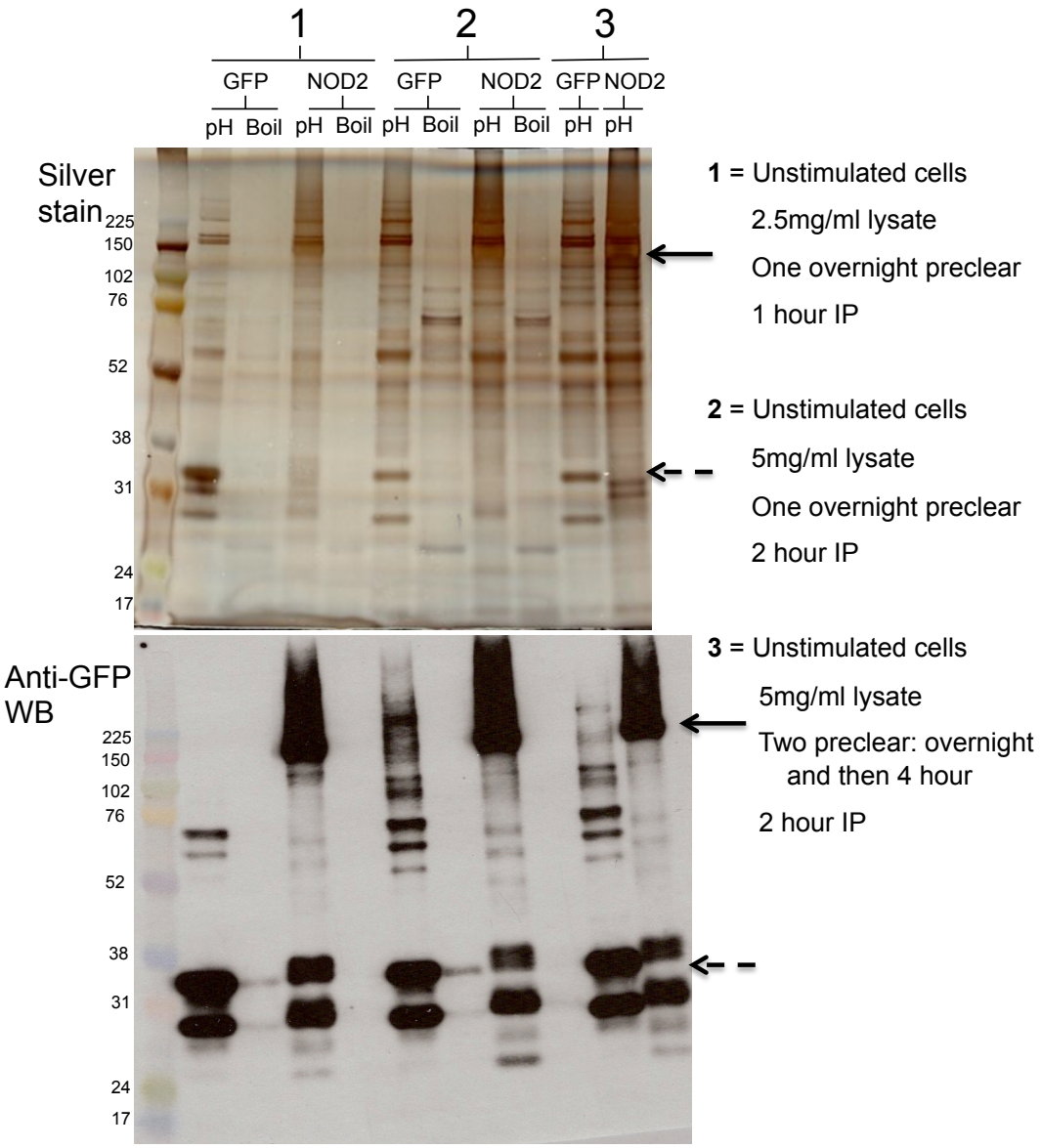


Figure 6.16 EGFP-C1 (GFP) or NOD2-GFP (NOD2) cells were left unstimulated, and then lysed as before. Bradford assay was used to adjust the lysates to 2.5 mg/ml or 5 mg/ml. The timing of the preclear step (using Ezview agarose; Sigma) and anti-GFP IP step were altered as shown, and the effect assessed by silver stain and western blot. The black arrow marks the weight of GFP-NOD2 (145 kDa) and the broken arrow of GFP (30 kDA).

I therefore changed the anti-GFP IP beads I was using, which use a conventional antibody with heavy and light chains, to GFP-Trap-A beads (Chromotek). These beads express an antibody that is derived from a llama single chain antibody (members of the Camelidae family express single domain heavy chain antibodies). This results in a small (13 kDa) but specific GFP-binding fragment[484]. The improved GFP-retrieval was immediately obvious as the agarose beads turned bright green after the IP step. The resultant silver stain demonstrated obvious bait proteins, and indeed differences between stimulated and unstimulated NOD2-GFP cells **(Fig. 6.17)**.

Figure 6.17 Optimised IP as assessed by silver stain

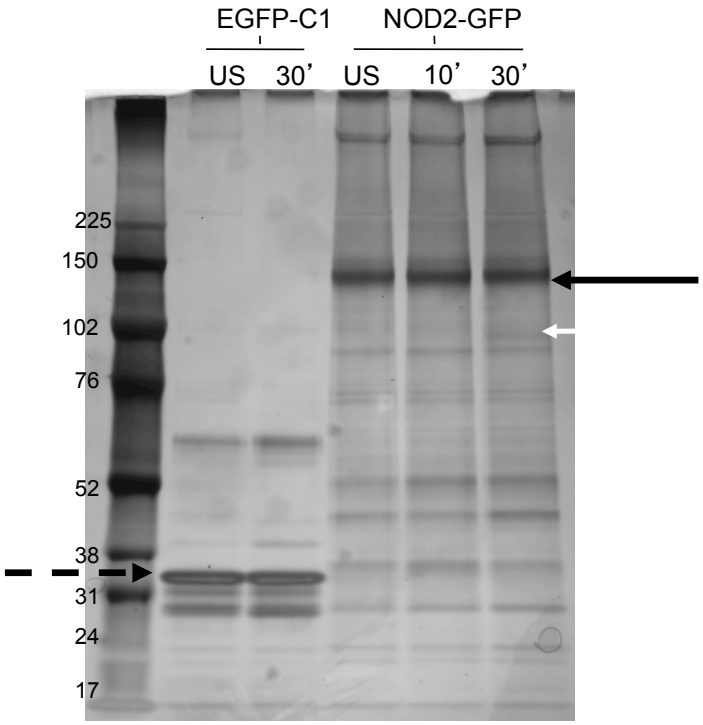


Figure 6.17 Silver Stain

EGFP-C1 and NOD2-GFP HEK293 cells were left unstimulated or stimulated in the normal way. After lysis in 0.5% NP40, the lysates were adjusted to 2.5 mg/ml. Overnight preclear at 4°C with agarose beads was followed by IP with 50 μl GFP-Trap-A beads (Chromotek) at 4°C for 1hr. The beads were washed 3x with 0.5% NP40 plus protease and phosphatase inhibitors, before elution of associated proteins using 200 μl 100 mM glycine pH 2.5.

GFP-NOD2 and GFP are clearly visible (black arrow and dashed arrow respectively). These bands were cut out, digested and analysed by MS, and confirmed presence of GFP-NOD2 and GFP. There are also visible differences between the stimulated and unstimulated conditions (white arrow).

6.10 Mass Spectrometry Analysis

I prepared the IP samples for mass spectrometry analysis as per the protocols established by Benedikt Kessler's laboratory (NDM, Oxford). These samples were run on an Agilent Q-TOF (quadrupole time-of-flight) mass spectrometer by a Kessler group member (Nicola Ternette), and the results are shown in **Table 6.2**.

Table 6.2 Mass Spectrometry results

Protein	Score	% AA coverage	EGFP-C1 US	EGFP-C1 Stim	NOD2-GFP US	NOD2-GFP Stim
NOD2	888.52	65			✓	✓
Tubulin β	322.13	60			✓	✓
Myosin 9	301.1	12			✓	✓
Raichu404X	249.87	14	✓	✓	✓	✓
Keratin 10	168.97	24	✓	✓	✓	✓
Actin γ1	168.16	42	✓	✓	✓	✓
Keratin 1	145.44	13	✓	✓	✓	✓
Ribosomal protein RPS18P5	37.2	19			✓	✓
Heat shock 70kDa	35.61	5			✓	✓
MIF	27.96	26	✓	✓	✓	✓
Erbin	13.33	6			✓	✓

Table 6.2 Mass Spectrometry results
IP samples were digested with trypsin and purified before Mass Spectrometry analysis. Proteins identified with the most significant peptide hits are represented in the table. The score in the table is the 'Distinct Summed MS/MS Search Score' (Agilent Spectrum Mill MS Proteomics Workbench), with the percentage amino acid coverage of the protein also shown.

6.11 Discussion

There is no doubt that immunoprecipitation of tagged proteins can yield substantial data of interest, as was neatly shown in a study of Flag-tagged AIRE (autoimmune regulator) in HEK293 cells[485]. Despite the careful steps

taken to set up my model system, unfortunately positive results are thin on the ground.

Although in my MS data there was robust identification of NOD2 peptides, indicating that the IP had worked well in the sense of NOD2 recovery, the other results were for the most part disappointing. The data are presented with accompanying Distinct Summed MS/MS Search Scores (which relates to the number of peptides identified from a particular protein to give a total score) and percentage protein amino acid coverage. Although the search score threshold set varies depending on the study, as a guide a figure of around 30 is often used as the threshold for further protein validation experiments[486]. Many of the most abundant peptides identified were from proteins involved in cell structure and polarity such as actin, myosin and tubulin, presumably in part due to their cytosolic abundance. NOD2 may be sequestered into actin cytoskeleton structures such as membrane ruffles and lamellipodia in association with Rac1 (a small RhoGTPase)[487], and changes in the actin cytoskeleton lead to NOD2-driven NFκB activation. However actin was found in all of my IP samples, not just in association with NOD2. Other hits include: keratin (contamination from dust entering the samples); the ribosomal protein hit, RPS18P5, a pseudogene of unknown function; and Raichu404X, a withdrawn gene sequence on the NCBI database, with the protein having unknown function.

The most encouraging result is the weak hit for Erbin (Erbb2IP) which has already been identified as a NOD2-binding partner[169,488]. Erbin has been shown to play roles in cytoskeleton organisation, cell polarity, receptor localisation[489], and the regulation of MAPK signalling[490]. Of all the NOD2-

interacting proteins, Erbin has some of the best evidence for a direct NOD2 interaction, with those studies already cited backed up by a recent study in paediatric mucosal biopsies[491] in which NOD2 and Erbin were co-precipitated from Crohn's biopsy lysates. Perhaps it is not surprising therefore that this was identified in my IP, although it is interesting that it appears in both stimulated and unstimulated samples.

HSP70 (heat shock protein 70kDa) is another weak hit, and changes in heat shock proteins have been previously identified in whole cell lysates of HEK293 cells transfected with NOD2 and FS1007insC NOD2[480]. Heat shock proteins (HSPs) are molecular chaperones that assist in ensuring protein quality through diverse processes such as protein folding, transport and degradation[492]. This interaction probably reflects that some of the over-expressed NOD2 is misfolded and being chaperoned for degradation, although some evidence for a protective effect of HSPs in inflammatory bowel disease and gastric ulceration exists[493]. Moreover, another heat shock protein, HSP90, interacts with NOD2 (and many other NLRs) along with SGT1 (suppressor of G2 allele of SKP1) a ubiquitin ligase-associated protein[494]. Their role with mammalian NLRs is homologous to that demonstrated with plant R protein function, in that they appear to be essential for inflammasome activation and IL-1β processing, and blocking HSP90 also reduces NOD2-driven NFκB activation and β-defensin production from keratinocytes[494]. It may be that the apparent NOD2 association with HSP70 therefore warrants further investigation, although again the function is questionable given that it is in both unstimulated and stimulated NOD2 samples.

Lastly, although MIF (macrophage migration inhibitory factor) would have been an interesting finding, the fact that it is present in both NOD2-GFP and EGFP-C1 samples implies that this is present through non-specific binding to GFP or agarose.

It is difficult to know why my IP failed to identify more interacting proteins, but the most likely explanation is that the interactions between NOD2 and other proteins were too weak to survive the protocol used. Further optimisation would include altering the stringency of the lysis buffer and the nature of the detergent, and reducing the timing of both the preclear and/ or of the IP steps.

In summary, this chapter presents the initiation and optimisation of a model method for detecting NOD2-interacting proteins.

7 General Discussion

7.1 Introduction

In this work I have investigated the innate immune receptor NOD2 in two ways. Firstly I have described the microRNAs that are expressed in human DCs after NOD2 stimulation, both in isolation and in conjunction with other PRRs. Secondly I have attempted to examine, and identify novel contributors to, the NOD2 signalosome.

7.2 IP Project

I can not be certain why this experiment failed to detect novel, or indeed more described, NOD2-interacting proteins, although it could be for a number of reasons. One of the most likely is that the partners were lost as either the interactions are weak, or the lysis buffer was too stringent. Another is that the NOD2 signalosome only forms momentarily after stimulation, prevented from chronic activation by counter-regulatory mechanisms, and that therefore an earlier stimulation time-point would have been more successful. In the past the lab have had success western blotting NOD2 in primary cells using lysis buffers that disrupt autophagosomal material (Triton X 114). It is possible that enriching for NOD2 in the autophagosomal fraction prior to IP of NOD2 might facilitate capture and detection of NOD2-interacting proteins by mass spectrometry. Further optimisation using my clones and experimental set-up as a basis, may yield more promising results.

7.3 miRNA Project

7.3.1 miRNA expression in human DCs

I have shown that NOD2 is involved in the expression of both miR-155, a microRNA with well-described immune functions, and for the miRNA-29 family. Other microRNA expression, for example miR-9[320] and miR-147[324], has been described in monocytes and macrophages through TLR2 triggering. These were not detected by my array of miRNA expression in MDDCs, and this may either be related to differences in DC function, or because these miRNAs were 'missed' by the array.

There is clearly synergy for miR-155 expression when NOD2 and TLR2 are co-stimulated. However, as the up-regulation of miR-155 is significantly greater when stimulating with the TLR4 ligand LPS than for other PRR ligands, and co-stimulating with MDP makes little impact on this, it appears that the role of NOD2 is probably redundant in a biological setting.

I therefore investigated the miR-29 family (29a, b, c) in more depth, and found that stimulation of NOD2 with MDP is critical for their up-regulation. This signal requires RIPK-2 expression but not MyD88, as demonstrated by the use of siRNAs. It is also lost in the presence of NOD2 CD-associated polymorphisms. These latter cells were derived from patients with terminal ileal Crohn's who are homozygous, or compound heterozygous, for the three most common LRR domain mutations. Although intact NOD2 function is required for miR-29 expression, interestingly only when stimulation is combined with TLR2 or TLR5 ligands is the up-regulation greater than a 2-fold change.

It is interesting to speculate why this may be, although how this is interpreted in part depends on how one views the role of NOD2 in the context of complex

immune responses. Certainly the relationship between NOD2 and TLR2, as already described, has been well studied and is for the most part considered to be complementary, if not frankly synergistic[193]. As both these PRRs respond to motifs derived from bacterial cell wall peptidoglycan, this is perhaps not surprising as it is likely that they would be co-triggered by most bacterial: DC interactions. Since this is the case, co-triggering with the resultant increases in pro-inflammatory cytokine production would need more robust anti-inflammatory mechanisms.

Although not all bacteria are flagellated, flagellin is present on most motile gut bacteria[495,496] and is therefore a critical PAMP in commensal: immune system 'dialogue' both via the intestinal epithelium[497] and directly with monocytes[498]. Flagellin has been suggested to be an immunodominant antigen in human CD, but not in UC[499], and a dominant negative TLR5 polymorphism (TLR5-stop) reduces circulating anti-flagellin antibodies, and reduces CD predisposition in a Jewish cohort[500]. In murine colitis models not only are similar anti-flagellin antibodies also present, but adoptive transfer of flagellin-specific $CD4^+$ T cells to severe combined immunodeficiency (SCID) mice induces a severe colitis[499].

NOD2: TLR5 interactions have not been studied in any depth. Although some studies have demonstrated no obvious synergy between NOD2 and TLR5 (in this case for TNFα[193]), the potentially cooperative, non-redundant, nature of their relationship was highlighted by a human case study examining the control of a GI infection[501]. *Yersinia enterocolitica*, a flagellated Gram-negative bacterium, normally causes a self-limiting ileitis, and this can be clinically difficult to distinguish from Crohn's disease. In a subset of cases the infection

becomes chronic, and this article describes one such case possibly related to the combined presence of homozygous FS1007insC NOD2, and compound heterozygous TLR5, loss-of-function mutations.

In intestinal epithelial cells stimulation with flagellin through TLR5, and to a lesser extent TLR2 with lipoteichoic acid (LTA), more powerfully up-regulates NOD2 expression than TLR4 ligand LPS[502], suggesting an important effector response loop. Moreover TLR5 is basolateral[497], and is therefore likely triggered in the context of disrupted epithelial integrity[503], or via bacteria attaining inappropriate epithelial locations in CD[504]. Since NOD2 is intracellular one could argue that in this context both these PRRs are physically located to be signallers of invasive infection. In this instance not only would the immune response have to be particularly robust, but once again the counter-regulatory mechanisms turning off the inflammation would also need to be exaggerated. miR-29 may play this role in GIT epithelial cells but this has yet to be determined.

By way of contrast, the response of intestinal epithelial cells to the gram-negative bacterial ligand LPS is quickly tolerised after birth in part via IRAK1 down-regulation, and intestinal macrophages are constitutively non-responsive[505], presumably to ensure that inappropriate inflammation does not occur as the gut is colonized. It may be that in the context of the gut, as opposed to in untolerised in vitro experiments, that LPS stimulation is constitutively dampened in both the intestinal and myelomonocytic compartments to a greater degree than for example TLR5 and NOD2 signalling pathways. This may in part explain why the apparently counter-

regulatory induction of miR-29 is predominantly via NOD2 and TLR2/ 5 co-stimulation.

One of the areas I have not investigated is the expression of miR-29 via other PRRs, for example NLRs. It would be interesting to know in particular whether there is any synergy between NOD2 and NLRP3, given the recent finding that co-stimulation leads to synergistic expression of both IL-12p40 and IL-23p19[233].

7.3.2 miR-29 targets

The miR-29 targets that I have identified in DCs, and their functional significance, together provide an interesting insight into how the NOD2-driven innate immune response is governed. Targeting MCL-1 appears to promote bacterial clearance from DCs, most probably by facilitating autophagy induction, and this may be a significant finding regarding the mechanism of NOD2-mediated autophagy. Targeting MCL-1 would help ensure an effective immune response, whilst the other targets together would ensure that inflammation is appropriately curtailed.

The finding that NOD2 promotes a direct mechanism for control of IL-23 is fascinating given the recently described associations between the Th17 pathway and CD. Co-targeting of IL-23 and CDC42 is particularly interesting in the context of the DC: T cell immune synapse, since the effector arm of IBD inflammation is generally acknowledged to be via activated $CD4^+$ Th17 T cells. Control of CX3CL1 should also reduce inflammatory cell recruitment, but also (speculatively) has the prospect of altering the DC: microbiome interactions by reducing transepithelial dendrite sampling.

Other possible miR-29 targets include TRAF4 and IL-1RAP identified by western blot and discussed in chapter 2, and a whole host of targeted and off-target effects on (mostly pro-inflammatory) mediators identified by DNA array and qPCR. Two of the most strongly affected are the bradykinin receptor B2 (BDKRB2), which contains two 7mer 3'UTR seed sequence targets (Targetscan), and the likely indirectly targeted CCL8. Bradykinin is a mediator of, amongst other effects, inflammation and pain, and is recognised by receptors 1 and 2. BDKRB2 is expressed in both normal and inflamed IBD epithelium, although expression is apparently constitutive and can be rapidly desensitised, whereas receptor 1 is inducible by pro-inflammatory cytokines and is increased in IBD[506]. The possible role of miR-29 in this context is therefore uncertain, although inhibitors of kallikrein (which releases bradykinin from plasma kininogen or tissue kallidin) can attenuate acute intestinal inflammation induced by peptidoglycan in Lewis rats[507], and chronic granulomatous inflammation in the same rat model[508]. CCL8 is chemotactic for inflammatory cells such as monocytes and lymphocytes, and is known to be up-regulated in inflamed IBD mucosa, particularly from infiltrating mononuclear cells[509].

Another interesting way of looking at the targets/ effects as a whole is via the number of CD-susceptibility genes that are affected by miR-29. These potentially not only include IL-12p40, but also IL-19, IL2RA, CARD9, and to a lesser extent TNFSF15 and DNMT3A by qPCR. Although only IL-12p40 and IL-19 are definitively demonstrated at the level of protein expression in DCs (and DNMT3A by another study[380]), this raises the possibility that despite CD clearly having a complex polygenic mode of inheritance, that many of these

polymorphisms affect immune pathways that are linked. This is similar to the recent finding that NOD2 and autophagy are part of the same xenophagy effector pathway[157,244].

Looking further afield at confirmed miR-29 targets in other cell types, some of the most interesting are those that relate to control of the extra-cellular matrix. As already described, miR-29 is known to be associated with fibrosis via control of collagen expression[345,348]. NOD2 polymorphisms in Crohn's are associated with a sub-phenotype of the disease - stricturing disease[128] where fibrosis occurs in the small bowel causing obstructive symptoms and requiring surgical intervention. It is possible that the inability of Crohn's NOD2 to induce miR-29 may contribute to this phenotype. This could be either directly through the failure of miR-29 induction in ileal fibroblasts, or indirectly through failure of miR-29 exosomal release from DCs. Exosomes are membrane vesicles released by various cell types, including DCs, and are a way of communicating signals in an autocrine and paracrine manner, and indeed are found in the circulation. miRNAs have been shown to be contained within exosomes[510], indeed miR-29 specifically in salivary exosomes[511], and so intestinal DC release of miR-29 could control collagen production from fibroblasts.

7.4 Further Work

Although my data suggest a role for NOD2 and miR-29 in the control of IL-23-driven immune responses, and in other aspects of NOD2 function, it is unclear whether this holds true in the setting of gastrointestinal immune responses.

Further work should include an attempt to demonstrate the effect of miR-29 in mouse models of colitis.

A number of obstacles present themselves to this approach. The first is that the control of miR-29 by NOD2, and indeed of IL-23 by miR-29, may be different in a murine setting. The second is the difficulty in producing a miR-29 knock-out model as there are four miR-29 family members spread across two chromosomes. A third is the mode of miRNA delivery – be that via retroviral transduction of miR-29 into DCs, or via some form of liposomal delivery[512]. Nevertheless this is the most important next experiment in order to determine the relative importance of miR-29 in the context of the complex GI environment.

As already discussed some of the demonstrated miR-29 targets would also be interesting to study further. In DCs this includes confirming the role of MCL-1 in autophagy induction, and demonstrating the effect CDC42 levels have on DC maturation and immune synapses. In GI epithelial cells, including fibroblasts and Paneth cells, this includes examining the expression of miR-29 after NOD2 stimulation, and any potential effects on ECM matrix formation, and defensin production via Wnt signalling, respectively.

Lastly, it may be that NOD2 is involved in the expression of other miRNAs both in DCs and other cell types. In DCs co-triggering with other PRRs, such as the NLRs or CLRs, may produce different results, and in the epithelial cell compartment NOD2 may induce an entirely different miRNA repertoire. Much of miRNA expression and function appears to be cell specific, so on going investigation in relation to NOD2 and other CD-polymorphisms is likely to yield further insights into CD pathogenesis.

Bibliography

1. Hooper, L.V. & Gordon, J.I. Commensal host-bacterial relationships in the gut. *Science* **292**, 1115-1118 (2001).
2. Whitman, W.B., Coleman, D.C. & Wiebe, W.J. Prokaryotes: the unseen majority. *Proc Natl Acad Sci U S A* **95**, 6578-6583 (1998).
3. Ley, R.E.*, et al.* Evolution of mammals and their gut microbes. *Science* **320**, 1647-1651 (2008).
4. Klein, J. Self-nonself discrimination, histoincompatibility, and the concept of immunology. *Immunogenetics* **50**, 116-123 (1999).
5. Sands, B.E.*, et al.* Risk of early surgery for Crohn's disease: implications for early treatment strategies. *Am J Gastroenterol* **98**, 2712-2718 (2003).
6. Mayberry, J.F.*, et al.* Crohn's disease in Jewish people--an epidemiological study in south-east Wales. *Digestion* **35**, 237-240 (1986).
7. Crohn, G. Regional ileitis: a pathologic and clinical entity. *JAMA* **99**, 1323-1329 (1932).
8. Halme, L.*, et al.* Family and twin studies in inflammatory bowel disease. *World J Gastroenterol* **12**, 3668-3672 (2006).
9. Monsen, U., Bernell, O., Johansson, C. & Hellers, G. Prevalence of inflammatory bowel disease among relatives of patients with Crohn's disease. *Scand J Gastroenterol* **26**, 302-306 (1991).
10. Hugot, J.P.*, et al.* Association of NOD2 leucine-rich repeat variants with susceptibility to Crohn's disease. *Nature* **411**, 599-603 (2001).
11. Franke, A.*, et al.* Genome-wide meta-analysis increases to 71 the number of confirmed Crohn's disease susceptibility loci. *Nature genetics* **42**, 1118-1125 (2010).
12. Lees, C.W., Barrett, J.C., Parkes, M. & Satsangi, J. New IBD genetics: common pathways with other diseases. *Gut* **60**, 1739-1753 (2011).
13. Massey, D.C. & Parkes, M. Genome-wide association scanning highlights two autophagy genes, ATG16L1 and IRGM, as being significantly associated with Crohn's disease. *Autophagy* **3**, 649-651 (2007).
14. Deretic, V. Autophagy in infection. *Curr Opin Cell Biol* **22**, 252-262.
15. Deretic, V. & Levine, B. Autophagy, immunity, and microbial adaptations. *Cell Host Microbe* **5**, 527-549 (2009).
16. McLeod, I.X. & He, Y. Roles of autophagy in lymphocytes: reflections and directions. *Cell Mol Immunol* **7**, 104-107 (2010).
17. Kuma, A., Mizushima, N., Ishihara, N. & Ohsumi, Y. Formation of the approximately 350-kDa Apg12-Apg5.Apg16 multimeric complex, mediated by Apg16 oligomerization, is essential for autophagy in yeast. *J Biol Chem* **277**, 18619-18625 (2002).
18. Fujita, N.*, et al.* The Atg16L complex specifies the site of LC3 lipidation for membrane biogenesis in autophagy. *Mol Biol Cell* **19**, 2092-2100 (2008).
19. Genome-wide association study of 14,000 cases of seven common diseases and 3,000 shared controls. *Nature* **447**, 661-678 (2007).

20. Rioux, J.D.*, et al.* Genome-wide association study identifies new susceptibility loci for Crohn disease and implicates autophagy in disease pathogenesis. *Nat Genet* **39**, 596-604 (2007).
21. Glas, J.*, et al.* The ATG16L1 gene variants rs2241879 and rs2241880 (T300A) are strongly associated with susceptibility to Crohn's disease in the German population. *Am J Gastroenterol* **103**, 682-691 (2008).
22. Latiano, A.*, et al.* Replication of interleukin 23 receptor and autophagy-related 16-like 1 association in adult- and pediatric-onset inflammatory bowel disease in Italy. *World J Gastroenterol* **14**, 4643-4651 (2008).
23. Prescott, N.J.*, et al.* A nonsynonymous SNP in ATG16L1 predisposes to ileal Crohn's disease and is independent of CARD15 and IBD5. *Gastroenterology* **132**, 1665-1671 (2007).
24. Van Limbergen, J.*, et al.* Autophagy gene ATG16L1 influences susceptibility and disease location but not childhood-onset in Crohn's disease in Northern Europe. *Inflamm Bowel Dis* **14**, 338-346 (2008).
25. Kuballa, P., Huett, A., Rioux, J.D., Daly, M.J. & Xavier, R.J. Impaired autophagy of an intracellular pathogen induced by a Crohn's disease associated ATG16L1 variant. *PLoS One* **3**, e3391 (2008).
26. Saitoh, T.*, et al.* Loss of the autophagy protein Atg16L1 enhances endotoxin-induced IL-1beta production. *Nature* **456**, 264-268 (2008).
27. Lapaquette, P., Glasser, A.L., Huett, A., Xavier, R.J. & Darfeuille-Michaud, A. Crohn's disease-associated adherent-invasive E. coli are selectively favoured by impaired autophagy to replicate intracellularly. *Cell Microbiol* **12**, 99-113.
28. Bekpen, C.*, et al.* The interferon-inducible p47 (IRG) GTPases in vertebrates: loss of the cell autonomous resistance mechanism in the human lineage. *Genome Biol* **6**, R92 (2005).
29. Parkes, M.*, et al.* Sequence variants in the autophagy gene IRGM and multiple other replicating loci contribute to Crohn's disease susceptibility. *Nat Genet* **39**, 830-832 (2007).
30. Fisher, S.A.*, et al.* Genetic determinants of ulcerative colitis include the ECM1 locus and five loci implicated in Crohn's disease. *Nat Genet* **40**, 710-712 (2008).
31. Franke, A.*, et al.* Replication of signals from recent studies of Crohn's disease identifies previously unknown disease loci for ulcerative colitis. *Nat Genet* **40**, 713-715 (2008).
32. Roberts, R.L.*, et al.* Confirmation of association of IRGM and NCF4 with ileal Crohn's disease in a population-based cohort. *Genes Immun* (2008).
33. Weersma, R.K.*, et al.* Confirmation of multiple Crohn's disease susceptibility loci in a large Dutch-Belgian cohort. *Am J Gastroenterol* **104**, 630-638 (2009).
34. Palomino-Morales, R.J.*, et al.* Association of ATG16L1 and IRGM genes polymorphisms with inflammatory bowel disease: a meta-analysis approach. *Genes Immun* **10**, 356-364 (2009).
35. Singh, S.B., Davis, A.S., Taylor, G.A. & Deretic, V. Human IRGM induces autophagy to eliminate intracellular mycobacteria. *Science* **313**, 1438-1441 (2006).

36. MacMicking, J.D., Taylor, G.A. & McKinney, J.D. Immune control of tuberculosis by IFN-gamma-inducible LRG-47. *Science* **302**, 654-659 (2003).
37. Collazo, C.M.*, et al.* Inactivation of LRG-47 and IRG-47 reveals a family of interferon gamma-inducible genes with essential, pathogen-specific roles in resistance to infection. *J Exp Med* **194**, 181-188 (2001).
38. Henry, S.C.*, et al.* Impaired macrophage function underscores susceptibility to Salmonella in mice lacking Irgm1 (LRG-47). *J Immunol* **179**, 6963-6972 (2007).
39. McCarroll, S.A.*, et al.* Deletion polymorphism upstream of IRGM associated with altered IRGM expression and Crohn's disease. *Nat Genet* (2008).
40. Prescott, N.J.*, et al.* Independent and population-specific association of risk variants at the IRGM locus with Crohn's disease. *Hum Mol Genet* **19**, 1828-1839.
41. Intemann, C.D.*, et al.* Autophagy gene variant IRGM -261T contributes to protection from tuberculosis caused by Mycobacterium tuberculosis but not by M. africanum strains. *PLoS Pathog* **5**, e1000577 (2009).
42. Brest, P.*, et al.* A synonymous variant in IRGM alters a binding site for miR-196 and causes deregulation of IRGM-dependent xenophagy in Crohn's disease. *Nature genetics* **43**, 242-245 (2011).
43. Singh, S.B.*, et al.* Human IRGM regulates autophagy and cell-autonomous immunity functions through mitochondria. *Nat Cell Biol* **12**, 1154-1165.
44. Neurath, M.F., Fuss, I., Kelsall, B.L., Stuber, E. & Strober, W. Antibodies to interleukin 12 abrogate established experimental colitis in mice. *The Journal of Experimental Medicine* **182**, 1281-1290 (1995).
45. Oppmann, B.*, et al.* Novel p19 protein engages IL-12p40 to form a cytokine, IL-23, with biological activities similar as well as distinct from IL-12. *Immunity* **13**, 715-725 (2000).
46. Yen, D.*, et al.* IL-23 is essential for T cell-mediated colitis and promotes inflammation via IL-17 and IL-6. *The Journal of clinical investigation* **116**, 1310-1316 (2006).
47. Uhlig, H.H.*, et al.* Differential activity of IL-12 and IL-23 in mucosal and systemic innate immune pathology. *Immunity* **25**, 309-318 (2006).
48. Hue, S.*, et al.* Interleukin-23 drives innate and T cell-mediated intestinal inflammation. *The Journal of Experimental Medicine* **203**, 2473-2483 (2006).
49. Kullberg, M.C.*, et al.* IL-23 plays a key role in Helicobacter hepaticus-induced T cell-dependent colitis. *The Journal of Experimental Medicine* **203**, 2485-2494 (2006).
50. Elson, C.O.*, et al.* Monoclonal anti-interleukin 23 reverses active colitis in a T cell-mediated model in mice. *Gastroenterology* **132**, 2359-2370 (2007).
51. Duerr, R.H.*, et al.* A genome-wide association study identifies IL23R as an inflammatory bowel disease gene. *Science* **314**, 1461-1463 (2006).
52. Kan, S.H., Mancini, G. & Gallagher, G. Identification and characterization of multiple splice forms of the human interleukin-23

receptor alpha chain in mitogen-activated leukocytes. *Genes and immunity* **9**, 631-639 (2008).
53. Aggarwal, S., Ghilardi, N., Xie, M.H., de Sauvage, F.J. & Gurney, A.L. Interleukin-23 promotes a distinct CD4 T cell activation state characterized by the production of interleukin-17. *The Journal of biological chemistry* **278**, 1910-1914 (2003).
54. Cua, D.J.*, et al.* Interleukin-23 rather than interleukin-12 is the critical cytokine for autoimmune inflammation of the brain. *Nature* **421**, 744-748 (2003).
55. Wilson, N.J.*, et al.* Development, cytokine profile and function of human interleukin 17-producing helper T cells. *Nature immunology* **8**, 950-957 (2007).
56. Weaver, C.T., Hatton, R.D., Mangan, P.R. & Harrington, L.E. IL-17 family cytokines and the expanding diversity of effector T cell lineages. *Annu Rev Immunol* **25**, 821-852 (2007).
57. Ahern, P.P.*, et al.* Interleukin-23 drives intestinal inflammation through direct activity on T cells. *Immunity* **33**, 279-288 (2010).
58. Liu, Z.*, et al.* The increased expression of IL-23 in inflammatory bowel disease promotes intraepithelial and lamina propria lymphocyte inflammatory responses and cytotoxicity. *J Leukoc Biol* **89**, 597-606 (2011).
59. Kleinschek, M.A.*, et al.* Circulating and gut-resident human Th17 cells express CD161 and promote intestinal inflammation. *The Journal of Experimental Medicine* **206**, 525-534 (2009).
60. Fujino, S.*, et al.* Increased expression of interleukin 17 in inflammatory bowel disease. *Gut* **52**, 65-70 (2003).
61. Iwakoshi, N.N., Pypaert, M. & Glimcher, L.H. The transcription factor XBP-1 is essential for the development and survival of dendritic cells. *The Journal of Experimental Medicine* **204**, 2267-2275 (2007).
62. Martinon, F., Chen, X., Lee, A.H. & Glimcher, L.H. TLR activation of the transcription factor XBP1 regulates innate immune responses in macrophages. *Nature immunology* **11**, 411-418 (2010).
63. Kaser, A.*, et al.* XBP1 links ER stress to intestinal inflammation and confers genetic risk for human inflammatory bowel disease. *Cell* **134**, 743-756 (2008).
64. Barrett, J.C.*, et al.* Genome-wide association defines more than 30 distinct susceptibility loci for Crohn's disease. *Nature genetics* **40**, 955-962 (2008).
65. Cantero-Recasens, G., Fandos, C., Rubio-Moscardo, F., Valverde, M.A. & Vicente, R. The asthma-associated ORMDL3 gene product regulates endoplasmic reticulum-mediated calcium signaling and cellular stress. *Human molecular genetics* **19**, 111-121 (2010).
66. Bertolotti, A.*, et al.* Increased sensitivity to dextran sodium sulfate colitis in IRE1beta-deficient mice. *The Journal of clinical investigation* **107**, 585-593 (2001).
67. Bengmark, S. Ecological control of the gastrointestinal tract. The role of probiotic flora. *Gut* **42**, 2-7 (1998).
68. Swidsinski, A.*, et al.* Mucosal flora in inflammatory bowel disease. *Gastroenterology* **122**, 44-54 (2002).

69. Darfeuille-Michaud, A.*, et al.* High prevalence of adherent-invasive Escherichia coli associated with ileal mucosa in Crohn's disease. *Gastroenterology* **127**, 412-421 (2004).
70. Lu, P.*, et al.* Colonic gene expression patterns of mucin muc2 knockout mice reveal various phases in colitis development. *Inflammatory bowel diseases* (2011).
71. Lees, C.W., Barrett, J.C., Parkes, M. & Satsangi, J. New IBD genetics: common pathways with other diseases. *Gut* (2011).
72. McAuley, J.L.*, et al.* MUC1 cell surface mucin is a critical element of the mucosal barrier to infection. *The Journal of clinical investigation* **117**, 2313-2324 (2007).
73. Cheng, H. & Leblond, C.P. Origin, differentiation and renewal of the four main epithelial cell types in the mouse small intestine. V. Unitarian Theory of the origin of the four epithelial cell types. *Am J Anat* **141**, 537-561 (1974).
74. Beau, I., Cotte-Laffitte, J., Amsellem, R. & Servin, A.L. A protein kinase A-dependent mechanism by which rotavirus affects the distribution and mRNA level of the functional tight junction-associated protein, occludin, in human differentiated intestinal Caco-2 cells. *Journal of virology* **81**, 8579-8586 (2007).
75. Berkes, J., Viswanathan, V.K., Savkovic, S.D. & Hecht, G. Intestinal epithelial responses to enteric pathogens: effects on the tight junction barrier, ion transport, and inflammation. *Gut* **52**, 439-451 (2003).
76. Marin, M.L., Greenstein, A.J., Geller, S.A., Gordon, R.E. & Aufses, A.H., Jr. A freeze fracture study of Crohn's disease of the terminal ileum: changes in epithelial tight junction organization. *The American journal of gastroenterology* **78**, 537-547 (1983).
77. Reuter, B.K. & Pizarro, T.T. Mechanisms of tight junction dysregulation in the SAMP1/YitFc model of Crohn's disease-like ileitis. *Ann N Y Acad Sci* **1165**, 301-307 (2009).
78. Kagan, B.L., Selsted, M.E., Ganz, T. & Lehrer, R.I. Antimicrobial defensin peptides form voltage-dependent ion-permeable channels in planar lipid bilayer membranes. *Proceedings of the National Academy of Sciences of the United States of America* **87**, 210-214 (1990).
79. Fellermann, K.*, et al.* A chromosome 8 gene-cluster polymorphism with low human beta-defensin 2 gene copy number predisposes to Crohn disease of the colon. *American journal of human genetics* **79**, 439-448 (2006).
80. Bentley, R.W.*, et al.* Association of higher DEFB4 genomic copy number with Crohn's disease. *The American journal of gastroenterology* **105**, 354-359 (2010).
81. Bevins, C.L., Stange, E.F. & Wehkamp, J. Decreased Paneth cell defensin expression in ileal Crohn's disease is independent of inflammation, but linked to the NOD2 1007fs genotype. *Gut* **58**, 882-883; discussion 883-884 (2009).
82. Wehkamp, J.*, et al.* The Paneth cell alpha-defensin deficiency of ileal Crohn's disease is linked to Wnt/Tcf-4. *Journal of immunology* **179**, 3109-3118 (2007).

83. Perminow, G.*, et al.* Defective paneth cell-mediated host defense in pediatric ileal Crohn's disease. *The American journal of gastroenterology* **105**, 452-459 (2010).
84. Cadwell, K.*, et al.* A key role for autophagy and the autophagy gene Atg16l1 in mouse and human intestinal Paneth cells. *Nature* **456**, 259-263 (2008).
85. Cadwell, K.*, et al.* Virus-plus-susceptibility gene interaction determines Crohn's disease gene Atg16L1 phenotypes in intestine. *Cell* **141**, 1135-1145.
86. Harper, P.H., Truelove, S.C., Lee, E.C., Kettlewell, M.G. & Jewell, D.P. Split ileostomy and ileocolostomy for Crohn's disease of the colon and ulcerative colitis: a 20 year survey. *Gut* **24**, 106-113 (1983).
87. Rutgeerts, P.*, et al.* Effect of faecal stream diversion on recurrence of Crohn's disease in the neoterminal ileum. *Lancet* **338**, 771-774 (1991).
88. Feller, M.*, et al.* Long-term antibiotic treatment for Crohn's disease: systematic review and meta-analysis of placebo-controlled trials. *Clin Infect Dis* **50**, 473-480 (2010).
89. Duchmann, R.*, et al.* T cell specificity and cross reactivity towards enterobacteria, bacteroides, bifidobacterium, and antigens from resident intestinal flora in humans. *Gut* **44**, 812-818 (1999).
90. Garrett, W.S.*, et al.* Communicable ulcerative colitis induced by T-bet deficiency in the innate immune system. *Cell* **131**, 33-45 (2007).
91. Elinav, E.*, et al.* NLRP6 inflammasome regulates colonic microbial ecology and risk for colitis. *Cell* **145**, 745-757 (2011).
92. Ivanov, II*, et al.* Specific microbiota direct the differentiation of IL-17-producing T-helper cells in the mucosa of the small intestine. *Cell Host Microbe* **4**, 337-349 (2008).
93. Rakoff-Nahoum, S., Paglino, J., Eslami-Varzaneh, F., Edberg, S. & Medzhitov, R. Recognition of commensal microflora by toll-like receptors is required for intestinal homeostasis. *Cell* **118**, 229-241 (2004).
94. Sartor, R.B. Microbial influences in inflammatory bowel diseases. *Gastroenterology* **134**, 577-594 (2008).
95. Sokol, H.*, et al.* Low counts of Faecalibacterium prausnitzii in colitis microbiota. *Inflammatory bowel diseases* **15**, 1183-1189 (2009).
96. Sokol, H.*, et al.* Faecalibacterium prausnitzii is an anti-inflammatory commensal bacterium identified by gut microbiota analysis of Crohn disease patients. *Proceedings of the National Academy of Sciences of the United States of America* **105**, 16731-16736 (2008).
97. Atarashi, K.*, et al.* Induction of colonic regulatory T cells by indigenous Clostridium species. *Science* **331**, 337-341 (2011).
98. Benjamin, J.L.*, et al.* Randomised, double-blind, placebo-controlled trial of fructo-oligosaccharides in active Crohn's disease. *Gut* **60**, 923-929 (2011).
99. Mazmanian, S.K., Round, J.L. & Kasper, D.L. A microbial symbiosis factor prevents intestinal inflammatory disease. *Nature* **453**, 620-625 (2008).
100. Baumgart, M.*, et al.* Culture independent analysis of ileal mucosa reveals a selective increase in invasive Escherichia coli of novel

phylogeny relative to depletion of Clostridiales in Crohn's disease involving the ileum. *Isme J* **1**, 403-418 (2007).
101. Martin, H.M.*, et al.* Enhanced Escherichia coli adherence and invasion in Crohn's disease and colon cancer. *Gastroenterology* **127**, 80-93 (2004).
102. Barnich, N.*, et al.* CEACAM6 acts as a receptor for adherent-invasive E. coli, supporting ileal mucosa colonization in Crohn disease. *The Journal of clinical investigation* **117**, 1566-1574 (2007).
103. Carvalho, F.A.*, et al.* Crohn's disease adherent-invasive Escherichia coli colonize and induce strong gut inflammation in transgenic mice expressing human CEACAM. *The Journal of Experimental Medicine* **206**, 2179-2189 (2009).
104. Kraehenbuhl, J.P. & Neutra, M.R. Epithelial M cells: differentiation and function. *Annu Rev Cell Dev Biol* **16**, 301-332 (2000).
105. Gullberg, E. & Soderholm, J.D. Peyer's patches and M cells as potential sites of the inflammatory onset in Crohn's disease. *Ann N Y Acad Sci* **1072**, 218-232 (2006).
106. Chassaing, B.*, et al.* Crohn disease--associated adherent-invasive E. coli bacteria target mouse and human Peyer's patches via long polar fimbriae. *The Journal of clinical investigation* **121**, 966-975 (2011).
107. Glasser, A.L.*, et al.* Adherent invasive Escherichia coli strains from patients with Crohn's disease survive and replicate within macrophages without inducing host cell death. *Infection and immunity* **69**, 5529-5537 (2001).
108. Zoetendal, E.G.*, et al.* Mucosa-associated bacteria in the human gastrointestinal tract are uniformly distributed along the colon and differ from the community recovered from feces. *Appl Environ Microbiol* **68**, 3401-3407 (2002).
109. Pei, Z.*, et al.* Bacterial biota in the human distal esophagus. *Proceedings of the National Academy of Sciences of the United States of America* **101**, 4250-4255 (2004).
110. Ahmed, S.*, et al.* Mucosa-associated bacterial diversity in relation to human terminal ileum and colonic biopsy samples. *Appl Environ Microbiol* **73**, 7435-7442 (2007).
111. Wang, X., Heazlewood, S.P., Krause, D.O. & Florin, T.H. Molecular characterization of the microbial species that colonize human ileal and colonic mucosa by using 16S rDNA sequence analysis. *J Appl Microbiol* **95**, 508-520 (2003).
112. Frank, D.N.*, et al.* Molecular-phylogenetic characterization of microbial community imbalances in human inflammatory bowel diseases. *Proceedings of the National Academy of Sciences of the United States of America* **104**, 13780-13785 (2007).
113. Eckburg, P.B.*, et al.* Diversity of the human intestinal microbial flora. *Science* **308**, 1635-1638 (2005).
114. Zoetendal, E.G., Rajilic-Stojanovic, M. & de Vos, W.M. High-throughput diversity and functionality analysis of the gastrointestinal tract microbiota. *Gut* **57**, 1605-1615 (2008).
115. Lay, C.*, et al.* Colonic microbiota signatures across five northern European countries. *Appl Environ Microbiol* **71**, 4153-4155 (2005).

116. Lepage, P.*, et al.* Biodiversity of the mucosa-associated microbiota is stable along the distal digestive tract in healthy individuals and patients with IBD. *Inflammatory bowel diseases* **11**, 473-480 (2005).
117. Stewart, J.A., Chadwick, V.S. & Murray, A. Investigations into the influence of host genetics on the predominant eubacteria in the faecal microflora of children. *J Med Microbiol* **54**, 1239-1242 (2005).
118. Muegge, B.D.*, et al.* Diet drives convergence in gut microbiome functions across mammalian phylogeny and within humans. *Science* **332**, 970-974 (2011).
119. Rehman, A.*, et al.* Nod2 is essential for temporal development of intestinal microbial communities. *Gut* (2011).
120. Tiihonen, K., Ouwehand, A.C. & Rautonen, N. Human intestinal microbiota and healthy ageing. *Ageing Res Rev* **9**, 107-116 (2010).
121. Seksik, P.*, et al.* Alterations of the dominant faecal bacterial groups in patients with Crohn's disease of the colon. *Gut* **52**, 237-242 (2003).
122. Ott, S.J.*, et al.* Reduction in diversity of the colonic mucosa associated bacterial microflora in patients with active inflammatory bowel disease. *Gut* **53**, 685-693 (2004).
123. Hugot, J.P.*, et al.* Mapping of a susceptibility locus for Crohn's disease on chromosome 16. *Nature* **379**, 821-823 (1996).
124. Ogura, Y.*, et al.* A frameshift mutation in NOD2 associated with susceptibility to Crohn's disease. *Nature* **411**, 603-606 (2001).
125. Lesage, S.*, et al.* CARD15/NOD2 mutational analysis and genotype-phenotype correlation in 612 patients with inflammatory bowel disease. *Am J Hum Genet* **70**, 845-857 (2002).
126. Cuthbert, A.P.*, et al.* The contribution of NOD2 gene mutations to the risk and site of disease in inflammatory bowel disease. *Gastroenterology* **122**, 867-874 (2002).
127. Ahmad, T.*, et al.* The molecular classification of the clinical manifestations of Crohn's disease. *Gastroenterology* **122**, 854-866 (2002).
128. Seiderer, J.*, et al.* Predictive value of the CARD15 variant 1007fs for the diagnosis of intestinal stenoses and the need for surgery in Crohn's disease in clinical practice: results of a prospective study. *Inflamm Bowel Dis* **12**, 1114-1121 (2006).
129. Franchi, L., Warner, N., Viani, K. & Nunez, G. Function of Nod-like receptors in microbial recognition and host defense. *Immunol Rev* **227**, 106-128 (2009).
130. Girardin, S.E.*, et al.* Nod2 is a general sensor of peptidoglycan through muramyl dipeptide (MDP) detection. *J Biol Chem* **278**, 8869-8872 (2003).
131. Inohara, N.*, et al.* Host recognition of bacterial muramyl dipeptide mediated through NOD2. Implications for Crohn's disease. *J Biol Chem* **278**, 5509-5512 (2003).
132. Sabbah, A.*, et al.* Activation of innate immune antiviral responses by Nod2. *Nat Immunol* **10**, 1073-1080 (2009).
133. Coussens, N.P., Mowers, J.C., McDonald, C., Nunez, G. & Ramaswamy, S. Crystal structure of the Nod1 caspase activation and recruitment domain. *Biochemical and biophysical research communications* **353**, 1-5 (2007).

134. Tanabe, T.*, et al.* Regulatory regions and critical residues of NOD2 involved in muramyl dipeptide recognition. *EMBO J* **23**, 1587-1597 (2004).
135. Hu, Y., Ding, L., Spencer, D.M. & Nunez, G. WD-40 repeat region regulates Apaf-1 self-association and procaspase-9 activation. *The Journal of biological chemistry* **273**, 33489-33494 (1998).
136. Srinivasula, S.M., Ahmad, M., Fernandes-Alnemri, T. & Alnemri, E.S. Autoactivation of procaspase-9 by Apaf-1-mediated oligomerization. *Mol Cell* **1**, 949-957 (1998).
137. Ogura, Y.*, et al.* Nod2, a Nod1/Apaf-1 family member that is restricted to monocytes and activates NF-kappaB. *The Journal of biological chemistry* **276**, 4812-4818 (2001).
138. Gutierrez, O.*, et al.* Induction of Nod2 in myelomonocytic and intestinal epithelial cells via nuclear factor-kappa B activation. *The Journal of biological chemistry* **277**, 41701-41705 (2002).
139. Ogura, Y.*, et al.* Expression of NOD2 in Paneth cells: a possible link to Crohn's ileitis. *Gut* **52**, 1591-1597 (2003).
140. Lala, S.*, et al.* Crohn's disease and the NOD2 gene: a role for paneth cells. *Gastroenterology* **125**, 47-57 (2003).
141. Reis e Sousa, C. Dendritic cells in a mature age. *Nat Rev Immunol* **6**, 476-483 (2006).
142. Soloff, A.C. & Barratt-Boyes, S.M. Enemy at the gates: dendritic cells and immunity to mucosal pathogens. *Cell Res* **20**, 872-885 (2010).
143. Trinchieri, G. & Sher, A. Cooperation of Toll-like receptor signals in innate immune defence. *Nat Rev Immunol* **7**, 179-190 (2007).
144. Medzhitov, R. Recognition of microorganisms and activation of the immune response. *Nature* **449**, 819-826 (2007).
145. Banchereau, J.*, et al.* Immunobiology of dendritic cells. *Annu Rev Immunol* **18**, 767-811 (2000).
146. Alvarez, D., Vollmann, E.H. & von Andrian, U.H. Mechanisms and consequences of dendritic cell migration. *Immunity* **29**, 325-342 (2008).
147. Niess, J.H. & Reinecker, H.C. Lamina propria dendritic cells in the physiology and pathology of the gastrointestinal tract. *Curr Opin Gastroenterol* **21**, 687-691 (2005).
148. Leon, B., Lopez-Bravo, M. & Ardavin, C. Monocyte-derived dendritic cells formed at the infection site control the induction of protective T helper 1 responses against Leishmania. *Immunity* **26**, 519-531 (2007).
149. Siddiqui, K.R., Laffont, S. & Powrie, F. E-cadherin marks a subset of inflammatory dendritic cells that promote T cell-mediated colitis. *Immunity* **32**, 557-567 (2010).
150. Herskovits, A.A., Auerbuch, V. & Portnoy, D.A. Bacterial ligands generated in a phagosome are targets of the cytosolic innate immune system. *PLoS pathogens* **3**, e51 (2007).
151. Marina-Garcia, N.*, et al.* Clathrin- and dynamin-dependent endocytic pathway regulates muramyl dipeptide internalization and NOD2 activation. *Journal of immunology* **182**, 4321-4327 (2009).
152. Lee, J.*, et al.* pH-dependent internalization of muramyl peptides from early endosomes enables Nod1 and Nod2 signaling. *The Journal of biological chemistry* **284**, 23818-23829 (2009).

153. Ismair, M.G., *et al.* hPepT1 selectively transports muramyl dipeptide but not Nod1-activating muramyl peptides. *Can J Physiol Pharmacol* **84**, 1313-1319 (2006).
154. Cossart, P. & Sansonetti, P.J. Bacterial invasion: the paradigms of enteroinvasive pathogens. *Science* **304**, 242-248 (2004).
155. Cloud-Hansen, K.A., *et al.* Breaching the great wall: peptidoglycan and microbial interactions. *Nat Rev Microbiol* **4**, 710-716 (2006).
156. Barnich, N., Aguirre, J.E., Reinecker, H.C., Xavier, R. & Podolsky, D.K. Membrane recruitment of NOD2 in intestinal epithelial cells is essential for nuclear factor-{kappa}B activation in muramyl dipeptide recognition. *J Cell Biol* **170**, 21-26 (2005).
157. Travassos, L.H., *et al.* Nod1 and Nod2 direct autophagy by recruiting ATG16L1 to the plasma membrane at the site of bacterial entry. *Nat Immunol* (2009).
158. Lecine, P., *et al.* The NOD2-RICK complex signals from the plasma membrane. *J Biol Chem* **282**, 15197-15207 (2007).
159. Kobayashi, K., *et al.* RICK/Rip2/CARDIAK mediates signalling for receptors of the innate and adaptive immune systems. *Nature* **416**, 194-199 (2002).
160. Nembrini, C., *et al.* The kinase activity of Rip2 determines its stability and consequently Nod1- and Nod2-mediated immune responses. *The Journal of biological chemistry* **284**, 19183-19188 (2009).
161. Abbott, D.W., Wilkins, A., Asara, J.M. & Cantley, L.C. The Crohn's disease protein, NOD2, requires RIP2 in order to induce ubiquitinylation of a novel site on NEMO. *Curr Biol* **14**, 2217-2227 (2004).
162. Park, J.H., *et al.* RICK/RIP2 mediates innate immune responses induced through Nod1 and Nod2 but not TLRs. *Journal of immunology* **178**, 2380-2386 (2007).
163. Hitotsumatsu, O., *et al.* The ubiquitin-editing enzyme A20 restricts nucleotide-binding oligomerization domain containing 2-triggered signals. *Immunity* **28**, 381-390 (2008).
164. Boone, D.L., *et al.* The ubiquitin-modifying enzyme A20 is required for termination of Toll-like receptor responses. *Nature immunology* **5**, 1052-1060 (2004).
165. Pickart, C.M. Mechanisms underlying ubiquitination. *Annu Rev Biochem* **70**, 503-533 (2001).
166. Bertrand, M.J., *et al.* Cellular inhibitors of apoptosis cIAP1 and cIAP2 are required for innate immunity signaling by the pattern recognition receptors NOD1 and NOD2. *Immunity* **30**, 789-801 (2009).
167. Krieg, A., *et al.* XIAP mediates NOD signaling via interaction with RIP2. *Proceedings of the National Academy of Sciences of the United States of America* **106**, 14524-14529 (2009).
168. Chen, C.M., Gong, Y., Zhang, M. & Chen, J.J. Reciprocal cross-talk between Nod2 and TAK1 signaling pathways. *J Biol Chem* **279**, 25876-25882 (2004).
169. McDonald, C., *et al.* A role for Erbin in the regulation of Nod2-dependent NF-kappaB signaling. *The Journal of biological chemistry* **280**, 40301-40309 (2005).

170. Till, A.*, et al.* A role for membrane-bound CD147 in NOD2-mediated recognition of bacterial cytoinvasion. *J Cell Sci* **121**, 487-495 (2008).
171. von Kampen, O.*, et al.* Caspase recruitment domain-containing protein 8 (CARD8) negatively regulates NOD2-mediated signaling. *The Journal of biological chemistry* **285**, 19921-19926 (2010).
172. Yamamoto-Furusho, J.K., Barnich, N., Xavier, R., Hisamatsu, T. & Podolsky, D.K. Centaurin beta1 down-regulates nucleotide-binding oligomerization domains 1- and 2-dependent NF-kappaB activation. *The Journal of biological chemistry* **281**, 36060-36070 (2006).
173. Bielig, H.*, et al.* A function for AAMP in Nod2-mediated NF-kappaB activation. *Mol Immunol* **46**, 2647-2654 (2009).
174. Barnich, N.*, et al.* GRIM-19 interacts with nucleotide oligomerization domain 2 and serves as downstream effector of anti-bacterial function in intestinal epithelial cells. *J Biol Chem* **280**, 19021-19026 (2005).
175. Rosenstiel, P.*, et al.* A short isoform of NOD2/CARD15, NOD2-S, is an endogenous inhibitor of NOD2/receptor-interacting protein kinase 2-induced signaling pathways. *Proceedings of the National Academy of Sciences of the United States of America* **103**, 3280-3285 (2006).
176. Kim, J.Y., Omori, E., Matsumoto, K., Nunez, G. & Ninomiya-Tsuji, J. TAK1 is a central mediator of NOD2 signaling in epidermal cells. *J Biol Chem* **283**, 137-144 (2008).
177. Agostini, L.*, et al.* NALP3 forms an IL-1beta-processing inflammasome with increased activity in Muckle-Wells autoinflammatory disorder. *Immunity* **20**, 319-325 (2004).
178. Windheim, M., Lang, C., Peggie, M., Plater, L.A. & Cohen, P. Molecular mechanisms involved in the regulation of cytokine production by muramyl dipeptide. *The Biochemical journal* **404**, 179-190 (2007).
179. Hsu, Y.M.*, et al.* The adaptor protein CARD9 is required for innate immune responses to intracellular pathogens. *Nat Immunol* **8**, 198-205 (2007).
180. Gross, O.*, et al.* Card9 controls a non-TLR signalling pathway for innate anti-fungal immunity. *Nature* **442**, 651-656 (2006).
181. LeibundGut-Landmann, S.*, et al.* Syk- and CARD9-dependent coupling of innate immunity to the induction of T helper cells that produce interleukin 17. *Nat Immunol* **8**, 630-638 (2007).
182. Oppenheim, J.J. & Yang, D. Alarmins: chemotactic activators of immune responses. *Curr Opin Immunol* **17**, 359-365 (2005).
183. Marques, R. & Boneca, I.G. Expression and functional importance of innate immune receptors by intestinal epithelial cells. *Cell Mol Life Sci* **68**, 3661-3673 (2011).
184. Zeytun, A., Chaudhary, A., Pardington, P., Cary, R. & Gupta, G. Induction of cytokines and chemokines by Toll-like receptor signaling: strategies for control of inflammation. *Crit Rev Immunol* **30**, 53-67 (2010).
185. Kawai, T. & Akira, S. Toll-like receptors and their crosstalk with other innate receptors in infection and immunity. *Immunity* **34**, 637-650 (2011).
186. Nish, S. & Medzhitov, R. Host defense pathways: role of redundancy and compensation in infectious disease phenotypes. *Immunity* **34**, 629-636 (2011).

187. Watanabe, T., Kitani, A., Murray, P.J. & Strober, W. NOD2 is a negative regulator of Toll-like receptor 2-mediated T helper type 1 responses. *Nat Immunol* **5**, 800-808 (2004).
188. Arkwright, P.D., Abinun, M. & Cant, A.J. Autoimmunity in human primary immunodeficiency diseases. *Blood* **99**, 2694-2702 (2002).
189. Akira, S. & Takeda, K. Toll-like receptor signalling. *Nat Rev Immunol* **4**, 499-511 (2004).
190. Botos, I., Segal, D.M. & Davies, D.R. The structural biology of Toll-like receptors. *Structure* **19**, 447-459 (2011).
191. Watanabe, T.*, et al.* Nucleotide binding oligomerization domain 2 deficiency leads to dysregulated TLR2 signaling and induction of antigen-specific colitis. *Immunity* **25**, 473-485 (2006).
192. Yang, Z.*, et al.* NOD2 transgenic mice exhibit enhanced MDP-mediated down-regulation of TLR2 responses and resistance to colitis induction. *Gastroenterology* **133**, 1510-1521 (2007).
193. Netea, M.G.*, et al.* Nucleotide-binding oligomerization domain-2 modulates specific TLR pathways for the induction of cytokine release. *J Immunol* **174**, 6518-6523 (2005).
194. Uehara, A.*, et al.* Muramyldipeptide and diaminopimelic acid-containing desmuramylpeptides in combination with chemically synthesized Toll-like receptor agonists synergistically induced production of interleukin-8 in a NOD2- and NOD1-dependent manner, respectively, in human monocytic cells in culture. *Cellular microbiology* **7**, 53-61 (2005).
195. van Heel, D.A.*, et al.* Synergy between TLR9 and NOD2 innate immune responses is lost in genetic Crohn's disease. *Gut* **54**, 1553-1557 (2005).
196. van Heel, D.A.*, et al.* Muramyl dipeptide and toll-like receptor sensitivity in NOD2-associated Crohn's disease. *Lancet* **365**, 1794-1796 (2005).
197. Yang, S.*, et al.* Synergistic effect of muramyldipeptide with lipopolysaccharide or lipoteichoic acid to induce inflammatory cytokines in human monocytic cells in culture. *Infection and immunity* **69**, 2045-2053 (2001).
198. Fritz, J.H.*, et al.* Synergistic stimulation of human monocytes and dendritic cells by Toll-like receptor 4 and NOD1- and NOD2-activating agonists. *Eur J Immunol* **35**, 2459-2470 (2005).
199. Correa-de-Santana, E.*, et al.* NOD2 receptors in adenopituitary folliculostellate cells: expression and function. *J Endocrinol* (2009).
200. Bonizzi, G. & Karin, M. The two NF-kappaB activation pathways and their role in innate and adaptive immunity. *Trends Immunol* **25**, 280-288 (2004).
201. Pan, Q.*, et al.* NF-kappa B-inducing kinase regulates selected gene expression in the Nod2 signaling pathway. *Infection and immunity* **74**, 2121-2127 (2006).
202. Richardson, W.M.*, et al.* Nucleotide-binding oligomerization domain-2 inhibits toll-like receptor-4 signaling in the intestinal epithelium. *Gastroenterology* **139**, 904-917, 917 e901-906 (2010).
203. Torok, H.P.*, et al.* Crohn's disease is associated with a toll-like receptor-9 polymorphism. *Gastroenterology* **127**, 365-366 (2004).
204. Torok, H.P.*, et al.* Epistasis between Toll-like receptor-9 polymorphisms and variants in NOD2 and IL23R modulates

susceptibility to Crohn's disease. *Am J Gastroenterol* **104**, 1723-1733 (2009).
205. Irie, T., Muta, T. & Takeshige, K. TAK1 mediates an activation signal from toll-like receptor(s) to nuclear factor-kappaB in lipopolysaccharide-stimulated macrophages. *FEBS Lett* **467**, 160-164 (2000).
206. Abbott, D.W.*, et al.* Coordinated regulation of Toll-like receptor and NOD2 signaling by K63-linked polyubiquitin chains. *Mol Cell Biol* **27**, 6012-6025 (2007).
207. Kim, J.Y., Omori, E., Matsumoto, K., Nunez, G. & Ninomiya-Tsuji, J. TAK1 is a central mediator of NOD2 signaling in epidermal cells. *The Journal of biological chemistry* **283**, 137-144 (2008).
208. Masumoto, J.*, et al.* Nod1 acts as an intracellular receptor to stimulate chemokine production and neutrophil recruitment in vivo. *The Journal of Experimental Medicine* **203**, 203-213 (2006).
209. Inohara, Chamaillard, McDonald, C. & Nunez, G. NOD-LRR proteins: role in host-microbial interactions and inflammatory disease. *Annu Rev Biochem* **74**, 355-383 (2005).
210. Poeck, H.*, et al.* Recognition of RNA virus by RIG-I results in activation of CARD9 and inflammasome signaling for interleukin 1 beta production. *Nature immunology* **11**, 63-69 (2010).
211. Canto, E.*, et al.* MDP-Induced selective tolerance to TLR4 ligands: Impairment in NOD2 mutant Crohn's disease patients. *Inflamm Bowel Dis* (2009).
212. Kullberg, B.J.*, et al.* Crohn's disease patients homozygous for the 3020insC NOD2 mutation have a defective NOD2/TLR4 cross-tolerance to intestinal stimuli. *Immunology* **123**, 600-605 (2008).
213. Jacinto, R., Hartung, T., McCall, C. & Li, L. Lipopolysaccharide- and lipoteichoic acid-induced tolerance and cross-tolerance: distinct alterations in IL-1 receptor-associated kinase. *Journal of immunology* **168**, 6136-6141 (2002).
214. Bagchi, A.*, et al.* MyD88-dependent and MyD88-independent pathways in synergy, priming, and tolerance between TLR agonists. *Journal of immunology* **178**, 1164-1171 (2007).
215. Medvedev, A.E. & Vogel, S.N. Overexpression of CD14, TLR4, and MD-2 in HEK 293T cells does not prevent induction of in vitro endotoxin tolerance. *J Endotoxin Res* **9**, 60-64 (2003).
216. Nakayama, K.*, et al.* Involvement of IRAK-M in peptidoglycan-induced tolerance in macrophages. *The Journal of biological chemistry* **279**, 6629-6634 (2004).
217. Li, C.H., Wang, J.H. & Redmond, H.P. Bacterial lipoprotein-induced self-tolerance and cross-tolerance to LPS are associated with reduced IRAK-1 expression and MyD88-IRAK complex formation. *J Leukoc Biol* **79**, 867-875 (2006).
218. Kramer, M., Netea, M.G., de Jong, D.J., Kullberg, B.J. & Adema, G.J. Impaired dendritic cell function in Crohn's disease patients with NOD2 3020insC mutation. *J Leukoc Biol* **79**, 860-866 (2006).
219. Chen, G., Shaw, M.H., Kim, Y.G. & Nunez, G. NOD-like receptors: role in innate immunity and inflammatory disease. *Annu Rev Pathol* **4**, 365-398 (2009).

220. Mariathasan, S. & Monack, D.M. Inflammasome adaptors and sensors: intracellular regulators of infection and inflammation. *Nat Rev Immunol* **7**, 31-40 (2007).
221. Schroder, K. & Tschopp, J. The inflammasomes. *Cell* **140**, 821-832 (2010).
222. Hu, B.*, et al.* Inflammation-induced tumorigenesis in the colon is regulated by caspase-1 and NLRC4. *Proceedings of the National Academy of Sciences of the United States of America* **107**, 21635-21640 (2010).
223. Suzuki, T.*, et al.* Differential regulation of caspase-1 activation, pyroptosis, and autophagy via Ipaf and ASC in Shigella-infected macrophages. *PLoS pathogens* **3**, e111 (2007).
224. Franchi, L.*, et al.* Cytosolic flagellin requires Ipaf for activation of caspase-1 and interleukin 1beta in salmonella-infected macrophages. *Nature immunology* **7**, 576-582 (2006).
225. Sutterwala, F.S. & Flavell, R.A. NLRC4/IPAF: a CARD carrying member of the NLR family. *Clin Immunol* **130**, 2-6 (2009).
226. Damiano, J.S., Oliveira, V., Welsh, K. & Reed, J.C. Heterotypic interactions among NACHT domains: implications for regulation of innate immune responses. *Biochem J* **381**, 213-219 (2004).
227. Mariathasan, S.*, et al.* Cryopyrin activates the inflammasome in response to toxins and ATP. *Nature* **440**, 228-232 (2006).
228. Kubota, T. & Koike, R. Cryopyrin-associated periodic syndromes: background and therapeutics. *Mod Rheumatol* **20**, 213-221 (2010).
229. Villani, A.C.*, et al.* Common variants in the NLRP3 region contribute to Crohn's disease susceptibility. *Nature genetics* **41**, 71-76 (2009).
230. Schoultz, I.*, et al.* Combined polymorphisms in genes encoding the inflammasome components NALP3 and CARD8 confer susceptibility to Crohn's disease in Swedish men. *The American journal of gastroenterology* **104**, 1180-1188 (2009).
231. Punzi, L.*, et al.* Clinical and genetic aspects of Blau syndrome: a 25-year follow-up of one family and a literature review. *Autoimmun Rev* **8**, 228-232 (2009).
232. Wagner, R.N., Proell, M., Kufer, T.A. & Schwarzenbacher, R. Evaluation of Nod-like receptor (NLR) effector domain interactions. *PLoS One* **4**, e4931 (2009).
233. Conforti-Andreoni, C.*, et al.* Synergism of NOD2 and NLRP3 activators promotes a unique transcriptional profile in murine dendritic cells. *J Leukoc Biol* **88**, 1207-1216 (2010).
234. Meixenberger, K.*, et al.* Listeria monocytogenes-infected human peripheral blood mononuclear cells produce IL-1beta, depending on listeriolysin O and NLRP3. *Journal of immunology* **184**, 922-930 (2010).
235. Martinon, F., Agostini, L., Meylan, E. & Tschopp, J. Identification of bacterial muramyl dipeptide as activator of the NALP3/cryopyrin inflammasome. *Curr Biol* **14**, 1929-1934 (2004).
236. Pan, Q.*, et al.* MDP-induced interleukin-1beta processing requires Nod2 and CIAS1/NALP3. *J Leukoc Biol* **82**, 177-183 (2007).

237. Marina-Garcia, N.*, et al.* Pannexin-1-mediated intracellular delivery of muramyl dipeptide induces caspase-1 activation via cryopyrin/NLRP3 independently of Nod2. *Journal of immunology* **180**, 4050-4057 (2008).
238. Martinon, F., Burns, K. & Tschopp, J. The inflammasome: a molecular platform triggering activation of inflammatory caspases and processing of proIL-beta. *Mol Cell* **10**, 417-426 (2002).
239. Hsu, L.C.*, et al.* A NOD2-NALP1 complex mediates caspase-1-dependent IL-1beta secretion in response to Bacillus anthracis infection and muramyl dipeptide. *Proc Natl Acad Sci U S A* **105**, 7803-7808 (2008).
240. Gregory, S.M.*, et al.* Discovery of a viral NLR homolog that inhibits the inflammasome. *Science* **331**, 330-334 (2011).
241. Xu, Y.*, et al.* Toll-like receptor 4 is a sensor for autophagy associated with innate immunity. *Immunity* **27**, 135-144 (2007).
242. Delgado, M.A., Elmaoued, R.A., Davis, A.S., Kyei, G. & Deretic, V. Toll-like receptors control autophagy. *The EMBO journal* **27**, 1110-1121 (2008).
243. Hampe, J.*, et al.* A genome-wide association scan of nonsynonymous SNPs identifies a susceptibility variant for Crohn disease in ATG16L1. *Nat Genet* **39**, 207-211 (2007).
244. Cooney, R.*, et al.* NOD2 stimulation induces autophagy in dendritic cells influencing bacterial handling and antigen presentation. *Nat Med* **16**, 90-97 (2010).
245. Homer, C.R., Richmond, A.L., Rebert, N.A., Achkar, J.P. & McDonald, C. ATG16L1 and NOD2 interact in an autophagy-dependent antibacterial pathway implicated in Crohn's disease pathogenesis. *Gastroenterology* **139**, 1630-1641, 1641 e1631-1632.
246. Ogata, M.*, et al.* Autophagy is activated for cell survival after endoplasmic reticulum stress. *Mol Cell Biol* **26**, 9220-9231 (2006).
247. Yang, L., Li, P., Fu, S., Calay, E.S. & Hotamisligil, G.S. Defective hepatic autophagy in obesity promotes ER stress and causes insulin resistance. *Cell Metab* **11**, 467-478 (2010).
248. Woo, C.W.*, et al.* Adaptive suppression of the ATF4-CHOP branch of the unfolded protein response by toll-like receptor signalling. *Nature cell biology* **11**, 1473-1480 (2009).
249. Asano, J.*, et al.* Nucleotide oligomerization binding domain-like receptor signaling enhances dendritic cell-mediated cross-priming in vivo. *Journal of immunology* **184**, 736-745 (2010).
250. Datta, S.K.*, et al.* A subset of Toll-like receptor ligands induces cross-presentation by bone marrow-derived dendritic cells. *Journal of immunology* **170**, 4102-4110 (2003).
251. Magalhaes, J.G.*, et al.* Nod2-dependent Th2 polarization of antigen-specific immunity. *Journal of immunology* **181**, 7925-7935 (2008).
252. Moreira, L.O.*, et al.* Modulation of adaptive immunity by different adjuvant-antigen combinations in mice lacking Nod2. *Vaccine* **26**, 5808-5813 (2008).
253. van Beelen, A.J.*, et al.* Stimulation of the intracellular bacterial sensor NOD2 programs dendritic cells to promote interleukin-17 production in human memory T cells. *Immunity* **27**, 660-669 (2007).

254. Shaw, M.H.*, et al.* T cell-intrinsic role of Nod2 in promoting type 1 immunity to Toxoplasma gondii. *Nature immunology* **10**, 1267-1274 (2009).
255. Porter, E.M., Bevins, C.L., Ghosh, D. & Ganz, T. The multifaceted Paneth cell. *Cell Mol Life Sci* **59**, 156-170 (2002).
256. Wehkamp, J.*, et al.* NOD2 (CARD15) mutations in Crohn's disease are associated with diminished mucosal alpha-defensin expression. *Gut* **53**, 1658-1664 (2004).
257. Elphick, D., Liddell, S. & Mahida, Y.R. Impaired luminal processing of human defensin-5 in Crohn's disease: persistence in a complex with chymotrypsinogen and trypsin. *Am J Pathol* **172**, 702-713 (2008).
258. Wehkamp, J.*, et al.* Reduced Paneth cell alpha-defensins in ileal Crohn's disease. *Proceedings of the National Academy of Sciences of the United States of America* **102**, 18129-18134 (2005).
259. Simms, L.A.*, et al.* Reduced alpha-defensin expression is associated with inflammation and not NOD2 mutation status in ileal Crohn's disease. *Gut* **57**, 903-910 (2008).
260. Kobayashi, K.S.*, et al.* Nod2-dependent regulation of innate and adaptive immunity in the intestinal tract. *Science* **307**, 731-734 (2005).
261. Garabedian, E.M., Roberts, L.J., McNevin, M.S. & Gordon, J.I. Examining the role of Paneth cells in the small intestine by lineage ablation in transgenic mice. *The Journal of biological chemistry* **272**, 23729-23740 (1997).
262. Wilson, C.L.*, et al.* Regulation of intestinal alpha-defensin activation by the metalloproteinase matrilysin in innate host defense. *Science* **286**, 113-117 (1999).
263. Biswas, A.*, et al.* Induction and rescue of Nod2-dependent Th1-driven granulomatous inflammation of the ileum. *Proceedings of the National Academy of Sciences of the United States of America* **107**, 14739-14744 (2010).
264. Bikker, F.J.*, et al.* Bacteria binding by DMBT1/SAG/gp-340 is confined to the VEVLXXXXW motif in its scavenger receptor cysteine-rich domains. *The Journal of biological chemistry* **279**, 47699-47703 (2004).
265. Rosenstiel, P.*, et al.* Regulation of DMBT1 via NOD2 and TLR4 in intestinal epithelial cells modulates bacterial recognition and invasion. *Journal of immunology* **178**, 8203-8211 (2007).
266. Hisamatsu, T.*, et al.* CARD15/NOD2 functions as an antibacterial factor in human intestinal epithelial cells. *Gastroenterology* **124**, 993-1000 (2003).
267. Lipinski, S.*, et al.* DUOX2-derived reactive oxygen species are effectors of NOD2-mediated antibacterial responses. *J Cell Sci* **122**, 3522-3530 (2009).
268. Park, H.S.*, et al.* Cutting edge: direct interaction of TLR4 with NAD(P)H oxidase 4 isozyme is essential for lipopolysaccharide-induced production of reactive oxygen species and activation of NF-kappa B. *Journal of immunology* **173**, 3589-3593 (2004).
269. Chen, L.W.*, et al.* The two faces of IKK and NF-kappaB inhibition: prevention of systemic inflammation but increased local injury following intestinal ischemia-reperfusion. *Nature medicine* **9**, 575-581 (2003).

270. Petnicki-Ocwieja, T.*, et al.* Nod2 is required for the regulation of commensal microbiota in the intestine. *Proceedings of the National Academy of Sciences of the United States of America* **106**, 15813-15818 (2009).
271. Bouskra, D.*, et al.* Lymphoid tissue genesis induced by commensals through NOD1 regulates intestinal homeostasis. *Nature* **456**, 507-510 (2008).
272. Frank, D.N.*, et al.* Disease phenotype and genotype are associated with shifts in intestinal-associated microbiota in inflammatory bowel diseases. *Inflammatory bowel diseases* **17**, 179-184 (2011).
273. Noguchi, E., Homma, Y., Kang, X., Netea, M.G. & Ma, X. A Crohn's disease-associated NOD2 mutation suppresses transcription of human IL10 by inhibiting activity of the nuclear ribonucleoprotein hnRNP-A1. *Nat Immunol* **10**, 471-479 (2009).
274. Maeda, S.*, et al.* Nod2 mutation in Crohn's disease potentiates NF-kappaB activity and IL-1beta processing. *Science* **307**, 734-738 (2005).
275. Netea, M.G.*, et al.* NOD2 3020insC mutation and the pathogenesis of Crohn's disease: impaired IL-1beta production points to a loss-of-function phenotype. *Neth J Med* **63**, 305-308 (2005).
276. O'Neill, L.A., Sheedy, F.J. & McCoy, C.E. MicroRNAs: the fine-tuners of Toll-like receptor signalling. *Nat Rev Immunol* **11**, 163-175 (2011).
277. Lee, R.C., Feinbaum, R.L. & Ambros, V. The C. elegans heterochronic gene lin-4 encodes small RNAs with antisense complementarity to lin-14. *Cell* **75**, 843-854 (1993).
278. Lim, L.P., Glasner, M.E., Yekta, S., Burge, C.B. & Bartel, D.P. Vertebrate microRNA genes. *Science* **299**, 1540 (2003).
279. Ibanez-Ventoso, C., Vora, M. & Driscoll, M. Sequence relationships among C. elegans, D. melanogaster and human microRNAs highlight the extensive conservation of microRNAs in biology. *PLoS One* **3**, e2818 (2008).
280. Filipowicz, W., Bhattacharyya, S.N. & Sonenberg, N. Mechanisms of post-transcriptional regulation by microRNAs: are the answers in sight? *Nat Rev Genet* **9**, 102-114 (2008).
281. Pillai, R.S.*, et al.* Inhibition of translational initiation by Let-7 MicroRNA in human cells. *Science* **309**, 1573-1576 (2005).
282. Petersen, C.P., Bordeleau, M.E., Pelletier, J. & Sharp, P.A. Short RNAs repress translation after initiation in mammalian cells. *Mol Cell* **21**, 533-542 (2006).
283. Wu, L., Fan, J. & Belasco, J.G. MicroRNAs direct rapid deadenylation of mRNA. *Proc Natl Acad Sci U S A* **103**, 4034-4039 (2006).
284. Taganov, K.D., Boldin, M.P., Chang, K.J. & Baltimore, D. NF-kappaB-dependent induction of microRNA miR-146, an inhibitor targeted to signaling proteins of innate immune responses. *Proc Natl Acad Sci U S A* **103**, 12481-12486 (2006).
285. Croce, C.M. & Calin, G.A. miRNAs, cancer, and stem cell division. *Cell* **122**, 6-7 (2005).
286. Carleton, M., Cleary, M.A. & Linsley, P.S. MicroRNAs and cell cycle regulation. *Cell Cycle* **6**, 2127-2132 (2007).
287. Lee, Y.*, et al.* MicroRNA genes are transcribed by RNA polymerase II. *EMBO J* **23**, 4051-4060 (2004).

288. Cai, X., Hagedorn, C.H. & Cullen, B.R. Human microRNAs are processed from capped, polyadenylated transcripts that can also function as mRNAs. *Rna* **10**, 1957-1966 (2004).
289. Borchert, G.M., Lanier, W. & Davidson, B.L. RNA polymerase III transcribes human microRNAs. *Nat Struct Mol Biol* **13**, 1097-1101 (2006).
290. Landthaler, M., Yalcin, A. & Tuschl, T. The human DiGeorge syndrome critical region gene 8 and Its D. melanogaster homolog are required for miRNA biogenesis. *Curr Biol* **14**, 2162-2167 (2004).
291. Gregory, R.I.*, et al.* The Microprocessor complex mediates the genesis of microRNAs. *Nature* **432**, 235-240 (2004).
292. Han, J.*, et al.* The Drosha-DGCR8 complex in primary microRNA processing. *Genes Dev* **18**, 3016-3027 (2004).
293. Yi, R., Qin, Y., Macara, I.G. & Cullen, B.R. Exportin-5 mediates the nuclear export of pre-microRNAs and short hairpin RNAs. *Genes Dev* **17**, 3011-3016 (2003).
294. Bohnsack, M.T., Czaplinski, K. & Gorlich, D. Exportin 5 is a RanGTP-dependent dsRNA-binding protein that mediates nuclear export of pre-miRNAs. *Rna* **10**, 185-191 (2004).
295. Lund, E., Guttinger, S., Calado, A., Dahlberg, J.E. & Kutay, U. Nuclear export of microRNA precursors. *Science* **303**, 95-98 (2004).
296. Ketting, R.F.*, et al.* Dicer functions in RNA interference and in synthesis of small RNA involved in developmental timing in C. elegans. *Genes Dev* **15**, 2654-2659 (2001).
297. Hutvagner, G.*, et al.* A cellular function for the RNA-interference enzyme Dicer in the maturation of the let-7 small temporal RNA. *Science* **293**, 834-838 (2001).
298. Hammond, S.M., Bernstein, E., Beach, D. & Hannon, G.J. An RNA-directed nuclease mediates post-transcriptional gene silencing in Drosophila cells. *Nature* **404**, 293-296 (2000).
299. Schwarz, D.S.*, et al.* Asymmetry in the assembly of the RNAi enzyme complex. *Cell* **115**, 199-208 (2003).
300. Xiao, C. & Rajewsky, K. MicroRNA control in the immune system: basic principles. *Cell* **136**, 26-36 (2009).
301. Krek, A.*, et al.* Combinatorial microRNA target predictions. *Nat Genet* **37**, 495-500 (2005).
302. Biton, M.*, et al.* Epithelial microRNAs regulate gut mucosal immunity via epithelium-T cell crosstalk. *Nature immunology* **12**, 239-246 (2011).
303. Park, C.*, et al.* MicroRNAs Dynamically Remodel Gastrointestinal Smooth Muscle Cells. *PLoS One* **6**, e18628 (2011).
304. Rodriguez, A.*, et al.* Requirement of bic/microRNA-155 for normal immune function. *Science* **316**, 608-611 (2007).
305. O'Connell, R.M., Taganov, K.D., Boldin, M.P., Cheng, G. & Baltimore, D. MicroRNA-155 is induced during the macrophage inflammatory response. *Proc Natl Acad Sci U S A* **104**, 1604-1609 (2007).
306. Ceppi, M.*, et al.* MicroRNA-155 modulates the interleukin-1 signaling pathway in activated human monocyte-derived dendritic cells. *Proc Natl Acad Sci U S A* **106**, 2735-2740 (2009).

307. Tang, B.*, et al.* Identification of MyD88 as a novel target of miR-155, involved in negative regulation of Helicobacter pylori-induced inflammation. *FEBS Lett* **584**, 1481-1486 (2010).
308. Huang, R.S., Hu, G.Q., Lin, B., Lin, Z.Y. & Sun, C.C. MicroRNA-155 silencing enhances inflammatory response and lipid uptake in oxidized low-density lipoprotein-stimulated human THP-1 macrophages. *J Investig Med* **58**, 961-967 (2010).
309. Ruggiero, T.*, et al.* LPS induces KH-type splicing regulatory protein-dependent processing of microRNA-155 precursors in macrophages. *Faseb J* **23**, 2898-2908 (2009).
310. Tili, E.*, et al.* Modulation of miR-155 and miR-125b levels following lipopolysaccharide/TNF-alpha stimulation and their possible roles in regulating the response to endotoxin shock. *J Immunol* **179**, 5082-5089 (2007).
311. O'Connell, R.M., Chaudhuri, A.A., Rao, D.S. & Baltimore, D. Inositol phosphatase SHIP1 is a primary target of miR-155. *Proc Natl Acad Sci U S A* **106**, 7113-7118 (2009).
312. Wang, P.*, et al.* Inducible microRNA-155 feedback promotes type I IFN signaling in antiviral innate immunity by targeting suppressor of cytokine signaling 1. *Journal of immunology* **185**, 6226-6233 (2010).
313. O'Connell, R.M.*, et al.* MicroRNA-155 promotes autoimmune inflammation by enhancing inflammatory T cell development. *Immunity* **33**, 607-619 (2010).
314. Martinez-Nunez, R.T., Louafi, F., Friedmann, P.S. & Sanchez-Elsner, T. MicroRNA-155 modulates the pathogen binding ability of dendritic cells (DCs) by down-regulation of DC-specific intercellular adhesion molecule-3 grabbing non-integrin (DC-SIGN). *J Biol Chem* **284**, 16334-16342 (2009).
315. Cameron, J.E.*, et al.* Epstein-Barr virus latent membrane protein 1 induces cellular MicroRNA miR-146a, a modulator of lymphocyte signaling pathways. *J Virol* **82**, 1946-1958 (2008).
316. Nahid, M.A., Pauley, K.M., Satoh, M. & Chan, E.K. miR-146a is critical for endotoxin-induced tolerance: IMPLICATION IN INNATE IMMUNITY. *J Biol Chem* **284**, 34590-34599 (2009).
317. Chassin, C.*, et al.* miR-146a mediates protective innate immune tolerance in the neonate intestine. *Cell Host Microbe* **8**, 358-368 (2010).
318. Hou, J.*, et al.* MicroRNA-146a feedback inhibits RIG-I-dependent Type I IFN production in macrophages by targeting TRAF6, IRAK1, and IRAK2. *Journal of immunology* **183**, 2150-2158 (2009).
319. Starczynowski, D.T.*, et al.* Identification of miR-145 and miR-146a as mediators of the 5q- syndrome phenotype. *Nature medicine* **16**, 49-58 (2010).
320. Bazzoni, F.*, et al.* Induction and regulatory function of miR-9 in human monocytes and neutrophils exposed to proinflammatory signals. *Proc Natl Acad Sci U S A* **106**, 5282-5287 (2009).
321. Li, M., Pascual, G. & Glass, C.K. Peroxisome proliferator-activated receptor gamma-dependent repression of the inducible nitric oxide synthase gene. *Mol Cell Biol* **20**, 4699-4707 (2000).

322. Ricote, M., Li, A.C., Willson, T.M., Kelly, C.J. & Glass, C.K. The peroxisome proliferator-activated receptor-gamma is a negative regulator of macrophage activation. *Nature* **391**, 79-82 (1998).
323. Jennewein, C., von Knethen, A., Schmid, T. & Brune, B. MicroRNA-27b contributes to lipopolysaccharide-mediated peroxisome proliferator-activated receptor gamma (PPARgamma) mRNA destabilization. *The Journal of biological chemistry* **285**, 11846-11853 (2010).
324. Liu, G.*, et al.* miR-147, a microRNA that is induced upon Toll-like receptor stimulation, regulates murine macrophage inflammatory responses. *Proc Natl Acad Sci U S A* **106**, 15819-15824 (2009).
325. Sheedy, F.J.*, et al.* Negative regulation of TLR4 via targeting of the proinflammatory tumor suppressor PDCD4 by the microRNA miR-21. *Nat Immunol* **11**, 141-147.
326. Lu, T.X., Munitz, A. & Rothenberg, M.E. MicroRNA-21 is up-regulated in allergic airway inflammation and regulates IL-12p35 expression. *Journal of immunology* **182**, 4994-5002 (2009).
327. Chen, X.M., Splinter, P.L., O'Hara, S.P. & LaRusso, N.F. A cellular micro-RNA, let-7i, regulates Toll-like receptor 4 expression and contributes to cholangiocyte immune responses against Cryptosporidium parvum infection. *J Biol Chem* **282**, 28929-28938 (2007).
328. Androulidaki, A.*, et al.* The kinase Akt1 controls macrophage response to lipopolysaccharide by regulating microRNAs. *Immunity* **31**, 220-231 (2009).
329. Iliopoulos, D., Hirsch, H.A. & Struhl, K. An epigenetic switch involving NF-kappaB, Lin28, Let-7 MicroRNA, and IL6 links inflammation to cell transformation. *Cell* **139**, 693-706 (2009).
330. Shaked, I.*, et al.* MicroRNA-132 potentiates cholinergic anti-inflammatory signaling by targeting acetylcholinesterase. *Immunity* **31**, 965-973 (2009).
331. Liu, Q.*, et al.* miR-16 family induces cell cycle arrest by regulating multiple cell cycle genes. *Nucleic Acids Res* **36**, 5391-5404 (2008).
332. Chang, T.C.*, et al.* Widespread microRNA repression by Myc contributes to tumorigenesis. *Nature genetics* **40**, 43-50 (2008).
333. Loffler, D.*, et al.* Interleukin-6 dependent survival of multiple myeloma cells involves the Stat3-mediated induction of microRNA-21 through a highly conserved enhancer. *Blood* **110**, 1330-1333 (2007).
334. Tarasov, V.*, et al.* Differential regulation of microRNAs by p53 revealed by massively parallel sequencing: miR-34a is a p53 target that induces apoptosis and G1-arrest. *Cell Cycle* **6**, 1586-1593 (2007).
335. Bueno, M.J.*, et al.* Genetic and epigenetic silencing of microRNA-203 enhances ABL1 and BCR-ABL1 oncogene expression. *Cancer Cell* **13**, 496-506 (2008).
336. Davis, B.N., Hilyard, A.C., Lagna, G. & Hata, A. SMAD proteins control DROSHA-mediated microRNA maturation. *Nature* **454**, 56-61 (2008).
337. Lee, E.J.*, et al.* Systematic evaluation of microRNA processing patterns in tissues, cell lines, and tumors. *Rna* **14**, 35-42 (2008).
338. Galardi, S., Mercatelli, N., Farace, M.G. & Ciafre, S.A. NF-kB and c-Jun induce the expression of the oncogenic miR-221 and miR-222 in

prostate carcinoma and glioblastoma cells. *Nucleic acids research* **39**, 3892-3902 (2011).
339. Mott, J.L.*, et al.* Transcriptional suppression of mir-29b-1/mir-29a promoter by c-Myc, hedgehog, and NF-kappaB. *J Cell Biochem* **110**, 1155-1164 (2010).
340. Kapinas, K., Kessler, C., Ricks, T., Gronowicz, G. & Delany, A.M. miR-29 modulates Wnt signaling in human osteoblasts through a positive feedback loop. *The Journal of biological chemistry* **285**, 25221-25231 (2010).
341. Lee, J.*, et al.* Maintenance of colonic homeostasis by distinctive apical TLR9 signalling in intestinal epithelial cells. *Nature cell biology* **8**, 1327-1336 (2006).
342. Blumenthal, A.*, et al.* The Wingless homolog WNT5A and its receptor Frizzled-5 regulate inflammatory responses of human mononuclear cells induced by microbial stimulation. *Blood* **108**, 965-973 (2006).
343. Wang, H.*, et al.* NF-kappaB-YY1-miR-29 regulatory circuitry in skeletal myogenesis and rhabdomyosarcoma. *Cancer Cell* **14**, 369-381 (2008).
344. Martinez, I., Cazalla, D., Almstead, L.L., Steitz, J.A. & DiMaio, D. miR-29 and miR-30 regulate B-Myb expression during cellular senescence. *Proceedings of the National Academy of Sciences of the United States of America* **108**, 522-527 (2011).
345. Roderburg, C.*, et al.* Micro-RNA profiling reveals a role for miR-29 in human and murine liver fibrosis. *Hepatology* **53**, 209-218 (2011).
346. van Rooij, E.*, et al.* Dysregulation of microRNAs after myocardial infarction reveals a role of miR-29 in cardiac fibrosis. *Proceedings of the National Academy of Sciences of the United States of America* **105**, 13027-13032 (2008).
347. Winbanks, C.E.*, et al.* TGF-{beta} Regulates miR-206 and miR-29 to Control Myogenic Differentiation through Regulation of HDAC4. *The Journal of biological chemistry* **286**, 13805-13814 (2011).
348. Maurer, B.*, et al.* MicroRNA-29, a key regulator of collagen expression in systemic sclerosis. *Arthritis Rheum* **62**, 1733-1743 (2010).
349. Guil, S. & Caceres, J.F. The multifunctional RNA-binding protein hnRNP A1 is required for processing of miR-18a. *Nat Struct Mol Biol* **14**, 591-596 (2007).
350. Tang, F.*, et al.* MicroRNAs are tightly associated with RNA-induced gene silencing complexes in vivo. *Biochemical and biophysical research communications* **372**, 24-29 (2008).
351. Diederichs, S. & Haber, D.A. Dual role for argonautes in microRNA processing and posttranscriptional regulation of microRNA expression. *Cell* **131**, 1097-1108 (2007).
352. Katoh, T.*, et al.* Selective stabilization of mammalian microRNAs by 3' adenylation mediated by the cytoplasmic poly(A) polymerase GLD-2. *Genes Dev* **23**, 433-438 (2009).
353. Zhang, Z.*, et al.* Uracils at nucleotide position 9-11 are required for the rapid turnover of miR-29 family. *Nucleic acids research* **39**, 4387-4395 (2011).
354. Jinek, M. & Doudna, J.A. A three-dimensional view of the molecular machinery of RNA interference. *Nature* **457**, 405-412 (2009).

355. Lewis, B.P., Shih, I.H., Jones-Rhoades, M.W., Bartel, D.P. & Burge, C.B. Prediction of mammalian microRNA targets. *Cell* **115**, 787-798 (2003).
356. Grimson, A.*, et al.* MicroRNA targeting specificity in mammals: determinants beyond seed pairing. *Mol Cell* **27**, 91-105 (2007).
357. Shin, C.*, et al.* Expanding the microRNA targeting code: functional sites with centered pairing. *Mol Cell* **38**, 789-802 (2010).
358. Zhou, X., Duan, X., Qian, J. & Li, F. Abundant conserved microRNA target sites in the 5'-untranslated region and coding sequence. *Genetica* **137**, 159-164 (2009).
359. Ritchie, W., Flamant, S. & Rasko, J.E. Predicting microRNA targets and functions: traps for the unwary. *Nat Methods* **6**, 397-398 (2009).
360. Thomson, D.W., Bracken, C.P. & Goodall, G.J. Experimental strategies for microRNA target identification. *Nucleic acids research* (2011).
361. Khan, A.A.*, et al.* Transfection of small RNAs globally perturbs gene regulation by endogenous microRNAs. *Nat Biotechnol* **27**, 549-555 (2009).
362. Lim, L.P.*, et al.* Microarray analysis shows that some microRNAs downregulate large numbers of target mRNAs. *Nature* **433**, 769-773 (2005).
363. Baek, D.*, et al.* The impact of microRNAs on protein output. *Nature* **455**, 64-71 (2008).
364. Guo, H., Ingolia, N.T., Weissman, J.S. & Bartel, D.P. Mammalian microRNAs predominantly act to decrease target mRNA levels. *Nature* **466**, 835-840 (2010).
365. Hendrickson, D.G., Hogan, D.J., Herschlag, D., Ferrell, J.E. & Brown, P.O. Systematic identification of mRNAs recruited to argonaute 2 by specific microRNAs and corresponding changes in transcript abundance. *PLoS One* **3**, e2126 (2008).
366. Mili, S. & Steitz, J.A. Evidence for reassociation of RNA-binding proteins after cell lysis: implications for the interpretation of immunoprecipitation analyses. *Rna* **10**, 1692-1694 (2004).
367. Chi, S.W., Zang, J.B., Mele, A. & Darnell, R.B. Argonaute HITS-CLIP decodes microRNA-mRNA interaction maps. *Nature* **460**, 479-486 (2009).
368. Hafner, M.*, et al.* Transcriptome-wide identification of RNA-binding protein and microRNA target sites by PAR-CLIP. *Cell* **141**, 129-141 (2010).
369. Vinther, J., Hedegaard, M.M., Gardner, P.P., Andersen, J.S. & Arctander, P. Identification of miRNA targets with stable isotope labeling by amino acids in cell culture. *Nucleic acids research* **34**, e107 (2006).
370. Zhu, S., Si, M.L., Wu, H. & Mo, Y.Y. MicroRNA-21 targets the tumor suppressor gene tropomyosin 1 (TPM1). *The Journal of biological chemistry* **282**, 14328-14336 (2007).
371. Muniyappa, M.K.*, et al.* MiRNA-29a regulates the expression of numerous proteins and reduces the invasiveness and proliferation of human carcinoma cell lines. *Eur J Cancer* **45**, 3104-3118 (2009).

372. Pekarsky, Y.*, et al.* Tcl1 expression in chronic lymphocytic leukemia is regulated by miR-29 and miR-181. *Cancer Res* **66**, 11590-11593 (2006).
373. Calin, G.A.*, et al.* Human microRNA genes are frequently located at fragile sites and genomic regions involved in cancers. *Proceedings of the National Academy of Sciences of the United States of America* **101**, 2999-3004 (2004).
374. Santanam, U.*, et al.* Chronic lymphocytic leukemia modeled in mouse by targeted miR-29 expression. *Proceedings of the National Academy of Sciences of the United States of America* **107**, 12210-12215 (2010).
375. Garzon, R.*, et al.* Distinctive microRNA signature of acute myeloid leukemia bearing cytoplasmic mutated nucleophosmin. *Proceedings of the National Academy of Sciences of the United States of America* **105**, 3945-3950 (2008).
376. Zhao, J.J.*, et al.* microRNA expression profile and identification of miR-29 as a prognostic marker and pathogenetic factor by targeting CDK6 in mantle cell lymphoma. *Blood* **115**, 2630-2639 (2010).
377. Mott, J.L., Kobayashi, S., Bronk, S.F. & Gores, G.J. mir-29 regulates Mcl-1 protein expression and apoptosis. *Oncogene* **26**, 6133-6140 (2007).
378. Park, S.Y., Lee, J.H., Ha, M., Nam, J.W. & Kim, V.N. miR-29 miRNAs activate p53 by targeting p85 alpha and CDC42. *Nat Struct Mol Biol* **16**, 23-29 (2009).
379. Porkka, K.P.*, et al.* MicroRNA expression profiling in prostate cancer. *Cancer Res* **67**, 6130-6135 (2007).
380. Fabbri, M.*, et al.* MicroRNA-29 family reverts aberrant methylation in lung cancer by targeting DNA methyltransferases 3A and 3B. *Proceedings of the National Academy of Sciences of the United States of America* **104**, 15805-15810 (2007).
381. Nguyen, T.*, et al.* Downregulation of microRNA-29c is associated with hypermethylation of tumor-related genes and disease outcome in cutaneous melanoma. *Epigenetics* **6**, 388-394 (2011).
382. Gebeshuber, C.A., Zatloukal, K. & Martinez, J. miR-29a suppresses tristetraprolin, which is a regulator of epithelial polarity and metastasis. *EMBO Rep* **10**, 400-405 (2009).
383. Taylor, G.A.*, et al.* A pathogenetic role for TNF alpha in the syndrome of cachexia, arthritis, and autoimmunity resulting from tristetraprolin (TTP) deficiency. *Immunity* **4**, 445-454 (1996).
384. Cushing, L.*, et al.* MIR-29 is a Major Regulator of Genes Associated with Pulmonary Fibrosis. *Am J Respir Cell Mol Biol* (2010).
385. Pandit, K.V., Milosevic, J. & Kaminski, N. MicroRNAs in idiopathic pulmonary fibrosis. *Transl Res* **157**, 191-199 (2011).
386. Villarreal, G., Jr., Oh, D.J., Kang, M.H. & Rhee, D.J. Coordinated Regulation of Extracellular Matrix Synthesis by the MicroRNA-29 Family in the Trabecular Meshwork. *Invest Ophthalmol Vis Sci* (2011).
387. Steinberger, P.*, et al.* Molecular characterization of human 4Ig-B7-H3, a member of the B7 family with four Ig-like domains. *Journal of immunology* **172**, 2352-2359 (2004).

388. Chapoval, A.I.*, et al.* B7-H3: a costimulatory molecule for T cell activation and IFN-gamma production. *Nature immunology* **2**, 269-274 (2001).
389. Xu, H., Cheung, I.Y., Guo, H.F. & Cheung, N.K. MicroRNA miR-29 modulates expression of immunoinhibitory molecule B7-H3: potential implications for immune based therapy of human solid tumors. *Cancer Res* **69**, 6275-6281 (2009).
390. Verrier, J.D.*, et al.* Peripheral myelin protein 22 is regulated post-transcriptionally by miRNA-29a. *Glia* **57**, 1265-1279 (2009).
391. Kozopas, K.M., Yang, T., Buchan, H.L., Zhou, P. & Craig, R.W. MCL1, a gene expressed in programmed myeloid cell differentiation, has sequence similarity to BCL2. *Proceedings of the National Academy of Sciences of the United States of America* **90**, 3516-3520 (1993).
392. Vaux, D.L., Cory, S. & Adams, J.M. Bcl-2 gene promotes haemopoietic cell survival and cooperates with c-myc to immortalize pre-B cells. *Nature* **335**, 440-442 (1988).
393. McDonnell, T.J.*, et al.* bcl-2-immunoglobulin transgenic mice demonstrate extended B cell survival and follicular lymphoproliferation. *Cell* **57**, 79-88 (1989).
394. Choi, S.S.*, et al.* A novel Bcl-2 related gene, Bfl-1, is overexpressed in stomach cancer and preferentially expressed in bone marrow. *Oncogene* **11**, 1693-1698 (1995).
395. Wei, M.C.*, et al.* Proapoptotic BAX and BAK: a requisite gateway to mitochondrial dysfunction and death. *Science* **292**, 727-730 (2001).
396. Shamas-Din, A., Brahmbhatt, H., Leber, B. & Andrews, D.W. BH3-only proteins: Orchestrators of apoptosis. *Biochim Biophys Acta* **1813**, 508-520 (2011).
397. Danial, N.N. & Korsmeyer, S.J. Cell death: critical control points. *Cell* **116**, 205-219 (2004).
398. Chen, L.*, et al.* Differential targeting of prosurvival Bcl-2 proteins by their BH3-only ligands allows complementary apoptotic function. *Mol Cell* **17**, 393-403 (2005).
399. Nijhawan, D.*, et al.* Elimination of Mcl-1 is required for the initiation of apoptosis following ultraviolet irradiation. *Genes Dev* **17**, 1475-1486 (2003).
400. Opferman, J.T.*, et al.* Development and maintenance of B and T lymphocytes requires antiapoptotic MCL-1. *Nature* **426**, 671-676 (2003).
401. Zhou, P.*, et al.* MCL1 transgenic mice exhibit a high incidence of B-cell lymphoma manifested as a spectrum of histologic subtypes. *Blood* **97**, 3902-3909 (2001).
402. Zhong, Q., Gao, W., Du, F. & Wang, X. Mule/ARF-BP1, a BH3-only E3 ubiquitin ligase, catalyzes the polyubiquitination of Mcl-1 and regulates apoptosis. *Cell* **121**, 1085-1095 (2005).
403. Marriott, H.M.*, et al.* Dynamic changes in Mcl-1 expression regulate macrophage viability or commitment to apoptosis during bacterial clearance. *The Journal of clinical investigation* **115**, 359-368 (2005).
404. Zychlinsky, A. & Sansonetti, P. Perspectives series: host/pathogen interactions. Apoptosis in bacterial pathogenesis. *The Journal of clinical investigation* **100**, 493-495 (1997).

405. Dockrell, D.H., *et al.* Alveolar macrophage apoptosis contributes to pneumococcal clearance in a resolving model of pulmonary infection. *Journal of immunology* **171**, 5380-5388 (2003).
406. Leu, J.I., Dumont, P., Hafey, M., Murphy, M.E. & George, D.L. Mitochondrial p53 activates Bak and causes disruption of a Bak-Mcl1 complex. *Nature cell biology* **6**, 443-450 (2004).
407. Liu, Q. & Gehring, K. Heterodimerization of BAK and MCL-1 activated by detergent micelles. *The Journal of biological chemistry* **285**, 41202-41210 (2010).
408. Willis, S.N., *et al.* Proapoptotic Bak is sequestered by Mcl-1 and Bcl-xL, but not Bcl-2, until displaced by BH3-only proteins. *Genes Dev* **19**, 1294-1305 (2005).
409. Pattingre, S., *et al.* Bcl-2 antiapoptotic proteins inhibit Beclin 1-dependent autophagy. *Cell* **122**, 927-939 (2005).
410. Levine, B., Sinha, S. & Kroemer, G. Bcl-2 family members: dual regulators of apoptosis and autophagy. *Autophagy* **4**, 600-606 (2008).
411. Kihara, A., Noda, T., Ishihara, N. & Ohsumi, Y. Two distinct Vps34 phosphatidylinositol 3-kinase complexes function in autophagy and carboxypeptidase Y sorting in Saccharomyces cerevisiae. *J Cell Biol* **152**, 519-530 (2001).
412. Erlich, S., *et al.* Differential interactions between Beclin 1 and Bcl-2 family members. *Autophagy* **3**, 561-568 (2007).
413. Germain, M., *et al.* MCL-1 is a stress sensor that regulates autophagy in a developmentally regulated manner. *The EMBO journal* **30**, 395-407 (2011).
414. Chou, C.H., Lee, R.S. & Yang-Yen, H.F. An internal EELD domain facilitates mitochondrial targeting of Mcl-1 via a Tom70-dependent pathway. *Molecular biology of the cell* **17**, 3952-3963 (2006).
415. Kapinas, K., Kessler, C.B. & Delany, A.M. miR-29 suppression of osteonectin in osteoblasts: regulation during differentiation and by canonical Wnt signaling. *J Cell Biochem* **108**, 216-224 (2009).
416. Manicassamy, S., *et al.* Activation of beta-catenin in dendritic cells regulates immunity versus tolerance in the intestine. *Science* **329**, 849-853 (2010).
417. Heasman, S.J. & Ridley, A.J. Mammalian Rho GTPases: new insights into their functions from in vivo studies. *Nat Rev Mol Cell Biol* **9**, 690-701 (2008).
418. Etienne-Manneville, S. Cdc42--the centre of polarity. *J Cell Sci* **117**, 1291-1300 (2004).
419. Garrett, W.S., *et al.* Developmental control of endocytosis in dendritic cells by Cdc42. *Cell* **102**, 325-334 (2000).
420. Pulecio, J., *et al.* Cdc42-mediated MTOC polarization in dendritic cells controls targeted delivery of cytokines at the immune synapse. *The Journal of Experimental Medicine* **207**, 2719-2732 (2010).
421. Hayden, M.S. & Ghosh, S. Shared principles in NF-kappaB signaling. *Cell* **132**, 344-362 (2008).
422. Opipari, A.W., Jr., Boguski, M.S. & Dixit, V.M. The A20 cDNA induced by tumor necrosis factor alpha encodes a novel type of zinc finger protein. *The Journal of biological chemistry* **265**, 14705-14708 (1990).

423. Dixit, V.M.*, et al.* Tumor necrosis factor-alpha induction of novel gene products in human endothelial cells including a macrophage-specific chemotaxin. *The Journal of biological chemistry* **265**, 2973-2978 (1990).
424. Krikos, A., Laherty, C.D. & Dixit, V.M. Transcriptional activation of the tumor necrosis factor alpha-inducible zinc finger protein, A20, is mediated by kappa B elements. *The Journal of biological chemistry* **267**, 17971-17976 (1992).
425. Beyaert, R., Heyninck, K. & Van Huffel, S. A20 and A20-binding proteins as cellular inhibitors of nuclear factor-kappa B-dependent gene expression and apoptosis. *Biochem Pharmacol* **60**, 1143-1151 (2000).
426. Ordureau, A.*, et al.* The IRAK-catalysed activation of the E3 ligase function of Pellino isoforms induces the Lys63-linked polyubiquitination of IRAK1. *The Biochemical journal* **409**, 43-52 (2008).
427. Kanayama, A.*, et al.* TAB2 and TAB3 activate the NF-kappaB pathway through binding to polyubiquitin chains. *Mol Cell* **15**, 535-548 (2004).
428. Wertz, I.E.*, et al.* De-ubiquitination and ubiquitin ligase domains of A20 downregulate NF-kappaB signalling. *Nature* **430**, 694-699 (2004).
429. Lee, E.G.*, et al.* Failure to regulate TNF-induced NF-kappaB and cell death responses in A20-deficient mice. *Science* **289**, 2350-2354 (2000).
430. Turer, E.E.*, et al.* Homeostatic MyD88-dependent signals cause lethal inflamMation in the absence of A20. *The Journal of Experimental Medicine* **205**, 451-464 (2008).
431. Arsenescu, R.*, et al.* Signature biomarkers in Crohn's disease: toward a molecular classification. *Mucosal Immunol* **1**, 399-411 (2008).
432. Stojanov, S. & McDermott, M.F. The tumour necrosis factor receptor-associated periodic syndrome: current concepts. *Expert Rev Mol Med* **7**, 1-18 (2005).
433. Lappalainen, M.*, et al.* Association of IL23R, TNFRSF1A, and HLA-DRB1*0103 allele variants with inflammatory bowel disease phenotypes in the Finnish population. *Inflammatory bowel diseases* **14**, 1118-1124 (2008).
434. Waschke, K.A.*, et al.* Tumor necrosis factor receptor gene polymorphisms in Crohn's disease: association with clinical phenotypes. *The American journal of gastroenterology* **100**, 1126-1133 (2005).
435. Takeshita, F.*, et al.* TRAF4 acts as a silencer in TLR-mediated signaling through the association with TRAF6 and TRIF. *Eur J Immunol* **35**, 2477-2485 (2005).
436. Marinis, J.M., Homer, C.R., McDonald, C. & Abbott, D.W. A novel motif in the Crohn's disease susceptibility protein, NOD2, allows TRAF4 to down-regulate innate immune responses. *The Journal of biological chemistry* **286**, 1938-1950 (2011).
437. Bazan, J.F.*, et al.* A new class of membrane-bound chemokine with a CX3C motif. *Nature* **385**, 640-644 (1997).
438. Lucas, A.D.*, et al.* The transmembrane form of the CX3CL1 chemokine fractalkine is expressed predominantly by epithelial cells in vivo. *Am J Pathol* **158**, 855-866 (2001).

439. Niess, J.H., *et al.* CX3CR1-mediated dendritic cell access to the intestinal lumen and bacterial clearance. *Science* **307**, 254-258 (2005).
440. Muehlhoefer, A., *et al.* Fractalkine is an epithelial and endothelial cell-derived chemoattractant for intraepithelial lymphocytes in the small intestinal mucosa. *Journal of immunology* **164**, 3368-3376 (2000).
441. Kostadinova, F.I., *et al.* Crucial involvement of the CX3CR1-CX3CL1 axis in dextran sulfate sodium-mediated acute colitis in mice. *J Leukoc Biol* **88**, 133-143 (2010).
442. Papadopoulos, E.J., *et al.* Fractalkine, a CX3C chemokine, is expressed by dendritic cells and is up-regulated upon dendritic cell maturation. *Eur J Immunol* **29**, 2551-2559 (1999).
443. Cullinan, E.B., *et al.* IL-1 receptor accessory protein is an essential component of the IL-1 receptor. *Journal of immunology* **161**, 5614-5620 (1998).
444. Wesche, H., *et al.* The interleukin-1 receptor accessory protein (IL-1RAcP) is essential for IL-1-induced activation of interleukin-1 receptor-associated kinase (IRAK) and stress-activated protein kinases (SAP kinases). *The Journal of biological chemistry* **272**, 7727-7731 (1997).
445. Huang, J., Gao, X., Li, S. & Cao, Z. Recruitment of IRAK to the interleukin 1 receptor complex requires interleukin 1 receptor accessory protein. *Proceedings of the National Academy of Sciences of the United States of America* **94**, 12829-12832 (1997).
446. Casadio, R., *et al.* Model of interaction of the IL-1 receptor accessory protein IL-1RAcP with the IL-1beta/IL-1R(I) complex. *FEBS Lett* **499**, 65-68 (2001).
447. Jensen, L.E., Muzio, M., Mantovani, A. & Whitehead, A.S. IL-1 signaling cascade in liver cells and the involvement of a soluble form of the IL-1 receptor accessory protein. *Journal of immunology* **164**, 5277-5286 (2000).
448. Buonocore, S., *et al.* Innate lymphoid cells drive interleukin-23-dependent innate intestinal pathology. *Nature* **464**, 1371-1375 (2010).
449. Geremia, A., *et al.* IL-23-responsive innate lymphoid cells are increased in inflammatory bowel disease. *The Journal of Experimental Medicine* **208**, 1127-1133 (2011).
450. Jeltsch, A. Beyond Watson and Crick: DNA methylation and molecular enzymology of DNA methyltransferases. *Chembiochem* **3**, 274-293 (2002).
451. Gamper, C.J., Agoston, A.T., Nelson, W.G. & Powell, J.D. Identification of DNA methyltransferase 3a as a T cell receptor-induced regulator of Th1 and Th2 differentiation. *Journal of immunology* **183**, 2267-2276 (2009).
452. El Gazzar, M., *et al.* G9a and HP1 couple histone and DNA methylation to TNFalpha transcription silencing during endotoxin tolerance. *The Journal of biological chemistry* **283**, 32198-32208 (2008).
453. Migone, T.S., *et al.* TL1A is a TNF-like ligand for DR3 and TR6/DcR3 and functions as a T cell costimulator. *Immunity* **16**, 479-492 (2002).
454. Papadakis, K.A., *et al.* Dominant role for TL1A/DR3 pathway in IL-12 plus IL-18-induced IFN-gamma production by peripheral blood and mucosal CCR9+ T lymphocytes. *Journal of immunology* **174**, 4985-4990 (2005).

455. Kunkel, E.J., *et al.* Lymphocyte CC chemokine receptor 9 and epithelial thymus-expressed chemokine (TECK) expression distinguish the small intestinal immune compartment: Epithelial expression of tissue-specific chemokines as an organizing principle in regional immunity. *The Journal of Experimental Medicine* **192**, 761-768 (2000).
456. Yamazaki, K., *et al.* Single nucleotide polymorphisms in TNFSF15 confer susceptibility to Crohn's disease. *Human molecular genetics* **14**, 3499-3506 (2005).
457. Tremelling, M., *et al.* Contribution of TNFSF15 gene variants to Crohn's disease susceptibility confirmed in UK population. *Inflammatory bowel diseases* **14**, 733-737 (2008).
458. Michelsen, K.S., *et al.* IBD-associated TL1A gene (TNFSF15) haplotypes determine increased expression of TL1A protein. *PLoS One* **4**, e4719 (2009).
459. Prehn, J.L., *et al.* The T cell costimulator TL1A is induced by FcgammaR signaling in human monocytes and dendritic cells. *Journal of immunology* **178**, 4033-4038 (2007).
460. Bamias, G., *et al.* Role of TL1A and its receptor DR3 in two models of chronic murine ileitis. *Proceedings of the National Academy of Sciences of the United States of America* **103**, 8441-8446 (2006).
461. Takedatsu, H., *et al.* TL1A (TNFSF15) regulates the development of chronic colitis by modulating both T-helper 1 and T-helper 17 activation. *Gastroenterology* **135**, 552-567 (2008).
462. Shih, D.Q., *et al.* Constitutive TL1A (TNFSF15) expression on lymphoid or myeloid cells leads to mild intestinal inflammation and fibrosis. *PLoS One* **6**, e16090 (2011).
463. Bamias, G., *et al.* Expression, localization, and functional activity of TL1A, a novel Th1-polarizing cytokine in inflammatory bowel disease. *Journal of immunology* **171**, 4868-4874 (2003).
464. Gallagher, G., *et al.* Cloning, expression and initial characterization of interleukin-19 (IL-19), a novel homologue of human interleukin-10 (IL-10). *Genes and immunity* **1**, 442-450 (2000).
465. Kunz, S., *et al.* Interleukin (IL)-19, IL-20 and IL-24 are produced by and act on keratinocytes and are distinct from classical ILs. *Exp Dermatol* **15**, 991-1004 (2006).
466. Huang, F., *et al.* Potentiation of IL-19 expression in airway epithelia by IL-17A and IL-4/IL-13: important implications in asthma. *J Allergy Clin Immunol* **121**, 1415-1421, 1421 e1411-1413 (2008).
467. Gallagher, G. Interleukin-19: multiple roles in immune regulation and disease. *Cytokine Growth Factor Rev* **21**, 345-352 (2010).
468. Liao, Y.C., *et al.* IL-19 induces production of IL-6 and TNF-alpha and results in cell apoptosis through TNF-alpha. *Journal of immunology* **169**, 4288-4297 (2002).
469. Wei, C.C., *et al.* Detection of IL-20 and its receptors on psoriatic skin. *Clin Immunol* **117**, 65-72 (2005).
470. Li, H.H., *et al.* Interleukin-19 upregulates keratinocyte growth factor and is associated with psoriasis. *Br J Dermatol* **153**, 591-595 (2005).
471. Azuma, Y.T., *et al.* Interleukin-19 protects mice from innate-mediated colonic inflammation. *Inflammatory bowel diseases* **16**, 1017-1028 (2010).

472. Hsing, C.H., Chiu, C.J., Chang, L.Y., Hsu, C.C. & Chang, M.S. IL-19 is involved in the pathogenesis of endotoxic shock. *Shock* **29**, 7-15 (2008).
473. Al-Salleeh, F. & Petro, T.M. Promoter analysis reveals critical roles for SMAD-3 and ATF-2 in expression of IL-23 p19 in macrophages. *Journal of immunology* **181**, 4523-4533 (2008).
474. El Gazzar, M. & McCall, C.E. MicroRNAs distinguish translational from transcriptional silencing during endotoxin tolerance. *The Journal of biological chemistry* **285**, 20940-20951 (2010).
475. Ma, F.*, et al.* MicroRNA-466l upregulates IL-10 expression in TLR-triggered macrophages by antagonizing RNA-binding protein tristetraprolin-mediated IL-10 mRNA degradation. *Journal of immunology* **184**, 6053-6059 (2010).
476. Hwang, H.W., Wentzel, E.A. & Mendell, J.T. A hexanucleotide element directs microRNA nuclear import. *Science* **315**, 97-100 (2007).
477. Napolitani, G., Rinaldi, A., Bertoni, F., Sallusto, F. & Lanzavecchia, A. Selected Toll-like receptor agonist combinations synergistically trigger a T helper type 1-polarizing program in dendritic cells. *Nature immunology* **6**, 769-776 (2005).
478. Khayrullina, T., Yen, J.H., Jing, H. & Ganea, D. In vitro differentiation of dendritic cells in the presence of prostaglandin E2 alters the IL-12/IL-23 balance and promotes differentiation of Th17 cells. *Journal of immunology* **181**, 721-735 (2008).
479. Becker, C.*, et al.* Constitutive p40 promoter activation and IL-23 production in the terminal ileum mediated by dendritic cells. *The Journal of clinical investigation* **112**, 693-706 (2003).
480. Weichart, D.*, et al.* Analysis of NOD2-mediated proteome response to muramyl dipeptide in HEK293 cells. *J Biol Chem* **281**, 2380-2389 (2006).
481. Dugan, J.W.*, et al.* Nucleotide oligomerization domain-2 interacts with 2'-5'-oligoadenylate synthetase type 2 and enhances RNase-L function in THP-1 cells. *Mol Immunol* **47**, 560-566 (2009).
482. Chakrabarti, A., Jha, B.K. & Silverman, R.H. New insights into the role of RNase L in innate immunity. *J Interferon Cytokine Res* **31**, 49-57 (2011).
483. Petrilli, V.*, et al.* Activation of the NALP3 inflammasome is triggered by low intracellular potassium concentration. *Cell Death Differ* **14**, 1583-1589 (2007).
484. Rothbauer, U.*, et al.* A versatile nanotrap for biochemical and functional studies with fluorescent fusion proteins. *Mol Cell Proteomics* **7**, 282-289 (2008).
485. Abramson, J., Giraud, M., Benoist, C. & Mathis, D. Aire's partners in the molecular control of immunological tolerance. *Cell* **140**, 123-135 (2010).
486. Ramirez, D.C.*, et al.* Cu,Zn-superoxide dismutase-driven free radical modifications: copper- and carbonate radical anion-initiated protein radical chemistry. *The Biochemical journal* **417**, 341-353 (2009).
487. Legrand-Poels, S.*, et al.* Modulation of Nod2-dependent NF-kappaB signaling by the actin cytoskeleton. *J Cell Sci* **120**, 1299-1310 (2007).

488. Kufer, T.A., Kremmer, E., Banks, D.J. & Philpott, D.J. Role for erbin in bacterial activation of Nod2. *Infection and immunity* **74**, 3115-3124 (2006).
489. Borg, J.P.*, et al.* ERBIN: a basolateral PDZ protein that interacts with the mammalian ERBB2/HER2 receptor. *Nature cell biology* **2**, 407-414 (2000).
490. Huang, Y.Z., Zang, M., Xiong, W.C., Luo, Z. & Mei, L. Erbin suppresses the MAP kinase pathway. *The Journal of biological chemistry* **278**, 1108-1114 (2003).
491. Negroni, A.*, et al.* Activation of NOD2-mediated intestinal pathway in a pediatric population with Crohn's disease. *Inflammatory bowel diseases* **15**, 1145-1154 (2009).
492. da Silva, K.P. & Borges, J.C. The molecular chaperone Hsp70 family members function by a bidirectional heterotrophic allosteric mechanism. *Protein Pept Lett* **18**, 132-142 (2011).
493. deFoneska, A. & Kaunitz, J.D. Gastroduodenal mucosal defense. *Curr Opin Gastroenterol* **26**, 604-610 (2010).
494. Mayor, A., Martinon, F., De Smedt, T., Petrilli, V. & Tschopp, J. A crucial function of SGT1 and HSP90 in inflammasome activity links mammalian and plant innate immune responses. *Nature immunology* **8**, 497-503 (2007).
495. Winstanley, C. & Morgan, J.A. The bacterial flagellin gene as a biomarker for detection, population genetics and epidemiological analysis. *Microbiology* **143 (Pt 10)**, 3071-3084 (1997).
496. Hayashi, F.*, et al.* The innate immune response to bacterial flagellin is mediated by Toll-like receptor 5. *Nature* **410**, 1099-1103 (2001).
497. Gewirtz, A.T., Navas, T.A., Lyons, S., Godowski, P.J. & Madara, J.L. Cutting edge: bacterial flagellin activates basolaterally expressed TLR5 to induce epithelial proinflammatory gene expression. *Journal of immunology* **167**, 1882-1885 (2001).
498. McDermott, P.F., Ciacci-Woolwine, F., Snipes, J.A. & Mizel, S.B. High-affinity interaction between gram-negative flagellin and a cell surface polypeptide results in human monocyte activation. *Infection and immunity* **68**, 5525-5529 (2000).
499. Lodes, M.J.*, et al.* Bacterial flagellin is a dominant antigen in Crohn disease. *The Journal of clinical investigation* **113**, 1296-1306 (2004).
500. Gewirtz, A.T.*, et al.* Dominant-negative TLR5 polymorphism reduces adaptive immune response to flagellin and negatively associates with Crohn's disease. *Am J Physiol Gastrointest Liver Physiol* **290**, G1157-1163 (2006).
501. Netea, M.G.*, et al.* Chronic yersiniosis due to defects in the TLR5 and NOD2 recognition pathways. *Neth J Med* **68**, 310-315 (2010).
502. Begue, B.*, et al.* Microbial induction of CARD15 expression in intestinal epithelial cells via toll-like receptor 5 triggers an antibacterial response loop. *J Cell Physiol* **209**, 241-252 (2006).
503. Rhee, S.H.*, et al.* Pathophysiological role of Toll-like receptor 5 engagement by bacterial flagellin in colonic inflammation. *Proceedings of the National Academy of Sciences of the United States of America* **102**, 13610-13615 (2005).

504. Swidsinski, A., Weber, J., Loening-Baucke, V., Hale, L.P. & Lochs, H. Spatial organization and composition of the mucosal flora in patients with inflammatory bowel disease. *Journal of clinical microbiology* **43**, 3380-3389 (2005).
505. Lotz, M.*, et al.* Postnatal acquisition of endotoxin tolerance in intestinal epithelial cells. *The Journal of Experimental Medicine* **203**, 973-984 (2006).
506. Stadnicki, A.*, et al.* Immunolocalization and expression of kinin B1R and B2R receptors in human inflammatory bowel disease. *Am J Physiol Gastrointest Liver Physiol* **289**, G361-366 (2005).
507. Stadnicki, A.*, et al.* Selective plasma kallikrein inhibitor attenuates acute intestinal inflammation in Lewis rat. *Dig Dis Sci* **41**, 912-920 (1996).
508. Stadnicki, A.*, et al.* Specific inhibition of plasma kallikrein modulates chronic granulomatous intestinal and systemic inflammation in genetically susceptible rats. *Faseb J* **12**, 325-333 (1998).
509. Banks, C., Bateman, A., Payne, R., Johnson, P. & Sheron, N. Chemokine expression in IBD. Mucosal chemokine expression is unselectively increased in both ulcerative colitis and Crohn's disease. *J Pathol* **199**, 28-35 (2003).
510. Hunter, M.P.*, et al.* Detection of microRNA expression in human peripheral blood microvesicles. *PLoS One* **3**, e3694 (2008).
511. Michael, A.*, et al.* Exosomes from human saliva as a source of microRNA biomarkers. *Oral Dis* **16**, 34-38 (2010).
512. Ibrahim, A.F.*, et al.* MicroRNA replacement therapy for miR-145 and miR-33a is efficacious in a model of colon carcinoma. *Cancer Res* (2011).